Universitat Ramon Llull

DOCTORAL THESIS

Title	GLYCOSYNTHASE TECHNOLOGY FOR ENZYMATIC SYNTHESIS OF FUNCTIONALIZED ARTIFICIAL POLYSACCHARIDES AS NEW BIOMATERIALS
Presented by	Mª Victoria Codera Pastor
Centre	IQS School of Engineering
Department	Bioengineering
Directed by	Dr. Antoni Planas and Dr. Magda Faijes

C. Claravall, 1-3
08022 Barcelona
Tel. 936 022 200
Fax 936 022 249
E-mail: urlsc@sec.url.es
www.url.es

A toda mi familia, especialmente

a mis padres y a Francesc.

Dream it, wish it, do it.

ACKNOWLEDGEMENTS

I have spent the last five years of my life as a member of the Biochemistry laboratory of the IQS School of Engineering. A Ph.D. teaches many things that go beyond the field you are studying, and it has been a real pleasure for me to work here all this time, growing up as a chemist and as a person. I am grateful for having had this opportunity and I would like to specially thank my advisor Professor Antoni Planas and my co-advisor Dr. Magda Faijes for offering me to participate in this challenging project.

Toni, thanks for everything, especially for introducing me into the amazing world of proteins and carbohydrates, these tricky molecules that are now a part of my life. Thank you for all the science we have shared and for all the good times in the symposiums: I could have not enjoyed myself more. I would like to thank you as well for being the best referee 'in-house'. With your love for little details you make us better scientists. Finally, early Saturday morning e-mails deserve a special place here as I realized that those e-mails usually contained the most challenging and motivating news I have gotten from you, giving me the energy that sometimes one lacks during a thesis. Thank you for always believing in me.

Magda, I would like to thank you for the days we spent back in 2007 in the undergrad laboratory. You were a passionate professor who spread your love for chemistry all around and I thank you for that spark that you ignited in me. Since then, science has a different meaning for me and I am not sure I would be here today otherwise. Thanks for all those mornings at 8 AM discussing carbohydrate science. I really enjoyed those moments, especially the ones talking about mono- and dirityls, tosyls, mesyls, bromides, iodides and chlorides. It was so much fun.

Dear Dr. Edgar, thank you for admitting me in your group. My stage in Blacksburg was a great experience for me where everything was perfect. You and the rest of the team were like family for me when I was there. I thank you as well for letting me attend the Polysaccharide Course you gave at Virginia Tech and for all the polysaccharide science you taught me in class and during the seminars. I really hope we can work together again in the future.

Dr. Xavier Batllori, I would like to thank you for all the help and good advice you have given to me. Thanks for all your time, all your patience and all the talks. It has been always a pleasure to go and run NMR experiments. Ms. Núria Ruiz, thanks for all the help with the IR, you always sent good news. Dr. Jordi Abellà, thanks for all the SEM experiments you performed for me. It was always an exciting time when we visualized the polymers on the screen. You transported me to a beautiful and awesome micro world. Finally, I want to thank Chema and David from the 'Stock room' for absolutely always being there with a huge smile ready to serve everyone. I have visited you thousands of times and you always cheered me up, always! Thanks!

I would like to thank Professor Carles Colominas, my good friend Dr. Rubén Ruiz and the always smiley Ana Ramos for the great team we formed several years ago when we were in charge of the Inorganic laboratory for undergrad students. The work with Professor Santi Nonell and the Physical Chemistry laboratory was also very challenging and I can sincerely say that I enjoyed myself there. I learned a lot and I thank you all for the opportunity and the freedom you gave me with the experiments and with the students.

During the thesis, the lab ends up being like your second home where a lot of people come and go. I would like to thank all my labmates for their company, their help, the talks, the good and the

bad moments that we have shared and that let us to know each other better. First, I would like to specially thank the actual members of the lab:

- Patri: you started to work in the lab at the same time I started my Ph.D. We have been through a lot and I thank you for always being there.

- Xavi Turón, I have enjoyed getting to know you between coffees and lunch times. I would sincerely like to run a bioreactor someday and scale up the growth of my cells!

- Xevi, thanks for your optimism and for always being up to help whoever whenever however. The presence of Biel (and now Martí as well) on Friday afternoons was always a motivation to go on and finish the week's work. They are lovely kids.

- Teresa, when I grow up I want to be like you. I learned so much from you. Thanks!

- Amanda, Pau and Marta Palomo, Cris Alsina, even though you arrived to the lab when I was about to leave I easily found out that you were great people and your presence was a gift! Thanks!

- Cris Val, you have been a great companion all this time, easy to talk with, realist, responsible, resilient, empathic and respectful… Dear pharmacist, I admire you much more than you think, as a person and as a scientist. Your work with the synthesis of carbohydrates has been enormous and in spite of all your tribulations you never gave up. That says a lot about you. There is always light at the end of the tunnel and all the efforts made during the way are worthwhile.

- Sergi, my dear friend and neighbor, thanks for all the support you have given me. I will never forget our daily breakfasts, specially the chocolate ones. And our hikes and visits to Caldes with Gabi and whoever wanted to join us.

- Carles, I would like to specially thank you for all the help with molecular biology. My polyacrylamide gels would not be the same without your wise lessons! Thanks for the company you gave me during many weekends. Will you be able to forget that literally 'black' Saturday?

- Javi, I would like to thank you for all the seminars you prepared trying to make us understand the biocomputational stuff you worked with. Furthermore, I have to say I will never forget that International Carbohydrate Symposium in Madrid. We had a lot of fun in that trip and it was a culinary experience for me thanks to you.

- Òscar, your presence in the lab was discreet but it was always nice to see you around.

- Hugo, I really want to thank you for introducing me to most of the analytical equipments you were in charge of, and for the good recommendations about molecular biology. I'm glad I had the opportunity to get to know you more during these last months. I hardly knew you before but now I can say you are my friend. And thanks for la 'Concha del Peregrino'! I will get to Santiago soon wearing it on my backpack.

- Estela, your presence is synonym of peace and good work in the lab. Thanks for your daily smile, your optimism, your empathy… You are always ready to help whoever needs it. Thanks!

- Nuria Abajo, I really enjoyed your nice company during the daily afternoons and evenings when you were still an undergrad. I wish you all the best with your bioreactors! Klaus, Oriol, Laia, Núria O., Marcos and Albert, good luck in your future. It has been a pleasure to share the lab with you all during these last months.

- Marta V., despite no longer sharing the IQS facilities I have to thank you for all the talks, the walks and for the summer days when we went to the beach after work. What could be better to restart next day feeling fresh?

I would also like to thank the people who is not working in the lab anymore:

- My old Ph.D. labmates, all of them already Doctors: Marta Marszalek, Neus Mora, Albert (Garcia) Colomer, Núria Martínez and Joan Nieto.

- My students, those who collaborated in different parts of my Ph.D. usually trying to optimize synthetic steps. Dear Mizanur, you were the first student I supervised. I am so glad we worked together and I think it was a great experience for both of us. I haven't forgotten you, and I don't think I will. Miquel, thanks for all the time you dedicated to the synthesis of carbohydrates after your undergrad classes, I will always remember your first fluorination, it was an adventure, wasn't it? José, your determination surprised me since the beginning and your work was very helpful. It was a real pleasure working with you. Annie, you continued the work of José and I really appreciate what you did despite it was a short stay.

- Postdocs, 'TFC', Master and undergrad students: Jenny, Montse, Susanna, Carme, Cristian Bene, Alba, Francesc Padrès, Damián, Ori and Ignasi. Special thanks to Cristian Calzada for introducing me to the expression and purification of proteins and to Ellen, whose dedication and patience have always been admirable. Elena Genescà and Inés Fonseca, we became friends during my first year of Ph.D. Despite only being together for less than a year we had a great time together and I will never forget you. David Álvarez, you came only for a few months to cover a maternity leave but you quickly became a part of the group. Thanks for all the help with the management stuff and for the beautiful friendship that came out. Edu and Xavi Pérez, I still miss you. Edu, thanks for all the carbohydrate synthesis that you taught me, it was the basis of my thesis, you were a great instructor. Xavi, thanks for your analytical vision, thanks for the precision and carefulness you showed in all the experiments you performed. You were always an example of good work.

- The visiting students Julio from Nicaragua, Anabella from Guatemala, Tania from Sweeden/Bolivia and Professor Mark Peczuh from Connecticut (USA). It's amazing having people from other countries in the lab. I had a great time with all of you. Thanks for letting me know more about your respective cultures. You will always have a friend in Barcelona.

My life in Blacksburg, Virginia (USA) would not have been the same without the lovely people I met there. First of all, I would like to thank my roommates Audrey, Kevin and Ariel for their hospitality and all the help they offered since the beginning of my stage. Thanks for all the tips, good hikes, English lessons, cooking experiments that we shared. My international group of labmates, Xiangtao, Ruoran, Haoyu, Tom, Joyanne, Amin and Nazzia. Special thanks to my labmates and friends Sidd, Çiğdem and Xueyan with whom I kept in touch after my departure. I miss you so much. Finally, I would like to thank Soheilla and Ying for the hikes and talks and my good friend Sheima for absolutely everything, you are a really good person who deserves all the best.

I had the great luck to have attended several important symposiums where I met really interesting and important scientists with whom I've had the pleasure to talk and discuss more than science. Dear Drs. Gemma Arsequell, Gregori Valencia, Jesús Trujillo Vázquez, Aloysius Siriwardena, Jesús Jiménez-Barbero, Manuel Martín-Lomas, Carlo Unverzagt, Monica Palcic, Marco Moracci, G. Davies, Laura Masgrau and Marcelo Guerín, I would like to thank you and your students and

co-workers for all your work and the moments we have shared in different meetings. Getting to know you made me want to do better in order to contribute to science the way you do. Special thanks to Dr. Régis Fauré. I admire your work, dedication and empathy: you are a model to follow and it has been a pleasure to work next to you for these last six months.

I specially thank my friends for their patience to understand all the issues that come by the hand of a Ph.D. Dear friends of school Claudia, Ana, Lorena, Ingrid, Marta and Raquel you have been next to me since we were 5 years old and I thank you for your unconditional love. Dear friends of College: Javi, Lorena and Víctor, I know that if I call you, you will always come. I really appreciate your presence in all the important events. Mireie, my life would not be the same without you. We all need a Mireie around to see the bright side of life. Mireia Ci. and Allan, the door of your house has always been opened for us. Thanks for being our adventure buddies. Albert Pell, I'm so glad I have gotten to know you much more during these last two years, you are great. Couple 'Montiña', thanks for your great company, all the laughs, good advices… you are an example for us. And finally, my dear Cris with whom I can say I have shared almost everything. The 'Camino de Santiago' joined us more than anything else. You are a great person and scientist and I thank you for all the experiences we have been through, for all the things you have taught me, etc, etc. Thanks, summing up, for being my friend.

I would also like to thank the Barcelona Guitar Orchestra I belong to since late 2007 and to its director Sergi Vicente for always leaving a place for me in the second guitar (viola) voice.

My political family was big since the beginning but it has starting to grow even more recently. Dolors and Jordi, Joan, Mateu, Benjamí, Liso, Aleix and little Gabriel, you are a great family and I specially thank you for your love and patience.

My own little family would deserve not only the 'thanks' but several monuments. They are some kind of warriors able to achieve whatever goals they have. Mom and dad, you are stronger than you think and I thank you for being literally here. And again, thanks for your patience, because a Ph.D. takes a long time and big efforts and sometimes it can seem endless. You can't imagine how important your support has been all this time, especially while writing the dissertation. Pili, thanks for your always supportive presence, this family would not be the same without you. Mª Dolores, Meri, thanks for all the communication we exchanged when I left to Virginia, I really enjoyed sending my almost daily reports and pictures. It would not have made sense if there was no one interested in at the other side.

And finally, last but not least, thank you Francesc. There were times that I think if it wasn't for you, my thesis would not be finished. You have been next to me all this time, during the experimental, cheering me up when my reactions failed, or coming to the office in order to see me at least for some minutes bringing something delicious to eat and giving me energy to come back to my experiments. You were there when preparing posters or presentations for the symposiums or for the lab seminars staying awake until late at night. You were waiting for me at the other side of the ocean when I left to the US, talking everyday through skype and watching movies or TV shows while synchronizing our laptops and chatting at the same time to comment the scenes. You helped me to improve my English, talking with me, reading with me for hours, correcting my compositions and writings. And you were there when I felt loneliest as ever while writing my dissertation. Without having done a Ph.D. you know better than anyone what is this like and I thank you for never having left me alone nor behind. Always together. We share a great passion for chemistry and science in general and I'm sure that it will always accompany us. I love you so much.

Victoria

SUMARI

La tecnologia glicosintasa ha esdevingut una eina important per a la síntesi d'oligosacàrids, polisacàrids i glicoconjugats. Les glicosintases són glicosidases mutades desproveïdes d'activitat hidrolítica però capaces de catalitzar eficientment la formació d'enllaços glicosídics amb rendiments elevats en fer ús d'un donador glicosídic activat. A més a més, el donador activat i el seu producte de transglicosidació poden actuar com acceptors donant lloc a l'autocondensació del donador o a l'elongació del producte de transglicosidació, produint polisacàrids.

En el present treball es pretén sintetitzar nous polisacàrids artificials funcionalitzats amb estructures definides mitjançant l'ús de la tecnologia glicosintasa. D'una banda, s'ha intentat augmentar la massa molecular dels polisacàrids fent ús d'un mòdul d'unió de carbohidrats (CBM). Aquest mòdul podria millorar la solubilitat dels nous polímers a mesura que es van sintetitzant durant la reacció de polimerització. L'efecte en el grau de polimerització ha estat estudiat tant pel mutant glicosintasa en presència de CBM com per la proteïna de fusió glicosintasa-CBM. D'altra banda, s'han sintetitzat polisacàrids artificials funcionalitzats a partir de donadors disacarídics activats on la funcionalització desitjada ha sigut prèviament introduïda a la posició C-6'. Aquests donadors funcionalitzats actuen com a substrat pel mutant glicosintasa que catalitzarà la reacció d'autocondensació. El grup azido va ser escollit com a un grup funcional adequat donada la seva versatilitat i mida, suficientment petit com per a ser acceptat per l'enzim. Els donadors fluorur de 6'-azidolaminaribiosa i fluorur de 6'-azidocel·lobiosa han estat sintetitzats i avaluats com a substrats per les reaccions glicosintasa amb el mutant E134S de la 1,3-1,4-β-glucanasa de *Bacillus licheniformis* i el mutant E197A de la cel·lulasa d'*Humicola insolens*, respectivament.

S'han sintetitzat 6-azido i 6-amino-6-deoxicel·luloses artificials amb una seqüència de funcionalització alternada. De forma oposada a la modificació química de cel·luloses on la seqüència de substitució és intrínsecament aleatòria, la polimerització catalitzada per glicosintases de donadors glicosídics modificats apropiadament, permet accedir a noves cel·luloses funcionalitzades amb seqüències de substitució definides i regulars.

SUMARIO

La tecnología glicosintasa se ha convertido en una herramienta importante para la síntesis de oligosacáridos, polisacáridos y glicoconjugados. Las glicosintasas son glicosidasas mutadas desprovistas de actividad hidrolítica pero capaces de catalizar eficientemente la formación de enlaces glicosídicos con rendimientos elevados utilizando un dador glicosídico activado. Además, el dador activo y su producto de transglicosidación pueden actuar como aceptores dando lugar a la autocondensación del dador o a la elongación del producto de transglicosidación, produciendo polisacáridos.

En el presente trabajo se pretenden sintetizar nuevos polisacáridos artificiales funcionalizados con estructuras definidas mediante el uso de la tecnología glicosintasa. Por un lado, se ha intentado aumentar la masa molecular de los polisacáridos utilizando un módulo de unión de carbohidratos (CBM). Este módulo podría mejorar la solubilidad de los nuevos polímeros a medida que se van sintetizando durante la reacción de polimerización. El efecto en el grado de polimerización ha sido estudiado tanto para el mutante glicosintasa en presencia de CBM como para la proteína de fusión glicosintasa-CBM. Por otro lado, se han sintetizado polisacáridos artificiales funcionalizados a partir de dadores disacarídicos activados donde la funcionalización deseada ha sido introducida previamente en la posición C-6'. Estos dadores funcionalizados actúan como sustrato para el mutante glicosintasa que catalizará la reacción de autocondensación. El grupo azido fue escogido por ser un grupo funcional adecuado dada su versatilidad y tamaño, suficientemente pequeño como para ser aceptado por el enzima. Los dadores fluoruro de 6'-azidolaminaribiosa y fluoruro de 6'-azidocelobiosa han sido sintetizados y evaluados como sustratos para las reacciones glicosintasa con el mutante E134S de la 1,3-1,4-β-glucanasa de *Bacillus licheniformis* y el mutante E197A de la celulasa de *Humicola insolens*, respectivamente.

Se han sintetizado 6-azido y 6-amino-6-deoxicelulosas artificiales con una secuencia de funcionalización alternada. De forma opuesta a la modificación química de celulosas donde la secuencia de sustitución es intrínsicamente aleatoria, la polimerización catalizada por glicosintasas de dadores glicosídicos modificados apropiadamente, permite acceder a nuevas celulosas funcionalizadas con secuencias de sustitución definidas y regulares.

SUMMARY

The glycosynthase technology has become a powerful enzymatic tool for the synthesis of oligosaccharides, polysaccharides and glycoconjugates. Glycosynthases are mutated glycosidases devoid of hydrolase activity but able to efficiently catalyze the formation of glycosidic bonds in high yields when using an activated glycosyl donor. In addition, the activated donor and its transglycosylation product, can both act as acceptors leading to the autocondensation of the donor or to the elongation of the transglycosylation product leading to polysaccharides.

The present work aims to synthesize novel artificial functionalized polysaccharides with defined structures by the use of the glycosynthase technology. On the one hand, an increase in the molecular weight of the polysaccharides is attempted by the use of a carbohydrate binding module (CBM). This module might improve the solubility of the new polymers that are synthesized during the polymerization reaction. The effect on the polymerization degree has been studied for both the glycosynthase mutant in the presence of CBM and for the fusion protein glycosynthase-CBM. On the other hand, functionalized artificial polysaccharides have been synthesized from activated disaccharidyl donors where the desired functionalization has been introduced at position C-6'. These functionalized donors act as a substrate for the glycosynthase mutant that will catalyze the autocondensation reaction. The azido group was chosen as a suitable functional group given its versatility and its size, small enough to be accepted by the enzyme. Donors 6'-azidolaminaribiosyl fluoride and 6'-azidocellobiosyl fluoride have been synthesized and evaluated as substrates for the glycosynthase reactions by the E134S 1,3-1,4-β-glucanase mutant and the E197A cellulase mutant from *Humicola insolens,* respectively.

Artificial 6-azido- and 6-amino-6-deoxicelluloses with an alternating functionalization pattern have been produced. As opposed to chemically modified celluloses where the substitution pattern is intrinsically random, the glycosynthase-catalyzed polymerization of properly modified glycosyl donors gives access to novel functionalized celluloses with defined and regular substitution patterns.

TABLE OF CONTENTS

LIST OF FIGURES

LIST OF TABLES

LIST OF ABBREVIATIONS

3D – Three dimensional

6-Tr – 6-*O*-Trityl

6'-Tr – 6'-*O*-Trityl

aa – amino acid

ACN – Acetonitrile

AcOH – Acetic acid

AGU – Anhydrous Glucose Unit

Ala – Alanine

Ap^r – Ampicillin resistant

aq – aqueous

arom – aromatic

Asp – Aspartate

B. licheniformis – *Bacillus licheniformis*

BARAC – Biarylazacyclooctynone

BCA – Bicinchoninic acid

BSE – Bovine Spongiform Encephalopathy

BTTES – 2-[4-{(bis[(1-tert-tert-butyl-1H-1,2,3,-triazol-4-yl)methyl}amino]methyl}-1H-1,2-3-triazol-1-yl)]-ethyl hydrogen sulfate

CAZy – Carbohydrate Active enZymes

CBM – Carbohydrate Binding Modules

CelF – β-D-Cellobiosyl fluoride

COSY – Correlation spectroscopy

CSA – (±)-10-Camphorsulfonic acid

CuAAC – Copper-catalyzed Azide - Alkyne Cycloaddition

Cy – Cyclohexane

d – doublet

DA – Degree of Acetylation

DBU – 1,8-Diazabicyclo[5.4.0]undec-7-ene

dd – doublet of doublets

ddd – doublet of doublet of doublets

DCM – Dichloromethane

Di – 6,6'-di-*O*-trityl

DIBO – Dibenzocyclooctyne

DIFO – Difluorinated cyclooctyne

Ditrityl – 6,6'-di-*O*-trityl

DNA – Deoxyribonucleic acid

DMAc – *N*,*N*-Dimethylacetamide

DMAP – 4-Dimethylaminopyridine

DMF – *N*,*N*-Dimethylformamide

DMSO – Dimethyl sulfoxide

DP – Degree of Polymerization

DS – Degree of Substitution

DXT – Dextran

E – Enzyme

ECM – Extracellular matrix

EGCase – Endoglycoceramidase

Em – Emission maximum

ENGase – Endo *N*-acetylglucosaminidase

eq – Equivalent

EtOAc – Ethyl acetate

Ex – Excitation maximum

Fc – Fragment, crystallizable

FTIR – Fourier transform infrared spectroscopy

Fuc – Fucose

GAG – Glycosaminoglycan

Gal – Galactose

GFP – Green Fluorescence Protein

Glc – Glucose

GlcNAc – *N*-Acetylglucosamine

GlcPNP – *p*-nitrophenyl β-D-glucopyranoside

Glu – Glutamate

GH – Glycosyl Hydrolase

GPC –Gel Permeation Chromatography

GS – Glycosynthase

HA – Hyaluronic acid

HPLC – High Performance Liquid Chromatography

HPSEC – High Performance Size Exclusion Chromatography

HSQC – Heteronuclear Single-Quantum Correlation Spectroscopy

IPTG – Isopropyl β-D-1-thiogalactopyranoside

L – β-D-Gal-(1→2)-α-D-Xyl-(1→6)-β-D-Glc (as a component of a xyloglucan oligosaccharide)

LB – Luria Bertani

LC/MS-TOF – Liquid Chromatography / Mass Selective– Time Of Flight

m – Multiplet

M – Mass

MALDI-TOF – Matrix-Assisted Laser Desorption/Ionization – Time Of Flight

Man – Mannose

MCC – Microcrystalline cellulose

MeOH – Methanol

Mesyl – Methanesulfonyl

M_n – Number average molecular mass

M_p – Molecular mass of the peak maximum

MS – Mass Spectrometry

M_w – Weight average molecular mass

MWCO – Molecular Weight Cut-Off

n – number of condensations

6'-N_3CelF – 6'-azido-6'-deoxy-β-D-cellobiosyl fluoride

N_3GlcPNP – *p*-nitrophenyl 6-azido-6-deoxy-2,3,4-tri-*O*-acetyl-β-D-glucopyranoside

NaAcO – Sodium acetate

NaOMe – Sodium methoxide

NBS – *N*-Bromosuccinimide

NIS – *N*-iodosuccinimide

NMR – Nuclear Magnetic Resonance

NOESY – Nuclear Overhauser Effect Spectroscopy

OMe – methoxy = methyl ether

P – Product

PDB – Protein Data Bank

PT – Proline – Threonine

PAMAM – Poly(amidoamine)

PDI – Polydispersity index

PMSF – Phenylmethylsulfonyl fluoride

***p*MP** – *p*-methoxyphenyl

***p*NP** – *p*-nitrophenyl

PSS – Polymer Standard Service

PPh_3 – Triphenylphosphine

Py – pyridine

RGD – Arginylglycylaspartic acid

RNA – Ribonucleic acid

RT – Room Temperature

S – substrate

s – singlet

SDS-PAGE – Sodium Dodecyl Sulfate-PoliAcrylamide Gel Electrophoresis

SEM – Scanning Electron Microscope

t – triplet

TALON – 50 mM Tris-HCl pH 8.0, 300 mM NaCl buffer

THF – Tetrahydrofuran

TLC – Thin Layer Chromatography

TMS – Trimethylsilyl

TMSOTF – Trimethylsilyl trifluoromethanesulfonate

Tosyl – *p*-toluenesulfonyl

TrCl – Trityl chloride

Triflate – Trifluoromethanesulfonate

Trityl – Triphenylmethyl

TsCl – Tosyl chloride

Tyr – Tyrosine

UV – Ultraviolet

VMD – Visual Molecular Dynamics

X – α-D-Xyl-(1→6)-β-D-Glc (isoprimeverose) (as a component of a xyloglucan oligosaccharide)

XLLG – xyloglucan-derived nonasaccharide

XXXG – xyloglucan-derived heptasaccharide

CHAPTER 1: LITERATURE REVIEW

1.1. CARBOHYDRATES AND GLYCOSCIENCE

Carbohydrates participate in almost every biological system and, in essence, life itself. They have multiple biological functions such as serving as energy sources for cells and living organisms, or as structural components of cell walls. Carbohydrates are part of the DNA and RNA molecules, furthermore they are mediators of cell-cell interactions, being central components in many important biological recognition processes such as cell adhesion and signaling, cancer progression, host-pathogen interactions, and immune responses.[1,2,3,4,5] Carbohydrates can be found as monosaccharides, oligosaccharides, polysaccharides or forming part of glycoconjugates (glycoproteins, glycolipids, glycosylated metabolites, etc). The biological processes in which carbohydrates are involved are typically associated to oligosaccharide structures of glycoconjugates and polysaccharides.

Glycoscience is an interdisciplinary field of research focused on the study of structures and functions of carbohydrates (glycans and glycoconjugates) and their relationship to other molecules in biological systems.[6] Glycobiology and glycochemistry are two main and usually intertwined subareas of glycoscience that study the structure, biosynthesis, and biology of glycans and their derivatives.[7]

Glycomics is part of analytical glycoscience and a subset of glycobiology. It consists on an emerging scientific discipline which studies the functions of glycomes (the set of glycans and glycoconjugates that the cells produce under specified conditions of space, time and environment) in biological systems.[7]

Glycomics focuses on glycans just as genomics is focused on nucleic acids and proteomics in proteins.[8] Each cell type has its own distinct glycome governed by local rules and cell's internal state.[7]

The glycome can be described at many hierarchical levels of complexity. The simplest level would be the deconstruction of glycome into an inventory of glycan structures. Next level would define which glycans are associated with individual proteins or lipids. A third level of complexity would determine which glycans or glycoconjugates are expressed on specific cells or tissues. Finally, the last and most complicated level would visualize how glycoconjugates are actually organized relative to each other within the cell, at the cell surface, and in the extracellular matrix.

Similar to the development in genomics and proteomics, high-throughput glycomics projects to decipher the role of carbohydrates in health and disease[9,10,11] and it is experiencing a rapid development as a result of advances in technologies for analyzing glycan structure, unraveling glycan-protein interactions and establishing the functional significance of glycans. Many aspects

of glycobiology will probably be understood with systems-level analysis by comparing data that define the glycome, genome, transcriptome and proteome of biological processes.

Glycobiology research has attracted increasing attention because glycosylation is the most complex and most frequently occurring post-translational modification in the biosynthesis of proteins with significant effects on protein folding, conformation, distribution, stability and activity.[12] During the glycosylation reaction a glycosyl donor is attached to an acceptor molecule (it can either be a glycosyl acceptor or another organic molecule such as a protein or a lipid) forming a glycosidic bond. This reaction works *via* the displacement of a leaving group on the donor with a free hydroxyl group from the acceptor.

Synthetic tools to access natural and non-natural glycosides and glycoconjugates have become a central issue in glycochemistry and glycobiology. Both for industrial applications in diverse fields such as medicine, pharma, food, cosmetics, etc, as well as in biological research in functional glycomic studies, there is the need for efficient synthetic approaches for structurally defined oligosaccharides and glycoconjugates. The development of efficient methodologies for the synthesis of oligo- and polysaccharides has been constantly explored and improved with the aim of studying biological activities and for its use as new biomaterials in biomedical applications. Polymers from natural sources are particularly useful as biomaterials given their similarity to the extracellular matrix and other polymers in the human body. Due to this biocompatibility they are nontoxic, relatively stable and degrade within the body as a result of natural biological processes, eliminating the need to remove them later. New natural-based biomedical polymers are interesting for applications such as implantable biomaterials, controlled-release carriers for local delivery of drugs, hormones, enzymes or growth factors. They can also be used as three dimensional scaffolds for tissue engineering or as polymer capsules in gene delivery systems, engineered to secrete a therapeutic agent for the therapy of a wide variety of diseases.[13]

The surfaces of these polymer-based biomaterials are chemically well-defined, have unique physicochemical properties and can be chemically modified to improve their functionality and suit specific needs.[14,15] Chemical synthesis is complicated due to the difficulty that results from trying to control the regioselective protection of polyhydroxyls by the use of suitable orthogonal protecting groups and anomeric stereoselective assembly of glycosidic linkages. This involves protection and deprotection steps, resulting in multi-step reactions with typically a low overall yield.[16]

In nature, enzymes are responsible of the synthesis of glycosidic bonds. Enzymatic synthesis, without the need of protecting groups, is characterized by a high catalytic activity, lack of undesirable side-reactions, mild reaction conditions, and high regio- and stereoselectivity.[17]

1.2. GLYCOSIDIC BOND FORMATION

There are two main carbohydrate active enzymes in nature involved in the synthesis of glycosidic bonds: glycosyltransferases and transglycosidases.

1.2.1. Glycosyltransferases

Glycosyltransferases catalyze the transfer of a sugar moiety from an activated glycosyl donor (nucleoside phosphate, phosphate, or lipid phosphate groups) to an acceptor forming a glycosidic bond. They have been widely studied and have been classified into more than 90 families (CAZymes, www.cazy.org).[18] When glycosyltransferases accept nucleotides as glycoside donors, the enzymes are termed Leloir glycosyltransferases, whereas if they accept non-nucleotide donors (sugar phosphates) then are termed non-Leloir glycosyltransferases.

Leloir glycosyltransferases have a high degree of specificity, many of them catalyzing the formation of a unique linkage. However, this type of glycosyltransferases are often membrane-bound proteins, present in low concentrations, difficult to isolate and purify, and unstable once they are isolated. These enzymes are also produced by recombinant technology but to date few commercial glycosyltransferases are available at high prices. In the case of Leloir glycosyltransferases which are extremely regio- and stereoselective, the need of glycosylated donors activated with nucleotides increases the already high cost of the reaction.[19]

Two main stereochemical outcomes exist for glycosyltransferases: *inverting* glycosyltransferases involve an inversion of the anomeric configuration of the carbohydrate while a retention of the anomeric configuration is observed with *retaining* glycosyltransferases (Figure 1. 1).

The mechanism of the inverting reaction is widely accepted and is mechanistically straightforward; the acceptor hydroxyl acts as a nucleophile and approaches the anomeric carbon from the opposite side to the donor-nucleoside linkage eventually resulting in inversion of anomeric stereochemistry as the nucleoside leaves (direct displacement S_N2-like reaction). On the contrary, the mechanism for retaining glycosyl transfer stereospecificity has been for a long time a matter of debate. They were broadly classified as proceeding with primarily dissociative (S_N1) or primarily associative (S_N2) character. The analysis of the structures, together with literature data from NMR, MS, kinetics, and computational studies, point to the orthogonal mechanism for retaining glycosyltransferases as both the simplest and the most consistent with the available data. The term ‘‘orthogonal’’ refers to a process involving the nucleophile and the leaving group on the same side (“front-side’’ attack) where the approach of the nucleophile is approximately orthogonal to the breaking bond axis, and proceeding in a single step from reactants to products without an intermediate.[20,21]

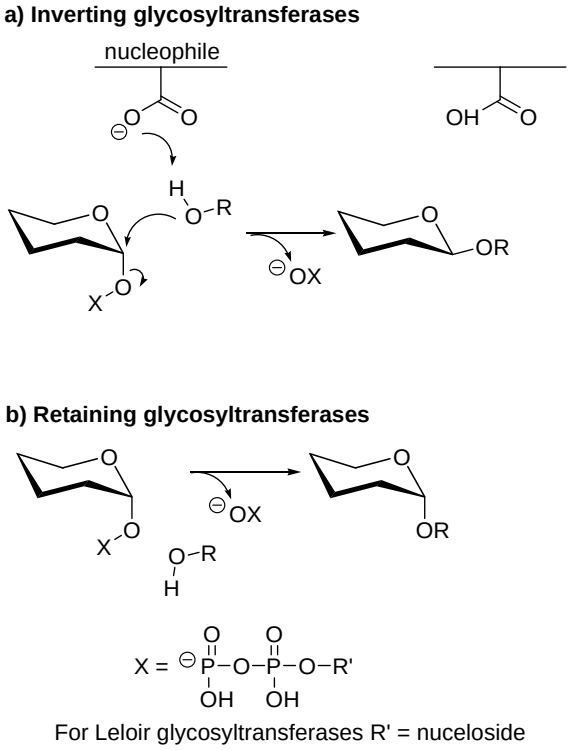

Figure 1. 1. Reaction mechanisms of inverting (A) and retaining (B) glycosyltransferases. R is an acceptor sugar molecule.

Phosphorylases, catalyze the phosphorolysis of polysaccharides. The reaction is reversible and these enzymes are also able to form glycosidic linkages using glycosyl phosphates as donors (Figure 1. 2).

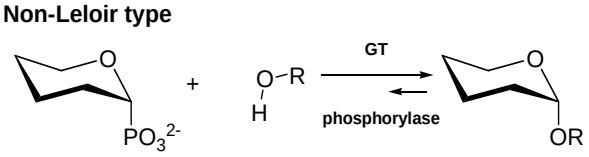

Figure 1. 2. Polysaccharide biosynthesis by a phosphorylase.

Phosphorylases are classified as members of glycosyl hydrolases families or glycosyltransferase families (CAZy). Like glycosyltransferases and glycosidases, phosphorylases can act with retention or inversion of configuration (Figure 1. 3).

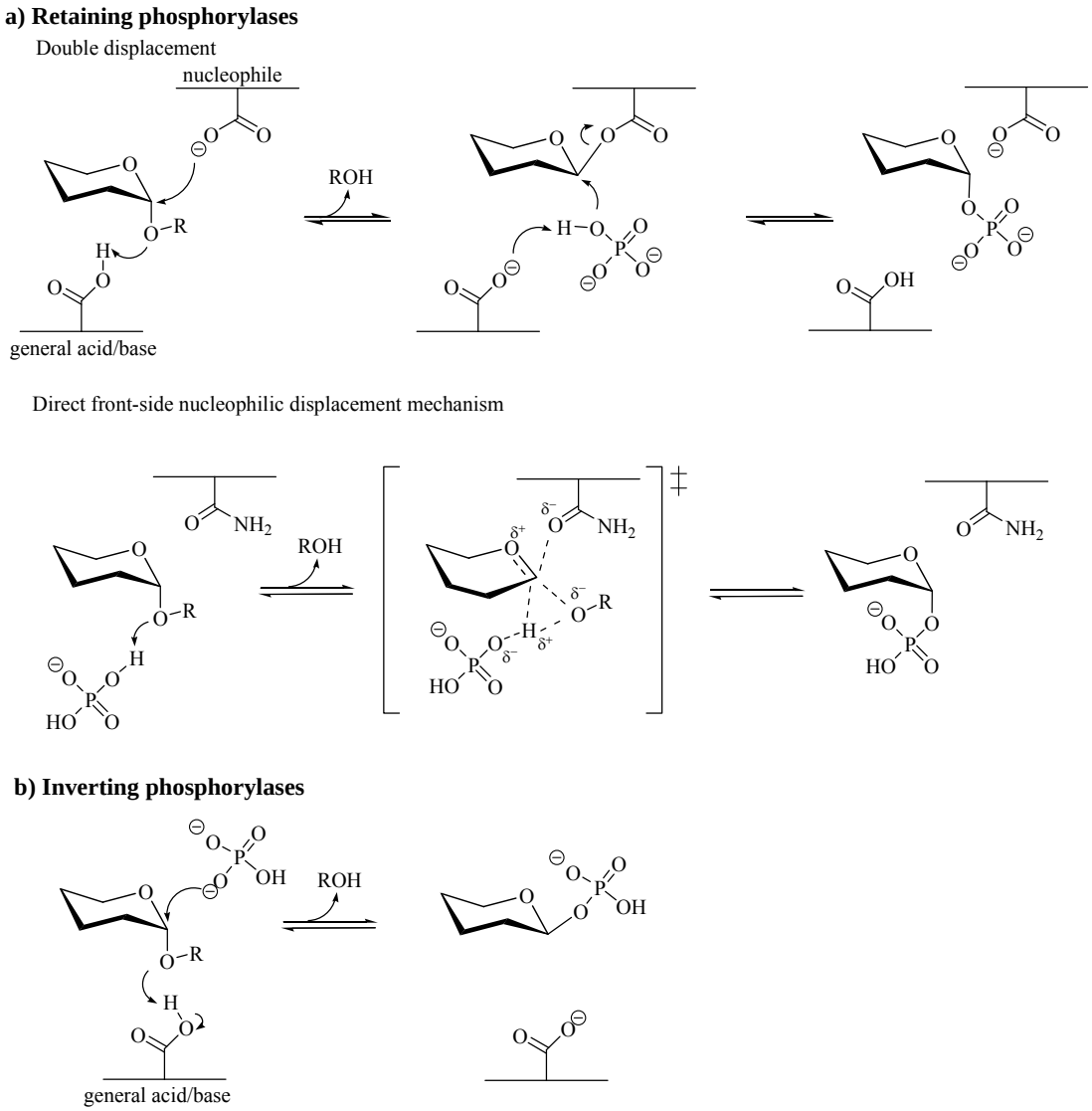

Figure 1. 3. Reaction mechanisms of phosphorylases: a) retaining phosphorylases, b) inverting phosphorylases.

Phosphorylases can be used for oligosaccharide synthesis *via* the reverse reaction (Figure 1. 4). Inverting glycosidases are highly regiospecific and *O*-glycosidic oligosaccharides are typically obtained with high regioisomeric purity.[22,23] The strict recognition of specific sugar 1-phosphate excludes substitution and modification of donor substrates, therefore, molecular design of novel phosphorylases is needed to obtain phosphorylases with altered donor specificity.[24,25] Sugar 1-fluoride proved to be an alternative to the donor sugar 1-phosphate making the reaction irreversible as no phosphate is released which can act as a general base catalyst in phosphorolysis of the obtained oligosaccharide product.

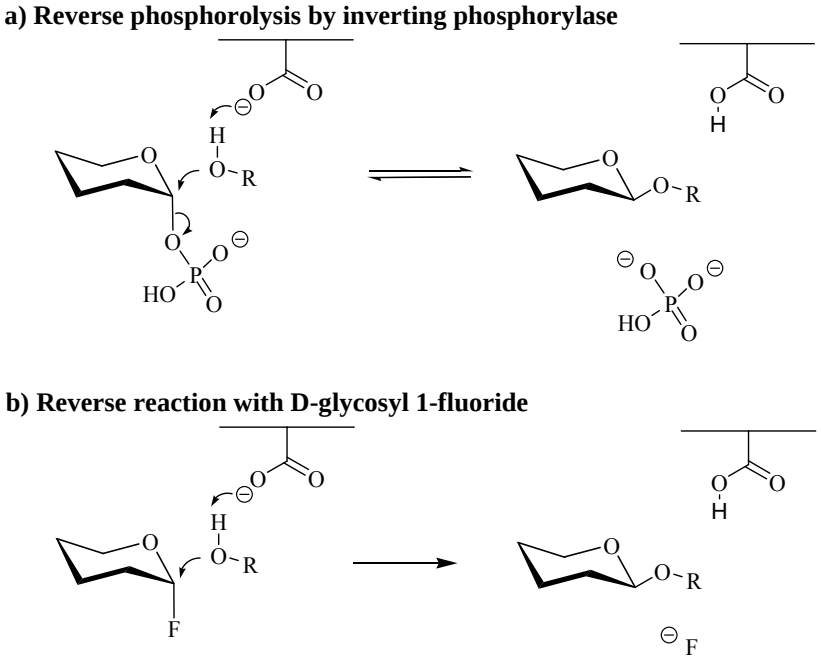

Figure 1. 4. Oligosaccharide synthesis *via* reverse reaction of inverting phosphorylases.

The number of existing phosphorylases is still low and therefore there are a few studies of these type of enzymes.[7] However, new phosphorylases have been discovered lately spreading the tools for oligosaccharide synthesis.[26]

1.2.2. Glycosidases

Glycosyl hydrolases or glycosidases are degrading enzymes that catalyze the stereospecific hydrolysis of a glycosidic bond in oligosaccharides, polysaccharides or glycoconjugates. Their hydrolytic activity is reversible under appropriate conditions and they can catalyze the synthesis of glycosides through transglycosylation reactions under appropriate conditions. Glycosyl hydrolases are a widespread group of carbohydrate active enzymes, with more than 130 families based on amino acid sequence similarities.[27] They are easy to produce, very stable and the required glycosyl donors are cheap and relatively easy to produce in large scale.

1.2.2.1. Endo/Exo glycosidases

Glycosidases can be classified in *exo*- or *endo*-enzymes depending on the position of the hydrolyzed glycosidic bond in the substrate chain. *Exo*-glycosidases remove a monosaccharide (or disaccharide) from one of the ends of the chain (most commonly from the non-reducing end), whereas *endo*-glycosidases act on internal glycoside bonds within the oligosaccharide chain (either randomly or processively). This regiospecificity for bond cleavage is a consequence of the active site topology. The carbohydrate binding site structure is reduced to three basic

topologies (Figure 1. 5): pocket, encountered in *exo*-glycosidases and optimal for recognition of a saccharide on the chain end; cleft, where an open grove structure allows binding of several sugar units in polymeric substrates and is commonly found in *endo*-acting enzymes; and tunnel, derived from the cleft topology with long loops that cover part of the cleft, as those found in cellobiohydrolases, where the resulting tunnel enables a polysaccharide chain to be theaded through it.[28]

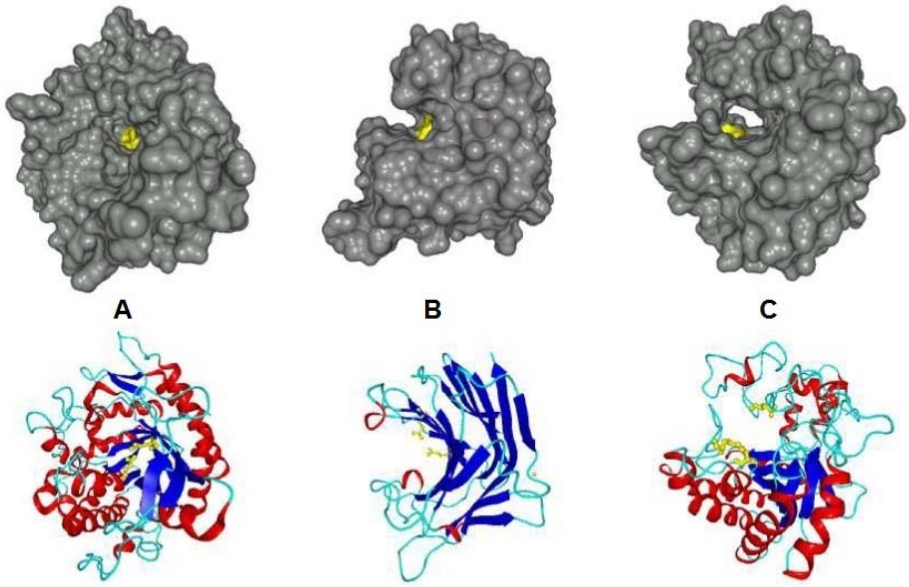

Figure 1. 5. The three different active sites found in glycosidases. At the upper side of the image, the molecular surface diagrams can be observed while at the lower side there are the secondary structure of the same proteins. Catalytic residues can be distinguished in yellow. A. The pocket (β-glucosidase from *Thermus thermophilus* HB8). B. The cleft (1,3-1,4-β-glucanase from *Bacillus licheniformis*).[29] C. The tunnel (*endo*-glucanase Cel6 from *Mycobacterium tuberculosis*).[30]

1.2.2.2. Retaining/Inverting glycosidases

Glycosyl hydrolases operate by general acid-base catalysis involving Asp, Glu or Tyr as catalytic residues, but differ in their mechanisms as a consequence of their active site topology.[31,32,33,34] Depending on their catalytic mechanism, glycosidases can act with retention or inversion of anomeric configuration.

For retaining glycosidases, the hydrolysis of the glycosidic bond is normally catalyzed by two amino acid residues of the enzyme: a general acid residue acting as a proton donor and a general base which acts as a nucleophile. A third catalytic residue is often involved in the modulation of the pK_a of the acid/base residues. Retaining glycosidases follow a double-displacement reaction *via* formation and hydrolysis of a glycosyl-enzyme intermediate, and have the catalytic residues

closer to each other at *c.a.* 5.5 Å (Figure 1. 6a). In the first step (glycosylation) the amino acid residue acting as a general acid protonates the glycosidic oxygen while the deprotonated carboxylate functioning as a nucleophile attacks the anomeric center with concomitant C-O breaking of the scissile glycosidic bond leading to a covalent glycosyl-enzyme intermediate. The second deglycosylation step involves the attack by a molecule of water assisted by the conjugate base of the general acid residue which renders the free sugar with overall retention of configuration, and the enzyme returns to its initial protonation state.[28]

Some retaining glycosidases catalyzing glycoside bond hydrolysis in 2-acetamido sugars (*i.e.* GH18 chitinases, GH20 hexosaminidases, GH52 hyaluronidases, and GH85, *endo*-β-acetylglucosaminidases) follow a variation of the retaining mechanism (Figure 1. 6b); they lack the enzyme's catalytic nucleophile and operate by substrate-assisted catalysis, where the *N*-acetyl group of the susbtrate acts as internal nucleophile forming an oxazolinium intermediate, which is then attacked by a water molecule assisted by the conjugate base of the general acid residue to yield the product with net retention of the anomeric configuration.[35] In this case, an auxiliary residue that hydrogen bonds with the NH- of the acetamido group assists the formation of the oxazolinium intermediate.

By contrast, inverting glycosidases operate by a single-step mechanism in which a water molecule (with general base catalysis) effects a direct displacement at the anomeric center with protonic assistance by the general acid residue on the departing glycosidic oxygen. The catalytic residues are located at approximately 10 Å apart to each other allowing binding of the substrate and a water molecule in a ternary productive complex (Figure 1. 6c).[34]

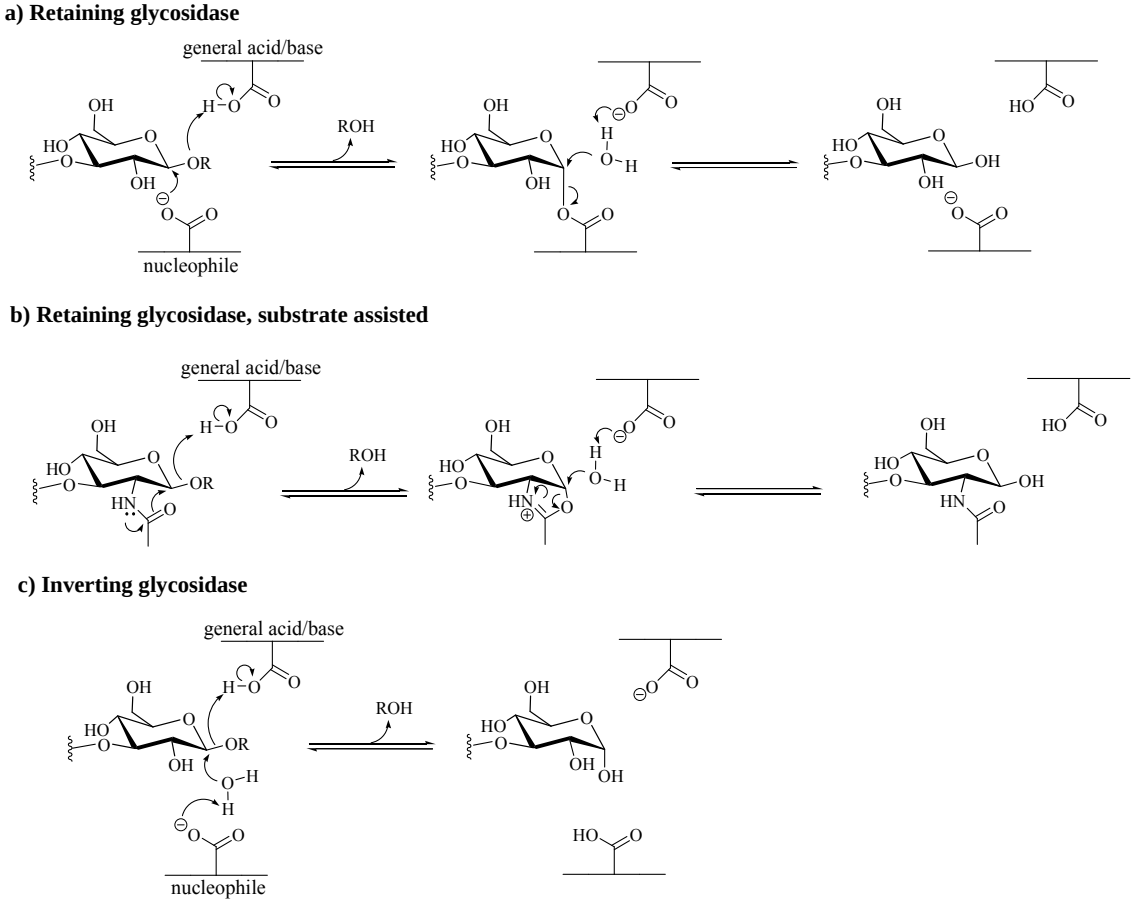

Figure 1. 6. Glycosidase mechanism: a) retaining glycosidase with enzyme nucleophile, *via* a glycosyl-enzyme intermediate in the two-step displacement mechanism, b) retaining glycosidase by substrate-assisted catalysis, *via* an oxazolonium ion intermediate. c) inverting glycosidase.

1.2.2.3. Glycosidases as synthetic tools

Retaining glycosidases are employed as biocatalysts in the preparation of diverse oligosaccharides and glycoconjugates. Classical approaches with wild type retaining glycosidases are based on reversal of their hydrolytic action. This is achieved either by displacing the equilibrium towards glycoside bond formation (thermodynamically controlled synthesis) or by using activated glycosyl donors (kinetically controlled transglycosylation).

Thermodynamically controlled reverse hydrolysis involves the shift of the equilibrium towards products by altering the reaction conditions minimizing the water activity in the reaction by adding water-miscible organic co-solvents (Figure 1. 7). The hydrolysis-synthesis equilibrium is balanced by approximately 4 kcal·mol^{-1} towards bond cleavage under aqueous conditions. Reactions at higher temperatures and the use of higher substrate concentrations also favor the transfer to the acceptor molecule and have proved to increase the synthetic yields. Reverse hydrolysis in nonaqueous solutions are not generally useful since the sugar substrates become insoluble. Most of the reported examples by the thermodynamic approach are for the preparation

of simple glycosides (mainly disaccharides) or glycosides of hydrophilic alcohols using *exo*-glycosidases.[36,37]

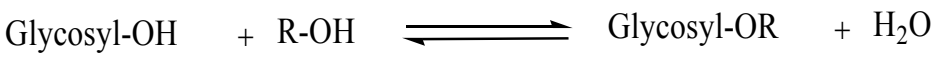

Figure 1. 7. Thermodynamically controlled reverse hydrolysis where R = sugar nucleophile or hydroxylated compound.

Kinetic control (transglycosylation) involves a more rapid trapping of the glycosyl-enzyme intermediate by a glycosyl acceptor acting as a nucleophile rather than by water. This approach relies on the fast formation of the reactive intermediate from a donor substrate with a good leaving group such as an aryl glycoside or a glycosyl fluoride. Under appropriate conditions, a nucleophilic acceptor other than water can intercept the glycosyl-enzyme intermediate and form a new glycosidic bond (transglycosylation product) with the same anomeric configuration in the product than in the glycosyl donor (overall retaining reaction). Although glycoside bond formation may be favored kinetically, hydrolysis always remains favored thermodynamically, because the product itself is a substrate for the enzyme, and the equilibrium is slowly shifted towards hydrolysis. The competing hydrolysis over transglycosylation is often referred as two processes: primary hydrolysis, meaning the hydrolysis of the glycosyl-enzyme intermediate (water attack in the deglycosylation step), and secondary hydrolysis, meaning hydrolysis of the transglycosylation product that is a substrate for the hydrolase activity of the enzyme (Figure 1.8 A). In the case of retaining glycosyl hydrolases (GH) acting by substrate-assisted catalysis (Figure 1.8. B) wild-type enzymes are also able to catalyze kinetically controlled transglycosylation using a -GlcNAc-sugar substrate or preferable, activated sugar oxazolines as glycosyl donors which bind to the enzyme to form directly the reaction intermediate.

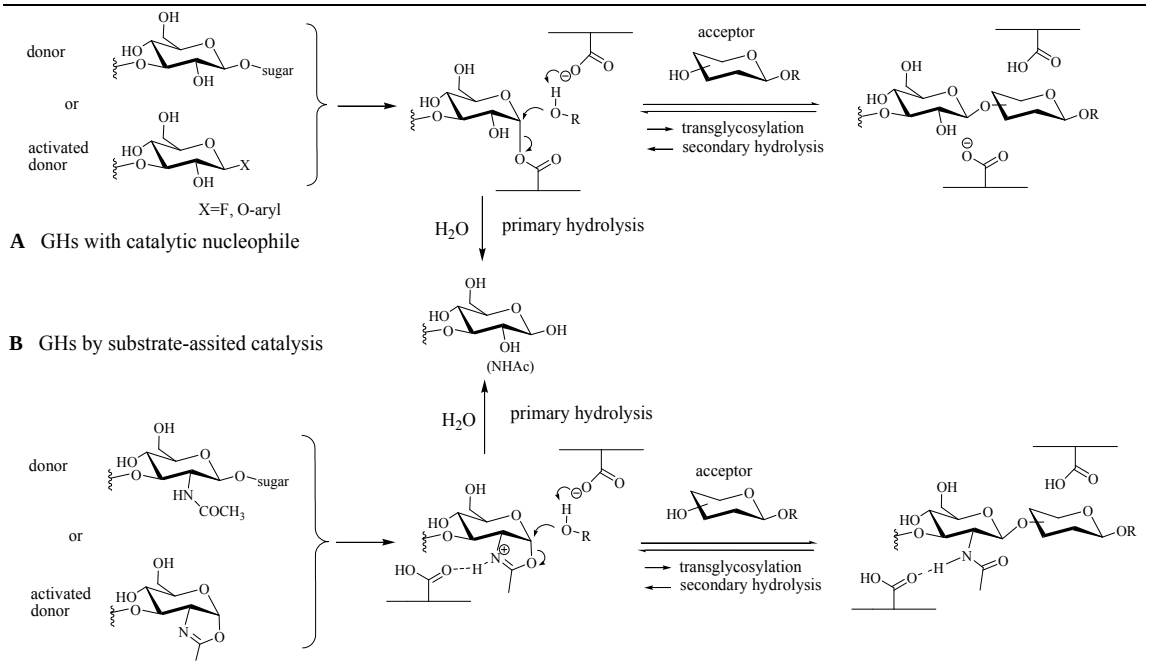

Figure 1. 8. Transglycosylation reactions catalyzed by retaining glycosidases. A. Glycosidases with catalytic nucleophile. B. Glycosidases operating by substrate-assisted catalysis.

Some other strategies were designed to maintain the displacement towards transglycosylation and avoid hydrolysis such as removal of the transglycosylation product from the reaction mixture, immobilization of the enzyme allowing re-use of the enzyme or the use of lipid-coated glycosidases which are stable in organic solvents and active in organic media and insoluble in buffer solutions.[38]

In 1991, Kobayashi produced in vitro artificial cellulose by using a cellulase to catalyze the polycondensation of β-cellobiosyl fluoride in acetonitrile/acetate buffer.[39] When a crude cellulase (mixture of enzymes) was used, the morphology of the obtained product consisted in the stable cellulose II allomorph with anti-parallel-chain packing. However, metastable crystalline cellulose I with parallel chain packing was obtained when using purified cellulases. In 2001, Kobayashi demonstrated that the relative intermolecular direction of growing glucan chains was controlled in the propagating process of enzymatic polymerization.[40,41] Therefore, it supposed a new method for the preparation of new higher-order molecular assemblies.

Other oligo- and polysaccharides such as maltooligosaccharides,[42] xylan,[42] chitin,[43] an hybrid cellulose-xylan[44] or mixed linked β-1,3 and β-1,4 glucans[45] were synthesized by enzymatic transglycosylation using different glycosidases, substrates and strategies. In all these cases, enzymes used glycosyl fluoride donors and the degrees of polymerization of the produced polysaccharides did not exceed 10 – 30 monosaccharide units.[17] Final yields rarely exceeded 50%

since the products become substrates of the enzyme since hydrolysis always remains favored thermodynamically and the equilibrium is slowly displaced.

Larger polysaccharides with higher DPs (6 – 80) which depended on the reaction conditions were synthesized by substrate-assisted catalysis. Homopolysaccharides such as chitin, chitosan and derivatives (chitanases derivatives in which C-2^{II} was functionalized with hydroxyl, amino or sulfonamide, C-3 was functionalized with a methyl group or C-6 was functionalized with carboxylate and fluorine groups) and heteropolysaccharides such as hybrids chitin-chitosan, cellulose-chitin, chitin-*N*-sulfonated chitosan. Hyaluran and chondroitin derivatives with different *N*-acyl groups and even a hybrid hyaluronic-chondroitin polysaccharide were successfully produced.[17]

1.3. Glycosynthases

In 1998, Withers and co-workers[46] engineered the first *exo*-glycosynthase, mutant of an *exo*-glycosidase, while Planas and co-workers[47] introduced the glycosynthase concept for *endo*-glycosidases. The new technology was developed to avoid the hydrolysis of the transglycosylation products by mutating the nucleophilic residue of the glycosidase, replacing it by an inert amino acid residue while using substrates such as glycosyl fluorides, with the opposite anomeric configuration to that of the natural substrate imitating the intermediate glycosyl-enzyme. In a one-step inverting mechanism, the remaining catalytic residue acts as a base to deprotonate the acceptor, activating it as a nucleophile that will attack the glucosyl donor in the active site creating the new glycosidic bond (Figure 1.9. A).

Most glycosynthases are derived from retaining glycosidases. 17 retaining glycosyl hydrolases, both *exo*- and *endoglycosidases*, have been converted into glycosynthases. *Endo*-glycosynthases typically exhibit high substrate specificity and regioselectivity and their products have higher degree of polymerization than *exo*-glycosynthases which are less regio- and stereoselective and produce shorter oligosaccharides.[48]

1.3.1. Activated substrates for glycosynthases

Most *endo*- and *exo*-glycosynthases use α-glycosyl fluorides as activated donors which imitate the glycosyl-enzyme intermediate synthesizing β-linkages (Figure 1. 9A). Some of the already known *endo*-glycosynthases (families GH 18 and GH 85) use activated oxazoline glycans as donors for the transglycosylation of 2-acetamido-β-glycans (Figure 1.9. B).[49,50,51,52,53] A few *exo*-glycosynthases from α-glycosidases can use a azido donor as an activated substrate synthesizing α-linkages instead of β-glycosyl fluorides because of their higher stability (Figure 1.9. C).[54] These glycosynthases were engineered with the objective of synthesizing α-L-fucosylated

oligosaccharides, molecules that exhibit prebiotic properties on cultured infant microbiota and might have potential application in biomedicine. α-glycosynthases were prepared from the GH29 α-L-fucosidases from *S. solfataricus* (Ssa-fuc) and *Thermotoga maritima*, and from the GH36 α-galactosidase from *T. maritima.*[55]

A) Retaining glycosynthases (from *exo*- and *endo*-glycosidases)

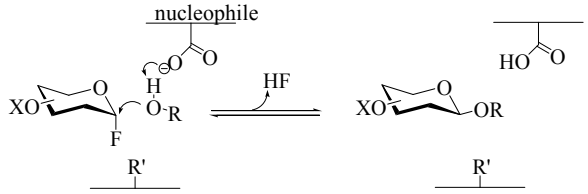

B) Retaining glycosynthase (from *endo*-glycosidases), substrate assisted

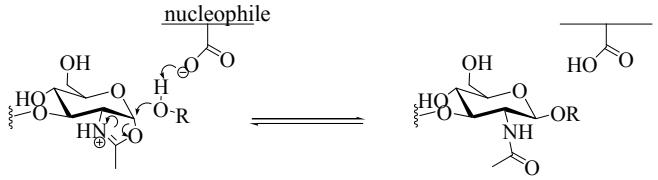

C) *Exo*-glycosynthases from retaining glycosidases (azido donor)

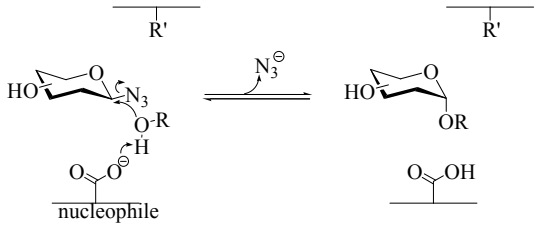

D) *Exo*-glycosynthases from retaining glycosidases (formate rescue)

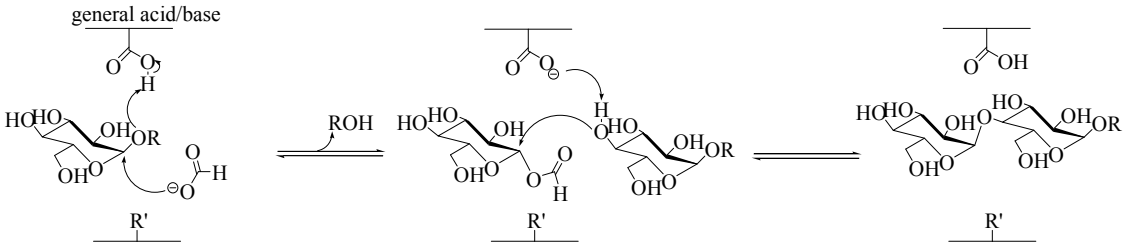

E) Inverting glycosynthase

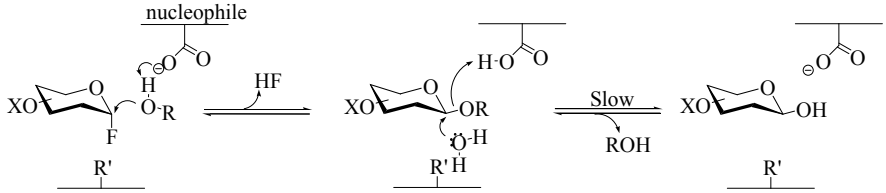

Figure 1. 9. Glycosynthase enzymes: a) nucleophile mutant of a retaining glycosidase with glycosyl fluoride donor, b) mutant at the assisting residue of a retaining glycosidase acting by substrate-assisted catalysis and a sugar oxazoline donor, c) nucleophile mutant of a retaining *exo*-glycosidase (thermophilic) with an azido donor, d) nucleophile mutant of a retaining glycosidase (thermophilic) with *in situ* generation of the glycosyl donor and exogenous nucleophile, e) glycosynthase-like mutant derived from an inverting glycosidase (general base mutant of an inverting β-glycosidase in the example).

The conventional glycosyl fluoride donor is unstable at high temperatures, therefore, some retaining glycosynthases from hyperthermophile *exo*-glycosidases, use formate/formic acid buffer as an external nucleophile to rescue the active site of the enzyme (Figure 1.9. D)[56,57,58]. The mutant E387G of GH1 *exo*-β-glycosidase from *Sulfolobus solfataricus* (Ssb-gly) functioned as glycosynthase by formate rescue of the substrate.[57]

In 2006, the first glycosynthase-like enzyme from an inverting glycosidase was engineered by mutating the nucleophilic catalytic residue and using an activated donor with the same anomeric configuration as the normal hydrolysis product. As inverting glycosidases operate by a single displacement mechanism, enzyme engineering for glycosynthesis in this case is based on a similar but slightly different concept. However, the normal hydrolytic process is substantially slowed but still significant[59]. An alternative approach was proposed by Honda et al 2008 by mutating a neighboring residue that holds the nucleophilic water molecule that interacts with the general base while keeping the general base residue intact (Figure 1.9. E) [60]. Higher transglycosylation yields where obtained because of the reduced hydrolysis. Since then, three more glycosynthases–like enzymes derived from three different families of inverting glycosidases have been reported.[61,62,63]

1.3.2. Synthesis of glycoconjugates and glycans

1.3.2.1. Glycoconjugates

Glycolipids and glycoproteins

Several *endo*-glycosynthases have been engineered lately using them in glycolipid and glycoprotein formation for a better understanding of their biological function avoiding the complex chemical synthesis.

The synthesis of the neurogenic ganglioside LLG-3 from *Linckia laevigata*, a tetrasaccharide present in starfish, was recently performed chemoenzymatically in high yields and with high regio- and stereospecificity in a minimum of synthetic steps by Rich and Withers[64] for the study of the influence of subtle structural alterations on the function of GSLs. The glycosynthase from *endo*-glycoceramidase II (EGCase) from *Rhodococcus sp*. transferred oligosaccharide fluorides to a diverse set of sphingolipids with transglycosylation yields over 70%.[65]

Since 2008, glycosynthases have been used to modify *N*-glycosylation sites making possible the preparation of homogeneous glycoforms for the study of the structural and functional roles of the attached glycans.[49] The glycoprotein of study has to be first hydrolyzed by the use of an *endo*-β-*N*-acetylglucosaminidase (ENGase) in order to remove its native glycans, only leaving the terminal GlcNAc residue. Then, an ENGase glycosynthase mutant is responsible of transferring

the oxazoline derivative of a homogenous *N*-glycan to the protein. Five mutants from ENGases have been reported so far: *Endo*-M, *Endo*-A, *Endo*-D, *Endo*-S and the new *Endo*-F3.

The mutant *Endo*-M from *Mucor hiemalis* transfers complex type *N*-glycans onto a synthetic peptide Saposin C58 on a five nanomole scale with a yield of 64%. *Endo*-A glycosynthase from *Arthrobacter protophormiae* was used to couple $Man_9GlcNAc$ and $Gal_1Glc_1Man_9GlcNAc$ to Ribonuclease B with yields over 78% producing 0.5 – 1.3 mg of glycoprotein. *Endo*-D from *Streptococcus pneumoniae* has a strict substrate specificity and it partially (because of the substrate specificity) catalyzes the transfer of Man3-GlcNAc oxazoline onto IgG-Fc. *Endo*-S from *Streptococcus pyogenes* removes the heterogeneous *N*-glycan from the Fc domain of the therapeutic antibody rituximab, leaving either the Fucα1,6-GlcNAc core or a single GlcNAc residue after treatment with a fucosidase. They then transferred the derivative oxazoline from a fully sialylated *N*-glycan or an azido-tagged glycoform onto the fucosylated protein quantitatively, and an asialylated *N*-glycan on to the nonfucosylated protein quantitatively, as well. The homogeneous nonfucosylated G2 glycoform displayed an increase in rituximab receptor affinity, which should translate to better activity in vitro.

Recently, several mutants of the *endo*-β-*N*-acetylglucosaminidase from *Elizabethkingia meningosepticum*, *Endo*-F3[66] were recently developed by site-directed mutagenesis. They transferred complex *N*-glycans to GlcNAc-peptide/protein. Unlike the other four ENGase glycosynthases, *Endo*-F3 was able to use triantennary glycan oxazolines as substrates for transglycosylation. Giddens et al synthesized CD52 antigen and efficiently remodeled Fc glycosylation of monoclonal antibody rituximab. This chemoenzymatic approach also provided an efficient synthesis of core fucosylated bi- and tri-antennary glycopeptides.

Glycosaminoglycans

Glycosaminoglycans (GAGs) are long unbranched polysaccharides composed of repeating disaccharide units which combine one uronic acid and one hexosamine (D-glucosamine or D-galactosamine). At least one of the monosaccharidic units contains a minimum of one sulfate or carboxylate group negatively charged. GAGs are located primarily on the surface of cells or in the extracellular matrix (ECM). Along with the high viscosity of GAGs comes low compressibility, which makes these molecules ideal for a lubricating fluid in the joints. At the same time, their rigidity provides structural integrity to cells and provides passageways between cells, allowing for cell migration. Apart from their structural importance to the integrity of the ECM, GAGs are also fundamental modulators of various biological processes at the level of cells (*i.e.,* adhesion, signaling and proliferation), tissue (*i.e.,* inflammation, wound repair, tissue morphogenesis and organogenesis) and organism (*i.e.,* cancer and developmental processes).[67]

The majority of GAGs in the body are linked to core proteins, forming proteoglycans (also called mucopolysaccharides).[68]

Traditionally, GAGs were obtained from mammalian tissues mainly generated in slaughterhouse but as a consequence of the concern due to the bovine spongiform encephalopathy (BSE) and other food chain crisis, the exploration of microorganism and marine organisms as source of those glycoconjugates or the synthetic preparations have received increasing attention.[69,70] Nevertheless, chemical synthesis of these polymers is particularly challenging and the use of enzymes recently showed remarkable successes.[71]

The glycosynthase derived from the β-glucuronidase from *Thermotoga maritima* (GH2) was able to transfer both glucuronic and galacturonic acid residues, main components of different GAGs.[72] This β-glucuronylsynthase recognized a great variety of acceptors (xylosides, glucosides, glucuronides, and disaccharide derivatives) and it was highly regiospecific producing in all cases β-(1,3) linkages with yields up to 83%. This *exo*-glycosynthase provided a promising way to synthesize GAG building blocks. However, it could not synthesize products longer than DP = 4 with yields not higher than 10%.

1.3.2.2. Glycans

Glycan inhibitors

Glycosynthases allow to produce a family of oligomeric products when searching for enzyme inhibitors. Goddard-Borger and co-workers[73] studied the production of xylanase inhibitors with a glycosynthase mutant from GH52 β-xylosidase from *Bacillus halodurans.* An α-xylosyl fluoride was used as a donor and several different inhibitory monosaccharides as acceptors creating inhibitors with different degrees of polymerization varying from 1 to 3. The produced trisaccharides were much more potent competitive inhibitors than their disaccharide counterparts.

Polymers

The use of glycosynthases increases the reaction yields if compared to transglycosylation yields of wild-type enzymes. One of the principal uses of glycosynthases is their use in the synthesis of polysaccharides by self-condensation of a glycosyl fluoride substrate that serves at the same time as donor and acceptor. This enzymatic polymerization is mainly catalyzed by *endo*-glycosynthases due to their extended active site which can accept larger complex oligosaccharides producing polysaccharides with high degrees of polymerization.

Eleven *endo*-glycosynthases out of the nineteen current *endo*-glycosynthases which use glycosyl fluorides as substrates have been able to polymerize their corresponding glycosyl donor.

Furthermore, there is one *exo*-glycosynthase from a retaining GH1 β-glycosidase from *Oryza sativa* and an *endo*-glycosynthase from an inverting GH19 β-glycosidase from *Bryum coronatum* able to autocondensate glycosyl fluoride donors as well. These polysaccharides have a higher degree of polymerization than the ones obtained with wild-type glycosidases under kinetic transglycosylation.

1.3.3. Glycosynthase-catalyzed synthesis of artificial polysaccharides

The glycosynthase reaction proved to be able to produce artificial polysaccharides by the use of E134 mutants of 1,3-1,4-β–glucanase from *Bacillus licheniformis.*[74] Other complex and homogenous glycopolymers using structurally diverse polysaccharides as acceptors have been produced as well by the use of other *endo*-xyloglycosynthases.[75,76]

Biologically relevant polymers like cellulose (E197 mutants of cellulose Cel7B from *Humicola insolens*), chitin, xylan (glycine mutants of several xylanases),[77] curdlan (E231 mutants of β-(1→3)-glucanase from barley) and functionalized derivatives have been synthesized with DP up to 30. Only few examples have yet been reported, but this is an emerging field for the preparation of new biomaterials with defined structures that either mimic natural polysaccharides or have unnatural structures and functionalities.

1) Mixed-linked β-glucans

It was shown in our laboratory that the *endo*-glycosynthase from *Bacillus licheniformis* β-1,3-1,4-β-glucanase catalyzed the polymerization of glycosyl fluoride donors (Glcβ4)nGlcβ3GlcαF (n = 0 – 2) leading to artificial mixed-linked β-glucans with regular sequences and variable β-1,3 to β-1,4 linkage ratios (Figure 1. 10).[78,74] With the E134A glycosynthase mutant, polymers had average molecular masses (M_w) of 10-15 kDa, and the morphology of the water-insoluble polysaccharides was dependent on the repeating unit. With the more active E134S glycosynthase mutant, polymerization led to high molecular mass polysaccharides, where Mw was linearly dependent on enzyme concentration. Remarkably, a homo-polysaccharide [4Glcβ4Glcβ4Glcβ3Glc]n with M_w as high as 30 kDa (n ≈ 42) was obtained, which contained a small fraction of products up to 70 kDa, a value that is in the range of the molecular masses of low viscosity cereal 1,3-1,4-β-glucans, and among the largest products produced by a glycosynthase.[78] It was demonstrated that the polysaccharide morphology depended on the β-1,3-linkage ratio content. Highly porous spherulitic crystalline polysaccharides composed of platelets were obtained when the disaccharide and tetrasaccharide fluoride donors n = 0, 2 were used as substrates whereas an amorphous precipitate was obtained after self-condensation of the trisaccharyl fluoride n = 1.[78]

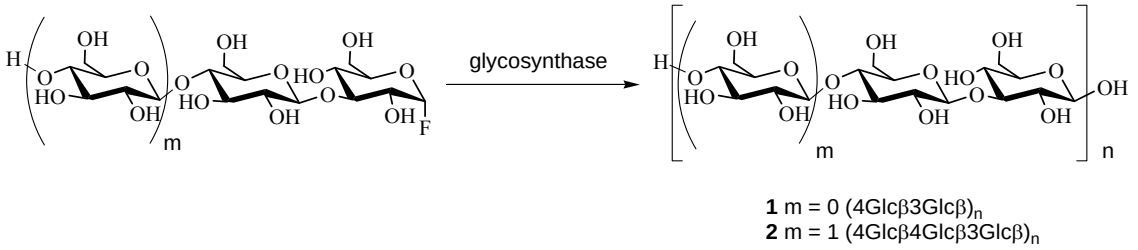

Figure 1. 10. Glycosynthase-catalyzed polymerization to produce β-1,3-1,4 mixed-linked glucans.

2) Cellulose

The E197A mutant of *endo*-cellulase Cel7B from *Humicola insolens* was shown to polymerize α-cellobiosyl fluoride to produce an insoluble crystalline β-1,4-glucan that was consistent with low molecular mass cellulose II.[79] This enzyme was able to polymerize, as well, cellobiosyl fluorides modified at the C-6^{II} position with amino, bromide or thioglycosyl functional groups generating functionalized polysaccharides. These chemical functionalities opened up possibilities to later modify and graft the polysaccharides with other biomolecules. The degree of polymerization of the generated polysaccharides was rather low (DP≈30) due to product insolubility.

3) β-1,3-curdlan

Crystalline β-1,3-linked polysaccharides were synthesized by the use of a glycosynthase derived from a barley β-1,3-glucan *endo*-hydrolase. The solid products from the polymerization of laminaribiosyl fluoride by the E231G glycosynthase mutant obtained with a DP of 30 were structurally similar in all respects to the recrystallized *β*-1,3-curdlan. Interestingly, 3-thiolaminaribiosyl fluoride (a *β*-1,3-S-linked disaccharide) was a suitable substrate for the glycosynthase and oligosaccharides with alternating *S*- and *O*-linkages between the sugar residues were obtained. The rate of formation and the degree of polymerization were lower than those of the homologous homo-polysaccharide but these novel hetero-polymers were much more resistant to enzymatic hydrolysis by 1,3-glucanases.[80]

4) Xylanases

Glycosynthases from GH10 xylanases from four different bacterial sources are able to produce polymeric β-1,4-linked xylopyranoside (DP≈30) efficiently using α-xylobiosyl fluoride (X2F) as donor, as well as from GH52 β-xylosidase.[77]

5) Xylan

Xyloglucan polymers have also been obtained by different glycosynthases. The Humicola insolens GH7 glycosynthase, HiCel7B E197S, is capable of synthesizing non-galactosylated,

XXXG-based homo-xyloglucan up to Mw 60000 Da [G=Glcβ(1→4); X=Xylα(1→6)Glcβ(1→4); L=Galβ(1→2)Xylα(1→6)Glcβ(1→4)]. More complex xyloglucans have been achieved by the glycosynthase based on the GH16 xyloglucan hydrolase from Tropaeolum majus (TmNXG1) which is capable of synthesizing XLLG-based xyloglucan oligosaccharides, but not higher polymers.[81] Interestingly, the glycosynthase derived from GH5 Paenibacillus pabuli *endo*-xyloglucanase catalyzes regio- and stereospecific homo- and hetero-condensations of α-xylogluco-oligosaccharyl fluoride donors XXXGαF and XLLGαF producing high molecular mass xyloglucan polymers with regular sidechain substitution patterns not available in nature.[82] The product range could be further extended by combination with an α(1→2)-fucosyltransferase to achieve the in vitro synthesis of fucosylated xyloglucans typical of dicot primary cell walls.[82]

Altogether, these glycosynthases provide a versatile method for the preparative synthesis of homogeneous xyloglucans with regular substitution patterns not available in nature.

In Table 1. 1, 1. 2 and 1. 3 all the glycosynthases engineered since the introduction of the technology in 1998 until June 2014 are presented with a breve description of each one.

Parental glycosidase	Family	Mutated residue	Reaction C[1]/P[2]	Linkage formed	Reference
***Exo*-glycosidases (fluoride donors)**					
Agrobacterium sp. β-glucosidase	GH 1	E358	C	β-1,4 (β-1,3) [3]	[46]
Sulfolobus solfataricus β-glycosidase	GH 1	E387	C	β-1,3/4/6	[83]
Thermosphaera aggregans β-glycosidase	GH 1	E386	C	β-1,3/4/6	[58]
Thermus thermophilus β-glycosidase	GH 1	E338	C	β-1,3	[84]
				(β-1,6) [3,4]	[85]
					[86]
Streptomyces sp. β-glucosidase	GH 1	E383	C	β-1,3 (β-1,4) [3,4]	[87]
Oryza sativa β-glucosidase	GH 1	E414	C / P	β-1,4 (β-1,3) [4]	[48]
					[88,89]
Thermus non-proteolyticus	GH 1	E338	C	β-1,3, β-1,4 [4]	[90]
Thermotoga neopolitana	GH 1	E349	C	β-1,3/4/6 [3]	[91]
Cellulomonas fimi β-mannosidase	GH 2	E519	C	β-1,3, β-1,4 [3,4]	[92]
Escherichia coli β-galactosidase	GH 2	E537	C	β-1,6	[93]
Thermotoga maritima β-glucuronidase	GH 2	E476	C	β-1,4	[72]
Escherichia coli β-glucuronidase	GH 2	E504	C	β-alcohol	[94]
Saccharopolyspora erythraea β-glucosidase	GH 3	D257		β-1,2	[95]
Candida albicans	GH 5	E292	C	β-1,6/3/4 [3]	[96]
Schizosaccharomyces pombe α-glucosidase	GH 31	D481	C	α-1,6/4	[97]
Bacillus circulans	GH 35	E233	C	β-1,3	[98]
Geobacillus stearothermophilus β-xylosidase	GH 52	E335	C	β-1,4 (β-1,3) [3]	[99]
Bacillus halodurans β-xylosidase	GH 52	E334	C	β-1,4 (β-1,3) [3,4]	[73]
***Exo*-glycosidases (formate rescue)**					
Sulfolobus solfataricus β-glycosidase (*)	GH 1	E387	C	β-1,3/4/6	[83]
Pyrococcus furiosus β-glycosidase	GH 1	E372	C	β-1,3	[58]
Thermoplasma acidophilum α-glucosidase	GH 31	D408G	C	α-1,4	[100]
					[56]
***Exo*-glycosidases (azide donor)**					
Sulfolobus solfataricus α-fucosidase	GH 29	E242	C	α-1,3 (α1,4/6/2) [3]	[54]
Thermotoga maritima α-fucosidase	GH 29	D224	C	α-1,3, α-1,4	[54]
Thermotoga maritima α-galactosidase	GH 36	D327	C	α-1,2/3/4/6 [3]	[101]

Table 1. 1. Retaining glycosynthases from *exo*-glycosidases. [1] Donor and acceptor condensation, and eventually, product elongation leading to short oligomers. [2] Polymerization by donor self-condensation to produce artificial polysaccharides. [3] Depending on the acceptor, mixture of both linkages are obtained [4] Regioselectivity changes depending on the acceptor.

Parental glycosidase	Family	Mutated residue	Reaction C[(1)]/P[(2)]	Linkage formed	Reference
***Endo*-glycosidases (fluoride donor)**					
Rhodococcus sp. Glycoceramidase	GH 5	E351	C	β-1,1	[102]
		E351/D324	C	β-1,1	[64]
Clostridium cellulolyticum Cel5A	GH 5	E307	C	β-1,3, β-1,4	[103]
Paenibacillus pabuli xyloglucanase	GH 5	E323	C / P	β-1,4	[82]
Humicola insolens cellulase	GH 7	E197	C / P	β-1,4, β-1,3 [(4)]	[79]
Trichoderma reesei cellulase	GH 7	E196	C	β-1,4	[104]
Clostridium stercorarium 1,4-β-xylanase	GH 10	E293	C / P	β-1,4	[77]
Bacillus halodurans 1,4-β-xylanase	GH 10	E301	C / P	β-1,4	[77]
Cellulomonas fimi Cex 1,4-β-xylanase	GH 10	E233	C / P	β-1,4	[77]
Thermotoga maritima 1,4-β-xylanase	GH 10	E259	C / P	β-1,4	[77]
Cellulomonas fimi CFX 1,4-β-xylanase	GH 10	E235	C	β-1,4	[105]
Geobacillus stearothermophilus 1,4-β-xylanase	GH 10	E265	C / P	β-1,4	[99]
Bacillus licheniformis xyloglucanase	GH 12	E155	C	unknown	[81]
Bacillus licheniformis 1,3-1,4-β-glucanase	GH 16	E134	C / P	β-1,4	[47]
Pyrococcus furiosus 1,3(4)-β-glucanase	GH 16	E170	C	β-1,4, β-1,3 [(4)]	[106]
Pttxyloglucan *endo*-transglycosylase	GH 16	E85	C / P	β-1,4	[107]
Tropaeolum majus xyloglucanase	GH 16	E94	C / P	β-1,4	[81]
Phanerochaete chrysosporium laminarinase	GH 16	E115S	C	β-1,3	[108]
Hordeum vulgare 1,3-β-glucanase	GH 17	E231	C / P	β-1,3	[80]
Cellvibrio japonicus β-mannanase	GH 26	E320	C	β-1,4	[109]
***Endo*-glycosidases (oxazoline)**					
Streptococcus pyogenes *Endo*-β-*N*-acetylglucosaminidase (*Endo*-S)	GH 18	D233	C	β-1,4	[49]
Mucor hiemalis *Endo*-β-*N*-acetylglucosaminidase (*Endo*-M)	GH 85	N175	C	β-1,4	[50]
Arthrobacter protophormiae *Endo*-β-*N*-acetylglucosaminidase (*Endo*-A)	GH 85	N171	C	β-1,4	[52]
Streptococcus pneumoniae *Endo*-β-*N*-acetylglucosaminidase (*Endo*-D)	GH 85	N322	C	β-1,4	[51]
Elizabethkingia meningosepticum *Endo*-β-*N*-acetylglucosaminidase (*Endo*-F)	GH 18	D126	C	β-1,4	[66]

Table 1. 2. Retaining glycosynthases (from *endo*-glycosidases). [(1)] Donor and acceptor condensation, and eventually, product elongation leading to short oligomers. [(2)] Polymerization by donor self-condensation to produce artificial polysaccharides. [(3)] Depending on the acceptor, mixture of both linkages are obtained [(4)] Regioselectivity changes depending on the acceptor.

Parental glycosidase	Family	Mutated residue	Reaction C[(1)]/P[(2)]	Linkage formed	Reference
***Exo*-glycosidases (fluoride donors)**					
Bacillus halodurans	GH 8	Y198	C	β-(1,4)	[59]
Eschericia coli	GH 63	E727/D324	C	β-1,3/4/6 [(3)]	[62]
Bifidobacterium bifidum	GH 95	D766	C	α-(1,2)	[63]
***Endo*-glycosidases (fluoride donors)**					
Bryum coronatum	GH 19	S102/E70	C/P	β-(1,4)	[61]

Table 1. 3. Inverting glycosynthases. [(1)] Donor and acceptor condensation, and eventually, product elongation leading to short oligomers. [(2)] Polymerization by donor self-condensation to produce artificial polysaccharides. [(3)] Depending on the acceptor, mixture of both linkages are obtained.

1.4. Aim of the thesis: new artificial polysaccharides

The use of polysaccharides as biomaterials has evolved over the past several decades finding applications in many fields of human life and activities. Polymers from natural sources are particularly useful as biomaterials given their similarity to the extracellular matrix and other polymers in the human body. Due to this biocompatibility they degrade within the body as a result of natural biological processes, eliminating the need to remove them later. The most intensely developing investigations on the design and application of polymer materials are related to biomedical and functional engineering materials. The surface of these polymer-based biomaterials is chemically well-defined, have unique physicochemical properties and can be chemically modified to improve their functionality and suit specific needs.[14,15] Implantable biomaterials such as coronary stents, vascular grafts and heart valves among other, controlled-release carriers for local delivery of drugs, hormones, enzymes or growth factors, or three dimensional scaffolds for regenerative medicine (artificial skins to treat burn victims, cardiac patches to regenerate cardiac muscle damaged by a heart attack) are applications that are transforming lives and improving the quality of living. The development of new functionalized artificial polysaccharides opens a large field of applications taking advantage of their specific properties, in particular, renewability, biodegradability and biological activity for some of them.[110,111,112,113] It is vitally important to control their surface properties so that they integrate well with host tissues.

1.4.1. Control of length

Polysaccharides have fundamental biological roles that depend on their length. Those polysaccharides that form macromolecular structures having structural or energy storage

functions (cellulose, hyaluronic acid (HA), starch, etc.) require physical and chemical properties that arise from high degrees of polymerization. However, polysaccharides that function in signaling tend to be shorter presumably because signaling depends on the recognition of distinct epitopes. Short HA polymers of only 100 monomeric units induce inflammatory responses and activate parts of the immune system, whereas full-length HA mediates the opposite effects. Therefore, control of length is critical for proper biological functions.

Carbohydrate polymers are synthesized by enzyme-catalyzed chain-growth polymerization reactions in which monomer units add successively to the growing end of an acceptor. The mechanism of length control depends on the mechanism of elongation, and elongation can occur by either a distributive or a processive mechanism. During distributive polymerizations the elongated polysaccharides are released into solution after each catalytic addition of monomer unit, whereas during processive polymerizations the elongated polysaccharides are retained through multiple catalytic rounds of monomer addition. In a distributive polymerization, product lengths occur statistically in a Poisson distribution. In a processive polymerization, however, product lengths are determined by when the enzyme releases the growing polymer into solution.

In the work developed by Planas and co-workers different glycosynthase mutants were evaluated in the synthesis of β-1,3 and β-1,4 mixed-linked β-glucans demonstrating that the DP can be modulated by the enzyme activity.[78] As the glycosynthase reaction takes place in solution, the polymerization can proceed until the products become insoluble and precipitate. The rate of polysaccharide formation and the amount of high molecular mass polymers produced at high donor and enzyme concentrations led to oversaturated solutions that entrapped the lower molecular mass polymers when precipitating, with the result of an insoluble polymer with a bimodal profile. Therefore, by increasing the rate of condensation (*i.e.*, more active glycosynthase), polymerization can be extended above the solubility limit as long as the product remains in solution due to oversaturation.

With the aim of obtaining more homogeneous polysaccharides, larger if possible, avoiding a fast initial precipitation and decreasing the PDI, the use of a carbohydrate binding module in combination with a glycosynthase mutant is proposed in this thesis.

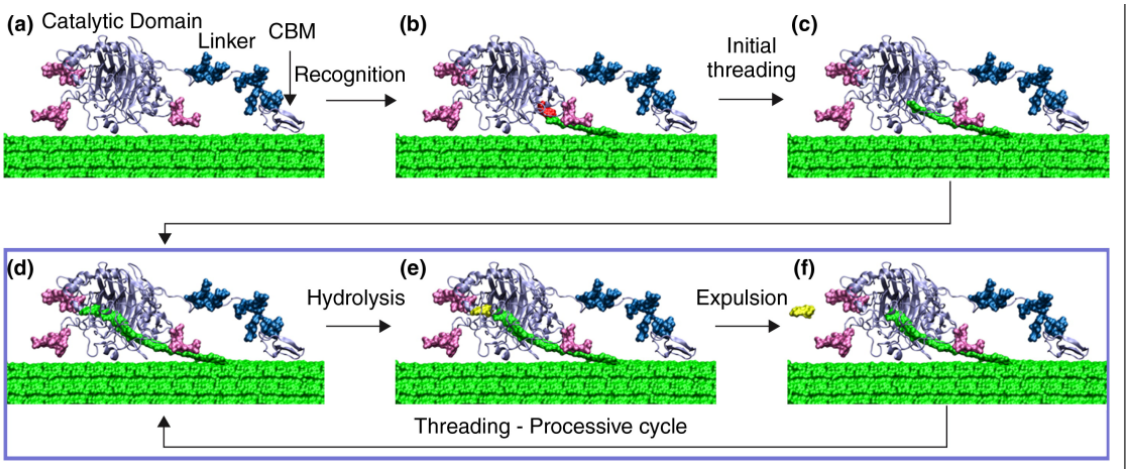

Figure 1. 11. CBMs in nature. (a) Cel7A binding to cellulose, (b) recognition of a reducing end of a cellulose chain, (c) initial threading of the cellulose chain into the catalytic tunnel, (d) threading and formation of a catalytically active complex, (e) hydrolysis in a processive cycle and (f) product expulsion and threading of another cellobiose (shown in yellow in e and f).[114]

Non-catalytic carbohydrate-binding modules (CBMs) play a critical role in the action of glycosyl hydrolases by localizing the appended catalytic domains onto the surface of insoluble polysaccharide substrates. Even nature selects these non-catalytic protein domains for important tasks such as the efficient and biotechnological conversion of cellulosic biomass (Figure 1. 11).[115] We envisioned the possible use of a CBM to enhance the solubility of the polysaccharide in the reaction medium becoming a tool to spread out the reaction time of glycosynthase-catalyzed polymerizations avoiding early precipitation of high polydispersed polysaccharides, improving their homogeneity and probably having an effect on their M_w.

1.4.2. Functionalization and derivatization

Biodegradable polymers with hydrolyzable chemical bonds are researched extensively for biomedical, pharmaceutical and 'green' chemistry applications.[111] Modifications and introduction of functionalizations into such polymers are often necessary in order to get polysaccharide-based functional biomaterials. Chemical modification is still an important route to structure and hence property design.[116] However, when working with polysaccharides chemical modification is challenging due to the similar reactivity toward electrophiles of the hydroxyl groups composing the polysaccharide. Esterification and etherification, as well as oxidation and nucleophilic displacement reactions are the most common reactions utilized in the modification of polysaccharides. Different chemical and enzymatic strategies are continuously being investigated to conveniently introduce direct modifications on the polysaccharides with high regioselectivity.

The azido group is a relatively small and versatile functional group, inert in most biological processes, that can undergo highly selective chemical reactions such as the Staudinger reduction from azides to amines (Figure 1. 12) or the [3+2] cycloaddition with activated alkynes. These reactions have been exploited for the selective labeling of azido-functionalized biomolecules, such as proteins, sugars and lipids.

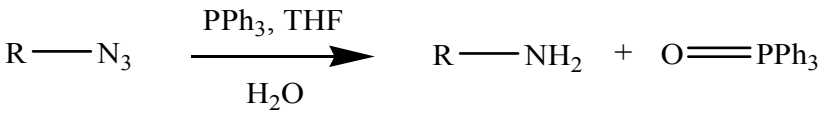

Figure 1. 12. Staudinger reduction of azides to amines.

Click chemistry (Figure 1. 13) was introduced in 2001 by Sharpless et al to describe experimentally simple reactions developed in mild reaction conditions, needing no protection from oxygen, requiring only stoichiometric amounts of starting materials with nearly quantitative yields.[117] The 1,3-dipolar cycloaddition of an azide moiety and a triple bond (Huisgen reaction) has rapidly become the most popular click reaction to date.[118,119] The Copper-catalyzed Azide - Alkyne Cycloaddition (CuAAC) allows the synthesis of the 1,4-disubstituted regioisomers specifically. This reaction features an enormous rate acceleration of 10^7 to 10^8 compared to the uncatalyzed 1,3-dipolar cycloaddition. The reaction succeeds over a broad temperature range, is insensitive to aqueous conditions and a pH range from 4 to 12, and tolerates a broad range of functional groups. Pure products can be isolated by simple filtration or extraction without the need for chromatography or recrystallization. The active Cu(I) catalyst can be generated from Cu(I) salts or Cu(II) salts using sodium ascorbate as the reducing agent. Addition of a slight excess of sodium ascorbate prevents the formation of oxidative homocoupling products.[120]

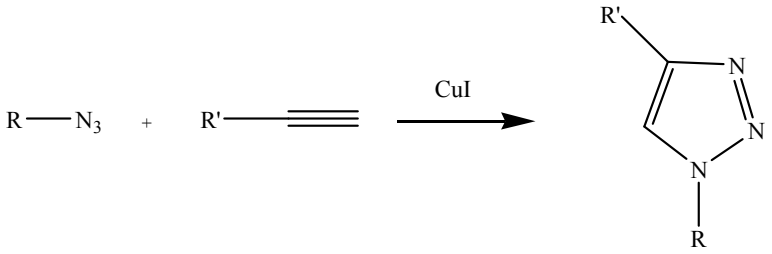

Figure 1. 13. Huisgen 1,3-dipolar cycloaddition of azides and terminal alkynes.

Different polysaccharides chemically modified with the azido functional group such as cellulose, starch, dextran, chitosan, hyaluronan, etc. have been already modified by the use of click chemistry for the synthesis of new materials and gels, new therapeutic or diagnostic agents, or to understand the reactivity and roles of glycan structures in living organisms. It has also been used for the synthesis of dendrimers[121] or the modification of proteins.[122] Click chemistry is becoming

a promising path for polysaccharide modification and it is broadening the structural diversity of polysaccharides yielding compounds that are not accessible via etherification, esterification, and the most commonly applied reactions.

Click chemistry with (1→3)-β-D-glucans

(1→3)-β-D-glucans have interesting structural features such as a rigid and triple-stranded helical structure,[123,124,125] pharmaceutical effects (anticancer activity),[126] and binding properties (with polynucleotides, single-walled carbon nanotubes).[127,128,129] Hasegawa et al synthesized a series of artificial (1→3)-β-D-glucans with various functional appendages in order to facilitate access to various polysaccharide-based materials (Figure 1. 14).

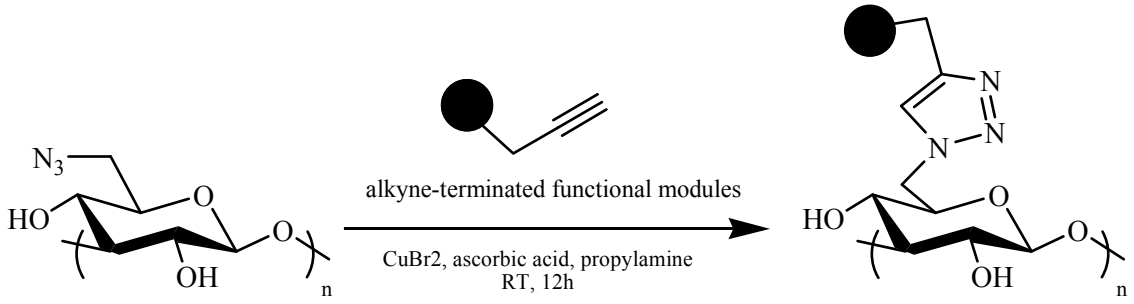

Figure 1. 14. Chemoselective coupling between 6-azido-6-deoxycurdlan and alkyne-terminated functional modules.

For instance, 6-azido-6-deoxycurdlan with different alkyne-terminated modules such as a β-lactoside (a strong ligand for asialo-glycoprotein receptors on hepatocytes), ferrocene (a redox-active unit), pyrene (a chromophore with strong fluorescence) and porphyrin (an essential component of native light-harvesting and oxygen-binding systems allowed the obtention of the correspondent derivatives. These new polymers had low cytoxicity and long blood circulation time, providing potential promise for biomedical application. Interactions between curdlan derivatives and polycytidylic acid formed stable macromolecular complexes that showed strong and specific lectin affinity, beneficial to use as polynucleotide carriers.[130]

Click chemistry with cellulose

The copper-catalyzed Huisgen reaction was first performed with cellulose in 2006 when Liebert et al studied different "click" reactions between 6-azido-6-deoxycellulose and methyl propiolate, 2-ethynylaniline and 3-ethynylthiophene[131] proving to be a very selective reaction. A novel cellulose-based hydrogel was synthesized by Heinze et al. by reacting carboxymethylated cellulose derivatives bearing azide and alkyne moieties and applying the CuAAC for the cross-linking.[132] The new gel contained up to 98.4% water and after lyophilization, a spongy material

with a porous structure was obtained. Cross-linking through 'click chemistry' between azido-polycaprolactone and undecynoate cellulose (DS 0.1) with a terminal alkyne developed biodegradable multilayer films with interesting properties for their application in drug delivery and tissue engineering.[133] A photobactericidal tissue was created in 2009 after direct cellulose azidation, followed by 'click' chemistry reaction in THF and water with acetylenic porphyrin.[134] Interestingly, the product displayed antibacterial activity agains *E. coli* and *S. aureus* under irradiation with visible light. Cellulose glycoclusters with improved water solubility were synthesized by grafting *O*-*N*-linked β-maltoside or β-lactoside containing a terminal alkyne onto C-6 positions of 6-azido-6-deoxycellulose. The product bound to carbohydrate-binding proteins in a non-specific manner.[135] Recently, the synthesis of ferrocene-modified cellulose for use as docking spot for cyclodextrin was performed by coupling 6-azido-6-deoxycellulose and ethynylferrocene via copper-catalyzed click-type cycloaddition under microwave-assisted conditions.[136] Rame-*β*-cyclodextrin could be supramolecularly attached to cellulose becoming a redox-sensitive system that could be switched by electrochemical *stimuli* and make it accessible to other guest molecules.[137]

With the aim of obtaining new functionalized artificial polysaccharides for a future use as biomaterials, in this work we address a powerful approach, whereby enzyme-catalyzed polymerization of properly modified building blocks is introduced as a simple route affording polysaccharides with controlled sequence and functionalization pattern (Figure 1.15).

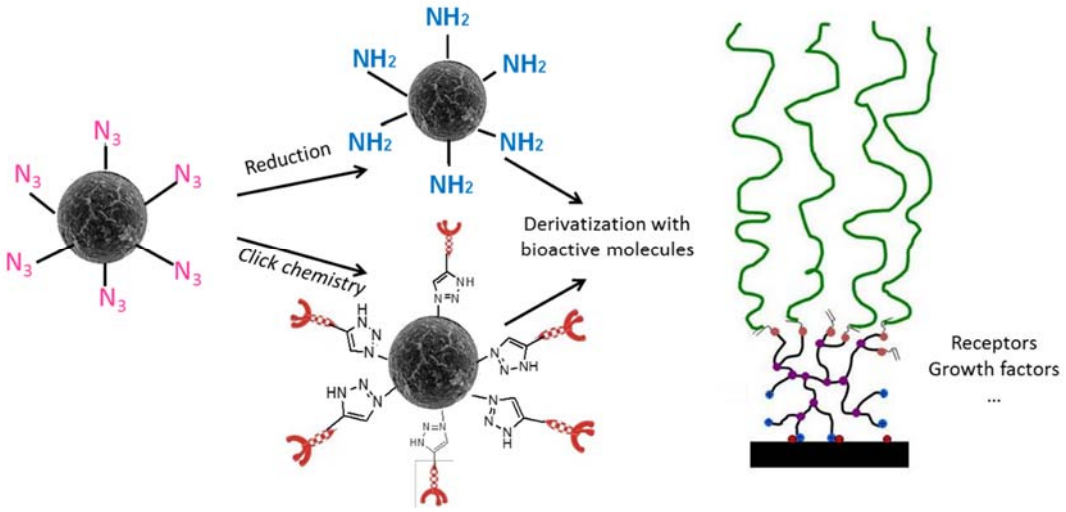

Figure 1. 15. Synthesis of new biomaterials. Versatility of the azido functional group. The azido functionalized polysaccharide surface might be reduced to amines or reacted by click chemistry attaching bioactive molecules such as growth factors, receptors, etc.

1.5. REFERENCES

(1) Dwek, R. A. *Chem. Rev.* **1996**, *96*, 683–720.

(2) Helenius, A.; Aebi, M. *Science (80-.).* **2001**, *291*, 2364–2369.

(3) Schwarz, F.; Aebi, M. *Curr. Opin. Struct. Biol. 2* **2011**, *21*, 576–582.

(4) Dube, D. H.; Bertozzi, C. R. *Nat Rev Drug Discov* **2005**, *4*.

(5) Adamczyk, B.; Tharmalingam, T.; Rudd, P. M. *Biochim. Biophys. Acta* **2012**, *1820*, 1347–1353.

(6) Glycoscience http://ncbes.eurhost.net/glycoscience.aspx.

(7) Varki A., Cummings R.D., Esko J.D., Freeze, H.H., Stanley, P., Bertozzi, C.R., Hart, G.W., Etzler, M. E. *Essentials of Glycobiology*; Second.; Cold Spring Harbor Press: Cold Spring Harbor (NY), 2009.

(8) Cummings, R. D.; Pierce, J. M. *Chem. Biol.* **2014**, *21*, 1–15.

(9) Blixt, O.; Head, S.; Mondala, T.; Scanlan, C.; Huflejt, M. E.; Alvarez, R.; Bryan, M. C.; Fazio, F.; Calarese, D.; Stevens, J.; Razi, N.; Stevens, D. J.; Skehel, J. J.; van Die, I.; Burton, D. R.; Wilson, I. A.; Cummings, R.; Bovin, N.; Wong, C.-H.; Paulson, J. C. *Proc. Natl. Acad. Sci. U. S. A.* **2004**, *101*, 17033–17038.

(10) Feizi, T.; Chai, W. *Nat Rev Mol Cell Biol* **2004**, *5*, 582–588.

(11) Pratt, M. R.; Bertozzi, C. R. *Chem. Soc. Rev.* **2005**, *34*, 58–68.

(12) Dell, A.; Morris, H. R. *Sci.* **2001**, *291* , 2351–2356.

(13) Dumitriu, S. *Polysaccharides: structural diversity and functional versatility*; CRC Press, 2012.

(14) Reis, R. L.; Neves, N. M.; Mano, J. F.; Gomes, M. E.; Marques, A. P.; Azevedo, H. S. *Natural-based polymers for biomedical applications*; Woodhead Publishing Limited: Cambridge, UK, 2008.

(15) Manjanna, K. M.; Pramod Kumar, T. M.; Shivakumar, B. *Int. J. ChemTech Res.* **2010**, *2*, 509–525.

(16) Demchenko, A. V. *Handbook of chemical glycosylation: advances in stereoselectivity and therapeutic relevance*; A.V. Demchenko, Ed.; WILEY-VCH Verlag GmbH & Co, 2008.

(17) Faijes, M.; Planas, A. *Carbohydr. Res.* **2007**, *342*, 1581–1594.

(18) Lombard, V.; Golaconda Ramulu, H.; Drula, E.; Coutinho, P. M.; Henrissat, B. *Nucleic Acids Res.* **2014**, *42*, 490–495.

(19) Kanekawa, Jun-ichi, Kaneko, Y. *Engineering of Polysaccharide Materials*; First edit.; Pan Standford Publishing Pte. Ltd.: Singapore, 2013.

(20) Schuman, B.; Evans, S. V; Fyles, T. M. *PLoS One* **2013**, *8*, e71077.

(21) Tvaroška, I. *Carbohydr. Res.* **2014**.

(22) Kitaoka, M.; Hayashi, K. *TRENDS GLYCOSCI GLYC* **2002**, *14*, 35–50.

(23) Luley-Goedl, C.; Nidetzky, B. *Biotechnol. J.* **2010**, *5*, 1324–1338.

(24) Yamamoto, T.; Yamashita, H.; Mukai, K.; Watanabe, H.; Kubota, M.; Chaen, H.; Fukuda, S. *Carbohydr. Res.* **2006**, *341*, 2350–2359.

(25) Nakai, H.; Petersen, B. O.; Westphal, Y.; Dilokpimol, A.; Abou Hachem, M.; Duus, J. Ø.; Schols, H. A.; Svensson, B. *Protein Eng. Des. Sel.* **2010**, *23*, 781–787.

(26) Nakai, H.; Kitaoka, M.; Svensson, B.; Ohtsubo, K. *Curr. Opin. Chem. Biol.* **2013**, *17*, 301–309.

(27) Cantarel, B. L.; Coutinho, P. M.; Rancurel, C.; Bernard, T.; Lombard, V.; Henrissat, B. *Nucleic Acids Res.* **2009**, *37*, D233–D238.

(28) Davies, G.; Henrissat, B. *Structure* **1995**, *3*, 853–859.

(29) Hahn, M.; Pons, J.; Planas, A.; Querol, E.; Heinemann, U. *FEBS Lett.* **1995**, *374*, 221–224.

(30) Varrot, A.; Leydier, S.; Pell, G.; Macdonald, J. M.; Stick, R. V; Henrissat, B.; Gilbert, H. J.; Davies, G. J. *J. Biol. Chem.* **2005**, *280*, 20181–20184.

(31) Withers, S. G. *Carbohydr. Polym.* **2001**, *44*, 325–337.

(32) Davies, G. J.; Mackenzie, L.; Varrot, A.; Dauter, M.; Brzozowski, A. M.; Schülein, M.; Withers, S. G. *Biochemistry* **1998**, *37*, 11707–11713.

(33) Sinnott, M. L. *Chem. Rev.* **1990**, *90*, 1171–1202.

(34) McCarter, J. D.; Withers, S. G. *Curr. Opin. Struct. Biol.* **1994**, *4*, 885–892.

(35) Tews, I.; Terwisscha van Scheltinga, A. C.; Perrakis, A.; Wilson, K. S.; Dijkstra, B. W. *J. Am. Chem. Soc.* **1997**, *119*, 7954–7959.

(36) Fernández-Mayoralas, A. *Top. Curr. Chem.* **1997**, *186*, 1–20.

(37) Rantwijk, F. Van; Oosterom, M. W.; Sheldon, R. A. *J. Mol. Catal. B Enzym.* **1999**, *6*, 511–532.

(38) Planas, A.; Faijes, M. *Afinidad* **2002**, *59*, 295–313.

(39) Kobayashi, S.; Kashiwa, K.; Kawasaki, T.; Shoda, S. *J. Am. Chem. Soc.* **1991**, *113*, 3079–3084.

(40) Kobayashi, S.; Sakamoto, J.; Kimura, S. *Prog. Polym. Sci.* **2001**, *26*, 1525–1560.

(41) Kobayashi, S.; Uyama, H.; Kimura, S. *Chem. Rev.* **2001**, *101*, 3793–3818.

(42) Kobayashi, S.; Shimada, J.; Kashiwa, K.; Shoda, S. *Macromolecules* **1992**, *25*, 3237–3241.

(43) Okada, G.; Genghof, D. S.; Hehre, E. J. *Carbohydr. Res.* **1979**, *71*, 287–298.

(44) Fujita, M.; Shoda, S.; Kobayashi, S. *J. Am. Chem. Soc.* **1998**, *120*, 6411–6412.

(45) Viladot, J.-L.; Moreau, V.; Driguez, H. *J. Chem. Soc., Perkin Trans* **1997**, 2383–2387.

(46) Mackenzie, L. F.; Wang, Q.; Warren, R. A. J.; Withers, S. G. *J. Am. Chem. Soc.* **1998**, *120*, 5583–5584.

(47) Malet, C.; Planas, A. *FEBS Lett.* **1998**, *440*, 208–212.

(48) Hommalai, G.; Withers, S. G.; Chuenchor, W.; Ketudat Cairns, J. R.; Svasti, J. *Glycobiology* **2007**, *17*, 744–753.

(49) Huang, W.; Giddens, J.; Fan, S.; Toonstra, C.; Wang, L. *J. Am. Chem. Soc.* **2012**.

(50) Umekawa, M.; Huang, W.; Li, B.; Fujita, K.; Ashida, H.; Wang, L.-X.; Yamamoto, K. *J. Biol. Chem.* **2008**, *283*, 4469–4479.

(51) Fan, S.-Q.; Huang, W.; Wang, L.-X. *J. Biol. Chem.* **2012**, *287*, 11272–11281.

(52) Huang, W.; Li, C.; Li, B.; Umekawa, M.; Yamamoto, K.; Zhang, X.; Wang, L.-X. *J. Am. Chem. Soc.* **2009**, *131*, 2214–2223.

(53) Smith, E. L.; Giddens, J. P.; Iavarone, A. T.; Godula, K.; Wang, L.-X.; Bertozzi, C. R. *Bioconjug. Chem.* **2014**, *25*, 788–795.

(54) Cobucci-Ponzano, B.; Conte, F.; Bedini, E.; Corsaro, M. M.; Parrilli, M.; Sulzenbacher, G.; Lipski, A.; Dal Piaz, F.; Lepore, L.; Rossi, M.; Moracci, M. *Chem. Biol.* **2009**, *16*, 1097–1108.

(55) Cobucci-Ponzano, B.; Strazzulli, A.; Rossi, M.; Moracci, M. *Adv. Synth. Catal.* **2011**, *353*, 2284–2300.

(56) Park, I.; Lee, H.; Cha, J. *Biotechnol. Lett.* **2014**, *36*, 789–796.

(57) Moracci, M.; Trincone, A.; Perugino, G.; Ciaramella, M.; Rossi, M. *Biochemistry* **1998**, *37*, 17262–17270.

(58) Perugino, G.; Trincone, A.; Giordano, A.; van der Oost, J.; Kaper, T.; Rossi, M.; Moracci, M. *Biochemistry* **2003**, *42*, 8484–8493.

(59) Honda, Y.; Kitaoka, M. *J. Biol. Chem.* **2006**, *281*, 1426–1431.

(60) Honda, Y.; Fushinobu, S.; Hidaka, M.; Wakagi, T.; Shoun, H.; Taniguchi, H.; Kitaoka, M. *Glycobiology* **2008**, *18*, 325–330.

(61) Ohnuma, T.; Fukuda, T.; Dozen, S.; Honda, Y.; Kitaoka, M.; Fukamizo, T. *Biochem. J.* **2012**, *444*, 437–443.

(62) Miyazaki, T.; Ichikawa, M.; Yokoi, G.; Kitaoka, M.; Mori, H.; Kitano, Y.; Nishikawa, A.; Tonozuka, T. *FEBS J.* **2013**, *280*, 4560–4571.

(63) Wada, J.; Honda, Y.; Nagae, M.; Kato, R.; Wakatsuki, S.; Katayama, T.; Taniguchi, H.; Kumagai, H.; Kitaoka, M.; Yamamoto, K. *FEBS Lett.* **2014**, *582*, 3739–3743.

(64) Rich, J. R.; Withers, S. G. *Angew. Chem. Int. Ed. Engl.* **2012**, *51*, 8640–8643.

(65) Hancock, S. M.; Rich, J. R.; Caines, M. E. C.; Strynadka, N. C. J.; Withers, S. G. *Nat Chem Biol* **2009**, *5*, 508–514.

(66) Giddens, J.; Lomino, J.; Wang, L.-X. *FASEB J.* **2014**, *28* .

(67) Perrimon, N.; Bernfield, M. *Cell Dev. Biol.* **2001**, *12*, 65–67.

(68) Esko, J. D.; Lindahl, U. *J. Clin. Invest.* **2001**, *108*, 169–173.

(69) Cobucci-Ponzano, B.; Moracci, M. *Nat. Prod. Rep.* **2012**, *29*, 697–709.

(70) Vázquez, J. A.; Rodríguez-Amado, I.; Montemayor, M. I.; Fraguas, J.; González, M. D. P.; Murado, M. A. *Mar. Drugs* **2013**, *11*, 747–774.

(71) Masuko, S.; Bera, S.; Green, D. E.; Weïwer, M.; Liu, J.; DeAngelis, P. L.; Linhardt, R. J. *J. Org. Chem.* **2011**, *77*, 1449–1456.

(72) Müllegger, J.; Chen, H.-M.; Chan, W. Y.; Reid, S. P.; Jahn, M.; Warren, R. A. J.; Salleh, H. M.; Withers, S. G. *ChemBioChem* **2006**, *7*, 1028–1030.

(73) Goddard-Borger, E. D.; Fiege, B.; Kwan, E. M.; Withers, S. G. *Chembiochem* **2011**, *12*, 1703–1711.

(74) Faijes, M.; Imai, T.; Bulone, V.; Planas, A. *Biochem. J.* **2004**, *380*, 635–641.

(75) Fauré, R.; Saura-Valls, M.; Brumer, H.; Planas, A.; Cottaz, S.; Driguez, H. *J. Org. Chem.* **2006**, *71*, 5151–5161.

(76) Saura-Valls, M.; Fauré, R.; Ragàs, S.; Piens, K.; Brumer, H.; Teeri, T. T.; Cottaz, S.; Driguez, H.; Planas, A. *Biochem. J.* **2006**, *395*, 99–106.

(77) Sugimura, M.; Nishimoto, M.; Kitaoka, M. *Biosci. Biotechnol. Biochem.* **2006**, *70*, 1210–1217.

(78) Pérez, X.; Faijes, M.; Planas, A. *Biomacromolecules* **2011**, *12*, 494–501.

(79) Fort, S.; Boyer, V.; Greffe, L.; Davies, G. J.; Moroz, O.; Christiansen, L.; Schülein, M.; Cottaz, S.; Driguez, H. *J. Am. Chem. Soc.* **2000**, *122*, 5429–5437.

(80) Hrmova, M.; Imai, T.; Rutten, S. J.; Fairweather, J. K.; Pelosi, L.; Bulone, V.; Driguez, H.; Fincher, G. B. *J. Biol. Chem.* **2002**, *277*, 30102–30111.

(81) Gullfot, F.; Ibatullin, F. M.; Sundqvist, G.; Davies, G. J.; Brumer, H. *Biomacromolecules* **2009**, *10*, 1782–1788.

(82) Spadiut, O.; Ibatullin, F. M.; Peart, J.; Gullfot, F.; Martinez-Fleites, C.; Ruda, M.; Xu, C.; Sundqvist, G.; Davies, G. J.; Brumer, H. *J. Am. Chem. Soc.* **2011**, *133*, 10892–10900.

(83) Trincone, A.; Perugino, G.; Rossi, M.; Moracci, M. *Bioorg. Med. Chem. Lett.* **2000**, *10*, 365–368.

(84) Drone, J.; Feng, H.; Tellier, C.; Hoffmann, L.; Tran, V.; Rabiller, C.; Dion, M. *European J. Org. Chem.* **2005**, *2005*, 1977–1983.

(85) Marton, Z.; Tran, V.; Tellier, C.; Dion, M.; Drone, J.; Rabiller, C. *Carbohydr. Res.* **2008**, *343*, 2939–2946.

(86) Teze, D.; Dion, M.; Daligault, F.; Tran, V.; André-Miral, C.; Tellier, C. *Bioorg. Med. Chem. Lett.* **2013**, *23*, 448–451.

(87) Faijes, M.; Saura-Valls, M.; Pérez, X.; Conti, M.; Planas, A. *Carbohydr. Res.* **2006**, *341*, 2055–2065.

(88) Pengthaisong, S.; Withers, S. G.; Kuaprasert, B.; Svasti, J.; Ketudat Cairns, J. R. *Protein Sci.* **2012**, *21*, 362–372.

(89) Pengthaisong, S.; Chen, C.-F.; Withers, S. G.; Kuaprasert, B.; Ketudat Cairns, J. R. *Carbohydr. Res.* **2012**, *352*, 51–59.

(90) Wei, J.; Lv, X.; Lü, Y.; Yang, G.; Fu, L.; Yang, L.; Wang, J.; Gao, J.; Cheng, S.; Duan, Q.; Jin, C.; Li, X. *European J. Org. Chem.* **2013**, *2013*, 2414–2419.

(91) Pozzo, T.; Plaza, M.; Romero-García, J.; Faijes, M.; Karlsson, E. N.; Planas, A. *J. Mol. Catal. B Enzym.* **2014**, *107*, 132–139.

(92) Nashiru, O.; Zechel, D. L.; Stoll, D.; Mohammadzadeh, T.; Warren, R. A. J.; Withers, S. G. *Angew. Chemie* **2001**, *113*, 431–434.

(93) Jakeman, D. L.; Withers, S. G. *Can. J. Chem.* **2002**, *80*, 866–870.

(94) Wilkinson, S. M.; Liew, C. W.; Mackay, J. P.; Salleh, H. M.; Withers, S. G.; McLeod, M. D. *Org. Lett.* **2008**, *10*, 1585–1588.

(95) Jakeman, D. L.; Sadeghi-Khomami, A. *Biochemistry* **2011**, *50*, 10359–10366.

(96) Nakatani, Y.; Larsen, D. S.; Cutfield, S. M.; Cutfield, J. F. *Biochemistry* **2014**.

(97) Okuyama, M.; Mori, H.; Watanaba, K.; Kimura, A.; Chiba, S. *Biosci. Biotechnol. Biochem.* **2002**, *66*, 928–933.

(98) Li, C.; Kim, Y.-W. *Chembiochem* **2014**, *15*, 522–526.

(99) Ben-David, A.; Bravman, T.; Balazs, Y. S.; Czjzek, M.; Schomburg, D.; Shoham, G.; Shoham, Y. *Chembiochem* **2007**, *8*, 2145–2151.

(100) Sungmin, H.; Seo, S.-H.; Park, I.; Choi, K.-H.; Kim, D.; Cha, J. *Korean Soc. Microbiol. Biotechnol.* **2012**, *40*, 104–110.

(101) Cobucci-Ponzano, B.; Zorzetti, C.; Strazzulli, A.; Carillo, S.; Bedini, E.; Corsaro, M. M.; Comfort, D. A.; Kelly, R. M.; Rossi, M.; Moracci, M. *Glycobiology* **2011**, *21*, 448–456.

(102) Vaughan, M. D.; Johnson, K.; DeFrees, S.; Tang, X.; Warren, R. A. J.; Withers, S. G. *J. Am. Chem. Soc.* **2006**, *128*, 6300–6301.

(103) Tao, A. R.; Habas, S.; Yang, P. *Small* **2008**, *4*, 310–325.

(104) Blanchard, S.; Cottaz, S.; Coutinho, P. M.; Patkar, S.; Vind, J.; Boer, H.; Koivula, A.; Driguez, H.; Armand, S. *J. Mol. Catal. B Enzym.* **2007**, *44*, 106–116.

(105) Kim, Y.-W.; Fox, D. T.; Hekmat, O.; Kantner, T.; McIntosh, L. P.; Warren, R. A. J.; Withers, S. G. *Org. Biomol. Chem.* **2006**, *4*, 2025–2032.

(106) Van Lieshout, J.; Faijes, M.; Nieto, J.; van der Oost, J.; Planas, A. *Archaea* **2004**, *1*, 285–292.

(107) Piens, K.; Henriksson, A.-M.; Gullfot, F.; Lopez, M.; Fauré, R.; Ibatullin, F. M.; Teeri, T. T.; Driguez, H.; Brumer, H. *Org. Biomol. Chem.* **2007**, *5*, 3971–3978.

(108) Vasur, J.; Kawai, R.; Jonsson, K. H. M.; Widmalm, G.; Engström, Å.; Frank, M.; Andersson, E.; Hansson, H.; Forsberg, Z.; Igarashi, K.; Samejima, M.; Sandgren, M.; Ståhlberg, J. *J. Am. Chem. Soc.* **2010**, *132*, 1724–1730.

(109) Jahn, M.; Stoll, D.; Warren, R. A. J.; Szabo, L.; Singh, P.; Gilbert, H. J.; Ducros, V. M.-A.; Davies, G. J.; Withers, S. G. *Chem. Commun.* **2003**, 1327–1329.

(110) Rinaudo, M. *Polym. Int. Int* **2008**, *430*, 397–430.

(111) Hasegawa, T.; Umeda, M.; Numata, M.; Li, C.; Bae, A.-H.; Fujisawa, T.; Haraguchi, S.; Sakurai, K.; Shinkai, S. *Carbohydr. Res.* **2006**, *341*, 35–40.

(112) Cumpstey, I. *ISRN Org. Chem.* **2013**, *2013*, 1–27.

(113) Vendra, V. K.; Wu, L.; Krishnan, S. In *Nanomaterials for the life sciences*; 2010; Vol. 5, pp. 1–54.

(114) Beckham, G. T.; Bomble, Y. J.; Bayer, E. a; Himmel, M. E.; Crowley, M. F. *Curr. Opin. Biotechnol.* **2011**, *22*, 231–238.

(115) Boraston, A.B., Bolam, D.N., Gilbert, H.J., Davies, G. J. *Biochem. J.* **2004**, *382*, 769–781.

(116) Heinze, T.; Liebert, T. *Prog. Polym. Sci.* **2001**, *26*, 1689–1762.

(117) Kolb, H. C.; Finn, M. G.; Sharpless, K. B. *Angew. Chem. Int. Ed. Engl.* **2001**, *40*, 2004–2021.

(118) Rostovtsev, V. V; Green, L. G.; Fokin, V. V; Sharpless, K. B. *Angew. Chemie* **2002**, *114*, 2708–2711.

(119) Lewis, W. G.; Green, L. G.; Grynszpan, F.; Radić, Z.; Carlier, P. R.; Taylor, P.; Finn, M. G.; Sharpless, K. B. *Angew. Chemie* **2002**, *114*, 1095–1099.

(120) Himo, F.; Lovell, T.; Hilgraf, R.; Rostovtsev, V. V; Noodleman, L.; Sharpless, K. B.; Fokin, V. V. *J. Am. Chem. Soc.* **2004**, *127*, 210–216.

(121) Wu, P.; Feldman, A. K.; Nugent, A. K.; Hawker, C. J.; Scheel, A.; Voit, B.; Pyun, J.; Fréchet, J. M. J.; Sharpless, K. B.; Fokin, V. V. *Angew. Chemie Int. Ed.* **2004**, *43*, 3928–3932.

(122) Tornøe, C. W.; Christensen, C.; Meldal, M. *J. Org. Chem.* **2002**, *67*, 3057–3064.

(123) Bot, A. *Carbohydr. Polym.* **2001**, *45*, 363–372.

(124) Yanaki, T.; Norisuye, T.; Fujita, H. *Macromolecules* **1980**, *13*, 1462–1466.

(125) Chuah, C. T.; Sarko, A.; Deslandes, Y.; Marchessault, R. H. *Macromolecules* **1983**, *16*, 1375–1382.

(126) Saitô, H.; Yoshioka, Y.; Uehara, N.; Aketagawa, J.; Tanaka, S.; Shibata, Y. *Carbohydr. Res.* **1991**, *217*, 181–190.

(127) Sakurai, K.; Shinkai, S. *J. Am. Chem. Soc.* **2000**, *122*, 4520–4521.

(128) Hasegawa, T.; Fujisawa, T.; Numata, M.; Umeda, M.; Matsumoto, T.; Kimura, T.; Okumura, S.; Sakurai, K.; Shinkai, S. *Chem. Commun.* **2004**, 2150–2151.

(129) Sakurai, K.; Uezu, K.; Numata, M.; Hasegawa, T.; Li, C.; Kaneko, K.; Shinkai, S. *Chem. Commun.* **2005**, 4383–4398.

(130) Zhang, R.; Edgar, K. J. *Biomacromolecules* **2014**, *15*, 1079–1096.

(131) Liebert, T.; Hänsch, C.; Heinze, T. *Macromol. Rapid Commun.* **2006**, *27*, 208–213.

(132) Koschella, A.; Hartlieb, M.; Heinze, T. *Carbohydr. Polym.* **2011**, *86*, 154–161.

(133) Krouit, M.; Bras, J.; Belgacem, M. N. *Eur. Polym. J.* **2008**, *44*, 4074–4081.

(134) Ringot, C.; Sol, V.; Granet, R.; Krausz, P. *Mater. Lett.* **2009**, *63*, 1889–1891.

(135) Negishi, K.; Mashiko, Y.; Yamashita, E.; Otsuka, A.; Hasegawa, T. *Polymers (Basel).* **2011**, *3*, 489–508.

(136) Ritter, H.; Knudsen, B.; Mondrzik, B. E.; Branscheid, R.; Kolb, U. *Polym. Int.* **2012**, *61*, 1245–1248.

(137) Harada, A. *Acc. Chem. Res.* **2001**, *34*, 456–464.

OBJECTIVES

OBJECTIVES

Given the important role of biomaterials in medicine, the glycosynthase-catalyzed synthesis of new functionalized artificial polysaccharides with a regular substitution pattern and sequence control could be an alternative new source of biocompatible materials for biomedical applications. Three main objectives are presented in this work taking advantage of the glycosynthase technology and with the aim of improving the properties of the new artificial polysaccharides.

1. The degree of polymerization of polysaccharides produced by glycosynthase-catalyzed polymerization is limited by product solubility. Can a carbohydrate binding module have an effect on solubility and degree of polymerization?

   Objective 1: Analyze the effect of a carbohydrate binding module (CBM11) upon the solubility and the length of artificial β–1,3-1,4-mixed-linked glucans produced by the E134S glycosynthase mutant of the 1,3-1,4-β-glucanase.

2. Mixed-linked β-glucans are among the artificial polysaccharides obtained by the glycosynthase technology with higher molecular weight and defined structure. Next step is the ability to introduce functionalized groups.

   Objective 2: Synthesize functionalized donors and acceptors of the glycosynthase reaction in order to study the subsite acceptance of the E134S mutant.

3. Selective modification of cellulose hydroxyl groups is a common way to achieve functionalized cellulose conferring new properties, such as better solubility or miscibility, interesting for use as biomaterial. So far, these modifications have been always introduced randomly on the polysaccharide surface. Glycosynthases can provide polysaccharides with controlled sequence and functionalization pattern.

   Objective 3: Synthesize azido-functionalized artificial cellulose *via* self-condensation of functionalized substrates with a glycosynthase derived from a GH-7 cellulase and derivatize them *via* ‘click chemistry’ or by reduction to amines.

CHAPTER 2: CARBOHYDRATE BINDING MODULE ASSISTING GLYCOSYNTHASE-CATALYZED POLYMERIZATIONS

2.1. INTRODUCTION

Non-catalytic carbohydrate-binding modules (CBMs) are components of multi-modular polysaccharide degrading enzymes where they play critical roles in the recognition of plant cell wall polysaccharides such as cellulose, β-glucans or insoluble storage polysaccharides.[1,2] CBMs promote the association of the enzyme with the substrate and this proximity effect enhances the activity of their cognate catalytic module and provides efficient hydrolysis.[3] Removal of CBMs greatly reduces the activity of the truncated enzymes against insoluble substrates.[4] In addition, there are examples where CBMs are components of substrate-binding sites or even the active site, playing a critical role in substrate specificity.[5,6,7]

To date, CBMs are classified in 71 families according to the CAZY database (Carbohydrate Active Enzymes, www.CAZY.org).[8] Some CBM families, typically those that recognize crystalline polysaccharides, present invariant ligand specificity, while other families cover a broad range of carbohydrate specificities. 6 protein domains from families 2, 4, 6, 11, 39 and 54 are able to accept β-1,3-1,4 linkages. Carbohydrate Binding Module 11 (CBM11) with a binding domain of *Ct*Lic26A-Cel5E from *Clostridium thermocellum* was selected as a suitable candidate for our experiments. It has a beta-sandwich structure with a concave side forming a substrate-binding cleft that displays affinity for both beta-1,4- and beta-1,3-1,4-mixed linked glucans.[9]

Mimicking the role of CBMs in polysaccharide hydrolysis in nature, we propose that CBMs may assist *in vitro* glycosynthase-catalyzed polymerization reactions. Glycosynthases, mutated glycosyl hydrolases lacking the catalytic nucleophile, have become powerful biocatalysts for the efficient synthesis of oligosaccharides and glycoconjugates.[10,11,12,13] They are able to catalyze glycosyl transfer from glycosyl fluoride donors, with opposite anomeric configuration to the natural substrate of the parental hydrolase, to an acceptor substrate with high yields of glycoside bond formation since products cannot be hydrolyzed. Our group extended the glycosynthase technology to polysaccharide synthesis.[14] Self-condensation of the laminaribiosyl donor by the E134A glycosynthase derived from *Bacillus licheniformis* 1,3-1,4-β-glucanase led to insoluble polymers with a regular structure of alternating β-1,3 and β-1,4 linkages $[4Glc\beta3Glc\beta]_n$ (Figure 2. 1).[14]

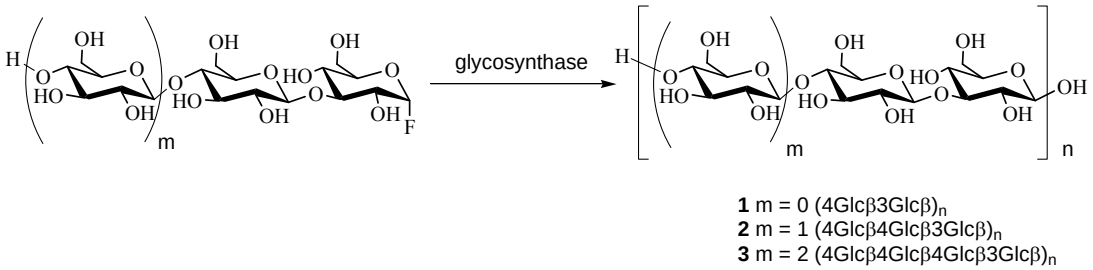

Figure 2. 1: Glycosynthase-catalyzed polymerization to produce 1,3-1,4-β-glucans.

With different glycosyl fluoride donors (Glcβ4)$_m$Glcβ3GlcαF (m = 0-2), artificial mixed-linked β-glucans with different ratios and patterns of β-1,3 and β-1,4 linkages were obtained.[15] Polysaccharide morphology depended on the repeating unit. Thus, (4Glcβ3Glcβ)$_n$ and (4Glcβ4Glcβ4Glcβ3Glcβ)$_n$ generated polysaccharides that were crystalline spherulites, while (4Glcβ4Glcβ3Glcβ)$_n$ polymers formed amorphous precipitates. The degree of polymerization (DP) with the original E134A glycosynthase was approximately constant and independent of donor and enzyme concentrations leading to polymers of average molecular mass (M_w) of 10-12 kDa. However, a linear dependence of M_w with enzyme concentration was observed with the more active E134S glycosynthase mutant. Polysaccharides with M_w of 30 kDa (DP 188) containing a small fraction of products up to 70 kDa were obtained, presenting a high polydispersity index. As the glycosynthase reaction takes place in solution, the polymerization can proceed until the products become insoluble and precipitate. The rate of polysaccharide formation and the amount of high molecular mass polymers produced led to oversaturated solutions and the resultant precipitation of the product entrapped the lower molecular mass polymers. Thus the insoluble polymer had a bimodal profile. Therefore, by increasing the rate of condensation relative to the rate of precipitation (*i.e.*, more active glycosynthase), polymerization can be extended above the apparent solubility limit as long as the product can remain in solution.

With the goal of extending the degree of polymerization, we proposed that CBMs could enhance solubility of the new polymers formed during the polymerization reaction by preventing inter-chain glycan-glycan interactions leading to increased turn-over of the enzyme and insoluble polymers of higher molecular mass that, probably, have low polydispersity indexes. Therefore, CBMs able to bind 1,3-1,4-β-glucans were considered among families 2, 4, 6, 11, 39 and 54, selecting the CBM11 domain from *Clostridium thermocellum* Lic26A-Cel5E.[9] This multimodular enzyme contains GH5 and GH26 catalytic domains that display beta-1,4 and 1,3-1,4-β-mixed linked endoglucanase activity respectively, and a CBM11 with a beta-sandwich structure with a concave face that forms a substrate-binding cleft that displays affinity for both beta-1,4- and beta-1,3-1,4-mixed linked glucans.[9]

Here we investigate the effect of CBM11 on the polymerization reaction catalyzed by the E134S glycosynthase to test the hypothesis that these modules can increase the DP of the product by reducing premature product precipitation. This will be studied by first adding CBM11 at different concentrations to the glycosynthase reaction, and next, the fusion protein E134S-CBM11 where the CBM11 is appended to the catalytic E134S enzyme through a linker spacer.

2.2. EXPERIMENTAL

2.2.1. Reagents and substrates

The donors Glcβ3GlcαF and Glcβ4Glcβ3GlcαF were prepared as previously reported,[16,17] by treatment of peracetylated laminaribiose and 3-O-β-cellobiosyl-α-D-glucose with hydrogen fluoride in pyridine, purification of the peracetylated α-glycosyl fluorides by flash chromatography, and de-*O*-acetylation with sodium methoxide in methanol.

2.2.2. Bioinformatics

The fusion protein composed of the E134S glycosynthase domain and the CBM11 domain linked by a $(PT)_7P$ was designed. Secondary structures of each domain at N-terminus or C-terminus of the fusion protein were predicted using the Secondary Structure Prediction Server (Jpred)[29] and compared with their crystal structures (PDB codes 1GBG and 1VOA for β-glucanase from *Bacillus licheniformis* and CBM11 from *Clostridium cellulolyticum* Lic26A-Cel5E enzyme).

3D structure models based on the construct E134S-linker-CBM11 were generated by means of homology modelling and simulated annealing. The models were based on templates from Bacillus licheniformis beta-glucanase (PDB code 1GBG) (98.6% sequence identity to E134S domain) and from familly 11CBM of Clostridium thermocellum Cel5E 1V0A (98.2% sequence identity to CBM11 domain). No structural template was used for the (PT)7 linker. A pool of 25 3D structures was generated with MODELLER v. 9.8 using a slow level refinement scheme based on simulated annealing molecular dynamics[19]. Those models in which E134S and CBM11 domains laid closer were selected for further analysis. Figures were generated using VMD[20].

2.2.3. Bacterial strains and plasmids

The *E. coli* strains and plasmids used in this study are listed in Table 2. 1. DH5α was used as host strain for routine cloning experiments and BL21 (DE3) Star® as expression strain. Plasmids pET16b and pET21a were used as cloning vectors. Plasmid pET16b-E134S was the source of 1,3-1,4- β-glucanase gene with the E134S mutation (Addington *et al*., 2009)[21] (E134S M_w of 24.3 kDa) while plasmid pET21a-CBM11 provided the gene encoding the family 11 *carbohydrate-binding module* (CtCBM11) from *Clostridium thermocellum*[9] (M_w of 18.4 kDa). Plasmid pUC57 was the source of the synthetic gene E134S-linker-CBM, synthesized by GenScript.

Gene, plasmid or *E. coli* strain	Relevant characteristic(s)	Reference or source
Strains		
DH5α	Host strain for routine cloning experiments	Invitrogen™
BL21 (DE3) Star®	Strain used to express and purify proteins; derived from K-12	Invitrogen™
Genes		
E134S	1,3-1,4-β-glucanase mutant (glycosynthase)	*E. coli*
CBM11	Carbohydrate binding module	*Clostridium thermocellum*
E134S-CBM11	Fusion protein	In situ synthesis, previously undescribed
Plasmids		
pET16b	Expression vector; pBR322 origin, Ap^r	Novagen
pET16b-E134S	pET16b carrying 1,3-1,4-β-glucanase gene with the mutation E134S	T. Addington[21]
pET21a	Expression vector; pBR322 origin, Ap^r	Novagen
pET21a-CBM11	pET21a carrying CBM11	H. Gilbert[9]
pUC57	Expression vector; pMB1 origin	GenScript
pET16b-E134S-CBM11	pET16b carrying the fusion protein E134S-CBM11	This work

Table 2. 1. Genes, plasmids and *E. coli* strains used in this study. Ap^r: ampicillin resistant

2.2.3.1. Construction of E134S-CBM11

The E134S-CBM11 fusion protein was designed to contain:

1) 10xHisTag sequence
2) E134S sequence (214 aa)
3) 15 aa $(PT)_7P$ linker
4) CBM11 sequence (167 aa)

The synthetic gene was cloned into pUC57 with flanking XhoI and BlpI restriction sites. *E. coli* DH5α cells were transformed and positive transformants were verified by DNA sequencing. *E. coli* BL21 (DE3) Star® cells were transformed with the plasmid for protein expression.

2.2.4. Culture conditions and growth media

For DNA manipulation and strain constructions, cultures were grown at 37 ºC in LB medium (Sigma). Ampicillin at 100 $\mu g \cdot mL^{-1}$ was added when it was appropriate. Recombinant *E. coli* BL21 DE3 star strains were also cultured overnight at 37 ºC in LB medium.

2.2.5. Protein expression and purification

Escherichia coli BL21 DE3 Star cells harboring the E134S plasmid were grown in 500 mL LB medium (100 μg/mL ampicillin, 2% glucose) for 8 h at 37 ºC and 250 rpm until late exponential phase. The medium was changed to 500 mL LB containing 1mM IPTG and 100 μg/mL ampicillin for protein expression (16 h at 25 ºC). Cells were harvested by centrifugation and resuspended in 100 mL phosphate buffer 50 mM, pH 7.0, 0.1mM $CaCl_2$ containing 1 mM PMSF. Cells were lysed in a cell-disrupter (Constant Systems, UK) and centrifuged at 23,000 x g. The supernatant containing the His-tagged protein was purified by immobilized metal ion affinity chromatography loading it onto a HiTrap 1mL column (GE Healthcare) previously equilibrated with loading buffer (50 mM phosphate pH 7.0, 0.1 mM $CaCl_2$). The column was rinsed to remove unbound proteins and then eluted with a gradient of 0.5 M imidazole in 50 mM phosphate pH 7.0, 0.1 mM $CaCl_2$ for 60 minutes. Protein fractions were dialyzed twice against 50 mM phosphate pH 7.0, 0.1 mM $CaCl_2$, followed by a last dialysis against water containing 0.1 mM $CaCl_2$.

The fusion protein E134S-CBM11 was expressed and purified in a similar way, however, some conditions were modified. The growth was done at 37ºC for 8 hours and the induction of the protein expression was done at 20 ºC for 6 h (final conditions) and the elution buffer consisted on phosphate buffer 50 mM, pH 7.0, 200 mM NaCl, 0.1 mM $CaCl_2$.

CBM11 was cloned in a pET16b vector. *E. coli* BL21 DE3 Star cells harboring the plasmid were grown in 500 mL LB medium (50 μg/mL ampicillin, 2% glucose) for 12 h at 37 ºC and 250 rpm until late exponential phase. The medium was changed to 500 mL LB containing 1 mM IPTG and 50 μg/mL ampicillin for protein expression (5.5 h at 21ºC). The cells were harvested by centrifugation and resuspended in 75 mL TALON buffer (50 mM Tris-HCl pH 8.0, 300 mM NaCl) containing 1 mM PMSF. Cells were lysed in a cell-disrupter (Constant Systems, UK) and centrifuged at 23,000 x g. The His-tagged protein was purified by immobilized metal ion affinity chromatography. The supernatant was loaded onto a HiTrap 5 mL column (GE Healthcare) previously equilibrated with loading buffer (TALON). The column was rinsed to remove unbound proteins and then eluted in a three step-gradient with 10%, 30% and 100% 100 mM imidazole in TALON buffer. Protein fractions were dialyzed three times against TALON buffer.

In all three cases the proteins were >95% homogeneous as judged by SDS-PAGE. The concentration of E134S was determined by absorbance at 280 nm using an extinction coefficient of $3.53 \cdot 10^5\ M^{-1}\ cm^{-1}$. For the fusion protein E134S-CBM11 and for CBM11 the concentration was determined by Bradford and BCA. E134S and E134S-CBM11 were lyophilized for storage and redissolved prior to use. No degradation of the fusion protein was observed after lyophilization

conserving the same activity than the non-lyophilized one. However, CBM11 had to be expressed and purified before its use and it was conserved in solution at 6 ºC.

2.2.6. Enzyme Kinetics for the E134S glycosynthase mutant and the E134S-CBM11 fusion protein

The trisaccharidyl fluoride (Glcβ4Glcβ3GlcαF) donor (0.05 – 2.00 mM) and the 4-nitrophenyl β-D-glucoside acceptor (20 mM) were dissolved in phosphate buffer (50 mM, pH 7.0) and $CaCl_2$ (0.1 mM). The reaction was developed in a 96 wells plate. After pre-incubation of the plate at 35 ºC for 5 minutes, reactions were initiated by addition of the enzyme (1.58 μM) and kept at 35 ºC. Aliquots were withdrawn at regular time intervals, diluted 1:10 with formic acid 2% (v/v) and analyzed by HPLC (Agilent equipment, Nova-Pak® C18 column, 4 μm, 3.9 × 150 mm from Waters, 1 mL/min, 14% MeOH in water, UV detector at 300 nm). Chromatographic peaks were assigned by co-injection with independent standards. Initial rates (v_o) were obtained from the linear progress curve of product formation (normalized area *vs* time) and expressed as $v_o/[E]$ in s^{-1}. Kinetic parameters k_{cat}, K_M, and k_{cat}/K_M were calculated by nonlinear regression to the Michaelis – Menten equation.

2.2.7. Enzymatic Polymerization Reactions

Reaction mixtures (0.4 mL) consisted of 30 mg donor substrate (290 mM laminaribiosyl fluoride or 150 mM trisaccharyl fluoride), 80 μL of phosphate buffer (100 mM phosphate, pH = 7.7, and 0.1 mM $CaCl_2$), 160 μL of E134S or E134S-CBM11 protein fusion in their phosphate buffer solution and finally, 150 μL of CBM11 in Talon buffer or TALON buffer. The reactions were run at pH 7.2, 37 ºC and 250 rpm in a microcentrifuge tube for one or three days as indicated. A precipitate was formed during the reaction and the presence of unreacted donor or hydrolysis product was checked by TLC (CH_3CN/H_2O 8:2). The precipitated product was isolated by centrifugation at 27,000 x g for 3 minutes, and it was thoroughly washed with cold water. Finally, the product was freeze-dried to yield water-insoluble polymers as white powders. Supernatants were also lyophilized to recover soluble oligomers. The products were analyzed by HPSEC to determine the polymer parameters (M_w, M_n, M_p, DP, PDI).

2.2.8. Polymer analysis by HPSEC and SEM

2.2.8.1. HPSEC

HPSEC analyses to determine molecular mass profiles were performed on an Agilent 1100 HPLC system equipped with a refractive index detector using a PSS Gram column (8.0 x 300 mm, 100Å, 10 μm) and a PSS GRAM pre-column (9.0 x 50 mm, 100 Å, 10 μm) thermostated at 50ºC, and

DMSO with lithium bromide (5 g/L) as eluent at a flow rate of 0.5 mL/min. The calibration curve was obtained with dextrans as standards (American Polymer Standards Corporation DXT1 – DXT55 kDa, see Appendix A3. 5). Freeze dried polymers and standards were dissolved in DMSO and filtered. From the chromatograms, M_p (molecular mass of the peak maximum), M_w (weight average molecular mass), M_n (number average molecular mass), DP (degree of polymerization), and PDI (polydispersity index) were calculated.

2.2.8.2. SEM

For SEM experiments, the dried product was fixed on a graphite tape, coated with gold/palladium by ion-sputtering, and observed at an accelerating voltage of 10 kV and working distance of 16 mm using a JEOL JSM-5310 microscope.

2.3. RESULTS AND DISCUSSION

The E134S glycosynthase mutant from *B. licheniformis* produced polysaccharides with high molecular weights due to its high catalytic efficiency.[11] For this reason, this mutant was selected as glycosynthase biocatalyst to explore the CBM11 effect on polysaccharides synthesis. E134S glycosynthase mutant was expressed as C-terminus His-tagged protein while CBM11 was expressed as N-terminus His-tagged protein. They were both obtained with the expected molecular weights of 27 kDa (23 mg/L culture) and 19.6 KDa (22 mg/L culture) respectively.

A starting study of the effect of CBM11 on polymerization reactions catalyzed by the E134S glycosynthase was developed using two different substrates. Different concentrations of CBM11 were added to the reactions in order to see the independent effect of this protein domain on the polysaccharide sizes and morphologies. After detecting a relation between the addition of CBM11 and an increase of solubility of the new polysaccharides, a new fusion protein was designed, cloned, subcloned, expressed, purified and finally characterized. Then, the polysaccharides produced by the new fusion protein E134S-CBM11 and the ones produced by the glycosynthase E134S were compared. Finally, reactions with different ratios of fusion protein and additional CBM11 were studied.

2.3.1. Effect of the CBM11 protein domain on polymerization reactions catalyzed by the glycosynthase E134S 1,3-1,4-β-glucanase

Polymerization reactions were carried out with laminaribiosyl fluoride (Glcβ3GlcαF) and 3-*O*-β-cellobiosyl-α-D-glucopyranosyl fluoride (Glcβ4Glcβ3GlcαF) donors at different E134S/CBM concentration ratios (Table 2. 2 and Table 2. 3). As expected, insoluble polymers were obtained with mixed β-1,3-β-1,4 linkages corresponding to $(4Glc\beta3Glc\beta)_n$ and $(4Glc\beta4Glc\beta3Glc\beta)_n$ when using the donors Glcβ3GlcαF and Glcβ4Glcβ3GlcαF, respectively, consistent with the specificity of the enzyme (Figure 2. 2).

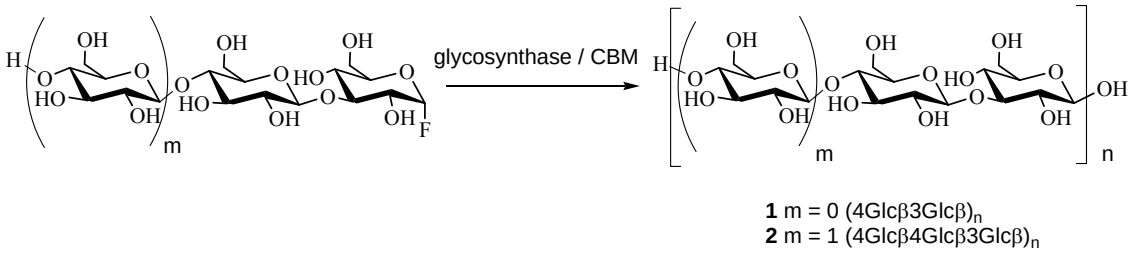

1 m = 0 $(4Glc\beta3Glc\beta)_n$
2 m = 1 $(4Glc\beta4Glc\beta3Glc\beta)_n$

Figure 2. 2. Glycosynthase-catalyzed polymerization to produce 1,3-1,4-β-glucans (polymers **1** and **2**).

- *(4Glcβ3Glcβ)$_n$, E134S/CBM*

Using the disaccharide donor and low enzyme activity, insoluble polymer yields did not exceed 70% after 1 and 3 days in all cases (polymers **1**-**5**, Table 2. 2). The soluble fraction contained soluble polymers and laminaribiose from donor hydrolysis. Molecular mass distributions of the insoluble polymers presented bimodal profiles (Figure 2. 3). Polymer **1** obtained without CBM11 showed two peaks with a molecular mass M_p of 16 kDa (DP 100) and 42 kDa (DP 260), respectively, corresponding to M_w of 16 kDa with a degree of polymerization of about 100 glucosyl units. In the presence of equimolar amount of CBM11 (polymer **2**) and in excess with respect to E134S (polymers **3** and **4**) Mp values were shifted to 21 and 44 kDa respectively. The resulting average Mw value was about 20 kDa, which corresponds to insoluble polymers of DP 123 glucosyl units.

		Glcβ3GlcαF 1 day					
Entry	**Molar Ratio E134S/CBM11**	**M_w (kDa)**	**n (DP)[a]**	**M_n (kDa)**	**Yield (%)**	**PDI**	**M_p (kDa)**
1	1:0	16	50 (100)	11	45	1.6	42, 16
2	1:1	17	53 (105)	10	48	1.7	43, 15
3	1:2	23	70 (140)	18	52	1.4	40, 21
4	1:3	20	62 (123)	11	69	1.5	44, 21
		Glcβ3GlcαF 3 days					
5	1:0	17	53 (105)	9	56	2.0	44, 17

Table 2. 2. Polymerization reactions of donor Glcβ3GlcαF by E134S/CBM. [a] n: number of disaccharyl donor units in the polymer, DP: degree of polymerization expressed as glucosyl units. Conditions: [Donor] = 290 mM. E134S: 0.21 U (for the reference glycosynthase reaction Glcβ4Glcβ3GlcαF + GlcpNP), [CBM11] = 0 – 360 μM), phosphate buffer pH 7.0, 0.1 mM $CaCl_2$, 37 ºC. Products analyzed after 1 or 3 days of reaction.

.

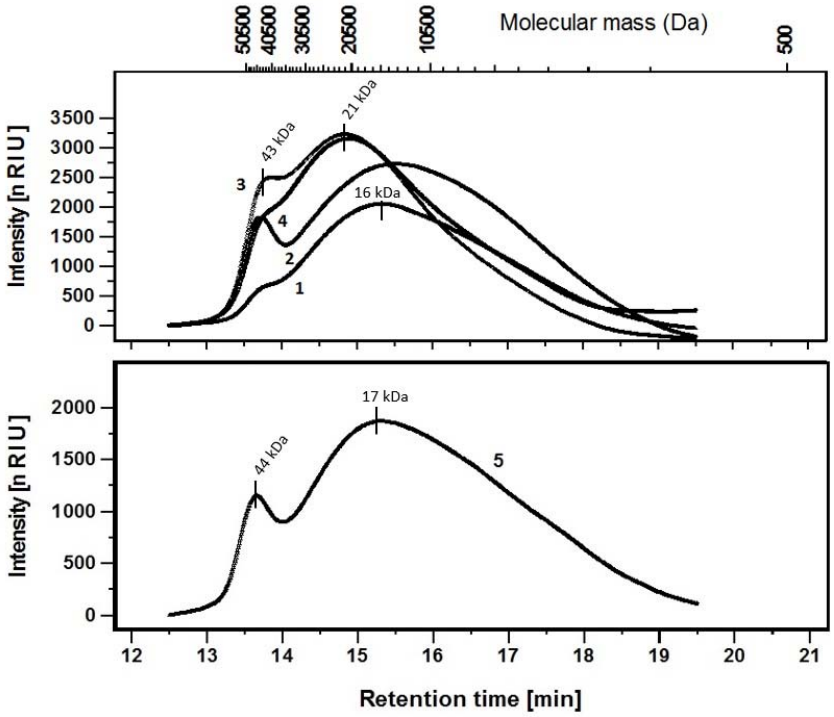

Figure 2. 3. HPSEC chromatograms of (Glcβ3Glcβ)$_n$ polymers **1** – **5** obtained under different conditions with E134S/CBM. Labels correspond to entries in Table 2. 2 and M_p values (maximum of the peaks) are indicated in kDa.

Moreover, the presence of CBM11 had an important effect on morphology (Figure 2. 4). Polymer **1** revealed the characteristic spherulitic morphology of polymers synthesized from laminaribiosyl fluoride, with an average diameter of 7-10 μm.[14] The spherulite formation is a spontaneous self-assembling process during the enzymatic polymerization since spherulites are directly observed by SEM after filtration and lyophilization of the precipitate. Polymer **2**, produced with an equimolar concentration of E134S and CBM, presented a similar morphology. However, when increasing the ratio of CBM, less spherulites were observed in polymer **3,** and polymer **4** contained no spherulites but an amorphous morphology. Therefore, the CBM extends the glycosynthase-catalyzed polymerization yielding up to 25% larger polymers probably due to disruption of the interaction between nascent polysaccharides resulting in increased solubility of the products. In addition to obtaining larger insoluble polymers, the CBM interferes with polysaccharide assembly to form spherulites. This *in vitro* effect resembles the disruption of the structure of crystalline polysaccharides by some CBMs. This function was first documented for the N-terminal family 2a CBM of Cel6A from *Cellulomonas fimi*.[22] The CBM mediated non-catalytic disruption of the crystalline structure of cellulose and enhanced the degradative capacity of the catalytic module. This function has not been described for CBM11 with respect to β-glucanase hydrolytic activity.

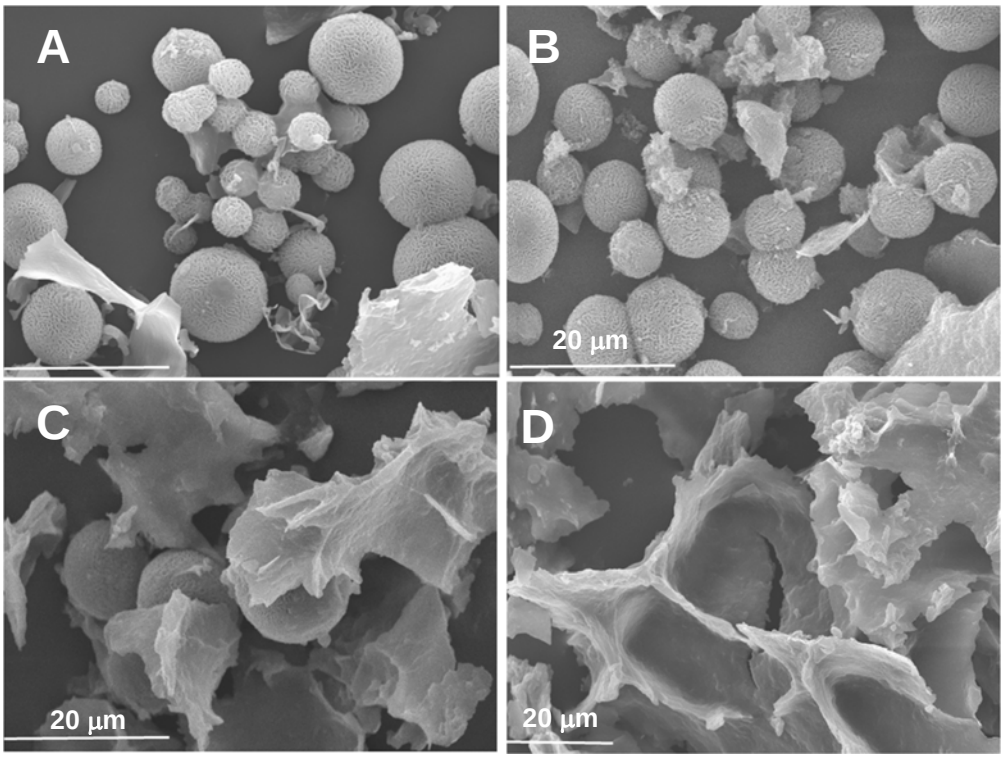

Figure 2. 4. SEM micrographs of freeze-dried polymers (Glcβ3Glcβ)$_n$ **1** - **4** (A - D).

- *(4Glcβ4Glcβ3Glc)$_n$, E134S/CBM*

Using the trisaccharyl donor, insoluble polymers **6** – **11** were obtained under the same conditions (Table 2. 3). As expected, due to the higher reactivity of the trisaccharyl donor compared to disaccharyl donor, yields of insoluble polysaccharides by E134S were higher reaching 82% yield after one or three days either at high or low enzyme activity (entries **6** and **9**, respectively). The molecular mass distribution of these two polymers presented bimodal profiles with M_p values of 20 and 40 kDa (Figure 2. 5). The M_w was 18 kDa (PDI 1.9) which corresponds to insoluble polymers with a degree of polymerization of about 110 glucosyl units. The liquid fraction after the reaction contained a small amount of soluble polymers, with no donor trisaccharide (Glcβ4Glcβ3GlcαF or Glcβ4Glcβ3Glc) evident, indicating that transglycosylation was complete and no hydrolysis occurred. Interestingly, with a 1:4 E134/CBM ratio the percentage of soluble polymers increased to 46% after 24 hours (entry **8**) and by three days, most of the polymers were found in the insoluble form (entry **10**). With E134S/CBM ratios from 1:0 to 1:4, the amount (yield) of insoluble polysaccharides decreased with a corresponding increase in the yield of soluble polysaccharides. After longer incubation times (3 days) most of the polysaccharides became insoluble (yields of 90%). The transient solubility of the synthesized polymers, after one day, did not affect the molecular mass of the polymers. With excess of CBM (entries **10** and **11**),

insoluble polymers had M_w values of around 20 kDa which is similar to polymer **9** produced in the absence of CBM. Most probably the trisaccharide donor was quickly self-condensed by the enzyme, polymers were elongated very fast and, although they remained soluble (oversaturated) due to the presence of CBM11 for one day, the reaction was already complete. The appearance of insoluble polysaccharides after three days reflected the gradual displacement of CBMs from the polymers, which was mediated by interactions between the glucan chains.

		Glcβ4Glcβ3GlcαF 1 day (E = 2.6 U)										
Entry	**Molar Ratio E134S/ CBM**	**Insoluble fraction**						**Soluble fraction**				
		M_w (kDa)	**n (DP)[a]**	M_n (kDa)	**yield** (%)	**PDI**	M_p	M_w (kDa)	**n (DP)[a]**	M_n (kDa)	**yield** (%)	**PDI**
6	1:0	18	37 (111)	11	82	1.9	20, 40	20	41 (123)	6	8	3.4
7	1:1	18	37 (111)	11	79	1.7	21, 40	13	27 (80)	4	9	3.2
8	1:4	17	35 (105)	11	51	1.5	18	16	33 (99)	8	46	1.6
		Glcβ4Glcβ3GlcαF 3 days (E = 0.21 U)										
9	1:0	19	39 (117)	11	82	1.7	22, 40	-	-	-	6	-
10	1:4	22	45 (136)	13	92	1.8	20, 40	-	-	-	4	-
11	1:6	18	37 (111)	11	92	1.6	18	-	-	-	-	-

Table 2. 3. Polymerization reaction of donor Glcβ4Glcβ3GlcαF by E134S/CBM11. [a] n: number of trisaccharyl donor units in the polymer, DP: degree of polymerization expressed as glucosyl units. Conditions: [Donor] = 150 mM; for polymers **6** – **8**, E134S: 2.6 U (for the reference glycosynthase reaction Glcβ4Glcβ3GlcαF + GlcpNP), for polymers **9** – **11**, E134S: 0.21 U, phosphate buffer pH 7.0, 0.1 mM $CaCl_2$, 37 ºC.

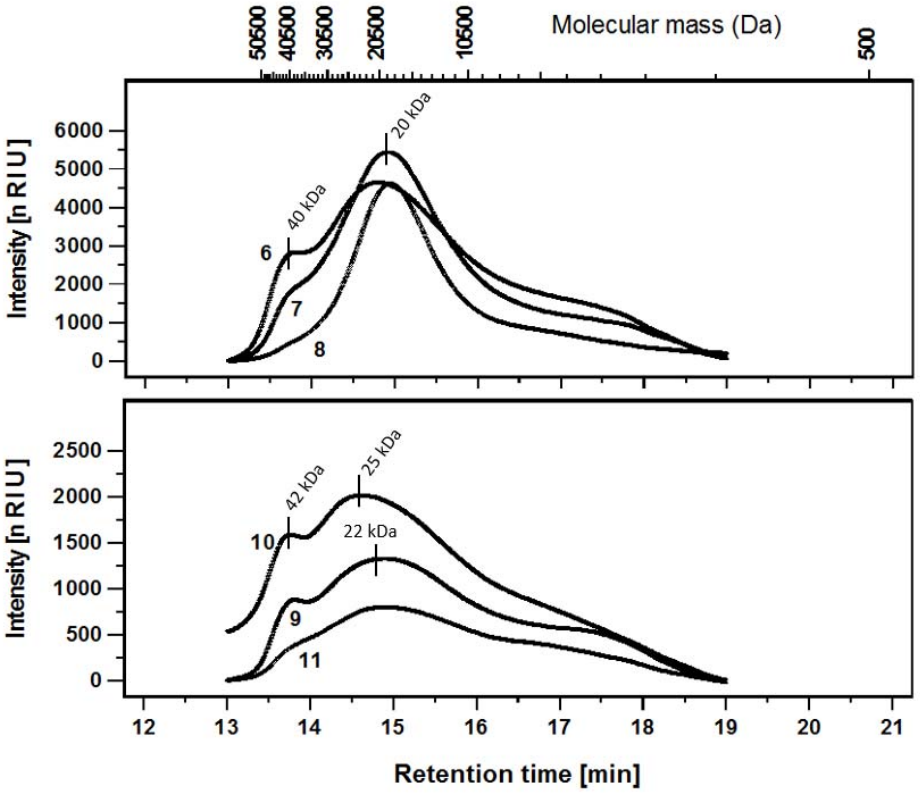

Figure 2. 5. HPSEC chromatograms of $(4Glc\beta4Glc\beta3Glc\beta)_n$ polymers **6** – **12** obtained under different conditions with E134S/CBM. Labels correspond to entries in Table 2. 3 and M_p values (maximum of the peaks) are indicated in kDa.

In conclusion, the addition of CBM11 to the polymerization reaction by E134S has several consequences. Polymerization of the slow-reacting disaccharyl donor gave insoluble polymers in 50-70% yields with 25% higher DP in the presence of CBM, where spherulite formation was clearly prevented (Figure 2. 6). Polymerization reactions with the fast-reacting trisaccharyl donor gave insoluble polymers in higher yields; the presence of CBM slowed down the kinetics of precipitation but had no effect on the molecular mass of the final polymers.

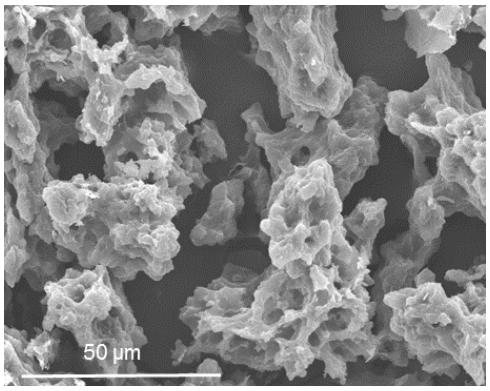

Figure 2. 6: SEM micrographs of freeze-dried polymer **11** $(4Glc\beta4Glc\beta3Glc\beta)_n$ (E134S, CBM).

2.3.2. Fusion protein

2.3.2.1. Design

Since CBMs are often appended to glycosyl hydrolases, the fusion protein consisting of a chimeric enzyme on which the glycosynthase was a appended to a single CBM11 module was designed. We hypothesize that the CBM in the fusion protein may accommodate the polymer as it is synthesized and achieve longer polysaccharides before their precipitation.

The linker between E134S and CBM11 was the first consideration in the fusion protein design. Although proteolysis is observed within protein domains, it is known to occur far more frequently within flexible or less compact regions of the folded polypeptide chain.[22] Inter-domain linkers are particularly susceptible to proteolysis. Unprotected and flexible regions of long linkers might be susceptible to proteolytic cleavage during recombinant protein expression whereas shorter linkers might overcome problems associated with protease degradation. Considering this facts, the design of the linker sequence was based on previous studies of Gustavsson *et al*.[23] and Kavoosi *et al*.[24] On the one hand, Gustavsson designed new proteolytically stable linkers to connect a lipase to a CBM. They considered different candidates with sequences that resembled different naturally occurring linkers. The results showed similar lipase hydrolytic activity for all the fusion proteins and concluded that unless an application is dependent on high flexibility, the use of short linkers should not become a problem. They finally selected a 13 amino acid long linker, composed of prolines and threonines.

On the other hand, Kavoosi studied the fusion between a GFP (Green Fluorescence Protein) and a CBM9, and analyzed the stability of 7 different linkers towards the proteolysis in the *E. coli* host. The protease specificity database MEROPSTM[25] developed to identify potential cleavage sites using genome-based assignment of peptidases and their associated putative specificities[26] was used to screen the linker sequences and assess their proteolytic stability. They concluded that the design of an effective linker had to consider proteolytic stability[27,28] as well as thermodynamic stability and spatial positioning of the fused proteins/domains that may alter expression levels and influence the overall performance of the fusion tag. Kavoosi's best spot consisted on a 15 proline-threonine $(PT)_7P$ sequence linker. We decided to use this $(PT)_7P$ linker for the design of our fusion protein due to its suitable properties.

Most of the CBMs are found in the C-terminus but before designing and cloning it, structural predictions of the fusion protein with E134S or CBM at the N-terminus were performed with the Secondary Structure Prediction Server (Jpred)[29] and compared to the crystal structures of the single proteins.

Visual Molecular Dynamics (VMD) was used to study the three dimensional structure of the protein domain CBM11 from *Clostridium cellulolyticum* (pdb: 1VOA), the E134S β-glucanase mutant from *Bacillus licheniformis* (pdb: 1GBG) and the complex composed of β-glucanase from *Bacillus macerans* crystallized with a trisaccharide in the active center (pdb: 1U0A[30]).

Figure 2. 7 shows the ribbon representation of the three-dimensional structure of *Ct*CBM11[9]. It shows the active-site cleft with only one ligand-binding region containing three Tyr residues at positions 22, 53 and 129 involved in the adhesion of the CBM11 to the glucan polysaccharides.

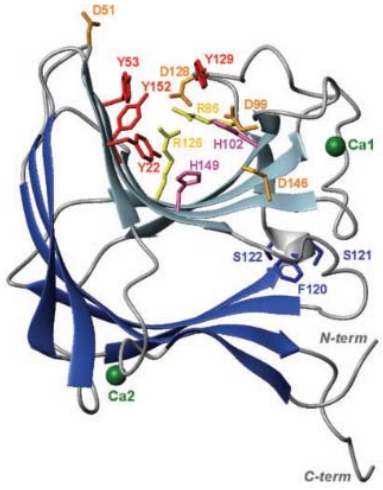

Figure 2. 7: 3D structure of CBM11 protein domain where the calcium ion can be distinguished in green.

Figure 2. 8 shows different views of β-glucanase from *Bacillus licheniformis.* The active-site cleft of the enzyme presents three main residues that form the catalytic triad: a glutamate acting as a nucleophile and an aspartate and another glutamate acting as acid-base residues.

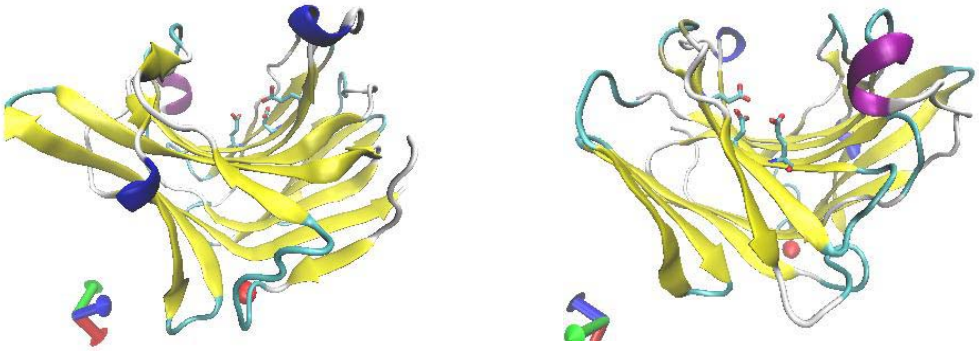

Figure 2. 8: Crystallographic structure of β-glucanase from *Bacillus licheniformis* with the catalytic cleft.

In Figure 2. 9 the structure of β-glucanase from *Bacillus macerans* is represented with a tetrasaccharide substrate binding to the active-site cleft.

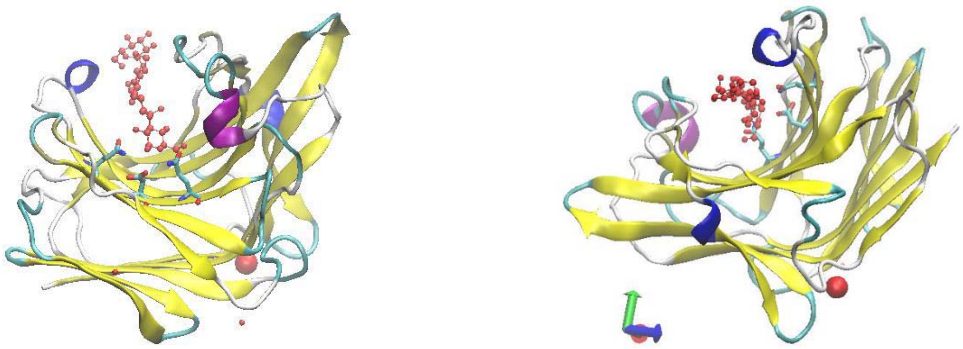

Figure 2. 9: Crystallographic structure of β-glucanase from *Bacillus macerans* binding to a tetrasaccharide substrate.

Figure 2. 10 shows the crystallographic structure of CBM11 and Figure 2. 11 shows the prediction of the secondary structure of CBM11.

Figure 2. 10: Crystallographic structure of CBM11 where SCOP corresponds to a classification of protein structural domains based on similarities of their structures and aa sequences, in this case *Endoglucanase H*. DSSP assigns the secondary structure to the aa of a protein. Site Record specify residues comprising catalytic, co-factor, anti-codon, regulatory or other essential sites or environments surrounding ligands present in the structure. PDB shows the amino acid sequence of the protein.

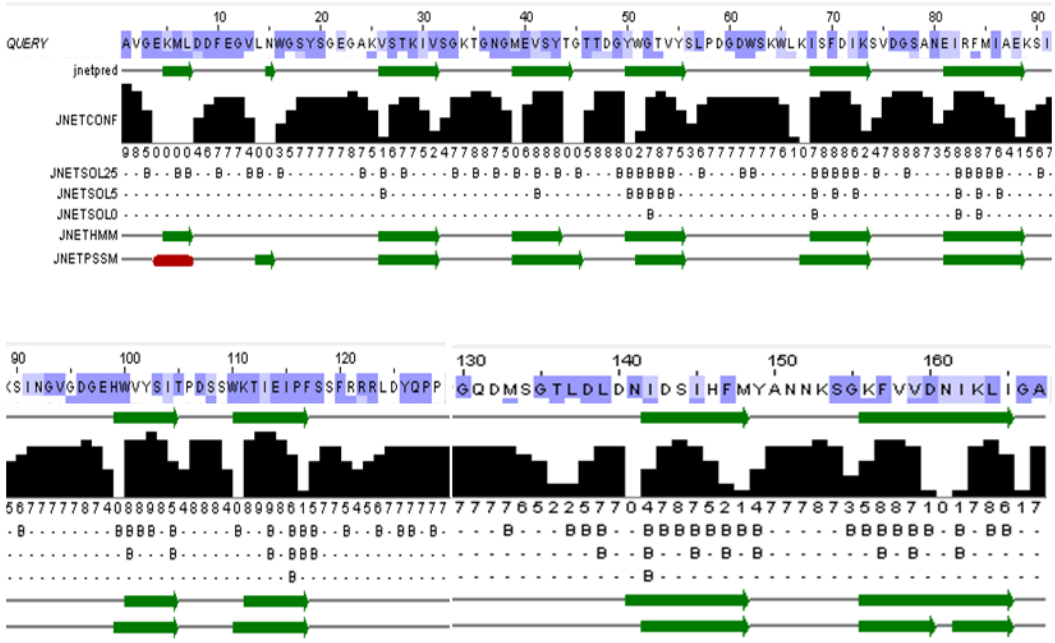

Figure 2. 11: Prediction of the secondary structure of CBM11. QUERY shows the aa sequence of the protein. Jnetpred shows the prediction of the secondary structure of the protein domain regions. JNETCONF indicates the probability of the prediction.

In the crystallographic structure of CBM11 (Figure 2. 10) 12 beta-sheets and 1 alpha-helix are identified. In the prediction of the secondary structure (Figure 2. 11), 11 out of the 12 β-sheets are observed (positions of β-sheets at Table 2. 4) and the α-helix at position 120 is not detected. In conclusion, the results of the prediction program were fair enough and it could be used to predict the secondary structure of the fusion protein E134S-CBM11.

β-sheet	1	2	3	4	5	6
Crystal	4→8	17→21	25→32	37→44	50→55	67→74
Prediction	5→7	15	25→31	39→44	50→55	68→73
β-sheet	7	8	9	10	11	12
Crystal	82→90	96→104	111→116	121→122	142→149	155→165
Prediction	81→88	99→104	110→116	------	142→148	155→165

Table 2. 4: Comparision of β-sheeet structure positions of CBM11 in the crystal structure *vs* the prediction.

The crystallographic structure of the β-glucanase (wild-type) from *Bacillus licheniformis* is presented in Figure 2. 12.

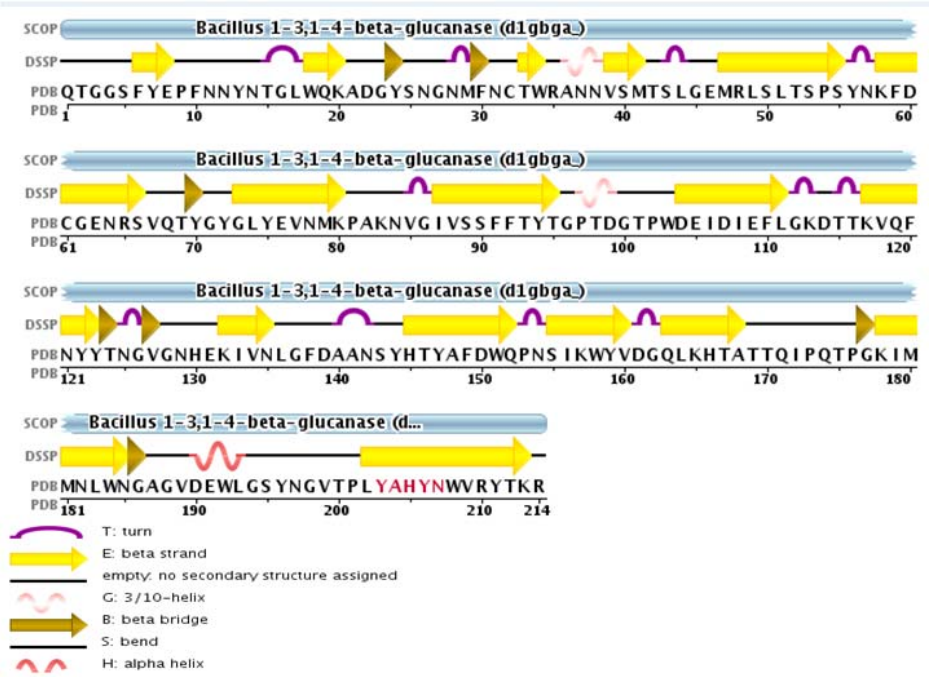

Figure 2. 12: Crystallographic structure of β-glucanase.

The prediction of the secondary structure of the E134S glycosynthase mutant is presented in Figure 2. 13.

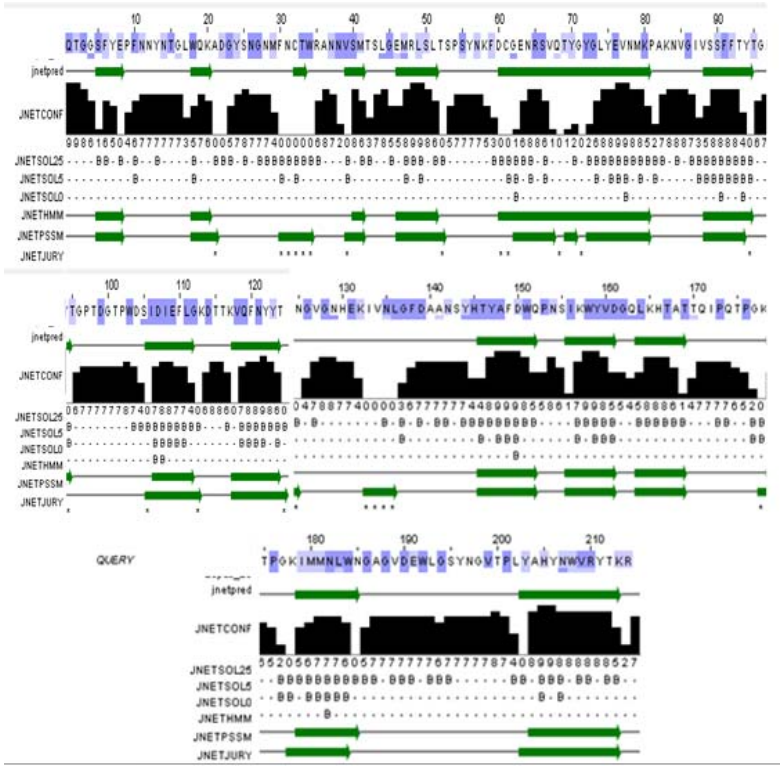

Figure 2. 13: Prediction of the secondary structure of E134S.

In the crystallographic structure of β-glucanase (Figure 2. 12), 16 β-sheets and 3 α-helices are detected. 15 out of 16 β-sheets were predicted (positions of β-sheets at Table 2. 5), however, α-helices at position 38, 98 and 191 were no predicted. Still, the correct prediction percentage was good enough.

β-sheet	1	2	3	4	5	6	7	8
Crystal	6→8	18→20	33→34	39→41	47→55	58→66	73→80	87→95
Prediction	5→8	18→20	32→33	39→41	46→51	60→80		88→94
β-sheet	**9**	**10**	**11**	**12**	**13**	**14**	**15**	**16**
Crystal	104→111	117→123	132→135	145→152	155→160	163→169	178→185	202→213
Prediction	105→111	117→123	------	145→151	155→161	164→169	179→185	202→213

Table 2. 5: Comparision of β-sheeet structure positions of the β-glucanase in the crystal structure *vs* the prediction.

The two possible designs of the new fusion protein consisted of a first construct containing the E134S glycosynthase at the N-terminus, followed by the linker and finally the CBM at the C-terminus or *vice versa*, a second construct consisting of the CBM11 at the N-terminus, followed by the linker and the E134S at the C-terminus. The fusion protein sequence had a total length of 396 amino acids. Predictions with the two possible fusion protein constructs were analyzed comparing them to the secondary structures of CBM11 (Figure 2. 11) and E134S (Figure 2. 13).

In Figure 2. 14 the secondary structure of the fusion protein composed of the E134S at the N-terminus is presented, followed by the linker and the CBM11 at the C-terminus. The comparison of this fusion protein structure *vs* the already predicted secondary structures of the glycosynthase and the CBM11 separately yields four differences: the absence of the three alpha-helices and one beta-sheet is still missing and new differences are not detected. These differences had been already detected when analyzing the predicted glycosynthase secondary structure of the E134S and the corresponding crystallographic structure of the beta-glucanase.

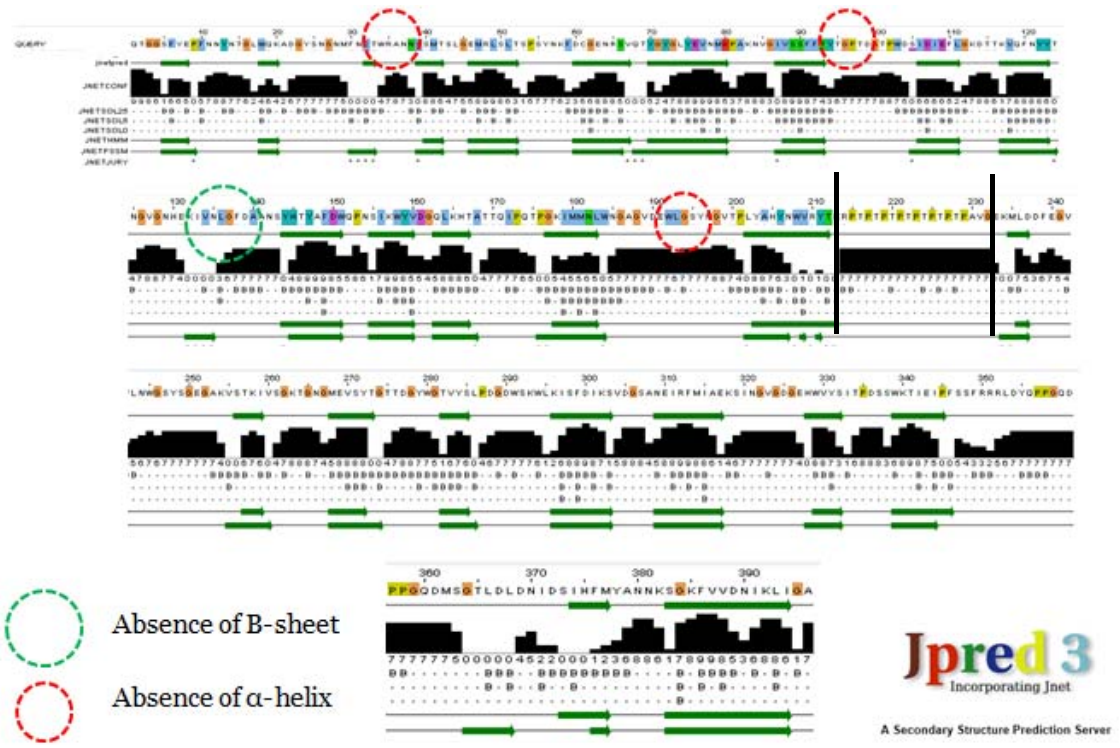

Figure 2. 14: Prediction of the secondary structure of the fusion protein composed of E134S (N-terminus), 15 aa linker and CBM11 (C-terminus).

By contrast, when analyzing the secondary structure of the fusion protein composed of the CBM11 at the N-terminus, followed by the linker and the E134S at the C-terminus some important changes were detected in the secondary structure of the CBM11 protein domain (Figure 2. 15). More specifically, β-sheets 1 and 2 (table 2. 4) disappear and an α-helix structure replaces them instead (from amino acid number 7 to 15). Furthermore, there is a decrease in the number of amino acids that compose the sequence involved in the formation of β-sheet 7.

Figure 2. 15 Prediction of the secondary structure of the fusion protein composed of CBM11 (N-terminus), 15 aa linker and E134S (C-terminus).

In both models the linker sequence was predicted to keep an extended conformation without adopting any secondary structure. Therefore in the fusion protein the E134S glycosynthase and CBM11 were located at the N- and C-termini, respectively (Figure 2. 16). The fusion protein was expressed as an N-terminal His_6-Tagged protein in good yield with a molecular mass of 47089 Da (confirmed by MALDI-TOF MS, demonstrating that no inter-domain occurred during protein expression or purification).

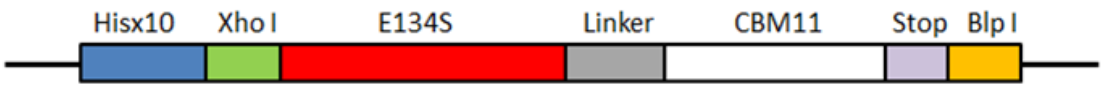

Figure 2. 16. Synthetic gene.

Furthermore, the 3D structure of this construct (E134S-linker-CBM11) was predicted by means of homology modelling (see methods). The structure of the single E134S and CBM11 domains are confidently solved. However, since the linker region is intrinsically disordered, a pool of structures were obtained with different relative orientations between the two domains. Two structures compatible with the catalytic activity of this construct are reported in Figure 2.17. The first model shows the shortest distance between the centers of masses of the domains E134S and

CBM11. This distance between domains is similar to Orzya sativa Chitinase I (PDB: 2DKV) which has a chitin binding domain linked to a GH19 hydrolytic domain through a nonresolved (PT)4P(PS)2 linker. The second model shows the shortest distance between substrate pockets of the E134S and CBM11 domains both facing each other.

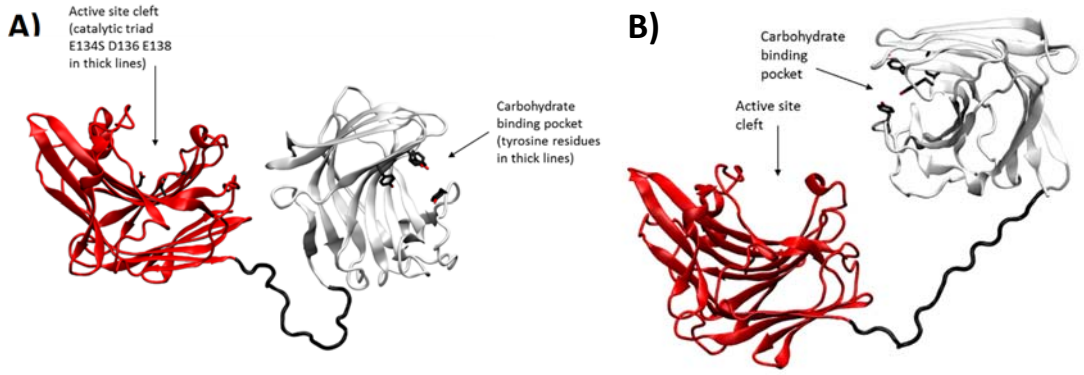

.

Figure 2. 17: E134S-$(PT)_7$-CBM11 3D structure. **A)** Model #1 (Contracted linker configuration); **B)** Model #18 (Extended linker configuration).

2.3.2.2. Fusion protein E134S-CBM11. Vector construction

Cloning

The synthetic gene which codified for the fusion protein E134S-CBM was prepared and supplied by GenScript in a pUC57 vector between XhoI and BlpI restriction sites. It consisted of a 10xHisTag sequence at the N-terminus end, the E134S glycosynthase composed of 214 aa (from the initial Q to the terminal R), the linker sequence composed of 15 aa $(PT)_7P$ and the 167 aa sequence of the CBM11 (from the initial A to the terminal A).

Subcloning

The synthetic gene from pUC57 gene was amplified by PCR using the primer pair FUP and RUP. The PCR-amplified fragment was composed of 1340 bp (lanes 2 and 4, figure 2. 18, A).

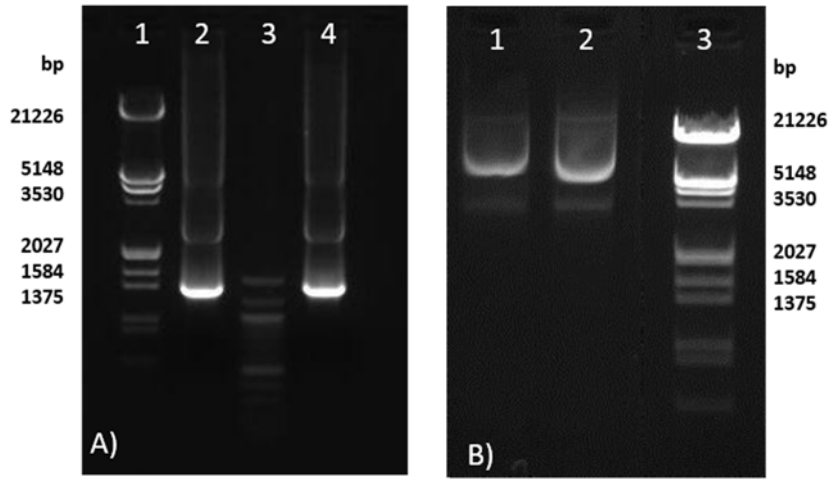

Figure 2. 18: 1% Agarose gels. A) Synthetic gene amplification from pUC57. Lane 1, DNA molecular weight marker III. Lane 3: DNA molecular weight marker XIV. Lanes 2 and 4: PCR-amplification product at T_m = 53ºC. B) Midiprep of vector pET16b. Lane 3, DNA molecular weight marker III. Lanes 1 and 2, purification product.

After PCR-amplification and further purification through DNA band extraction from the agarose gels, the fragments containing the synthetic gene and the pET16b plasmid were digested with Xho I and Blp I restriction enzymes. A first digestion was performed with Xho I *overnight* followed by a second 12 hours-long digestion with Blp I. The result after both digestions is presented in Figure 2. 19. The agarose gel shows a band of 1200 bp (Figure 2. 19, lane 1) corresponding to the digested synthetic gene. Another band of 5650 bp corresponds to the digested pET16b vector (Figure 2. 19, lane 2). Both bands were removed from the agarose gel and were purified by use of a Miniprep kit GenElute.

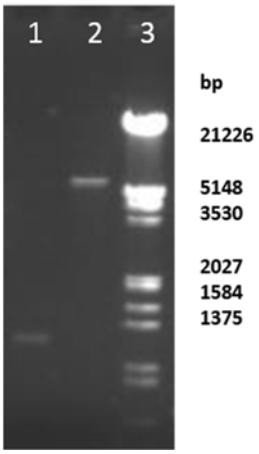

Figure 2. 19: 1% Agarose gel. Lane 3, DNA molecular weight marker III. Lane 1, insert digestion. Lane 2, vector digestion. 2 μL of simple were loaded to check the results of the digestion.

Both vector and insert were mixed and ligated using the T4 ligase. Different vector/insert ratios were performed (See table 2. 6) and following ligation, chemically component E. coli cells were transformed and the resulting transformant colonies were screened for insertion by PCR using primers (T7 promoter and pET16b-Reverse) flanking the insertion site (Figure 2. 20).

PCR of colonies-Ligation analysis			
Ligation	Vector/Insert	Number of transformant colonies	Number of colonies with insert
1	1:3	1	1
2	1:5	11	0
3	1:6	4	2
4	1:7	0	-
5	1:10	0	-

Table 2. 6: Screening of ligation by PCR.

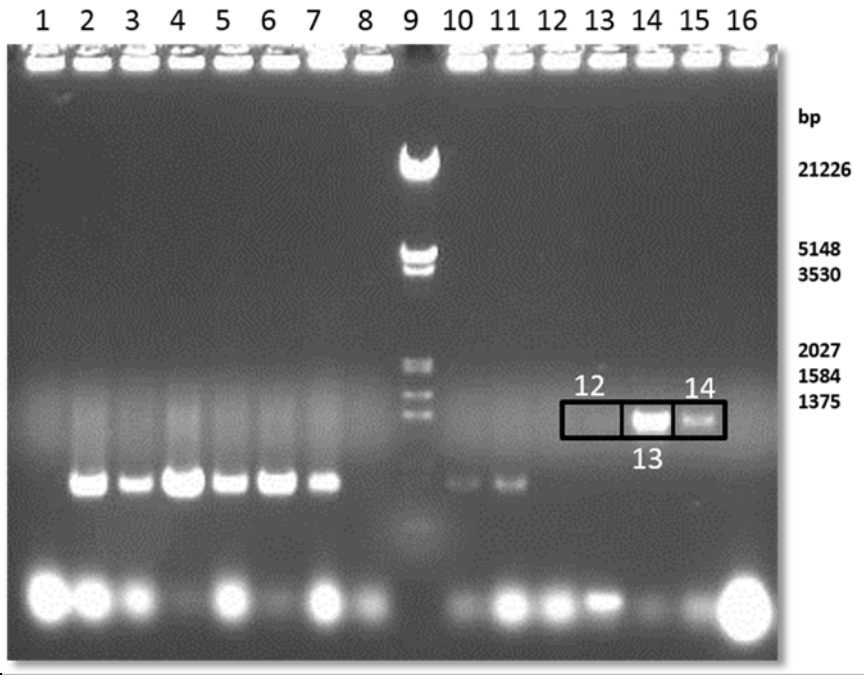

Figure 2. 20: 1% Agarose gel of flanking primer insertion screen of the 16 transformant colonies. Lanes 1 – 8 and 10 -16, transformant colonies. Lane 9, DNA molecular weight marker III. Note gene insertion bands in lanes 12, 13 and 14.

The colonies with insert (Figure 2. 20, lanes 12, 13 and 14) presented a band corresponding to 1360 bp. One of these colonies was obtained after ligation with a ratio of vector/insert 1:3 and two of the colonies with a ratio 1:6. Colonies screened positive for the synthetic gene insertion were subsequently bulked up for DNA purification and nucleotide sequence. The three ligations were confirmed by performing two different digestion strategies. On the one hand, a digestion with Xho I and Blp I restriction enzymes and on the other hand, a digestion with Xho I and Hind

III yielding a fragment of 1442 bp composed of the synthetic gene and a first part of the vector and another fragment of 5416 bp that corresponds to the remaining vector.

The plasmidic DNA of the three colonies containing the insert was sequenced to confirm the correct sequence of the nucleotides corresponding to the vector pET16b-synthetic gene. The sequencing reaction was performed with the kit *BigDye® Terminator* v3.1 and the resulting fragments were analyzed by capillary electrophoresis at the Sequencing Service of the Parc Científic of the University of Barcelona. The sequence of the fusion protein was confirmed (See Appendix, Fusion protein sequence). The vector from colony 14 was further used for the fusion protein expression and purification.

2.3.2.3. Expression and purification of the fusion protein

E. coli BL21 (DE3) competent cells were used as a host for the production of the fusion protein. Transformants were grown for 9 hours at 37 ºC and 250 rpm in 1 L LB medium containing 100 µg/mL ampicillin in a 2 L Erlenmeyer flask. The volume of the culture was splitted in three and expression was induced by addition of IPTG and continued at 20 ºC and 150 rpm for 6, 9 and 16 hours respectively. Cells were harvested by centrifugation, resuspended in phosphate buffer 50 mM, pH 7.5, 200 mM NaCl, 0.1 mM $CaCl_2$, and after lysed with a cell-disrupter, centrifuged at 23,000 x g. The pellets were analyzed to determine if the overexpression of fusion protein generates insoluble fractions of protein (Figure 2. 21).

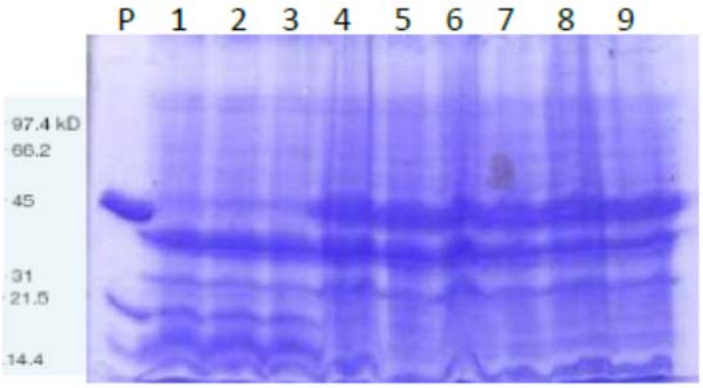

Figure 2. 21: 14% SDS-PAGE with Coomassie stain of 3 the insoluble fractions obtained during the expression of the fusion protein. Lane P, fusion protein from the supernatant obtained after the lysis. Lanes 1-3, insoluble fraction from 6 hours of induction. Lanes 4-6, insoluble fraction from 9 hours of induction. Lanes 7-9, insoluble fraction from 16 hours of induction.

No protein was observed in the insoluble fraction at 6 hours of induction. After 9 hours, though, the overexpression of the protein caused the precipitation of a considerable amount of protein losing yield. To avoid protein loss, 6 hours was set as the best induction time.

To purify the fusion protein, an IMAC purification was performed by the use of a 1 mL HisTrap^{TM} column. The intracellular soluble fraction was then injected into a precharged Ni^{2+} Sepharose HisTrap^{TM} 1 mL column. The column was subsequently washed with phosphate buffer 50 mM-0.1 mM $CaCl_2$-200 mM NaCl and then a linear imidazol gradient ranging from 0 to 500 mM for 60 minutes was applied. Subsequent elution of the bound fusion protein is shown by chromatogram below (Figure 2. 22). Note that the primary elution peak is of nonspecifically bound proteins whereas the secondary elution peak is of the fusion protein E134S-CBM11.

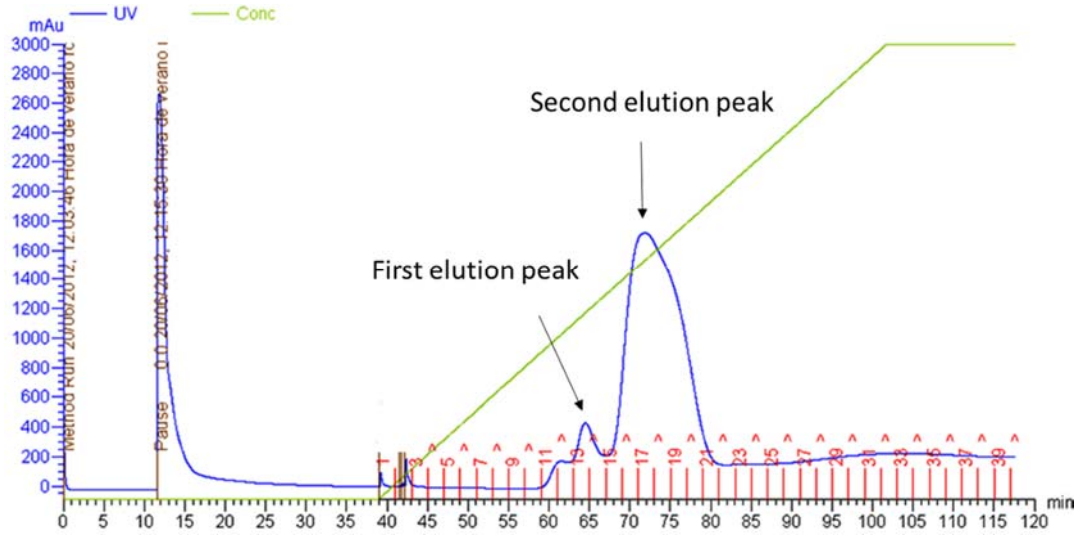

Figure 2. 22: Chromatogram of the fusion protein E134S-CBM11 affinity chromatography purification. The blue line represents 280nm absorbance units while the green line shows the linear imidazole gradient. The elution tube number are shown in red. Note the primary elution peak at 64 mL that corresponds to non-specifically bound proteins whereas the secondary elution peak at 68 mL corresponds to the fusion protein.

In order to evaluate the His-tag purification efficiency, samples of each of the purification steps were saved for subsequent analysis by SDS-PAGE with Coomassie stain (Figure 2. 23).

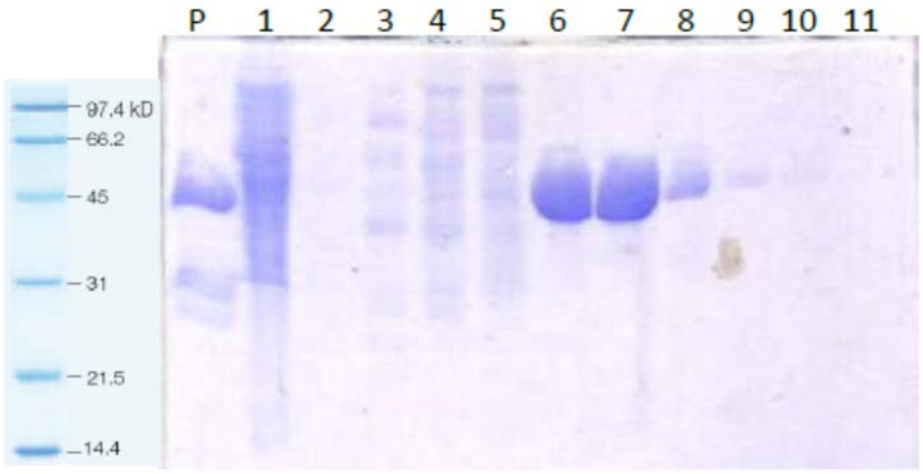

Figure 2. 23: 14% SDS-PAGE with Coomassie stain of the E134S-CBM11 protein purification shown in the chromatogram above (Figure 2. 22). Left lane, low range protein standard. Lane P, impure positive sample, Lane 1, impure protein standard, Lane 2, column flow-through, Lanes 3-5, primary elution peak (tubes 12, 13 and 14), Lanes 6-10, correspond to secondary elution peak (tubes 16, 18, 21, 27 and 37, respectively). Lane 11, blank.

Samples of tubes 16 – 21 (lanes 6 -8, Figure 2. 23) containing the fusion protein were dialyzed in 3 x 1L 50 mM phosphate buffer-0.1 mM $CaCl_2$-200 mM NaCl at pH 7.5. The quantity of fusion protein was calculated by Bradford assay, resulting in 64 milligrams of purified protein from a 1 liter culture. The protein sample was analyzed by MALDI-TOF (See appendix, Figure A2. 1). The chromatogram shows a peak of 47089 Da that corresponds to the monocharged fusion protein. A second peak of 23549 Da corresponds to the doubly charged protein.

2.3.2.4. Fusion protein characterization.

The fusion protein E134S-CBM11 was characterized by performing the glycosynthase reaction between the donor Glcβ4Glcβ3GlcαF and the acceptor GlcβPNP (Figure 2. 24).

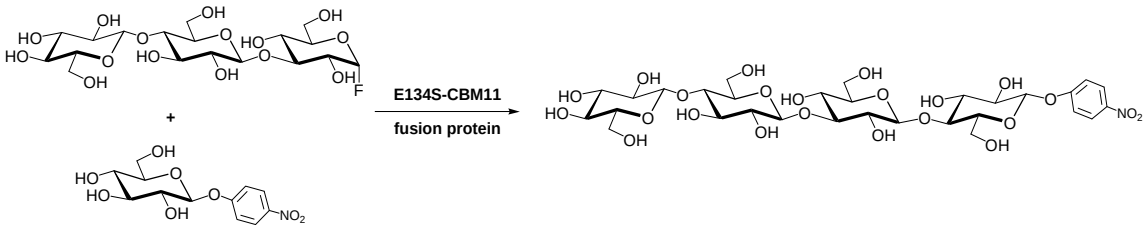

Figure 2. 24: Formation of the glycosidic bond during the activity assay. Conditions: 20 mM GlcPNP, 2 mM Glcβ4Glcβ3GlcαF, 35 ºC, 50 mM phosphate buffer-0.1 mM $CaCl_2$, pH 7.0.

Transglycosylation rates at constant acceptor concentration (20 mM) and different donor concentrations (0 – 2 mM) showed that tetrasaccharide product formation followed saturation kinetics (Figure 2. 25) with an apparent k_{cat} value of 16.6 min^{-1} and K_M of 0.25 mM (k_{cat}/K_M of 66.2 min^{-1} mM^{-1}) (Table 2. 7). Compared to E134S, the k_{cat} of fusion protein is two-fold lower and the K_M value is 2.5-fold higher, resulting in a 7-fold decrease in k_{cat}/K_M. Therefore, the fusion protein is active but this construct could be optimized.

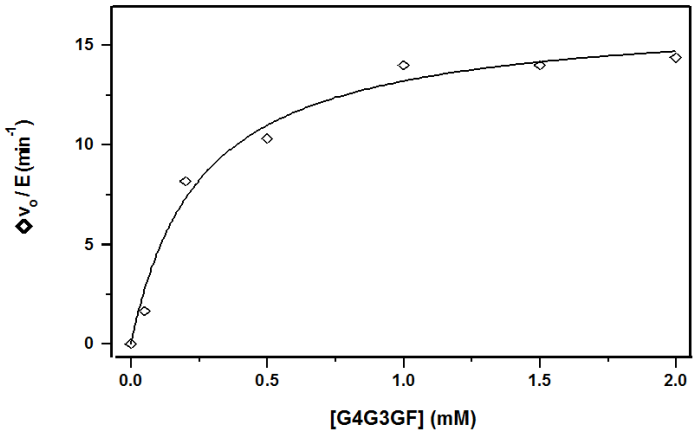

Figure 2. 25. Reaction kinetics of the fusion protein E134S-CBM11 (1.58 µM). Cellobiosyl fluoride donor and 4-nitrophenyl β-D-glucopyranoside acceptor (20 mM), 50 mM phosphate buffer-0.1 mM $CaCl_2$ at pH 7.2 and 35 °C.

Enzyme	k_{cat} (min^{-1})	K_M (mM)	k_{cat}/K_M (M^{-1} s^{-1})
E134S	40.8 ± 0.6	0.09 ± 0.01	$7.55 \cdot 10^3$
E134S-CBM11	16.6 ± 0.98	0.25 ± 0.06	$1.10 \cdot 10^3$

Table 2. 7: Kinetic parameters for the glycosynthase reactions Glcβ4Glcβ3GlcαF + GlcpNP catalyzed by E134S and E134S-CBM11 fusion protein. Conditions: 0.1 – 2.0 mM Glcβ4Glcβ3GlcαF donor, 50 – 100 mM phosphate buffer pH 7.2, 0.1 mM $CaCl_2$ and 35 ºC. For E134S, 7.8 mM GlcPNP acceptor and 0.1 µM enzyme were used. For E134S-CBM11, 20 mM GlcpNP acceptor and 1.58 µM enzyme were used.

2.3.2.5. E134S-CBM11 vs E134S

Polymerization reactions of the trisaccharyl donor with E134S-CBM11 and E134S were compared, using enzyme activities standardized against the glycosynthase reaction between Glcβ4Glcβ3GlcαF and GlcPNP (Table 2. 8).

Insoluble polysaccharides synthesized by E134S were obtained in 60% yields after one day (Table 2. 8, entries **12** and **14**). Since the enzyme concentration used was relatively low if compared to reaction 6 (Table 2. 3), soluble polymers and unreacted donor were recovered. The molecular mass distribution presented a bimodal profile (polymers **12** and **14,** Figure 2. 26) at M_p values of 17 kDa and around 7 KDa. The M_w value of 15 kDa corresponds to insoluble polymers with DP

of 90 glucosyl units. Interestingly, reactions catalyzed by E134S-CBM11 gave insoluble polysaccharides in 68% yield at low enzyme activity but quantitative yield at high enzyme activity (Table 2. 8, entries 13 and 15). Molecular mass distribution of polymer **15** presented a bimodal profile (M_p of 39 and 21 kDa) resulting in a M_w value of 20 KDa composed of 121 glucosyl units (Figure 2. 26). In these conditions, E134S-CBM11 generated slighly longer insoluble polysaccharides compared to E134S (≈33%; **14**). But the effect of the CBM11 appended to the E134S is not conclusive since these DP values were also obtained at higher E134S concentrations (polymers **6** and **9**). The morphology of polymer **15** (Figure 2. 27) showed the typical amorphous precipitate of the $(4Glc\beta4Glc\beta3Glc\beta)_n$ structures obtained by E134S.[15,14]

Entry	Enzyme	activity (U)[a]	M_w (kDa)	n (DP)[b]	M_n (kDa)	Yield (%)	PDI	M_p (kDa)
12	E134S	0.38	15	30 (90)	8	57	1.7	17, 4
13	E134S-CBM11	0.35	18	37 (110)	9	68	1.9	39, 19
14	E134S	0.94	15	30 (90)	9	60	1.7	17, 7
15	E134S-CBM11	0.85	20	40 (121)	10	100	2.0	39, 21

Table 2. 8. Polymerization reactions of donor Glcβ4Glcβ3GlcαF by E134S *vs* E134S-CBM11 fusion protein. [a] enzyme activity for the reference glycosynthase reaction Glcβ4Glcβ3GlcαF + GlcpNP. [b]n: number of trisaccharyl donor units in the polymer, DP: degree of polymerization expressed as glucosyl units. Conditions: [Donor] = 150 mM, phosphate buffer pH 7.0, 0.1 mM $CaCl_2$, 37 ºC, 24 h.

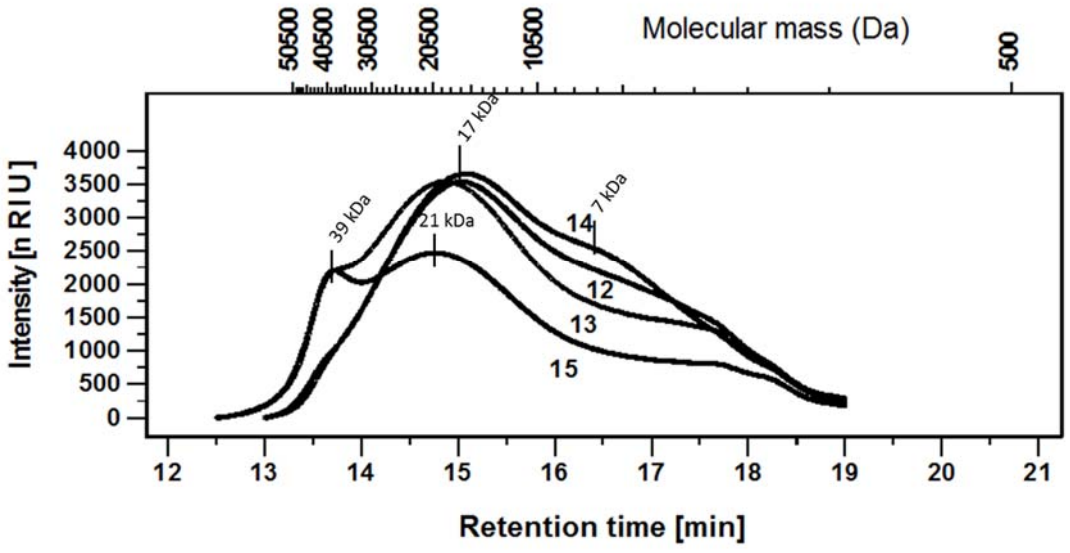

Figure 2. 26. HPSEC chromatograms of $(4Glc\beta4Glc\beta3Glc\beta)_n$ polymers **12** – **15** where the reactivity of E134S and E134S-CBM11 are compared under the same specific activity. Polymers **12** and **14** were synthesized with E134S while polymers **13** and **15** were obtained with E134S-CBM11. Labels correspond to entries in Table 2. 8 and M_p values (maximum of the peaks) are indicated in kDa. [Donor] = 150 mM.

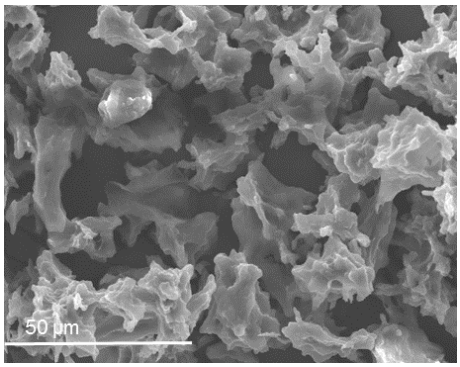

Figure 2. 27: SEM micrographs of freeze-dried polymers $(4Glc\beta4Glc\beta3Glc\beta)_n$ where A corresponds to polymer **15**

2.3.2.6. Effect of the CBM11 protein domain on polymerization reactions catalyzed by the fusion protein E134S-CBM11

When CBM11 was added to the polymerization reactions performed by E134S-CBM11, no significant change in product profile was observed with respect to DP, M_p, M_w, and morphology (Table 2. 9, Figure 2. 28 and Figure 2. 29).

		Glcβ4Glcβ3GlcαF 1day					
Entry	**Molar Ratio E134S-CBM11 /CBM11**	M_w (kDa)	**n (DP)[a]**	M_n (kDa)	**Yield** (%)	**PDI**	M_p (kDa)
16	1:1	17	35 (105)	9	91	1.9	
17	1:2	17	35 (105)	12	87	1.9	39, 18
18	1:3	16	33 (99)	8	81	1.9	
		Glcβ4Glcβ3GlcαF 3 days					
19	1:3	18	37 (111)	9	80	1.9	39, 18
20	1:6	17	35 (105)	8	91	2.0	

Table 2. 9. Polymerization reactions by E134S-CBM11 fusion protein with added CBM11 (Glcβ4Glcβ3GlcαF donor). [a] n: number of trisaccharyl donor units in the polymer, DP: degree of polymerization expressed as glucosyl units. Conditions: [Donor] = 150 mM, enzyme 0.5 U (for the reference glycosynthase reaction Glcβ4Glcβ3GlcαF + GlcpNP), phosphate buffer pH 7.0, 0.1 mM $CaCl_2$, 37 ºC, 24 or72 h.

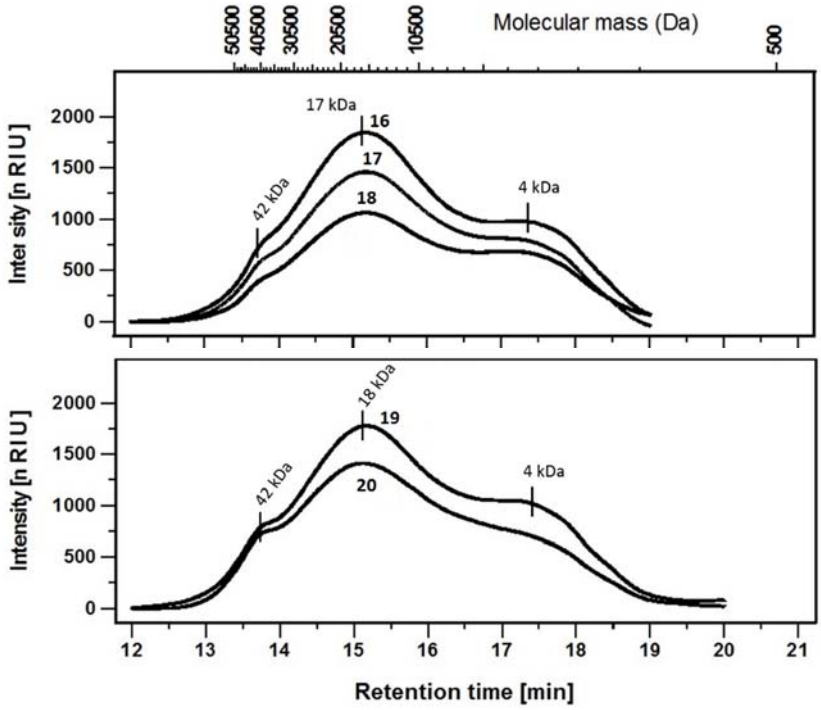

Figure 2. 28. HPSEC chromatograms of $(4Glc\beta4Glc\beta3Glc\beta)_n$ polymers **16** – **20**. Labels correspond to entries in Table 2. 9.

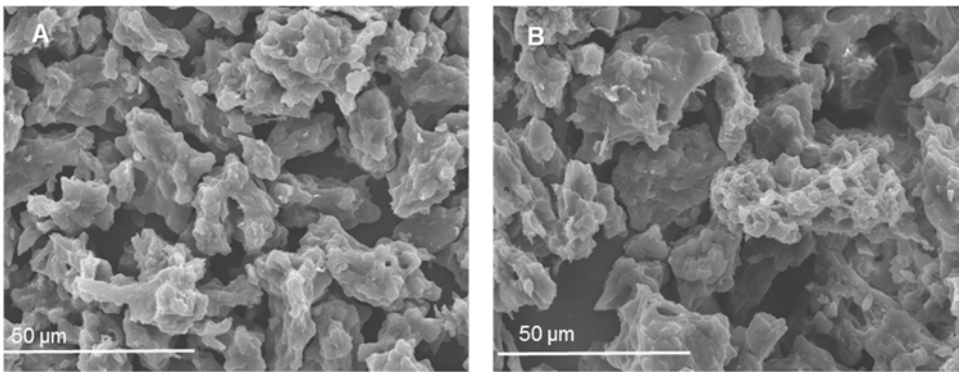

Figure 2. 29. SEM micrographs of freeze-dried polymers $(4Glc\beta4Glc\beta3Glc\beta)_n$ where B corresponds to polymer **17** and A to polymer **20**; (E134S-CBM11/CBM).

All insoluble polymers obtained by self-condensation of the trisaccharyl donor are quite similar when yields are over 80%. Polysaccharides with M_w of 17-20 kDa (DP 100-120) are obtained when the reaction is either catalysed by the E134S mutant or by E134S-CBM11, with or without extra addition of CMB11 (Tables 2. 3 and 2. 9). The rates of polymerization were high, thus there was not sufficient time for inter-chain interactions to occur, which leads to polymer precipitation around these M_w values. By contrast, when yields do not reach 80% due to lower rate of polymerization, addition of CBM11 or the fusion protein enable longer insoluble polysaccharides to be generated compared to the E134S-catalyzed reaction. Here the CBM11

prevented the *nascent* polymers from interchain interactions enabling continued polymerization of these molecules in solution before the reaction was termined by product precipitation.

2.4. CONCLUSIONS

We explored the effect of a CBM on glycosynthase-catalyzed polymerization to generate mixed-linked 1,3-1,4-β-glucans with regular sequences. The observed effect is dependent on the rate of polysaccharide formation. When the rate of polymerization is high, polymer yields are higher than 80% and CBM11, either as a discrete protein or appended to E134S, had no effect on the DP. In contrast, when the rate of polymerization was low and polymer yields were below 80%, the CBM11 facilitated oversaturation of the polymers and longer insoluble polysaccharides were obtained. Moreover, in the case of the alternating polysaccharide $(4Glc\beta3Glc\beta)_n$, the presence of the CBM disrupts the crystallinity of the insoluble polymer obtained yielding amorphous precipitates instead of the characteristic spherulite morphology.

For the system studied, the observed effect on DP is small but significant, probably reflecting the non-processive behavior of *endo*-1,3-1,4-β-glucanase. For a truly processive glycosynthase it might be expected that the synthesized oligomeric chain protruding from the active site binds the CBM which may keep the polymer in solution during chain extension. For a non-processive enzyme, polymer extension occurs by association and dissociation of intermediate products into the active site, and the concentration of the intermediate polymers in solution is higher than the concentration of CBM (in the rage of enzyme concentration). Therefore the solubilization effect provided by the CBM is not as extensive as it would be expected for a processive enzyme. The effect on DP increase here observed for slow polymerization reactions agrees with this hypothesis.

In conclusion, CBM assists glycosynthase-catalyzed polymerizations to achieve longer polysaccharides, potentially being a general strategy in the design of efficient glycosynthases aimed at the production of artificial polysaccharides.

2.5. REFERENCES

(1) Gilbert, H. J.; Knox, J. P.; Boraston, A. B. *Curr. Opin. Struct. Biol.* **2013**, *23*, 669–677.

(2) Boraston, A. B.; Bolam, D. N.; Gilbert, H. J.; Davies, G. J. *Biochem. J* **2004**, *781*, 769–781.

(3) Gilbert, H. J. *Plant Physiol.* **2010**, *153*, 444–455.

(4) Hervé, C.; Rogowski, A.; Blake, A. W.; Marcus, S. E.; Gilbert, H. J.; Knox, J. P. *Proc. Natl. Acad. Sci. U. S. A.* **2010**, *107*, 15293–15298.

(5) Cuskin, F.; Flint, J. E.; Gloster, T. M.; Morland, C.; Baslé, A.; Henrissat, B.; Coutinho, P. M.; Strazzulli, A.; Solovyova, A. S.; Davies, G. J.; Gilbert, H. J. *Proc. Natl. Acad. Sci. U. S. A.* **2012**, *109*, 20889–20894.

(6) Meekins, D. a; Raththagala, M.; Husodo, S.; White, C. J.; Guo, H.-F.; Kötting, O.; Vander Kooi, C. W.; Gentry, M. S. *Proc. Natl. Acad. Sci. U. S. A.* **2014**, *111*, 7272–7277.

(7) Montanier, C.; Money, V. a.; Pires, V. M. R.; Flint, J. E.; Pinheiro, B. A.; Goyal, A.; Prates, J. A. M.; Izumi, A.; Stalbrand, H.; Morland, C.; Cartmell, A.; Kolenova, K.; Topakas, E.; Dodson, E. J.; Bolam, D. N.; Davies, G. J.; Fontes, C. M. G. A.; Gilbert, H. J. *PLoS Biol.* **2009**, *7*, 687–697.

(8) Lombard, V.; Golaconda Ramulu, H.; Drula, E.; Coutinho, P. M.; Henrissat, B. *Nucleic Acids Res.* **2014**, *42*, 490–495.

(9) Carvalho, A. L.; Goyal, A.; Prates, J. A. M.; Bolam, D. N.; Gilbert, H. J.; Pires, V. M. R.; Ferreira, L. M. A.; Planas, A.; Romão, M. J.; Fontes, C. M. G. A. *J. Biol. Chem.* **2004**, *279*, 34785–34793.

(10) Wang, L.-X.; Huang, W. *Curr. Opin. Chem. Biol.* **2009**, *13*, 592–600.

(11) Faijes, M.; Planas, A. *Carbohydr. Res.* **2007**, *342*, 1581–1594.

(12) Shaikh, F. A.; Withers, S. G. *Biochem. Cell Biol.* **2008**, *86*, 169–177.

(13) Perugino, G.; Trincone, A.; Rossi, M.; Moracci, M. *Trends Biotechnol.* **2004**, *22*, 31–37.

(14) Faijes, M.; Imai, T.; Bulone, V.; Planas, A. *Biochem. J.* **2004**, *380*, 635–641.

(15) Pérez, X.; Faijes, M.; Planas, A. *Biomacromolecules* **2011**, *12*, 494–501.

(16) Malet, C.; Planas, A. *FEBS Lett.* **1998**, *440*, 208–212.

(17) Malet, C.; Vallés, J.; Bou, J.; Planas, A. *J. Biotechnol.* **1996**, *48*, 209–219.

(18) Cuff, J. A.; Clamp, M. E.; Siddiqui, A. S.; Finlay, M.; Barton, G. J. *Bioinformatics* **1998**, *14*, 892–893.

(19) Eswar, N.; Webb, B.; Marti-Renom, M.-A.; M.S., M.; Eramian, D.; Shen, M.; Pieper, U.; Sali, A. *Curr Protoc Bioinforma.* **2006**, *65*, 712–7254448.

(20) Humphrey, W.; Dalke, A.; Schulten, K. *J. Mol. Graph.* **1996**, *14*, 33–38.

(21) Addington, T. Doctoral thesis, IQS, 2009.

(22) Din, N.; Damude, H. G.; Gilkes, N. R.; Miller, R. C.; Warren, R. A. J.; Kilburn, D. G. *Proc. Nati. Acad. Sci. USA* **1994**, *91*, 11383–11387.

(23) Fontana, A.; Zambonin, M.; Polverino de Laureto, P.; De Filippis, V.; Clementi, A.; Scaramella, E. *J. Mol. Biol.* **1997**, *266*, 223–230.

(24) Gustavsson, M.; Lehtio, J.; Denman, S.; Teeri, T. T.; Hult, K.; Martinelle, M. *Protein Eng.* **2001**, *14*, 711–715.

(25) Kavoosi, M.; Creagh, A. L.; Kilburn, D. G.; Haynes, C. A. *Biotechnol. Bioeng.* **2007**, *98*, 599–610.

(26) Rawlings, N. D.; Morton, F. R.; Barrett, A. J. *Nucleic Acids Res.* **2006**, *34*, D270–D272.

(27) Boyd, S. E.; Pike, R. N.; Rudy, G. B.; Whisstock, J. C.; Garcia de la Banda, M. *J. Bioinform. Comput. Biol.* **2005**, *03*, 551–585.

(28) Parsell, D. A.; Sauer, R. T. *J. Biol. Chem.* **1989**, *264*, 7590–7595.

(29) Wriggers, W.; Chakravarty, S.; Jennings, P. A. *Pept. Sci.* **2005**, *80*, 736–746.

(30) Gaiser, O. J.; Piotukh, K.; Ponnuswamy, M. N.; Planas, A.; Borriss, R.; Heinemann, U. *J. Mol. Biol.* **2006**, *357*, 1211–1225.

APPENDIX CHAPTER 2

APPENDIX

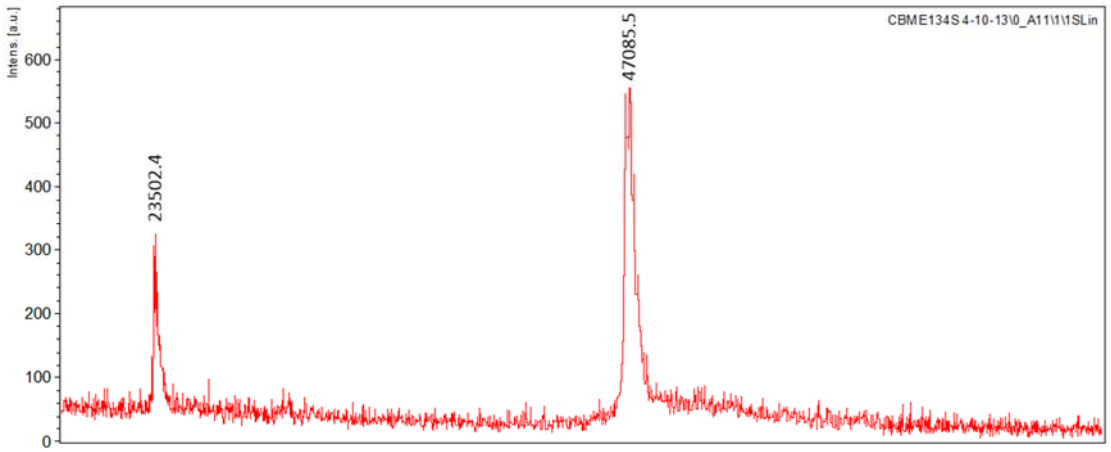

Figure A2. 1: MALDI-TOF spectrum of the fusion protein E134S-CBM11

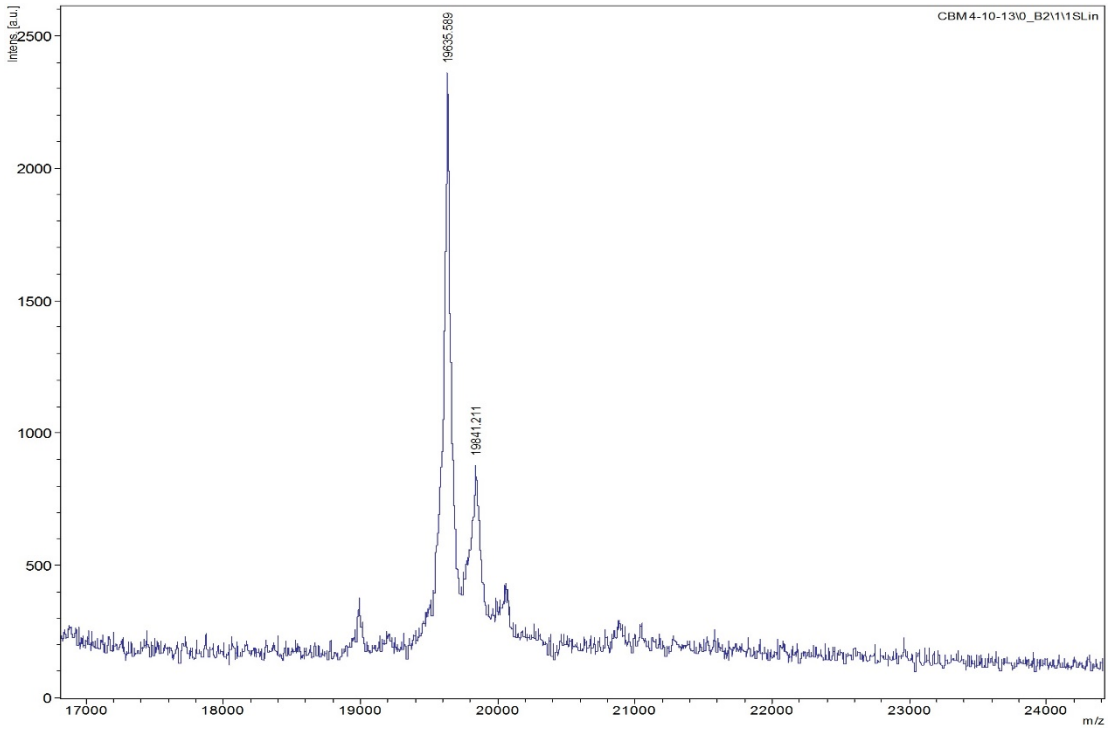

Figure A2. 2: MALDI-TOF spectrum of the protein domain CBM11

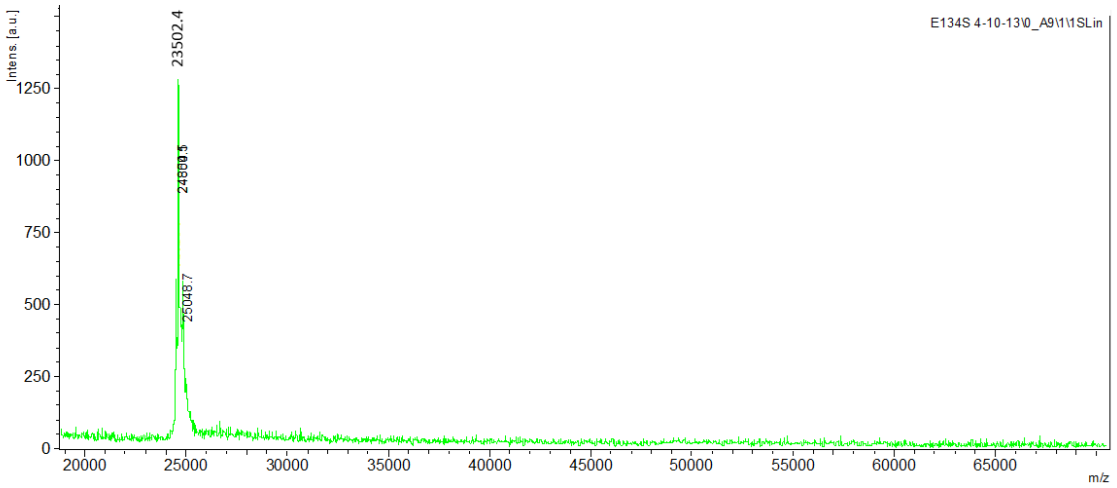

Figure A2. 3: MALDI-TOF of the glycosynthase mutant E134S

Figure A2. 4. Fusion protein sequence (Number of amino acids: 422 Molecular weight: 47241.3)

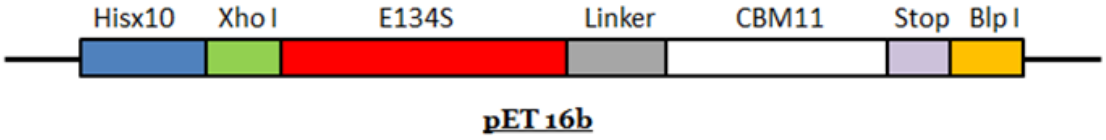

pET 16b

```
atgggccatcatcatcatcatcatcatcatcacagcagcggccatatcgaaggtcgt
 M  G  H  H  H  H  H  H  H  H  H  H  S  S  G  H  I  E  G  R
catatgctcgagcagaccggcggctccttctacgaaccgtttaacaactacaacacgggc
 H  M  L  E  Q  T  G  G  S  F  Y  E  P  F  N  N  Y  N  T  G
ctgtggcaaaaagcagatggctactcaaatggtaatatgtttaattgcacgtggcgcgca
 L  W  Q  K  A  D  G  Y  S  N  G  N  M  F  N  C  T  W  R  A
aacaatgtttcaatgacctcgctgggtgaaatgcgtctgagtctgaccagcccgtcttat
 N  N  V  S  M  T  S  L  G  E  M  R  L  S  L  T  S  P  S  Y
aataaattcgattgtggcgaaaaccgcagcgtgcagacctatggctacggtctgtacgaa
 N  K  F  D  C  G  E  N  R  S  V  Q  T  Y  G  Y  G  L  Y  E
gttaatatgaaaccggcgaaaaacgtgggtattgtgagcagcttttcacctatacgggt
 V  N  M  K  P  A  K  N  V  G  I  V  S  S  F  F  T  Y  T  G
ccgacggacggtaccccgtgggattccattgacatcgaatttctgggtaaagataccacg
 P  T  D  G  T  P  W  D  S  I  D  I  E  F  L  G  K  D  T  T
aaagttcagttcaactcttataccaatggcgaaggtaaccatgaaaaaattgtgaatctg
 K  V  Q  F  N  S  Y  T  N  G  E  G  N  H  E  K  I  V  N  L
ggctttgatgcggccaacagttatcacacctacgcattcgactggcagccgaactccatc
 G  F  D  A  A  N  S  Y  H  T  Y  A  F  D  W  Q  P  N  S  I
aaatggtatgtggatggtcaactgaaacatacggctaccacgcagattccgcaaaccccg
 K  W  Y  V  D  G  Q  L  K  H  T  A  T  T  Q  I  P  Q  T  P
ggcaaaatcatgatgaacctgtggaatggcgcgggtgtcgatgaatggctgggtagctat
 G  K  I  M  M  N  L  W  N  G  A  G  V  D  E  W  L  G  S  Y
aatggcgtgacgccgctgtatgcccactacaactgggttcgctacaccaaacgtccgacc
 N  G  V  T  P  L  Y  A  H  Y  N  W  V  R  Y  T  K  R  P  T
ccgacgccgacgccgaccccgaccccgacgccgaccccggcggtcggcgaaaaaatgctg
 P  T  P  T  P  T  P  T  P  T  P  T  P  A  V  G  E  K  M  L
gatgactttgaaggtgtgctgaattggggcagttactccggcgaaggtgccaaagtcagt
 D  D  F  E  G  V  L  N  W  G  S  Y  S  G  E  G  A  K  V  S
acgaaaattgtgtccggtaaaaccggcaacggtatggaagttagctatacgggcaccacg
 T  K  I  V  S  G  K  T  G  N  G  M  E  V  S  Y  T  G  T  T
gatggttattggggcaccgtctactctctgccggatggtgactggtcaaaatggctgaaa
 D  G  Y  W  G  T  V  Y  S  L  P  D  G  D  W  S  K  W  L  K
atctcgttcgatatcaaaagcgtggacggctctgcaaatgaaattcgtttcatgatcgct
 I  S  F  D  I  K  S  V  D  G  S  A  N  E  I  R  F  M  I  A
gaaaaatcaattaacggcgttggtgacggcgaacattgggtctactcgatcacgccggat
 E  K  S  I  N  G  V  G  D  G  E  H  W  V  Y  S  I  T  P  D
agttcctggaaaaccattgaaatcccgttttcatcgttccgtcgccgtctggattatcag
 S  S  W  K  T  I  E  I  P  F  S  S  F  R  R  R  L  D  Y  Q
ccgccgggtcaagacatgagcggcaccctggatctggacaatattgattctatccacttt
 P  P  G  Q  D  M  S  G  T  L  D  L  D  N  I  D  S  I  H  F
atgtacgcaaataacaaaagcggtaaattcgtcgtggacaacattaaactgattggtgcc
 M  Y  A  N  N  K  S  G  K  F  V  V  D  N  I  K  L  I  G  A
taagctgagc
 -  A  E
```

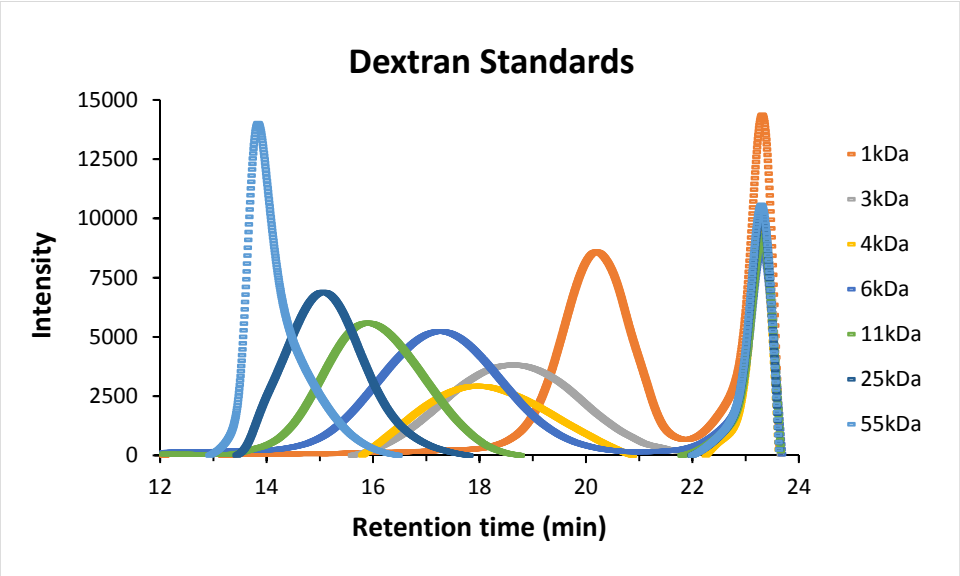

Figure A2. 5: HPSEC dextran standards

M_p Standards	log M_p	t_r (min)
1000	3.0000	20.1384
2800	3.4472	18.5688
3400	3.5315	17.9028
4440	3.6474	17.2008
9900	3.9956	15.8400
20500	4.3118	15.0048
50200	4.7007	13.7808

Table A2. 1: Determination of the retention time (t_r) of dextran standards

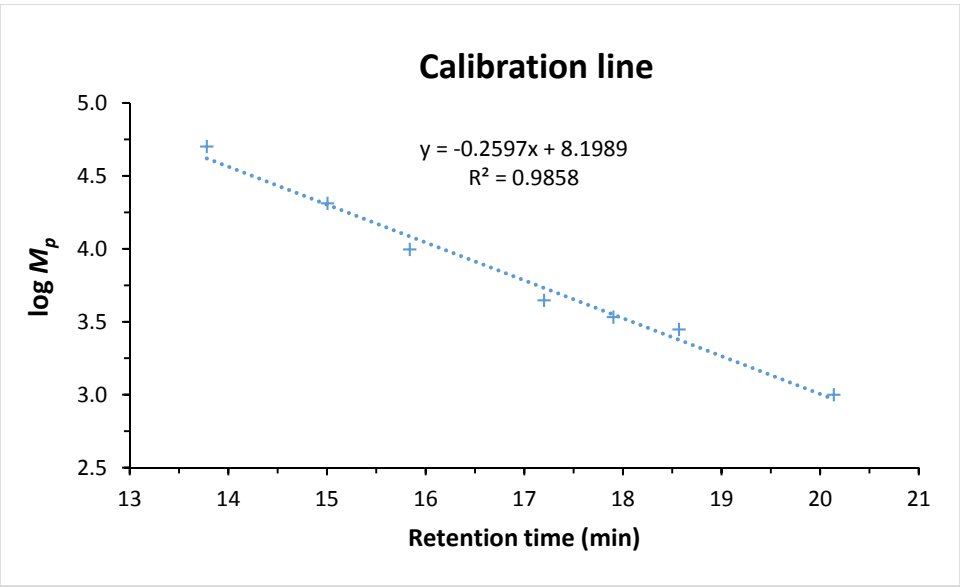

Figure A2. 6: HPSEC. Calibration line

CHAPTER 3: TOWARDS THE SYNTHESIS OF ARTIFICIAL FUNCTIONALIZED 1,3-1,4-β-GLUCANS

3.1. INTRODUCTION

Biocompatibility, biodegradability and stability are the main characteristics of polymers used as biomaterials. Complex carbohydrate structures containing functional groups have been extensively investigated for a wide range of biomedical applications. Further functionalizations have aimed to improve solubility and miscibility allowing the binding of the polymers to target compounds and improve their efficiency as drug delivery systems.[1] Successful examples are the cationic polysaccharides obtained by modifying polymers that are reported to efficiently encapsulate proteins and DNA and enhance gene transfection such as cellulose, schizophyllan, curdlan and chitosan.[2,3,4,5,6,7] The modifications can be performed chemically on natural polysaccharides by functionalizing C-6 positions with amine side chains or azido groups that later can be reduced to amines or can be reacted by click-chemistry.[8,9]

Alternatively, enzymatic synthesis have provided artificial polysaccharides that mimic natural polysaccharides in an efficient way. It takes advantage of the regio- and stereoselectivity of enzymes to form new linkages and provide polysaccharides with perfectly regular and homogenous structures that are impossible to obtain from natural sources.

The glycosynthase technology has been expanded to the synthesis of artificial polysaccharides by promoting the donor self-condensation reaction.[10,11] The glycosynthase approach provides a new generation of polysaccharides with different polymerization and functionalization properties than those obtained by chemical modification routes. Therefore glycosyl donors containing functional groups can be suitable candidates to synthesize this *in situ*-modified polysaccharides by the use of glycosynthases. The introduction of a functionality in substrates that will fit in the donor and acceptor subsites might be determinant for the enzyme having a different effect in every subsite. This effect will depend on the interactions between the enzyme and the new functionalized substrate.

In this context, our goal is to evaluate the chemoenzymatic synthesis of functionalized artificial mixed-linked 1,3-1,4-β-glucans.

The crystal structure of 1,3-1,4-β-D-glucan 4-glucanohydrolase from *Bacillus macerans*,[12] from the hybrid *Bacillus* β-glucanase H(A16-M),[13] and from *Bacillus licheniformis*[14] were solved in an effort to reveal the degree of redundancy to which the three-dimensional structure of protein domains is encoded by the amino acid sequence.[15] These 1,3-1,4-β-glucanases are homologous enzymes having a similar β-sandwich structure with a compact jellyroll domain. In 2006, Gaiser *et al*. reported the high-resolution crystal structure of the hybrid 1,3-1,4-β-glucanase

H(A16-M)$^{E105Q/E109Q}$ in complex with a β-glucan tetrasaccharide Glcβ4Glcβ4Glcβ3Glc covering donor subsites from subsite -1 to -4 (Figure 3. 1).[16]

The catalytic residues of *Bacillus* 1,3-1,4-β-glucanases were identified by means of mutational analysis, affinity labeling, and X-ray crystallography. Ten active-site residues Asn26, Glu63, Arg65, Phe92, Tyr94, Glu105, Asp107, Glu109, Asn182 and Trp184 (*Bacillus macerans* numeration) form a network of hydrogen bonds and hydrophobic stacking interactions with the substrate. We had previously shown that these residues are significant for stabilization of the enzyme–carbohydrate complex[17] and mutational analyses on the *Bacillus licheniformis* and *B. macerans* enzymes identified Glu105 and Glu109 as the catalytic nucleophile and the general acid/base, respectively[18] (H(A16-M), *Bacillus macerans* numbering).

In β-glucans two neighboring glucopyranosyl units linked by a β-1,3 bond have the orientation with the 6-CH_2-OH side-chains on the same side of the glucopyranosyl rings. In the complex, binding of a laminaribiosyl unit in subsites –2 / -1 is accomplished by strong hydrogen bond interactions of Asn26 and Glu63 with the O^6 hydroxyl of Glc-2, as well as Trp184 $N^{\varepsilon 1}$ and Gln109 with the O^6 hydroxyl of Glc-1 in the catalytic subsite (Figure 3. 1).

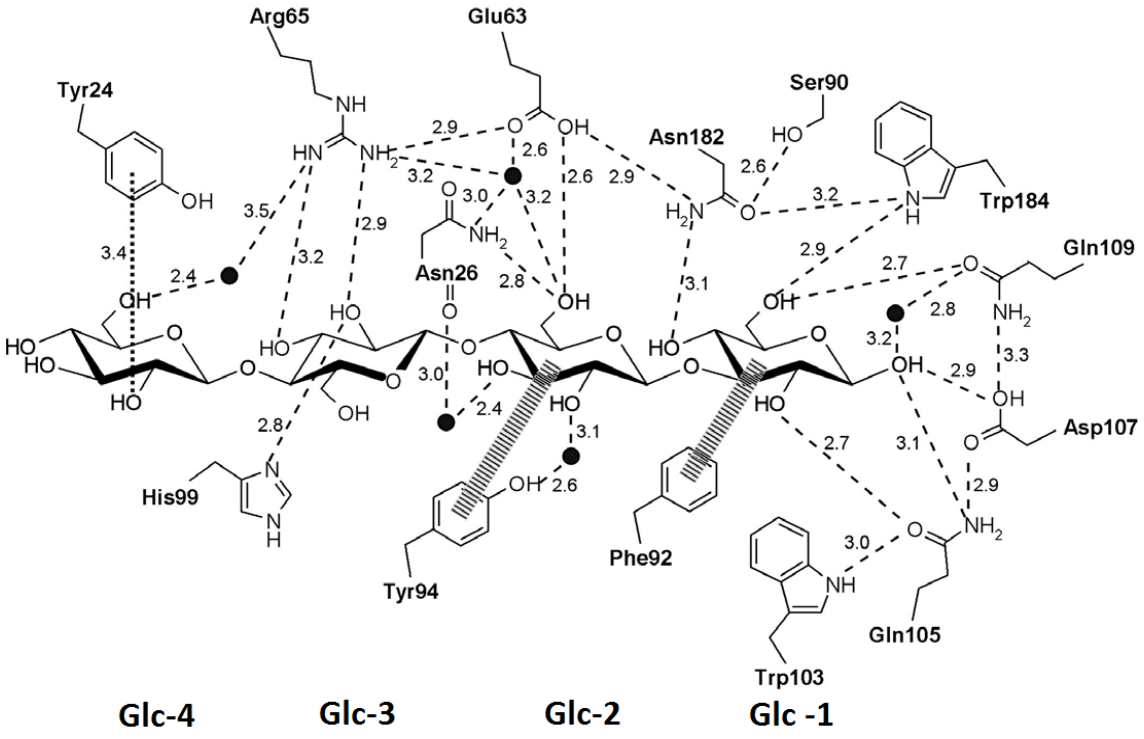

Figure 3. 1: Scheme of enzyme–carbohydrate interactions in subsites -1 to -4. Schematic depiction of hydrogen bond and hydrophobic stacking interactions in the enzyme–ligand complex. Glc-1 to Glc-4 mark glucosyl residues bound in subsites -1 to -4. Amino acid side-chains are shown with their functional groups. Hydrogen bonds with donor-acceptor distance below 3.5 Å are shown as broken lines (numbers are donor-acceptor distances in Å). Water molecules mediating hydrogen bonds are depicted as black balls. Hydrophobic interactions are also indicated. Note that the β-1,3 linkage between Glc-2 and Glc-1 positions both 6-CH_2-OH glucosyl side-chains on the same side of the tetrasaccharide.

Asn121 and Glu131 were proposed as potential interaction partners for the O^6 hydroxyl group of the glucosyl residue bound in subsite +1. Interestingly, the side-chain functional group of Gln109 is nearly parallel with the glucopyranosyl ring in subsite -1 and allows interactions with both the glycosidic oxygen of the scissile bond and the O^6 hydroxyl.[19,16,20] The direct interaction of the acid/base catalyst with the O^6 hydroxyl group of Glc-1 appears to be an important feature of catalysis.[16]

Therefore, the introduction of a functional group at C-6 could compromise the enzyme-substrate binding. By contrast C-6' seems less restrictive despite the interaction of O^6 and Asn 26 and Glu 63 (Asn55 and Glu92 for *Bacillus licheniformis numeration)* through hydrogen bonds.

We tentatively proposed 6'-azido-6'-deoxy-α-D-laminaribiosyl fluoride (6'N_3-Glcβ3GlcαF) as a functionalized substrate for the further production of *in situ*-modified 1,3-1,4-β-glucan by the use of the glycosynthase derived from 1,3-1,4-β-glucanase from *B. licheniformis* as a model enzyme (Figure 3. 2).

We chose the azide functional group as a highly versatile functionality which can be later either reduced to amine, or be functionalized by click chemistry as it has been done for a broad variety of chemically modified polysaccharides. Furthermore, it is a relatively small functional group which will probably not affect the binding of the substrate increasing the probability of acceptance of the functionalized substrate by the enzyme. However, direct evolution of the enzyme will be probably needed in the future in order to improve the enzyme activity with this azido-substrate. To the best of our knowledge, no direct and selective azidation of laminaribiose on the primary hydroxyl positions has been described before in the literature. The functionalities introduced in the glycosyl donors will be inherited in the resulting heteropolymer and should confer new properties while retaining the biodegradability given by its unaltered sugar backbone.

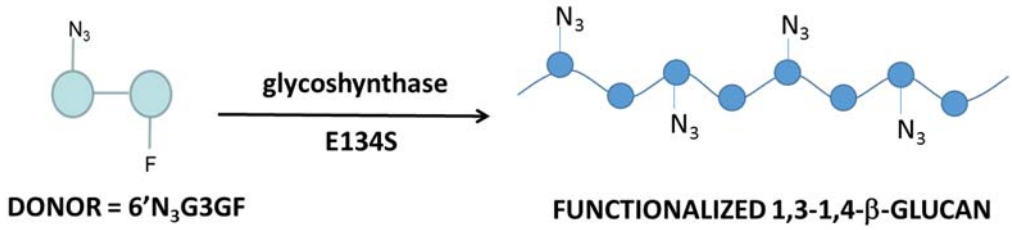

Figure 3. 2: Synthesis of alternating 6-azido-6-deoxy-1,3-1,4-β-glucan by glycosynthase-catalyzed polymerization of the 6'-azido-6'-deoxylaminarbiosyl fluoride donor.

In the polymerization reaction the same glycosyl donor binds in the donor and acceptor subsites. As the introduction of the new functionality might affect the acceptance of subsites -2 and +1,

different donors and acceptors have been synthesized in this work to study the independent effect of the azido group on the different subsites by using the glycosynthase reaction. On the one hand, $6N_3$-GlcβPNP was synthesized as an acceptor for the acceptance study of subsite +1. On the other hand $6'N_3$-Glcβ3GlcαF was synthesized for the study of subsite -2 (Figure 3. 3).

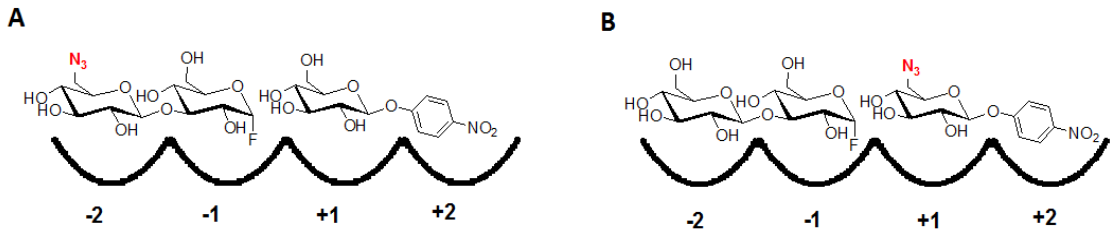

Figure 3. 3: Study of subsites. A) Study of the introduction of the azide in subsite -2. B) Study of the introduction of the azide in subsite +1.

We present here the synthesis of the functionalized acceptor *p*-nitrophenyl 6-azido-6-deoxy-β-D-glucopyranoside and two different approaches for the synthesis of the 6'-azido-6'-deoxylaminaribiosyl fluoride donor. The first 'Total synthesis' approach (Figure 3. 4) starts from individual monosaccharides where the different positions are easily differentiated before its chemical coupling to obtain the disaccharide. By properly choosing orthogonal protecting groups, the functionality was either introduced first in the disaccharide product after glycosylation ('Total synthesis 1', Figure 3. 4A) or in the donor before glycosylation ('Total synthesis 2', Figure 3. 4B). Alternatively, the 'Polymer approach' (Figure 3. 5) takes advantage of a natural raw material to easily access to a disaccharide where position C-6' can be selectively modified.

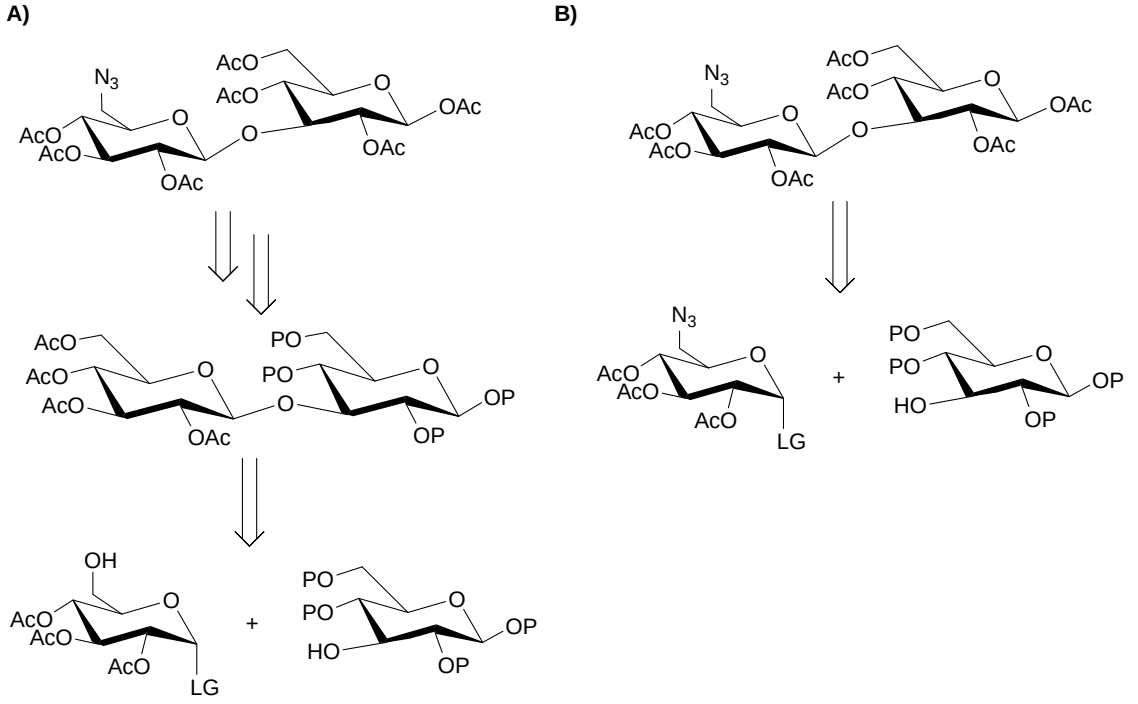

Figure 3. 4: A) 'Total synthesis 1': introduction of the azide after glycosylation of a glycosyl donor and acceptor. B) 'Total synthesis 2': introduction of the azide in the glycosyl donor before glycosylation. LG = leaving group; P = Protecting group.

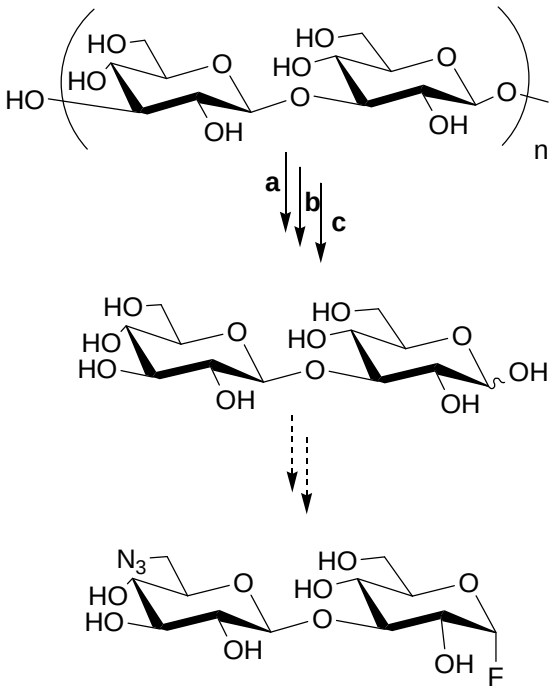

Figure 3. 5: Polymer approach: degradation of curdlan and further functionalization.

3.2. RESULTS AND DISCUSSION

The effect of the introduction of the azide functional group was evaluated studying subsite -2 using donors 6'N_3-Glcβ3GlcαF and Glcβ3GlcαF as a reference. In addition, the effect on subsite +1 was studied using acceptors 6N_3-GlcβPNP and GlcβPNP as a reference (Figure 3. 3).

3.2.1. Synthesis of the glycosynthase donors

3.2.1.1. Total synthesis: design

Several glycosyl donors were designed for the synthesis of the target azido laminaribiosyl derivative. In order to generate a β-(1→3) linkage during the glycosylation reaction, the synthesis of alpha glucosyl donors was required. 2,3,4,6-tetra-*O*-acetyl-α-D-glycopyranosyl bromide (**5**) was chosen as the best donor candidate for the introduction of the azide after glycosylation. However, if the azide was to be introduced before glycosylation, it should be introduced at C-6 of glucose (previous tosylation) before the formation of the trichloroacetimidate on the anomeric carbon (Figure 3. 6, compound **14**). By contrast, if the introduction of the bromide group on the anomeric carbon of acetyl 6-azido-6-deoxy-2,3,4-tri-*O*-acetyl-D-glucopyranoside was attempted, the azido group would be displaced by the bromide and dibrominated glucose would be obtained.

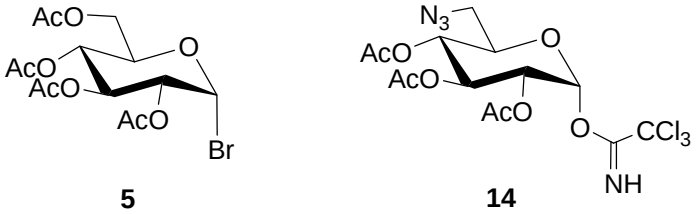

Figure 3. 6: Design of glycosyl donors. 2,3,4,6-tetra-*O*-acetyl-α-D-glucopyranosyl bromide **5** (for further introduction of the azide) and 6-azido-6-deoxy-2,3,4-tri-*O*-acetyl-α-D-glucopyranosyl trichloroacetimidate **14**.

In order to generate a β-(1→3) linkage during the glycosylation reaction, the synthesis of glucosyl acceptors with a free hydroxyl at C-3 acting as a nucleophile was required. The other hydroxyls of the acceptor had to be protected in order to avoid side-reactions. Several acceptors were designed with a methoxy (OMe) or a *p*-methoxyphenyl (*p*MP) group protecting the anomeric carbon, a benzylidene or an isopropylidene group protecting C-4 and C-6, and an allyl, a benzyl or a benzoyl group protecting C-2 (Figure 3. 7).

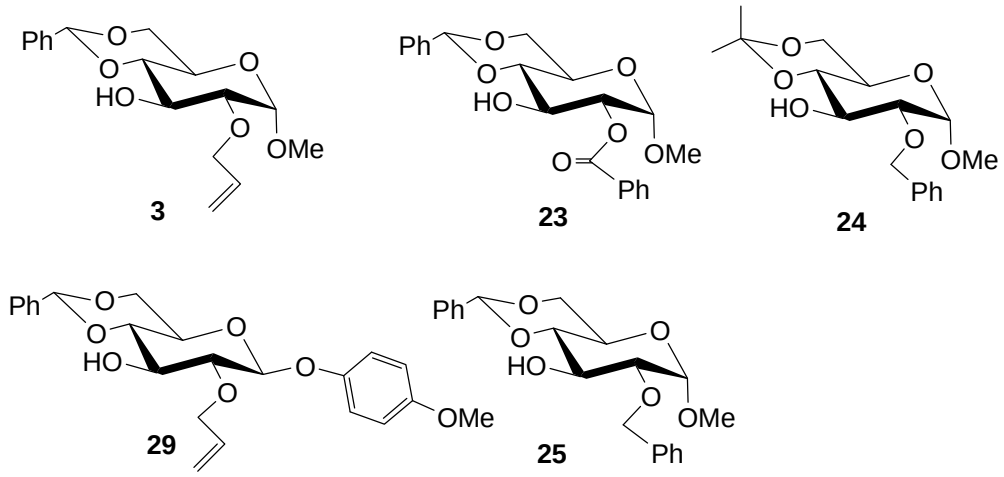

Figure 3. 7: Design of glucosyl acceptors. **3**) Methyl 2-*O*-allyl-4,6-*O*-benzylidene-α-D-glucopyranoside. **23**) Methyl 2-*O*-benzoyl-4,6-*O*-benzylidene-α-D-glucopyranoside. **24**) Methyl 2-*O*-benzyl-4,6-*O*-isopropylidene-α-D-glucopyranoside. **29**) *p*-methoxyphenyl 2-*O*-allyl-4,6-*O*-benzylidene-β-D-glucopyranoside. **25**) Methyl 2-*O*-benzyl-4,6-*O*-benzylidene-α-D-glucopyranoside.

Two preferential approaches were designed by combining different donors and acceptors. The first approach (Figure 3. 4A, 'Total synthesis 1') consisted in the condensation of 2,3,4,6-tetra-*O*-acetyl-α-D-glucopyranosyl bromide (**5)** with the acceptor methyl 2-*O*-allyl-4,6-*O*-benzylidene-α-D-glucopyranoside (**3**). In this case, the azide would be further introduced into the disaccharide and the target product could be obtained after further deprotection of benzylidene, allyl and methyl protecting groups. On the other hand, the second approach (Figure 3. 4B, 'Total synthesis 2') introduces first the azido group on glucose and then forms the trichloroacetimidate synthesizing the 6-azido-6-deoxy-2,3,4-tri-*O*-acetyl-α-D-glucopyranosyl trichloroacetimidate (**14**). This donor could condensate with an acceptor by the Schmidt glycosylation reaction and the target product could be further obtained. There are different possible ways to introduce the azide in the target molecule. As Figure 3. 8 shows, in these approaches the azide is introduced after previous tosylation of C-6.

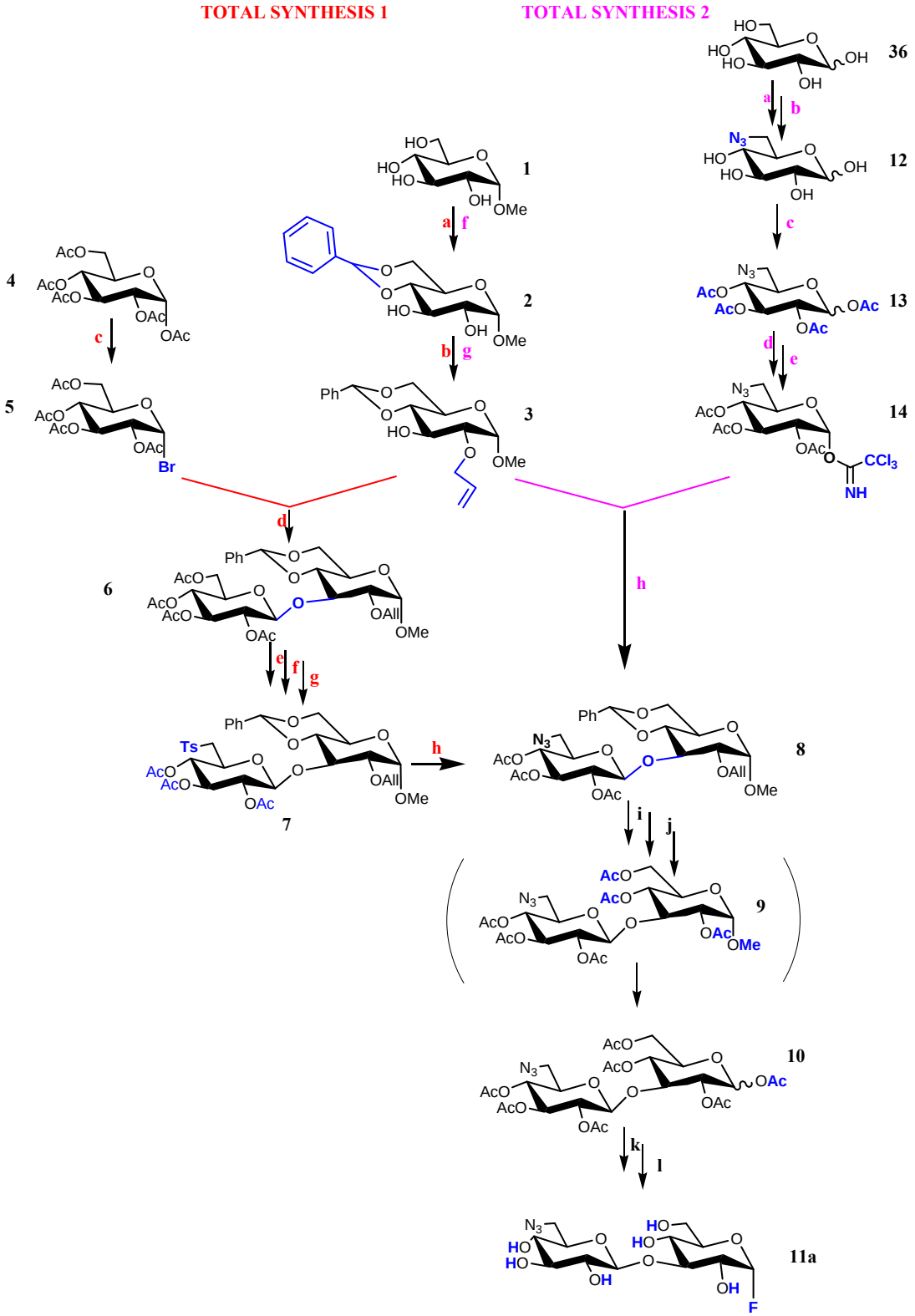

Figure 3. 8: Synthesis of 6'-azido-6'-deoxy-α-D-laminaribiosyl fluoride. Aproach 'Total synthesis I' (left, conditions in red). a) $PhCH(OMe)_2$/CSA/Bz; b) $(Bu_3Sn)_2O$/AllBr; c) HBr/AcOH; d) $HgBr_2/Hg(CN)_2$; e) NaOMe/MeOH; f) TsCl/py; g) Ac_2O/py; h) NaN_3/DMF. Approach 'Total synthesis II' (right, conditions in purple). a) TsCl/py; b) NaN_3/DMF; c) Ac_2O/py; d) Hydrazine acetate/DMF; e) Cl_3CCN/DBU/CH_2Cl_2; f) $PhCH(OMe)_2$/CSA/Bz; g) $(Bu_3Sn)_2O$/AllBr; h) TMSOTf/CH_2Cl_2; i) $PdCl_2$/NaOAc/AcOH; j) H^+; k) HF/py; l) NaOMe/MeOH.

3.2.1.2. Total synthesis: results

In 'Total synthesis 1' a glucosyl bromide donor was first synthesized in high yield whereas in 'Total synthesis 2' the azido group was first introduced through tosylation. However, the trichloroacetimidate group was introduced in the anomeric carbon in lower overall yields. Therefore, 'Total synthesis 1' was selected for the synthesis of substrate $6N_3$-Glcβ3GlcαF using the glucosyl bromide as donor and exploring five different glucosyl acceptors with the aim of choosing the best conditions for a straightforward synthesis in the highest possible yields (Figure 3. 8).

The synthesis of acceptor **24** (Figure 3. 9) proved to be trickiest than expected due to the obtention of a mixture of isomers, one containing the benzyl group at C-2 and the other one at C-3, both products showing the same R_f on TLC.

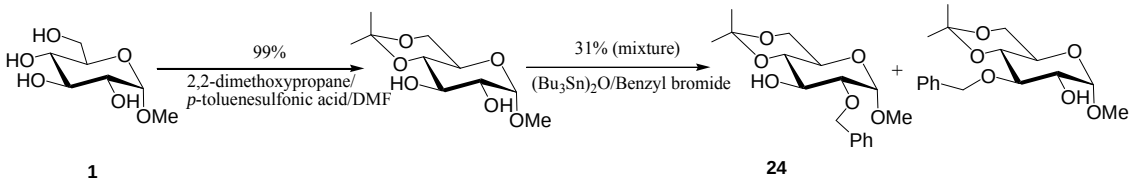

Figure 3. 9: Synthesis of acceptor **24**.

Therefore, the isolation of methyl 2-*O*-benzyl-4,6-*O*-benzylidene-α-D-glucopyranose became a challenge as no eluent nor mixture of eluents was found to separate the isomers. As **24** could not be isolated, it was not considered as a possible acceptor for the glycosylation reaction.

The syntheses of 2,3,4,6-tetra-*O*-acetyl-α-D-glucopyranosyl bromide donor (**5**) and the methyl 2-*O*-allyl-4,6-*O*-benzylidene-α-D-glucopyranoside acceptor (**3**) as precursors for glycosylation according to 'Total synthesis 1' were successfully performed (Figure 3. 8) (see characterization of the products in the Experimental section).

The synthesis of the methyl 2-*O*-allyl-4,6-*O*-benzylidene-α-D-glucopyranose acceptor (**3**) was accomplished in two steps with an overall yield of 53% (Figure 3. 10).

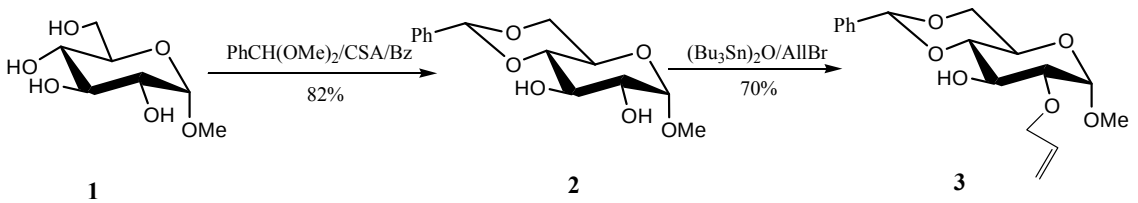

Figure 3. 10: Synthesis of acceptor **3**.

The 2,3,4,6-tetra-*O*-acetyl-α-D-glucopyranoside bromide donor (**5**) was synthesized from peracetylated glucose quantitatively and once it was synthesized, it was immediately used in the glycosylation reaction to avoid the hydrolysis of the bromide (Figure 3. 11).

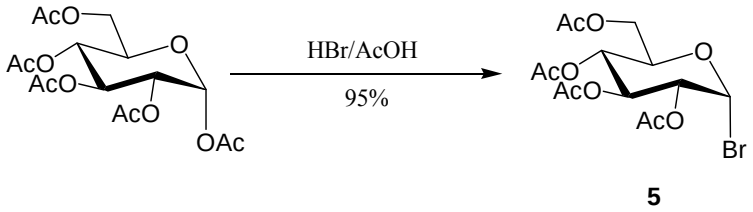

Figure 3. 11: Synthesis of donor **5**.

The donor was activated during the glycosylation reaction with mercury salts and the glycosylation reaction was performed under strict anhydrous conditions (nitrogen atmosphere) in the presence of molecular sieves and the laminaribiosyl derivative **6** was obtained in 55 % yield (Figure 3. 12) (see characterization of the product in the Experimental section). Some hydrolysis of the benzylidene protecting group occurred always after glycosylation. However, the benzylidene group could be easily reintroduced. The disaccharide acetyl groups were removed by performing the Zemplen reaction of **6**.

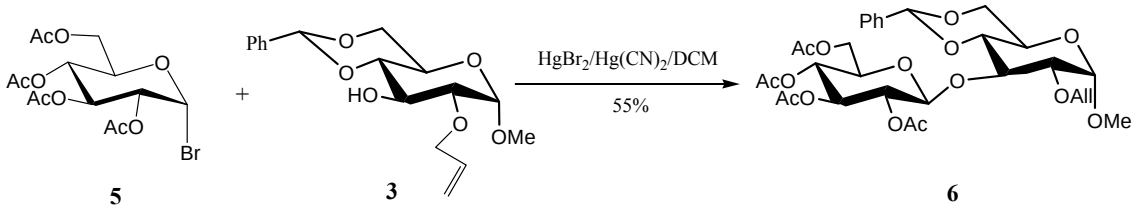

Figure 3. 12: Schmidt glycosylation reaction. Synthesis of **6**.

The synthesis of **8** was performed by tosylation and further azidation (Figure 3. 13) (see characterization of the product in the Experimental section). Due to the preference of tosyl groups for primary hydroxyls, it was easily introduced at C-6' and further substituted by the azido functional group by the use of NaN_3 in DMF. Finally, acetylation of C-2', C-3' and C-4' allowed a better chromatographic purification.

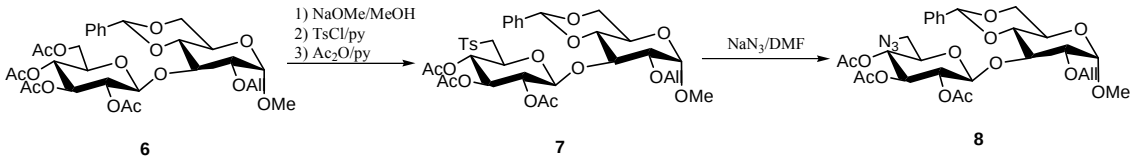

Figure 3. 13: Introduction of the azide. Synthesis of **8** (25% yield, 4 steps).

Before the introduction of the fluoride on the anomeric carbon, the removal of the remaining protecting groups of **8** was needed. The allyl group could be removed by a reaction of **8** with $PdCl_2$, NaOAc and AcOH. Previous results from Lohman and Seeberger[21] commented the possibility of removing the allyl group in the presence of benzyl, benzoyl, methoxy and acetyl groups in 85% yield. During the reaction, the substrate reacts with equimolar or slightly higher amounts of $PdCl_2$ in aqueous acetic acid in the presence of sodium acetate at temperatures between 25 – 70 ºC. Following this procedure the allyl group at C-2 was removed and a new acetyl was introduced instead (Figure 3. 14).

Methoxy and benzylidene groups can be generally removed by the use of acidic conditions. It was found in the literature[22] that the methoxy group of the anomeric carbon of methyl 3,4-di-*O*-acetyl 2-*O*-(2,3,4-tri-*O*-acetyl-α-L-rhamnopyranosyl-)-β-D-fucopyranoside could be deprotected by dissolving it in a mixture of acetic anhydride and 1.5% (v/v) sulfuric acid-acetic anhydride, stirring it at RT for 3.5 hours without hydrolyzing the glycosidic bond and obtaining the α-anomer in 42% yield and the β-anomer in 37% yield. Therefore, these conditions were applied on the deallylated intermediate disaccharide in order to obtain **10**. However, the laminaribiosyl derivative was hydrolyzed in these acidic conditions and two monosaccharides were obtained. Different ratios of acetic anhydride – sulfuric acid were tested and it was found that when using lower amounts of sulfuric acid the benzylidene could be removed but the methoxy group stayed at the anomeric position. Even when the disaccharide was hydrolyzed the methoxy group was present in one of the monosaccharides (Figure 3. 14).

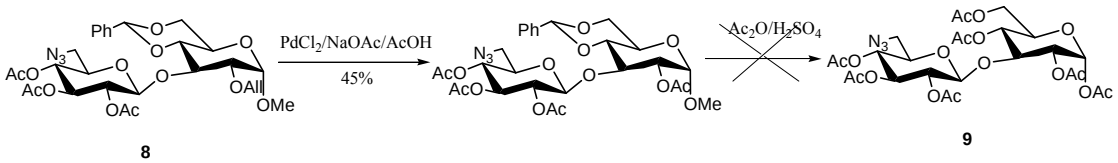

Figure 3. 14: Deprotection of the allyl group and test of deprotection of the methoxy and benzylidene groups.

Extensive bibliography search about removal of methoxy groups was performed and only reference reactions on monosaccharides were found. A lot of bibliography described protic acid deprotections of methoxy groups. For instance, Greene's group[23] described the methoxy group as a very stable group in front of other reactants. They suggested its removal in aqueous conditions at pH < 1, at high temperature or with a Lewis acid in different conditions ($AlCl_3$, 25 – 80 ºC; $SnCl_4$, 25 ºC, $BF_3 \cdot Et_2O$). None of these reactions worked in our hands, though.

In the work of Kumar *et al.*[24] the authors proposed a mild and chemoselective procedure in order to hydrolyze the methoxy group at anomeric positions in the presence of other protective groups such as benzyls, acyls, amides and carbamates. They could deprotect the methoxy group from methyl 2,3,4,6-tetra-*O*-benzyl-α-D-glucopyranoside when dissolving it in dichloromethane and adding trityl tetrafluoroborate at RT under stirring for 8 hours in yields up to 78%. Unsuccessful results were obtained when testing this reaction with our substrate.

Some other authors described the deprotection of methoxy groups with trifluoroacetic acid on molecules containing azides. Bird *et al.*[25] deprotected the methoxy group of methyl 5-azido-5-deoxy-2,3,6-tri-*O*-benzyl-D-glucofuranoside by stirring it in aqueous trifluoroacetic acid (79 eq) for 6 hours in 83% yields. Dauban *et al.*[26] could perform a similar deprotection under similar conditions (70 eq trifluoroacetic acid and longer reaction times, 70 hours) when working with a methyl D-ribose derivative containing an azido group. Instead of testing these conditions directly on our disaccharide, the first experiments were assayed on the monosaccharide methyl 2,3,4,6-tetra-*O*-acetyl-α-D-glucopyranoside (Figure 3. 15).

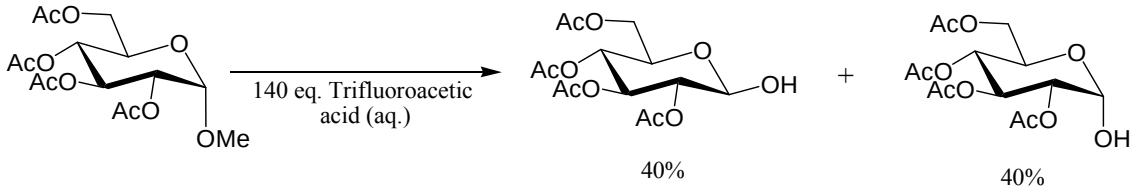

Figure 3. 15: Methoxy group deprotection: obtention of isomers.

The evolution of the reaction was followed by TLC and after 70 hours only traces of deprotected glucose (mixture of isomers) were obtained. The starting product was recovered in 71 % yield, 2,3,4,6-tetra-*O*-acetyl-α-D-isomer in 20% and the deprotected β-isomer in 9% yield. Better results were obtained when doubling the equivalents of trifluoroacetic acid from 70 to 140 eq. Then, the starting product was recovered in 20 % yield and a mixture of isomers alpha/beta (1:1) was obtained in 80% yields. Given the difficulties on the removal of the methoxy group on the

monosaccharide and the mixture of anomers that was recovered when working with the monosaccharide, the experiments with this protecting group were stopped.

Alternatively, the aromatic *p*-methoxyphenyl group was chosen as the new protecting group for the anomeric carbon of the acceptor due to its milder deprotection conditions. *p*MP was introduced on 2,3,4,6-tetra-*O*-acetyl-β-D-glucopyranose and a deprotection test was first performed to confirm the straightforward removal of the aromatic *p*MP. This deprotection reaction was performed successfully with ammonium cerium (IV) nitrate in toluene/acetonitrile/water (1:1:1) (Figure 3. 16).

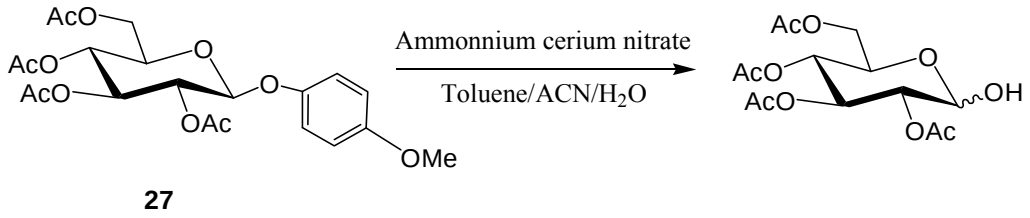

27

Figure 3. 16: *p*MP deprotection test.

Therefore, the synthesis of acceptor **29**, containing a *p*-methoxyphenyl group (*p*MP) at the anomeric position was designed and its synthesis developed (Figure 3. 17). First, the *p*MP is introduced at the anomeric carbon, then positions O-4 and O-6 are protected with a benzylidene group and finally, O-2 should be protected with an allyl group. However, the introduction of the allyl on the acceptor occurred at the two free hydroxyls (O-2 and O-3) and an equimolar mixture of isomers always with the same R_f in different solvents was obtained. Due to the difficulty in the isolation of *p*-methoxyphenyl 2-*O*-allyl-6-azido-6-deoxy-β-D-glucopyranoside no glycosylation reaction was further performed with this acceptor.

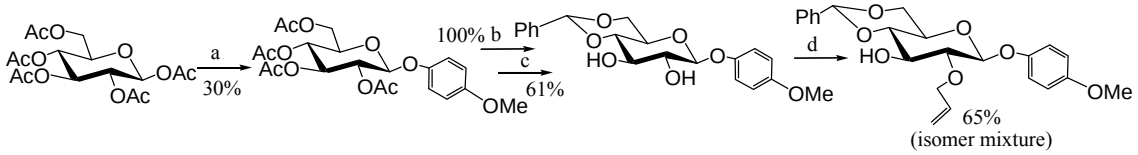

26 **27** **28** **29**

Figure 3. 17: Synthesis of acceptor **29**. a) *p*-methoxyphenol, TMSOTf, DCE; b) NaOMe/MeOH; c) Benzaldehyde dimethyl acetal, CSA, benzene; d) AllBr, $(Bu_3Sn)_2O$, toluene.

In conclusion, two different 'Total synthesis' approaches were designed. The good results in the synthesis of the bromide glucosyl donor (Total synthesis 1) and further glycosylation comparing to the results obtained in the synthesis of the trichloroacemidate donor (Total synthesis 2) brought

us to focus on 'Total synthesis 1' for the synthesis of substrate 6'N_3-Glcβ3GlcαF. This approach allowed the synthesis of methyl *O*-(6-azido-6-deoxy-2,3,4-tri-*O*-acetyl-β-D-glucopyranosyl)-(1→3)-2,4,6-tri-*O*-acetyl-α-D-glucopyranoside (**9**). Removal of the methoxy group at the anomeric position of **9** was not possible after testing several deprotecting reaction conditions. Consequently, acetylation and further activation of the disaccharide with a fluoride for the synthesis of the alpha 6'N_3-Glcβ3GlcαF (**11a**) substrate was not possible. Therefore, our efforts focused on the 'Polymer approach' where the degradation of the polysaccharide curdlan allowed the direct obtention of laminaribiose and, after several protection/deprotection steps, the target 6'-azido-6'-deoxy-α-D-laminaribiosyl fluoride **11a** could be obtained.

3.2.1.3. Polymer approach: design

Figure 3. 18 delineates the synthesis of the functionalized donor **11a** starting from laminaribiose (**16**). This disaccharide was previously obtained in our group by acetolysis of sclereoglucan affording the corresponding laminaribiose octacacetate in 23% yield.[27] After the survey of different chemical[28,29] and enzymatic degradation methods[30,31,32,33] we considered the enzymatic hydrolysis of curdlan by a kitalase from *Rhizoctonia solani* to synthesize laminaribiose in 51 % yields as reported by Wang.[32]

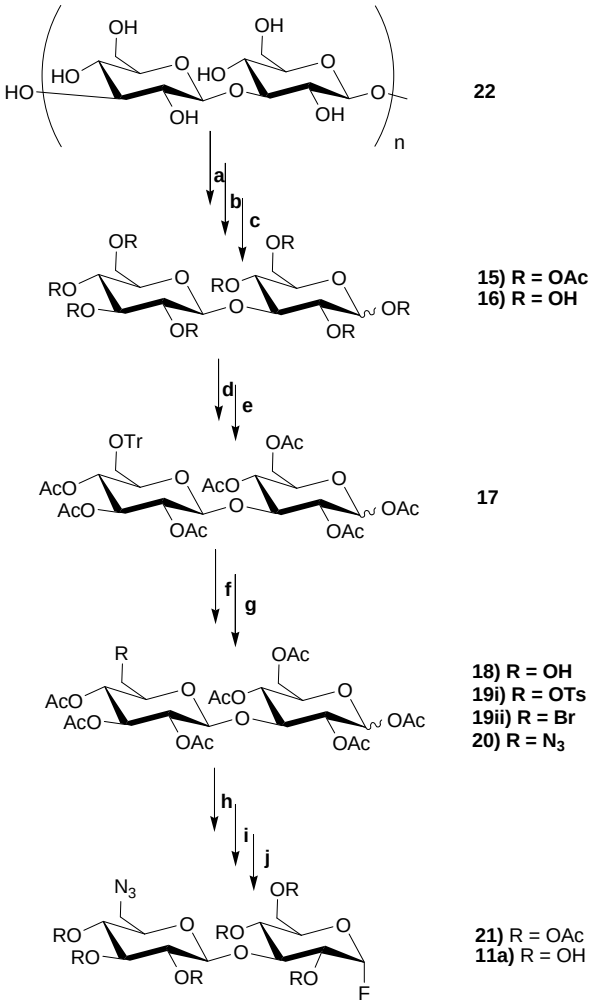

Figure 3. 18: Synthesis of the 6'-azido-6'-deoxy-β-D-laminariobyl fluoride donor (**11a**). a) Kitalase/NaOAc 10 mM/pH 5.0, 6 h, 42 ºC; b) Ac_2O/py; c) NaOMe/MeOH; d) TrCl/py; e) Ac_2O/py; f) $FeCl_3 \cdot 6H_2O/CH_2Cl_2$; g) If R = OTs, TsCl/py; If R = Br, NBS/PPh_3/DMAc; h) NaN_3/DMF; i) HF/py; j) NaOMe/MeOH.

The 'Polymer approach' was designed in order to allow a quick and direct obtention of laminaribiose (Glcβ3Glc) **16**. The degradation of curdlan, a polymer composed of glucoses linked by β-1,3 linkages, with a kitalase (enzyme preparation of culture filtrates of *Rhizoctonia solani* containing *exo* and *endo*-(1,3)-β-glucanases) would allow an easy isolation of the target disaccharide avoiding the synthetic glycosylation step.[32]

Once in possession of the disaccharide building block, the introduction of the azide into position 6' of the molecule would become the most important step in the synthesis of the target substrate **11a.** A selective reaction able to differentiate the two primary alcohols (OH-6' and OH-6) would be needed (Figure 3. 18) and different strategies were studied and evaluated in this work prior to the final synthesis.

Many works describe the substitution of all the primary hydroxyl groups by azides to achieve polyazides either in mono-, di-, oligo- or polysaccharides.

6-Azido-6-deoxy-α-D-glucopyranose was first prepared by selective tosylation (2 days at 20 °C; 55% yield) with a subsequent displacement with azide after isolation of the 6-*O*-tosylate.[34] In 1972, Hanessian *et al.* studied the selective halogenation reaction of primary hydroxyl groups by treatment of a solution of a polyhydroxy compound in DMF with two equivalents per alcohol of PPh_3 and two equivalents of the appropriate *N*-halosuccinimide per alcohol under rigorously anhydrous conditions[25] (55 – 65 % yield). Later on, they published the extension of this reaction to the preparation of primary azides by carrying out the halogenation reaction, and the subsequent conversion of the intermediate halogen derivative into the corresponding azide, in a single flask[36] (70% yield). Direct azidation reaction of several monosaccharide methyl glycopyranosides with NaN_3 in the presence of PPh_3-CBr_4 yielding the primary azidodeoxy compounds in quantitative yields was reported by Jimenez-Blanco *et al.* in 1997.[26] Moreover, direct azidation of unprotected carbohydrates was performed in a similar way by Gouin *et al.* in 2007 demonstrating that modulation of the number and position of azido groups on different saccharides was possible when varying the number of equivalents of reagents.[38]

In 1964, Dutton *et al.* synthesized several 6'-substituted maltoses (Glcα4Glc), the 6'-azido derivative among them.[39] Tritylation of 1,6-anhydrous-β-maltose yielded only the 6'-*O*-trityl derivative (40%). Acetylation, followed by detritylation with aqueous acetic acid gave a pentaacetate with only the 6'-hydroxyl free (97%). Subsequent *p*-toluenesulfonation yielded the acetylated 1,6-anhydro-6'-*O*-tosyl-β-maltose in high yield (82%) and a final replacement of the sulfonate with azide yielded acetylated 1,6-anhydro-6'-azido-6'-deoxy-β-maltose in 87% yield.

The ratio of halogenating mixture (PPh_3/NBS) and the reaction time and temperature proved to play an important role in determining whether mono- or dibromination occured at the primary positions of α,α-trehalose. Although the formation of a certain proportion of dibromo derivative could not be avoided even with a deficiency of halogenating agent, a reproducible procedure yielding 6'-bromo-6'-deoxy-α,α-trehalose was developed (37 – 40 % yields).[40]

Gouin *et al.*[38] extended their methodology to unprotected di- and trisaccharides: maltose, lactose and maltotriose. They observed differences on the reactivity and selectivity between lactose and maltose that indicated the importance of the spatial orientation of the hydroxyl groups. When using 2 eq PPh_3/CBr_4 per monosaccharide unit, first azidation occurred at C-6 position for maltose and maltotriose whereas a complex mixture of side-products was obtained for lactose. When increasing the reagent to substrate ratio, all substrates gave substituted derivatives containing azides at both anomeric and primary positions. The β anomers of glycosyl azides were

preferentially or exclusively formed obtaining a single isomer for lactose in 13% yield and the corresponding derivative from maltose in 49% yield.

Thiebault *et al.* performed the synthesis of 6''-6'-6-trideoxy-6'',6',6-trichloromaltotriose and 6''-6'-6-trideoxy-6'',6',6-triiodomaltotriose derivatives by direct chlorination of totally unprotected maltotriose.[41] They found that ratio of PPh_3/maltotriose and CCl_4/maltotriose was crucial for the complete halogenation of all the primary positions. The use of less than 9 equivalents of each reagent lead to the mixtures of di- and trihalogenated maltotriose derivatives. Triiodomaltotriose was prepared in 85% yield from acetylated 6-deoxy-6-trichloromaltotriose. A broad range of halogenous reagents were tested finding that couples of PPh_3/CBr_4, PPh_3/NBS, PPh_3/CI_4 or PPh_3/NIS under various conditions of temperature and time gave only traces of a monohalogeno derivative.

The discrimination between the two primary hydroxyl groups of a β-1,3-linked disaccharide is particularly tricky since reactivities of 4-OH and 6-OH are similar. Several procedures to selectively introduce a functional group at C-6' on a disaccharide have been described. Bulky groups such as triphenylmethyl (trityl), tert-butyldimethylsilyl, thexyldimethylsilyl (2,3-dimethyl-2-butyl) are known preferentially to block the readily accessible primary hydroxyl groups. Among these groups, the trityl moiety appears to provide the greatest regioselectivity. Klemm *et al.*[47] used a trityl group to modify C-6 positions on cellulose. Later, Kern *et al.*[48] used *p*-methoxytrityl with the same purpose for the synthesis of 2,3-di-*O*-methylcellulose due to its better reactivity and a more rapid deprotection. Tritylation of laminaribiose followed by further acetylation was reported by Wang *et al.*[39] who obtained a mixture of 6'-*O*-trityl-, 6,6'-di-*O*-trityl- and 6-*O*-trityl- in a 5:2:1 ratio respectively.

To obtain the target $6'N_3$-Glcβ3GlcαF (**11a**), the selective tritylation reaction was deeply studied in this work as it is shown in Figure 3. 18. As direct substitution of the trityl group with the azide is not possible, several studies of deprotection and further halogenation and esterification reactions were analyzed for the final introduction of the azide and the results are presented in this work.

3.2.1.4. Polymer approach: results

First, using the same conditions as Wang,[32] the reaction with curdlan (**37**) (300 mg) and a kitalase (4.5 mg, 9 U) at pH 5.0, 42 ºC at 250 rpm was monitored for 20 h in order to optimize the production of laminaribiose (Figure 3. 19). Aliquots were withdrawn and after enzyme inactivation, the soluble fraction was freeze-dried and acetylated before TLC analysis.

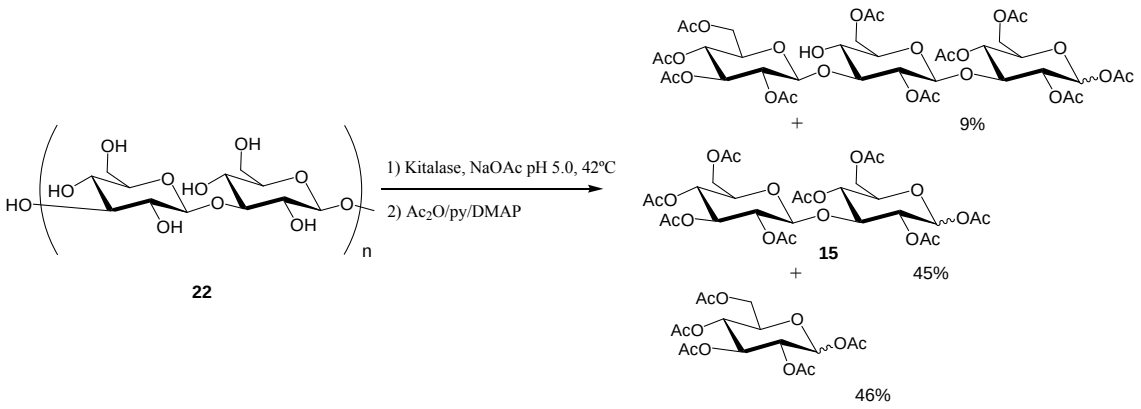

Figure 3. 19: Enzymatic degradation of curdlan.

A mixture of peracetylated mono-, di- and trisaccharides was present along the reaction and the disaccharide maximum yield of 40% was reached between 4 and 6 hours. At that moment, the ratio of mono-, di- and trisaccharides was 47:39:14 respectively (Figure 3. 20). After 6 hours of reaction, laminaribiose started to be hydrolyzed and the production of glucose increased remarkably.

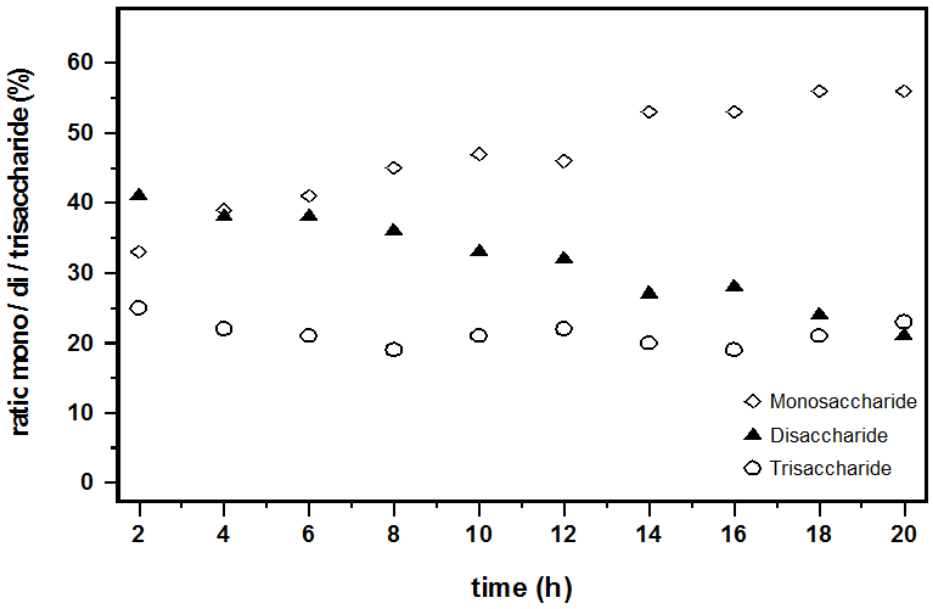

Figure 3. 20: Degradation of curdlan reaction.

The enzymatic reaction was scaled up, followed by further acetylation and purification affording the peracetylated laminaribioside (**15**) in 45% yield (see characterization of the product in the Experimental section), the peracetylated glucoside (46%) and higher oligosaccharides (9%). Finally *O*-deacetylation by Zemplen afforded laminaribiose (**16**) in quantitative yields.

First attempts of direct tritylation of laminaribiose were carried out by using 1.2 equivalents of trityl chloride in pyridine containing DMAP at room temperature for one week similarly to the conditions reported by Wang (Figure 3. 21). The bulky group preferred the C-6' position than C-6 in a 1.3:1 ratio, however, the desired product **17** (6'-Tr) was only obtained in 20% yield and mainly laminaribiose **16** (64%) was recovered after acetylation and further purification (see characterization of 17 in the Experimental section). A tritylation study was done in order to improve the reaction yields. Therefore, reactions with laminaribiose and different trityl chloride equivalents followed by acetylation were performed, the products were purified, quantified and analyzed to determine the ratio of 6'-trityl (**17**), 6-trityl (**17i**) and 6,6'-ditrityl (**17ii**) compounds.

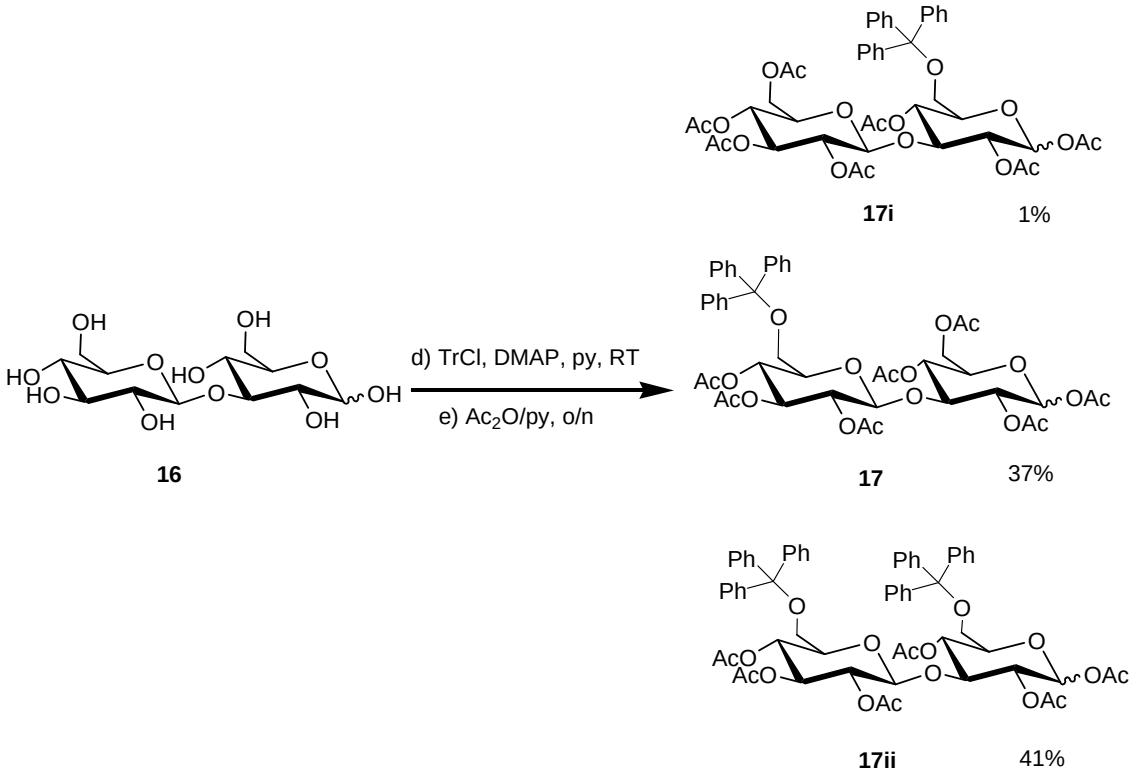

Figure 3. 21: Tritylation reaction.

In Figure 3. 22 it can be seen how the starting laminaribiose decreases as it reacts with TrCl to form the tritylated products. The higher the amount of TrCl added, the higher the ratio of monotritylated (6'-Tr and 6-Tr) and ditritylated products synthesized. With TrCl additions higher than 4.25 equivalents, the ratio of monotritylated product decreases while the ditritylated increases.

We found that the ratio of trityl chloride/disaccharide was crucial for the complete protection of the primary positions. The maximum yield of monotritylated products was found when using 2.5 – 4.5 equivalents of trityl chloride, whereas at lower amounts of TrCl, laminaribiose still

unreacted was the main product recovered. Higher amounts of TrCl (≥ 4.5 eq.) mainly led to the ditritylated compound. In the optimum conditions, the monotritylated products were obtained in 50 – 60% yields. With additions of 2 – 4.5 equivalents of TrCl the target 6'-Tr product was obtained in 30 – 37% yields. There was a preferential regioselectivity for 6'-tritylation *vs* 6-tritylation (average ratio of 2 – 2.5:1 respectively) and typically 6-Tr was obtained in 10 – 17% yields.

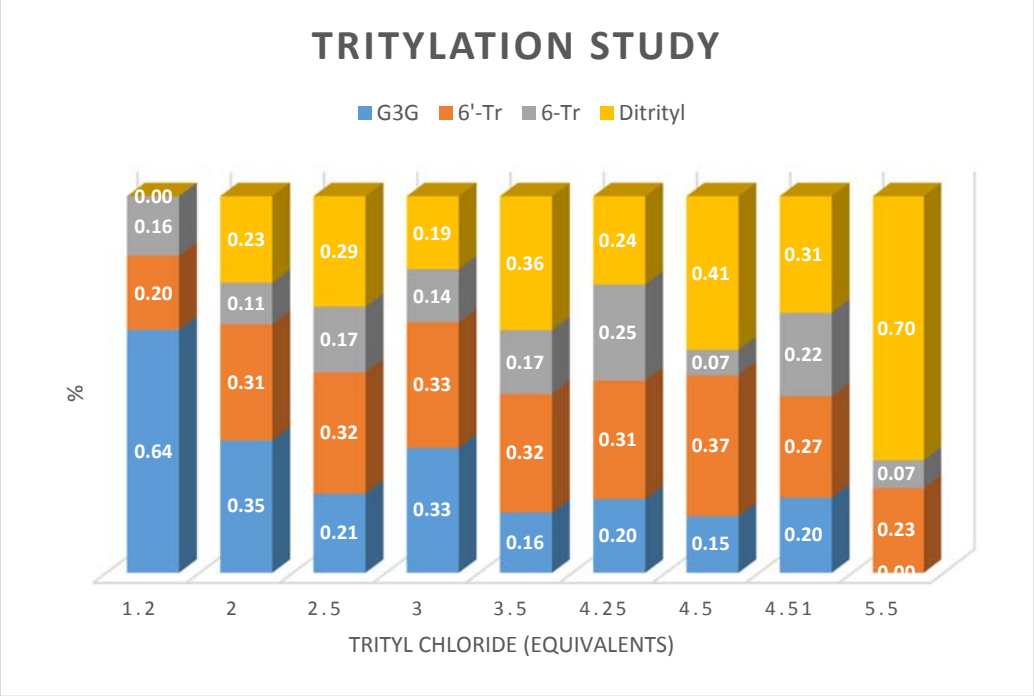

Figure 3. 22. Ratio of tritylated products *vs* equivalents of TrCl.

Detritylation of compound **17** was first performed in 80% aqueous acetic acid at 70 ºC. After 5 hours, detritylation was complete. However, unexpectedly if compared to the good results obtained by Wang et al., three new products were formed (Figure 3. 23). Additionally to compound **18**, two other products were obtained in similar ratios due to migration of acetyl groups after the deprotection of C-6' as commented in literature.[49,50] No re-insertion of trityl nor any other possible side-reaction was observed.

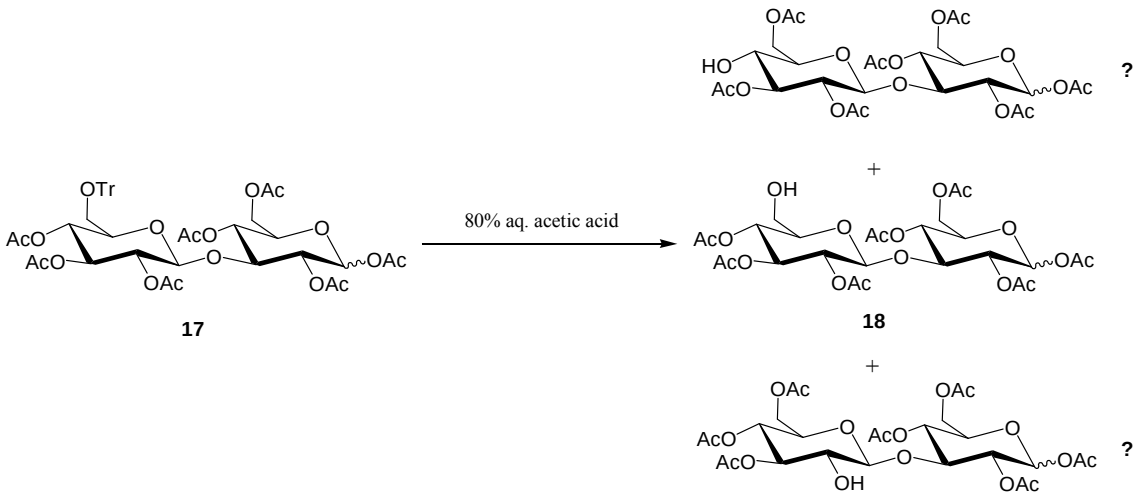

Figure 3. 23: Detritylation reaction. Acetyl migrations.

The facile migrations of acyl groups in partially acylated polyhydroxylic compounds were first noted by E. Fischer and Ohle between 1920 – 1924. They observed the conversion of 3-*O*-benzoyl-1,2-*O*-isopropylidene-α-D-glucofuranose into the 6-*O*-benzoyl isomer under the influence of traces of alkali. Since this observation, these migrations have been observed under neutral, basic, and acidic conditions, and have been reported to originate at all positions except C-6 in the hexose series. As a consequence, the number of reactions that may be carried out in partially acetylated sugars without affecting the acetylated positions is severely limited because of acyl migrations.[51]

It has been suggested that those acyl migrations which span a large number of carbon atoms may proceed *via* a series of consecutive migrations each spanning fewer carbons (*i.e.*, C2→C6 *via* C4→C6, C3→C4, and C2→C3) and each involving ortho acid ester intermediates of smaller ring size.[47]

With the idea of improving the yields by avoiding acyl migrations, we studied two more detritylation procedures. On the one hand, the use of 2 equivalents of iron chloride per trityl group and short reaction times was known to detritylate quantitatively mono- and disaccharide derivatives[47] as well as trisaccharides derivatives without acetyl migration.[39] On the other hand, Ogawa et al also described the absence of migrations in detritylations of 1,6-disaccharide derivatives with aq. acetic acid in the presence of NaI at 80 ºC.[48] While this last reaction was the fastest, producing compound **18** in 2.5 hours and avoiding migrations in the next synthetic steps, detritylation was always incomplete and not reproducible. By contrast, the use of $FeCl_3 \cdot 6\ H_2O$ allowed the complete detritylation of compound **17** (87% yield) in higher yields.

The introduction of the azide was performed following two different approaches (Figure 3. 24). Several reactions were studied introducing two different leaving groups (tosyl and bromide) at C-6'in order to displace them with the desired azido group.

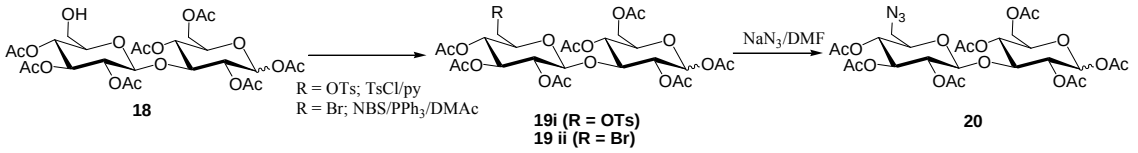

Figure 3. 24: Introduction of the azide.

Our studies on the tosylation reaction demonstrated that sequential tosylation was completely necessary for the development of the reaction. However, migration was observed when compound **18** was obtained by detritylation with $FeCl_3 \cdot 6\ H_2O$ (see characterization in the Experimental section) and two main products with R_f 0.36 (Compound **19i,** 50% yield) and R_f 0.27 were obtained always in a reproducible way eluted in EtOAc/Toluene (1:1). Further substitution of **19i** with NaN_3 yielded the target acetylated 6'N_3-Glcβ3Glc (compound **19ii**) in 24% yield (two steps of reaction: tosylation and azidation). We also performed halogenation of compound **18** with NBS produced several brominated products. 6'Br-Glcβ3Glc (**8bii**) (R_f 0.49 eluted in EtOAc/Toluene (1:1)) was later azidated with NaN_3 synthesizing **19ii** in 17% yield (two steps of reaction). The signal at δ 51 ppm of the ^{13}C NMR spectrum verified the presence of the azido group at C-6' in compound **20**. The total yield from laminaribiose (**16)** to acetylated 6'N_3-Glcβ3Glc (**20**) was in average of 7% (for the five steps). In all cases, an anhydrous conditions was required, and the reactants and solvents must be of high purity. Finally, the activated donor was synthesized by fluorination with HF/py (yields around 25 – 35%) (see characterization of **11b** in the Experimental section) and further deacetylation. In this way, the target compound **11a** was obtained (Figure 3. 25).

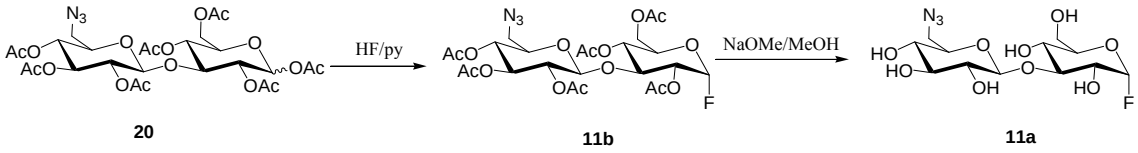

Figure 3. 25: Synthesis of **11a**. Introduction of the fluoride in the anomeric position and further deacetylation.

In summary, the main bottleneck of this process was the differentiation of the two primary hydroxyl groups at C-6 and C-6'. The tritylation reaction was deeply studied and its yield was

improved. However, the introduction of the azide involved a previous introduction of a leaving group. Therefore, tosylation and bromination reactions were studied but in all cases, several functionalized products were obtained due to acetyl migrations, altogether decreasing the yield of the isolated target compound. The functionalized donor 6'N_3-Glcβ3GlcαF **11a** was successfully achieved using the 'Polymer approach'.

3.2.2. Synthesis of acceptors for the glycosynthase reaction

As Figure 3. 3 shows, the other target was *p*-nitrophenyl 6-azido-6-deoxy-β-D-glucoside (6N_3-GlcβPNP, **35**) that will act as an acceptor in the glycosynthase reaction for the subsite acceptance study. As far as we know this compound was not synthesized before. Therefore, we designed a simple set of reactions for the synthesis of **35** presented in Figure 3. 26. It could be obtained after regiospecific tosylation of *p*-nitrophenyl β-D-glucoside (GlcβPNP, **31**) and further substitution by sodium azide with an overall yield of 50% (see characterization of the products in the Experimental section).

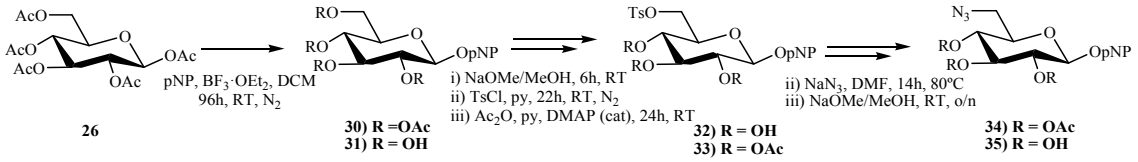

26

30) R =OAc
31) R = OH

32) R = OH
33) R = OAc

34) R = OAc
35) R = OH

Figure 3. 26. Synthesis of the acceptor 6N_3-GlcβPNP (**35**).

3.2.3. Enzyme characterization: docking and kinetics.

3.2.3.1. Docking

Docking approaches directly model physical interactions focusing on the final configuration of the complex. They become useful tools for a first structural analysis of the active site of the enzyme. In order to study the effect of the new functional group on subsites –2 and +1 the binding of different susbtrates (GlcβPNP and 6N_3-GlcβPNP) to the active site of the E134S glycosynthase mutant of the 1,3-1,4-β-glucanase from *Bacillus licheniformis* was predicted by means of computational docking. The 3D structure of the enzyme was taken from the Protein Data Bank, accession code 1UOA, which corresponds to an enzyme complex with the tetrasaccharide Glcβ4Glcβ4Glcβ3Glc. From this structure, the Glcβ3GlcαF and 6N_3-Glcβ3GlcαF were manually built and kept in the same position as in the X-ray structure. The structures of the two acceptors to be tested (GlcβPNP and 6N_3-GlcβPNP) were generated from the coordinates of a GlcβPNP molecule taken from the PDB (accession code: 3AI0).

The study of subsite +1 is illustrated in Figure 3.27 where Glcβ3GlcαF is located in the donor subsites and $6N_3$-GlcβPNP is in the acceptor subsites. There is apparently enough room in the active site for the azido group to fit in the active site. Moreover, the distance between the anomeric carbon of the donor (see the fluoride in green, figure 3. 27A) and the nucleophilic 3-OH of the functionalized acceptor is less than 4 Å. It seems that the acceptor substrate should be able to get activated through general base catalysis and perform the reaction.

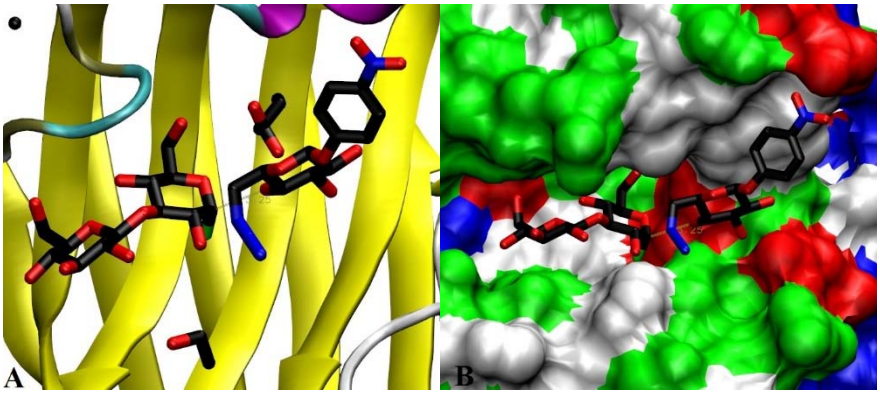

Figure 3. 27: Close up to the active site of the E134S glycosynthase mutant of 1,3-1,4-β-glucanase from *Bacillus licheniformis*. $6N_3$-GlcβPNP (**35**) is located at +1 and +2 subsites and Glcβ3GlcαF (**36**) at -2 and -1 subsites. Figure A shows the active site at molecular surface. In Figure B the protein surface is represented as well.

On the other hand, in Figure 3. 28 the subsite -2 is evaluated using the donor $6'N_3$-Glcβ3GlcαF and the acceptor GlcβPNP. In this case, the donor containing the azido groups fits in the active site placing the azide outwards the active site. The position that the backbone of both acceptors (**31** and **35**) adopt in the active site is exactly the same in Figures 3. 27 and 3. 28, and the distance between the anomeric carbon of the donor and the nucleophilic 3-hydroxyl of the acceptor slightly higher than 4 Å. Therefore, after the two computational docking studies, it looked like the functionalized molecules could bind to the active site and should be able to react and develop synthase activity.

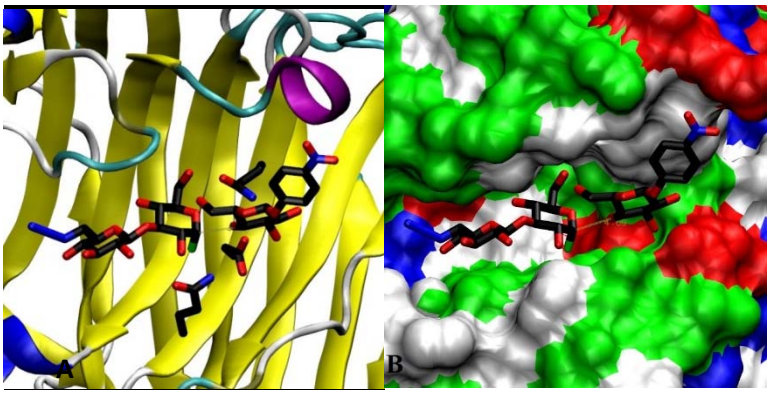

Figure 3. 28: Close up to the active site of the E134S glycosynthase mutant of 1,3-1,4-β-glucanase from *Bacillus licheniformis*. Figure A: GlcβPNP (**31**) has been located at +1 and +2 subsites and 6N_3-Glcβ3GlcαF (**26**) at -2 and -1 subsites. In Figure B the protein surface is represented as well.

3.3.3.2. Kinetics

Condensation reactions between laminaribiosyl fluoride donors (Glcβ3GlcαF and 6'N_3-Glcβ3GlcαF) and *p*-nitrophenyl glucoside acceptors (GlcβPNP and 6N_3-GlcβPNP) were performed (Figure 29) in order to study the acceptance of the new functionality by the enzyme.

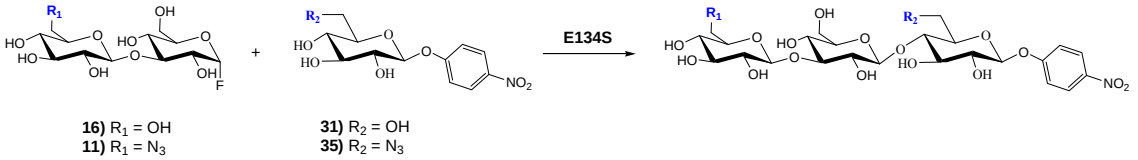

16) R_1 = OH
11) R_1 = N_3

31) R_2 = OH
35) R_2 = N_3

Reaction	R_1	R_2	s.a. (%)
16 + 31	OH	OH	100
16 + 35	OH	N_3	100
11a + 31	N_3	OH	0.15

Figure 3. 29. E134S glycosynthase subsite studies. Conditions: 5 mM R_2Glc*p*NP, 1 mM Glcβ3GlcαF, 35ºC, 50 mM phosphate buffer pH 7.0. [E134S] = 0.1 μM.

Reaction was performed at saturating donor concentrations according to K_M of Glcβ3Glc (1mM). To avoid the self-condensation of the donor, an excess of acceptor was used in all reactions with a ratio donor-acceptor of 1:5 and reaction conditions of pH 7, 35 ºC. The reference reaction to study the acceptance of the subsites was Glcβ3GlcαF + GlcβPNP **(16 + 31)** yielding the Glcβ3Glcβ4GlcβPNP trisaccharide. On the one hand, to evaluate subsite -2, 6'N_3-Glcβ3GlcαF and GlcβPNP were used as a donor and as an acceptor respectively **(16+35)** introducing the azide in the laminaribiosyl donor and yielding the 6'N_3-Glcβ3Glcβ4GlcβPNP trisaccharide. On the other hand, to study subsite +1 Glcβ3GlcαF and 6N_3-GlcβPNP were used **(11a+31)** introducing the azide in the *p*-nitrophenyl acceptor and yielding the Glcβ3Glcβ4-6N_3-GlcβPNP trisaccharide. The specific activity of the enzyme (E134S) when studying subsite +1 was of 64 min^{-1}, exactly

the same value obtained for the reference reaction. When studying subsite -2 with 6'N_3-Glcβ3GlcαF (**11a**) and GlcβPNP (**31**), the specific activity was 629 times slower than the reaction Glcβ3GlcαF + GlcβPNP.

These results reflect that E134S can accommodate a functionalized azido substrate in both subsites, but with very low activity when placing the azido group in the -2 subsite. This fact is very typical for both *endo*- and *exo*- glycosidases where the donor subsite is more restrictive than the more promiscuous acceptor subsite.

In other endo-glycosynthases, promiscuity of subsite -2 has been observed. Fort *et al*. described the chemosenzymatic synthesis of a variety of regioselectively modified β-(1,4)-oligo- and polysaccharides by the use of the E197A glycosynthase mutant from the retaining cellulase endoglucanase I from *Humicola insolens*.[49] After first examining the information given by the X-ray structures of wild type and mutated cellulases they rationally designed different modified donors and acceptors for the glycosynthase reaction. Their results confirmed those of the X-ray structure of the complexed wild type enzyme in which the 6-OH and 2-OH of the glucosyl unit in subsite +1 were not involved in key polar interactions. When using α-lactosyl fluoride as a donor and a 6,6'-dibrominated α-cellobiosyl fluoride as an acceptor for the glycosynthase reaction the corresponding functionalized tetrasaccharide was obtained in 80% yields. These results demonstrated that subsites -1 and -2 could accept the new functionalizations at C6. Furthermore, in subsite -2, 6-OH was extremely solvent exposed and frequently disordered and this lack of steric restriction on the C6-OH interactions was exploited for the synthesis of substituted β-(1,4)-glucans.

Therefore, despite the low activities obtained with donor **11a**, the polymerization reaction is expected to occur. However, it is not studied in this work and it is open for future research. The reaction yields will probably be low and directed evolution will be needed to optimize the enzyme and improve substrate recognition.

3.3. CONCLUSIONS

The synthesis of 6'N_3-Glcβ3GlcαF, donor for the glycosynthase reaction and not synthesized before, was achieved after exploring different approaches ('Total synthesis 1 and 2' and 'Polymer approach'). The polymer approach afforded laminaribiose after enzymatic digestion and the substrate was synthesized chemically after several protection and deprotection steps with low overall yield. The critical differentiation between C-6 and C-6' of laminaribiose was approached by the use of trityl chloride (sequential addition) which had a preference for C-6' (tritylation ratio, C-6'*vs* C-6 of 2 – 2.8 to 1). The best tritylation conditions were achieved when using 4.5 equivalents of TrCl (37% yield of 6'-trityl derivative). After the detritylation reaction with iron chloride, the introduction of the azide was achieved by displacement of a leaving group (tosyl or bromide). However, acetyl migration occurred after detritylation. In the future, the overall process should be redesigned in order to increase the reaction yields.

When working in the 'Total synthesis 1' approach different donors and acceptors were explored. However, due to problems in the protection and deprotection of some groups of the acceptors that could not be overcome, the desired 6'N_3-Glcβ3GlcαF donor could not be achieved through this chemical path.

Computational docking studies allowed a first approximation structural analysis of the active site of the E134S glycosynthase mutant. The effect of the new functional group, an azide introduced in a C-6 position of different substrates, was studied at subsites -2 and +1. The results predicted the binding of the functionalized molecules to the active site of the enzyme and the syntheses of a functionalized acceptor (6N_3-GlcβPNP) and a functionalized donor (6'N_3-Glcβ3GlcαF) were performed.

Condensation reactions between laminaribiosyl fluoride donors (Glcβ3GlcαF and 6'N_3-Glcβ3GlcαF) and *p*-nitrophenyl glucoside acceptors (GlcβPNP and 6N_3-GlcβPNP) catalyzed by the E134S mutant yielded in both cases the corresponding functionalized trisaccharides. Subsite +1 is not affected by the presence of the new functional group. However, subsite –2 is affected the enzyme activity decreases 629 times *vs* the non-functionalized donor. Therefore, the enzyme should be modified for better results if self-condensation of the donor is going to be performed in the future for the production of artificial alternating azido β-glucans.

3.4. EXPERIMENTAL

3.4.1. Materials

Benzene (anhydrous), methyl α-D-glucopyranoside and acetyl 2,3,4,6-tetra-*O*-acetyl-β-D-glucopyranoside were purchased from Sigma-Aldrich. (±)-camphor-10-sulfonic acid was purchased from Sigma-Aldrich and was recrystallized twice from dried EtOAc.

Cyclohexane, chloroform and DCM were distilled over $CaCl_2$. In some cases DCM was distilled a second time over P_2O_5 for a higher desiccation. Ethyl acetate was distilled over K_2CO_3. DMF was purified by drying overnight over KOH pellets and distilling later from BaO. Pyridine was distilled over KOH. 1,2-dichloroethane was first dried with $MgSO_4$ and further distilled over P_2O_5. $HgBr_2$ and $Hg(CN)_2$ were dried at 70 ºC in a desiccator for 12 hours before their use. Molecular sieves were activated in the oven at 450 ºC for 3 - 4 hours. Celite was washed with sodium bicarbonate before filtration of the product of glycosylation.

Curdlan was purchased from Wako Pure Chemical Industries, Ltd. and kitalase (300 units/g) from Wako Chemicals USA, Inc. *N*-bromosuccinimide (NBS, Sigma) was recrystallized from boiling water and dried for two days under reduced pressure over anhydrous calcium chloride. Triphenylphosphine (PPh_3, Sigma) was recrystallized from boiling ethanol and dried overnight under reduced pressure over anhydrous calcium chloride. Dimethylacetamide (DMAc, Fisher Scientific) was kept over 4 Å molecular sieves and stored under dry nitrogen after the first use. DMF and pyridine were freshly distilled before its use over BaO or $MgSO_4$ and KOH respectively.

3.4.2. Synthesis of glycosynthase donors

3.4.2.1.Total synthesis 1

Methyl 4,6-*O*-benzylidene-α-D-glucopyranoside (2)

A mixture of methyl α-D-glucopyranoside (**1a**) (10.50 g, 51.70 mmol), α,α-dimethoxytoluene (25 mL, 169 mmol), (±)-10-camphorsulfonic acid (0.21 g, 1.00 mmol) and anhydrous benzene (500 mL) was heated under reflux for 6 hours under nitrogen atmosphere. Most of the solvent was evaporated under reduced pressure and the resulting crude was dissolved in DCM and washed with saturated aq. $NaHCO_3$, saturated aq. NaCl and water. The organic layer was dried over $MgSO_4$, concentrated and the residue was triturated with hexane to give after filtration compound **2** (11.90 g, 42.40 mmol) in 82% yield.

^{1}H NMR (400MHz, $CDCl_3$) δ 7.49 – 7.35 (m, 5H, ArH), 5.53 (s, 1H, C*H*Ph), 4.80 (d, 1H, $J_{1,2}$ = 3.9 Hz, H-1), 4.29 (dd, 1H, $J_{6a,6b}$ = 9.7, $J_{5,6b}$ = 4.3 Hz, 1H, H-6_a), 3.93 (t, 1H, $J_{3,4}$ = 9.2 Hz, H-3), 3.84 – 3.71 (m, 2H, H-5, H-6_b), 3.63 (dd, 1H, $J_{1\text{-}2}$ = 3.6 Hz, $J_{2,3}$ = 9.0 Hz, H-2), 3.49 (t, 1H, $J_{3,4}$ = 9,2, H-4), 3.46 (s, 3H, OMe).

Methyl 2-*O*-benzoyl-4,6-*O*-benzylidene-α-D-glucopyranoside (23)

Imidazole (5.78 g, 0.08 mol) was dissolved in purified chloroform (150 mL), and benzoyl chloride (4.93 mL, 0.04 mol) was added slowly with cooling. The suspension was filtered to remove imidazole hydrochloride and the filtrate was added to **2** (11.99 g, 0.04 mol) in chloroform (200 mL) and heated for 13 hours at reflux. After being extracted with sodium hydrogen carbonate solution (50 mL) and two portions of saturated sodium chloride solution (50 mL), the solution was dried with magnesium sulfate and concentrated to give crude **23** which was recrystallized from acetone-water (8.67 g, 0.02 mol) in 57% yield.

^{1}H NMR (400MHz, $CDCl_3$) δ 8.11 – 7.37 (m, 10H, ArH), 5.58 (s, 1H, C*H*Ph), 5.08 (d, 1H, $J_{1,2}$ = 3.8 Hz, H-1), 5.04 (dd, 1H, $J_{2,3}$ = 9.5, $J_{1,2}$ = 3.8 Hz, H-2), 4.38 – 4.31 (m, 2H, H-3, H-6_b), 3.90 (dd, 1H, $J_{5,6a}$ = 9.9 Hz, $J_{4,5}$ = 4.7 Hz, H-5), 3.80 (t, 1H, $J_{6a,6b}$ = 10.2 Hz, H-6_a), 3.63 (t, 1H, $J_{4,3}$ = 9.4 Hz, H-4), 3.40 (s, 3H, OMe).

Methyl 2-*O*-benzyl-4,6-*O*-benzylidene-α-D-glucopyranoside (25)

Compound **2** (0.45 g, 1.59 mmol) was dispersed in toluene (30 mL) in a flask fitted with a Dean-Stark apparatus. One third of the toluene was distilled off and the required quantity of $(Bu_3Sn)_2O$ (1.8 mL, 3.02 mmol) was added. More toluene (half of the remaining volume) was removed by distillation, the Dean-Stark assembly was replaced with a condenser, and the mixture was refluxed for 3 hours. The mixture was concentrated, the syrupy residue was dried thoroughly and then the mixture was treated with benzyl bromide (4.0 mL, 33.6 mmol) and stirred under N_2 at 90 ºC for 48 hours. Then, the reaction mixture was introduced in an ice-bath and MeOH (40 mL) was slowly added to eliminate the excess of benzyl bromide. The syrupy product was transferred onto a dry silica gel column and purified by flash chromatography (gradient 1:3 → 1:2 EtOAc - cyclohexane) obtaining **25** (0.52 g, 1.40 mmol) in 89% yield.

^{1}H NMR (400MHz, $CDCl_3$) δ 7.46 – 7.31 (m, 10H, ArH), 5.47 (s, 1H, C*H*Ph), 4.76 – 4.65 (m, 2H, CH_2Ph), 4.57 (d, 1H, $J_{1,2}$ = 3.6 Hz, H-1), 4.22 (dd, 1H, $J_{6a,6b}$ = 10.0, $J_{5,6a}$ = 4.7 Hz, H-6_a), 4.11 (t, 1H, H-3), 3.80 – 3.74 (m, 1H, H-5), 3.66 (t, 1H, $J_{6a,6b}$ = 10.0 Hz, H-6_b), 3.47 – 3.41 (m, 2H, H-4, H-2), 3.33 (s, 3H, OMe).

Methyl 2-*O*-allyl-4,6-*O*-benzylidene-α-D-glucopyranoside (3)

Compound **2** (12.29 g, 43.54 mmol) was dispersed in toluene (487 mL) in a flask fitted with a Dean-Stark apparatus. One third of the toluene was distilled off and the required quantity of $(Bu_3Sn)_2O$ (38 mL, 63.74 mmol) was added. More toluene (half of the remaining volume) was removed by distillation, the Dean-Stark assembly was replaced with a condenser, and the mixture was refluxed for 3 hours. The mixture was concentrated, the syrupy residue was dried thoroughly and then the mixture was treated with allyl bromide (sequential addition of 35 mL, 673.9 mmol) and stirred under N_2 at 100 ºC for 15 hours. Then, the reaction mixture was introduced in an ice-bath and MeOH (50 mL) was slowly added to eliminate the excess of allyl bromide. The syrupy product was transferred onto a dry silica gel column and purified by flash chromatography (gradient 1 → 1:2 → 2:1 → 1:5 cyclohexane – EtOAc) obtaining **3** (9.89 g, 30.68 mmol) in 70% yield. MS m/z 667.2766 $[2M+Na]^+$.

^{1}H NMR (400MHz, $CDCl_3$) δ 7.51 – 7.35 (m, 5H, ArH), 6.01 – 5.91 (m, 1H, CH_2-C*H*=CH_2), 5.54 (s, 1H, C*H*Ph), 5.32 – 5.24 (m, 2H, CH_2-CH=C*H*$_2$), 4.84 (d, 1H, $J_{1,2}$ = 3.5 Hz, H-1), 4.29 (dd, 1H, $J_{6a,6b}$ = 10.0, $J_{5,6a}$ = 4.4 Hz, H-6$_a$), 4.22 (m, 2H, C*H*$_2$-CH=C*H*$_2$, H-5), 4.12 (m, 1H, H-3), 3.86 – 3.80 (m, 1H, C*H*$_2$-CH=C*H*$_2$), 3.74 (t, 1H, $J_{6a,6b}$ = 10.0 Hz, H-6$_b$), 3.53 (t, 1H, $J_{4,3}$ = 9.3 Hz, H-4), 3.47 – 3.43 (m, 1H, H-2), 3.45 (s, 3H, OMe).

Methyl 2-*O*-benzyl-4,6-*O*-isopropylidene-α-D-glucopyranoside (24)

Synthesis of methyl 4,6-O-isopropylidene-α-D-glucopyranoside

A mixture of methyl α-D-glucopyranoside (**1**) (2.45 g, 12.6 mmol), 2,2-dimethoxypropane (7.7 mL, 63 mmol), *p*-toluenesulfonic acid (159 mg, 0.84 mmol) and anhydrous DMF (120 mL) was stirred at room temperature for 1.5 hours. Et_3N (4 mL) was added to the mixture and the solvent was evaporated under reduced pressure. The resulting crude was purified by flash chromatography ($CHCl_3$/EtOAc/MeOH, 5:2:1) obtaining the desired methyl 4,6-*O*-isopropylidene-α-D-glucopyranoside (3.11 g, 13.28 mmol) in 100 % yield.

^{1}H NMR (400MHz, $CDCl_3$) δ 4.78 (d, 1H, $J_{1,2}$ = 4.0 Hz, H-1), 3.89 (dd, 1H, $J_{6a,6b}$ = 10.8, $J_{5,6b}$ = 5.2 Hz, 1H, H-6$_b$), 3.82 – 3.74 (m, 2H, H-3, H-5), 3.67 – 3.52 (m, 3H, H-6$_b$, H-4, H-2), 3.44 (s, 3H, OMe), 1.53 (s, 3H, C*H*$_2$C isopropylidene), 1.46 (s, 3H, C*H*$_2$C isopropylidene). (Figure A3. 5).

Methyl 4,6-*O*-isopropylidene-α-D-glucopyranoside (3.11 g, 13.28 mmol) was dispersed in toluene (230 mL) in a flask fitted with a Dean-Stark apparatus. One third of the toluene was distilled off and the required quantity of $(Bu_3Sn)_2O$ (15 mL, 29.50 mmol) was added. More

toluene (half of the remaining volume) was removed by distillation, the Dean-Stark assembly was replaced with a condenser, and the mixture was refluxed for 2.5 hours. The mixture was concentrated, the syrupy residue was dried thoroughly and then the mixture was treated with benzyl bromide (33 mL, 280.6 mmol) and stirred under N_2 at 90 ºC for 48 hours. Then, the reaction mixture was introduced in an ice-bath and MeOH (40 mL) was slowly added to eliminate the excess of benzyl bromide. The syrupy product was transferred onto a dry silica gel column and purified by flash chromatography (gradient 1 → 2:1 cyclohexane - EtOAc) obtaining a mixture of benzylated isomers (methyl 4,6-*O*-benzylidene-α-D-glucopyranoside benzylated at C-2 and C-3) with the same R_f (1.34 g, 4.13 mmol) in 31% yield. NMR data of the mixture of isomers was obtained showing that the isomer benzylated at C-2 was majoritary (Figure A3. 6). ^{13}C NMR ($CDCl_3$, 100 MHz) δ 79.6 (C-2, 3-OBn), 79.0 (C-2, 2-OBn).

p-methoxyphenyl 2-*O*-allyl-4,6-*O*-benzylidene-β-D-glucopyranoside (29)

Synthesis of p-methoxyphenyl 2,3,4,6-tetra-O-acetyl-β-D-glucopyranoside

To a solution of acetyl 2,3,4,6-tetra-*O*-acetyl-β-D-glucapyranoside (10.0 g, 25.62 mmol) and *p*-methoxyphenol (4.8 g, 38.67 mmol) in dried dichloroethane (80 mL) was added TMSOTf (0.5 mL, 2.76 mmol) at 0 ºC. The mixture was kept at 0 ºC and stirred under inert conditions (N_2) for 4.5 hours, diluted with EtOAc (120 mL), washed with aq satd $NaHCO_3$ (3 x 40 mL) and water (3 x 40 mL). The organic layer was dried with $MgSO_4$, filtered and concentrated. The crude was purified by flash chromatography (5:1 toluene – EtOAc) and *p*-methoxyphenyl 2,3,4,6-tetra-*O*-acetyl-β-D-glucopyranoside (6.20 g, 13.63 mmol) was obtained in 30 % yield.

^{1}H NMR (400MHz, $CDCl_3$) δ 6.96 – 6.83 (2 m, 4H, Aromatics), 4.93 (d, 1H, $J_{1,2}$ = 7.4 Hz, H-1), 4.30 (dd, 1H, $J_{6a,6b}$ = 12.0, $J_{6a,5}$ = 2.3 Hz, 1H, H-6_a), 3.76 (s, 3H, OMe), 2.09, 2.08, 2.05, 2.04 (s, 12H, 4Ac).

Test of deprotection of the p-methoxyphenyl group

To a solution of *p*-methoxyphenyl 2,3,4,6-tetra-*O*-acetyl-β-D-glucopyranoside (0.4 g, 0.88 mmol) in 1:1:1 toluene – ACN – water (89 mL) was added ammonium cerium nitrate (6.0 g, 10.94 mmol). The mixture was stirred for 30 minutes, diluted with EtOAc (100 mL) and washed with aqueous saturated $NaHCO_3$ (3 × 30 mL) and water (3 × 30 mL). The solution was dried with $MgSO_4$, filtered and concentrated.

Synthesis of p-methoxyphenyl 4,6-O-benzylidene-β-D-glucopyranoside

To a solution of *p*-methoxyphenyl 2,3-di-*O*-acetyl-β-D-glucopyranoside (3.1 g, 6.86 mmol) in methanol (40 mL) was added of methanolic NaOMe 1M (0.345 mL) was added and the solution

was stirred overnight at room temperature. Then, Amberlyst® 15 resin was added to neutralize the mixture and it was filtered and concentrated to give *p*-methoxyphenyl β-D-glucopyranoside.

The crude *p*-methoxyphenyl β-D-glucopyranoside was dissolved in dry DMF (22 mL). Benzaldehyde dimethyl acetal (1.1 mL, 7.33 mmol) and *p*-toluensulfonic acid (30 mg, 0.16 mmol) were added to the mixture and it was stirred overnight. The mixture was neutralized with Amberlyst® 21 resin, filtrated and concentrated. The crude was purified by flash chromatography (5:1 DCM – acetone) obtaining *p*-methoxyphenyl 4,6-*O*-benzylidene-β-D-glucopyranoside (1.57 g, 4.19 mmol) in 61% yield.

^{1}H NMR (400MHz, $CDCl_3$) δ 7.51 – 7.48 (2m, 5H, C_6H_5CH), 7.04 – 6.83 (2 m, 4H, $C_6H_4OCH_3$), 5.58 (s, 1H, C_6H_5CH), 4.89 (d, 1H, $J_{1,2}$ = 7.7 Hz, H-1), 3.78 (s, 3H, OMe).

Synthesis of *p*-methoxyphenyl 2-*O*-allyl-4,6-*O*-benzylidene-β-D-glucopyranoside (29)

p-methoxyphenyl 4,6-*O*-benzylidene-β-D-glucopyranoside (6.13 g, 16.37 mmol) was dispersed in toluene (460 mL) in a flask fitted with a Dean-Stark apparatus. One third of the toluene was distilled off and the required quantity of the $(Bu_3Sn)_2O$ (17 mL, 28.78 mmol) was added. More toluene (half of the remaining volume) was removed by distillation, the Dean-Stark assembly was replaced with a condenser, and the mixture was refluxed for 2 hours. The mixture was concentrated, the syrupy residue was dried thoroughly and then the mixture was treated with allyl bromide (sequential addition of 32 mL, 613.3 mmol) and stirred under N_2 at 100 ºC for 16 hours. Then, the reaction mixture was introduced in an ice-bath and MeOH (50 mL) was slowly added to eliminate the excess of allyl bromide. The syrupy product was dried, concentrated and transferred onto a dry silica gel column and purified by flash chromatography (gradient 1 → 1:2 → 2:1 → 1:5 cyclohexane – EtOAc) obtaining **29** (4.46 g, 10.61 mmol) in 65% yield. ^{1}H NMR, ^{13}C NMR, COSY and HSQC spectra showed a mixture (50:50) of *p*-methoxyphenyl 2-*O*-allyl-4,6-*O*-benzylidene-β-D-glucopyranoside and *p*-methoxyphenyl 3-*O*-allyl-4,6-*O*-benzylidene-β-D-glucopyranoside. ^{1}H NMR (400MHz, $CDCl_3$) δ 4.95 (d, 1H, $J_{1,2}$ = 7.6 Hz, H-1, isomer 1), 4.91 (d, 1H, $J_{1,2}$ = 7.6 Hz, H-1, isomer 2).

Synthesis of the donor 2,3,4,6-tetra-*O*-acetyl-α-D-glucopyranosyl bromide (5)

Methyl 2,3,4,6-tetra-*O*-acetyl-α-D-glucopyranoside (4.11 g, 10.51 mol) was slowly added upon hydrobromic acid solution (33 wt. % in acetic acid) (13 mL, 70 mmol) and stirred for 1.5 hours under anhydrous conditions. The resulting solution was poured into ice-water (50 mL), the white solid that precipitated was filtered off and extracted with $CHCl_3$ (4 x 20 mL), and the solution

washed with saturated aq. $NaHCO_3$ (3 x 25 mL) until neutral pH, followed by water. After drying over $MgSO_4$ and filtering, evaporation of the solvent afforded compound **5** as a white amorphous solid (4.11 g, 9.98 mmol) in 95 % yield.

^{1}H NMR (400MHz, $CDCl_3$) 6.61 (d, 1H, $J_{1,2}$ = 4.0 Hz, H-1), 5.56 (t, 1H, $J_{3,4}$ = 9.7 Hz, H-3), 5.16 (t, 1H, $J_{4,3}$ = 9.6 Hz, H-4), 4.84 (dd, 1H, $J_{2,3}$ = 10.0 Hz, $J_{2,1}$ = 4.1 Hz, H-2), 4.35 – 4.29 (m, 2H, H-6_a, H-5), 4.15 – 4.12 (m, 1H, H6_b), 2.11, 2.10, 2.06, 2.04 (4s, 12H, 4Ac).

Synthesis of methyl *O*-(2,3,4,6-tetra-O-acetyl-β-D-glucopyranosyl)-(1→3)-2-*O*-allyl-4,6-*O*-benzylidene-α-D-glucopyranoside (6)

Compound **3** (2.00 g, 6.20 mmol), $HgBr_2$ (11.04 g, 30.63 mmol), $Hg(CN)_2$ (7.78 g, 30.81 mmol), powdered 4 Å molecular sieves (3.56 g), and DCM[1] (20 mL) were mixed and stirred in the dark under Ar for 1 h. Compound **5** (6.90 g, 16.79 mmol) in DCM (60 mL) was added and the mixture was stirred for 37 h with rigorous exclusion of light and moisture, then filtered over Celite, extracted with DCM, and washed with saturated aqueous saturated $NaHCO_3$ and water. After drying over $MgSO_4$ and evaporating the solvent, the residue was purified by flash chromatography over silica gel (gradient 65:35 → 50:50 → 35:65 → 1:5 Cy – EtOAc) to yield compound **6** (2.21 g, 3.38 mmol) in 55 % yield (R_f = 0.57, 2:1 EtOAc – cychlohexane). MS m/z 675.2280 $[M+Na]^+$.

^{1}H NMR ($CDCl_3$, 400 MHz) δ 7.47 – 7.34 (m, 5H, aromatic), 5.95 – 5.85 (m, 1H, CH_2-C*H*=CH_2), 5.52 (s, 1H, C*H*Ph), 5.30 – 5.19 (m, 2H, CH_2-CH=CH_2), 5.13 – 4.99 (m, 3H, H-3^{II}, H-4^{II}, H-2^{II}), 4.81 (d, 1H, $J_{1II,2II}$ = 8.0 Hz, H-1^{II}), 4.75 (d, 1H, $J_{1I,2I}$ = 4.0 Hz, H-1^{I}), 4.24 (dd, 1H, J = 9.6 Hz, J = 4.2 Hz, CH_2-CH=CH_2), 4.20 – 4.10 (m, 2H, H-5^{II}, H-6^{Ia}), 4.06 – 4.00 (m, 2H, H-6^{IIa}, H-6^{Ib}), 3.84 (dd, 1H, $J_{5II,6IIb}$ = 12.2 Hz, $J_{6IIa,6IIb}$ = 2.4 Hz, H-6^{IIb}), 3.78 (dd, 1H, $J_{4I,3I}$ = $J_{4I,5I}$ =9.4 Hz, H-4^{I}), 3.73 (t, 1H, J = 9.6 Hz, CH_2-CH=CH_2), 3.60 (t, 1H, $J_{3I,4I}$ = $J_{3I,2I}$ = 9.2 Hz, H-3^{I}), 3.46 (dd, 1H, $J_{2I,1I}$ = 3.8 Hz, $J_{2I,3I}$ = 9.3 Hz, H-2^{I}), 3.42 (s, 3H, OMe), 3.41 – 3.38 (m, 1H, H-5^{I}), 2.04, 1.97, 1.96, 1.95 (4s, 12H, 4 Ac).

^{13}C NMR ($CDCl_3$, 100 MHz) δ 170.48, 170.16, 169.31, 169.18 (CO), 134.46 (CH_2-*C*H=CH_2), 128.98, 128.08, 125.85 (Aromatic), 118.07 (CH_2-CH=*C*H_2), 101.21 (*C*HPh), 100.69 (C-1^{II}), 98.59 (C-1^{I}), 80.36 (C-3^{I}), 78.27 (C-2^{I}), 77.89 (C-5^{II}), 73.01 (C-3^{II}), 72.87 (C-6^{I}), 71.71 (C-2^{II}), 71.55 (C-5^{I}), 68.85 (*C*H_2-CH=CH_2), 67.97 (C-4^{II}), 61.93 (C-4^{I}), 61.57 (C-6^{II}), 51.14 (OMe), 20.65, 20.52, 20.45, 20.40 (CH_3).

Some hydrolysis of the benzylidene protecting group occurred after glycosylation and 0.721 g (1.159 mmol) (R_f = 0.16, 2:1 EtOAc – Cychlohexane) of the disaccharide deprotected at C-4 and C-6 were recovered (See Appendix Figure A3.11 and Figure A3.12). However, the benzylidene group could be easily reintroduced.

^{1}H NMR Methyl *O*-(2,3,4,6-tetra-*O*-acetyl-β-D-glucopyranosyl)-(1→3)-2-*O*-allyl-α-D-glucopyranoside ($CDCl_3$, 400 MHz) δ 5.95 – 5.85 (m, 1H, CH_2-C*H*=CH_2), 5.32 – 5.18 (m, 3H, CH_2-CH=C*H*$_2$, H-3^{II}), 5.08 – 5.02 (m, 2H, , H-4^{II}, H-2^{II}), 4.80 (d, 1H, $J_{1I,2I}$ = 3.6 Hz, H-1^{I}), 4.76 (d, 1H, $J_{1II,2II}$ = 8.0 Hz, H-1^{II}), 4.19 – 4.11 (m, 1H, C*H*$_2$-CH=CH_2), 4.03 (dd, 1H, *J* = 12.8 Hz, *J* = 6.4 Hz, C*H*$_2$-CH=CH_2), 3.94 – 3.74 (m, 4H, H-6^{Ia}, H-3^{I}, H-6^{Ib}, H-5^{II}), 3.63 – 3.59 (m, 2H, H-6^{IIa}, H-4^{I}), 3.51 (t, 1H, *J* = 9.2 Hz, H-5^{I}), 3.43 (s, 3H, OMe), 3.42 – 3.37 (m, 2H, H-6^{IIb}, H-2^{I}), 2.08, 2.04, 2.03, 2.01 (4s, 12H, Ac).

^{13}C NMR ($CDCl_3$, 100 MHz) δ 169.58, 169.13, 168.42, 168.32 (CO), 133.46 (CH_2-*C*H=CH_2), 117.22 (CH_2-CH=*C*H$_2$), 100.14 (C-1^{II}), 96.64 (C-1^{I}), 82.41 (C-3^{I}), 76.62 (C-2^{I}), 71.86 (C-3^{II}), 71.17 (*C*H$_2$-CH=CH_2), 70.78 (C-5^{II}), 70.32 (C-4^{II}), 69.88 (C-4^{I}), 68.35 (C-5^{II}), 67.39 (C-2^{II}), 66.92 (C-6^{II}), 61.41 (C-6^{I}), 54.16 (OMe), 19.74, 19.57, 19.54, 19.53 (CH_3).

Synthesis of methyl *O*-(6-azido-6-deoxy-2,3,4-tri-O-acetyl-β-D-glucopyranosyl)-(1→3)-2-*O*-allyl-4,6-*O*-benzylidene-α-D-glucopyranoside (8)

To a solution of **6** (1.07g, 1.64 mmol) in methanol (40 mL) was added of methanolic NaOMe 1M (0.570 mL) was added and the solution was stirred for 7 hours at room temperature. Then, Amberlyst® IR 120 acid resin was added to neutralize the mixture and it was filtered and concentrated to give methyl *O*-(β-D-glucopyranosyl)-(1→3)-2-*O*-allyl-4,6-*O*-benzylidene-α-D-glucopyranoside. 678 mg of the previous crude were dissolved in dry pyridine (18 mL) and TsCl (1.34 g, 6.97 mmol) was slowly and sequentially added to the mixture and it was securely stoppered and stirred for 18 hours at room temperature. Acetic anhydride (20 mL) and DMAP (30 mg) were directly added to the solution in order to acetylate the tosylated laminaribiosyl derivative. The mixture was stirred for 24 hours at room temperature. Finally, methanol (50 mL) was added to quench the reaction and after evaporation until dryness, the crude was redissolved with ethyl acetate, washed with water, dried and concentrated. 2.03 g (2.65 mmol) of crude *O*-(6-*O*-tosyl-2,3,4-tri-*O*-acetyl-β-D-glucopyranosyl)-(1→3)-2-*O*-allyl-4,6-*O*-benzylidene-α-D-glucopyranoside was dissolved in dry DMF (40 mL). Sodium azide (689 mg, 10.59 mmol) was added to the solution and stirred at 80 ºC for 12 hours. Saturated sodium bicarbonate and ethyl acetate were added to the solution and the organic phase was finally washed with water, dried, concentrated and purified by flash chromatography (toluene-ethyl acetate 20:1). Compound **8** (0.246 g, 0.393 mmol) was obtained in 25 % yield.

^{1}H NMR ($CDCl_3$, 400 MHz) δ 7.51 – 7.35 (m, 5H, aromatic), 5.99 – 5.84 (m, 1H, CH_2-C*H*=CH_2), 5.53 (s, 1H, C*H*Ph), 5.31 – 5.14 (m, 2H, CH_2-CH=C*H*$_2$), 5.09 (t, 1H, $J_{3II,4II}$ = 9.2 Hz, H-3^{II}), 5.02 – 4.93 (m, 2H, H-4^{II}, H-2^{II}), 4.88 (d, 1H, $J_{1II,2II}$ = 7.7 Hz, H-1^{II}), 4.76 (d, 1H, $J_{1I,2I}$ = 3.8 Hz, H-1^{I}), 4.24 (dd, 1H, *J* = 9.8 Hz, *J* = 4.4 Hz, C*H*$_2$-CH=CH_2), 4.19 – 4.01 (m, 3H, H-5^{II}, H-6^{Ia}, H-6^{Ib}), 3.83 – 3.63 (m, 2H, H-4^{I}, C*H*$_2$-CH=CH_2), 3.58 (t, 1H, $J_{3I,4I}$ = 9.2 Hz, H-3^{I}), 3.46 (dd, 1H, $J_{2I,1I}$ = 3.7 Hz, $J_{2I,3I}$ = 9.4 Hz, H-2^{I}), 3.42 (s, 3H, OMe), 3.41 – 3.38 (m, 1H, H-5^{I}), 3.18 (dd, 1H, $J_{5II,6IIa}$ = 13.2 Hz, $J_{6IIa,6IIb}$ = 6.4 Hz, H-6^{IIa}), 2.96 (dd, 1H, $J_{5II,6IIb}$ = 13.6 Hz, $J_{6IIa,6IIb}$ = 2.8 Hz, H-6^{IIb}), 2.04, 1.98, 1.97 (3s, 9H, 3 Ac).

^{13}C NMR ($CDCl_3$, 100 MHz) δ 170.29, 169.47, 169.40 (CO), 134.60 (CH_2-*C*H=CH_2), 129.10, 128.22, 126.25 (Aromatic), 118.27 (CH_2-CH=*C*H_2), 101.60 (*C*HPh), 100.38 (C-1^{II}), 98.67 (C-1^{I}), 80.41 (C-3^{I}), 78.81 (C-2^{I}), 77.47 (C-5^{II}), 73.02 (C-3^{II}), 73.01 (C-6^{I}), 72.10 (C-5^{I}), 71.97 (C-4^{II}), 69.52 (C-2^{II}), 68.99 (*C*H_2-CH=CH_2), 62.12(C-4^{I}), 55.30 (OMe), 50.93 (C-6^{II}), 20.80, 20.62, 20.60 (CH_3).

Synthesis of methyl *O*-(6-azido-6-deoxy-2,3,4-tri-*O*-acetyl-β-D-glucopyranosyl)-(1→3)-2-*O*-acetyl-4,6-*O*-benzylidene-α-D-glucopyranoside

Compound **8** (500 mg, 0.78 mmol), $PdCl_2$ (618 mg, 3.53 mmol), and NaOAc (588 mg, 7.17 mmol) were dissolved in AcOH (6.69 mL) and water (0.37 mL) and stirred for 7 hours. $NaHCO_3$ (250 mL) was added to the mixture and the product was extracted with EtAcO (3 x 250 mL), washed with water, dried over $MgSO_4$ and concentrated. The crude was purified by flash chromatography obtaining compound methyl *O*-(6-azido-6-deoxy-2,3,4-tri-*O*-acetyl-β-D-glucopyranosyl)-(1→3)-2-*O*-acetyl-4,6-*O*-benzylidene-α-D-glucopyranoside (228 mg, 0.36 mmol) in 45 % yield.

^{1}H NMR ($CDCl_3$, 400 MHz) δ 7.53 – 7.36 (m, 5H, aromatic), 5.56 (s, 1H, C*H*Ph), 5.10 (t, 1H, $J_{3II,4II}$ = 9.2 Hz, H-3^{II}), 5.00 – 4.94 (m, 2H, H-4^{II}, H-2^{II}), 4.89 – 4.87 (m, 2H, H-1^{I}, H-2^{I}), 4.82 (d, 1H, $J_{1I,2I}$ = 7.8 Hz, H-1^{II}), 4.30 – 4.24 (m, 2H, H-5^{I}, H-6^{Ia}), 3.87 – 3.74 (m, 2H, H-4^{I}, H-6^{Ib}), 3.69 – 3.65 (m, 2H, H-3^{I}, H-4^{I}), 3.52 – 3.47 (m, 1H, H-5^{II}), 3.40 (s, 3H, OMe), 3.28 (dd, 1H, $J_{5II,6IIa}$ = 6.9 Hz, $J_{6IIa,6IIb}$ = 13.3 Hz, H-6^{IIa}), 3.06 (dd, 1H, $J_{5II,6IIb}$ = 2.7 Hz, $J_{6IIa,6IIb}$ = 13.3 Hz, H-6^{IIb}), 2.17, 2.04, 2.00, 1.99 (4s, 12H, 4 Ac). (Figures A3. 15 and A3. 16).

^{13}C NMR ($CDCl_3$, 100 MHz) δ 169.30, 169.14, 168.41, 168.19 (4 CO), 128.06, 127.16, 125.23, (Aromatic), 100.55 (*C*HPh), 99.06 (C-1^{II}), 96.42 (C-1^{I}), 78.75 (C-3^{I}), 74.06 (C-5^{I}), 72.18 (C-5^{II}), 71.96 (C-2^{I}), 71.81 (C-3^{II}), 70.72 (C-4^{II}), 68.48 (C-2^{II}), 67.78 (C-6^{I}), 61.38 (C-4^{I}), 54.31 (OMe), 50.00 (C-6^{II}), 19.84, 19.58, 19.57, 19.51 (CH_3). (Figures A3. 15 and A3. 16).

3.4.2.2.Polymer approach

2,3,4,6-tetra-*O*-acetyl-β-D-glucopyranosyI-(1→3)-1,2,4,6-tetra-*O*-acetyl-D-glucopyranose (15)

A suspension of curdlan **37** (10.0 g) in 10 mM sodium acetate buffer (pH 5.0, 500 mL) containing kitalase (150 mg, 2000 units/g) was incubated for 6 h at 42 ºC[32]. Then the kitalase was deactivated by heating the mixture for 30 min at 100 ºC. The reaction mixture was filtered and lyophilized. To a solution of the residue was added acetic anhydride/pyridine (200 mL, 1:1 v/v) and 4-dimethylaminopyridine (10 mg, 0.08 mmol). After 12 hours, methanol was poured into the mixture once cold and after concentration, diluted with ethyl acetate. The organic layer was washed with saturated aq. $NaHCO_3$ and water. After drying over $MgSO_4$ and evaporation of the solvent, the residue was purified by flash chromatography (ethyl acetate/toluene 5:1 v/v) to give, in order of elution: peracetylated glucose (11.8 g, 58%), peracetylated laminaribiose **15** (9.4g, 28%) and a mixture of higher oligosaccharides (14%).

Laminaribiose octaacetate **3** (α/β, 1:1):^{1}H NMR (400MHz, $CDCl_3$) δ 6.24 (d, 0.5H, $J_{1,2}$ = 3.6 Hz, H-1^{I}), 5.62 (d, 0.5H, $J_{1,2}$ = 8.3 Hz, H-1^{I}), 5.18 – 4.99 (m, 3H, H-3^{II}, H-4^{II}, H-2^{I}), 4.90 (t, 1H, J = 8.4 Hz, H-2^{II}), 4.65 (d, 0.5H, $J_{1,2}$ = 8 Hz, H-1^{II}), 4.60 (d, 0.5H, $J_{1,2}$ = 8.4 Hz, H-1^{II}), 4.42 – 4.36 (m, 1H, H-6^{Ia}), 4.30 – 4.04 (m, 4.5H, H-6^{Ib}, H-6^{IIa}, H-6^{IIb}, H-4^{I}, H-3^{Iβ}), 3.94 (t, 0.5H, $J_{3,4}$ = 9.6 Hz, H-3^{Iα}), 3.81 – 3.77 (m, 1H, H-5^{II}), 3.76 – 3.67 (m, 1H, H-5^{I}), 2.36 – 1.97 (m, 24H, CH_3).

^{13}C-NMR (400MHz, $CDCl_3$) δ 170.72-168.68 (8C, CO), 100.93, 100.77 (C-1^{II}), 91.73 (C-1^{Iβ}), 89.18 (C-1^{Iα}), 78.84 (C-3^{Iα}), 76.11 (C-3^{Iβ}), 72.85 (C-3^{II}), 72.79, 71.84 (C-5^{II}, C-5^{I}), 71.29, 71.17 (C-2^{I}, C-2^{II}), 69.89 (C-4^{I}), 68.03 (C-4^{II}), 61.67, 61.65 (C-6^{I}, C-6^{II}), 21-43-20.29 (8C, *C*H$_3$).

Acetyl *O*-(2,3,4-tri-*O*-acetyl-6-*O*-trityl-β-D-glucopyranosyl)-(1→3)-2,4,6-tri-*O*-acetyl-D-glucopyranose (17)

Freshly prepared sodium methoxide (1M in methanol, 100 µL) was added to a stirred solution of **15** (300 mg, 0.44 mmol) in anhydrous methanol (10 mL), and the mixture was stirred at RT for 12 hours. The reaction mixture was neutralized with Amberlite® IR-120 (H^+) resin, filtered and the filtered and lyophilized to give deacetylated laminaribiose (**16**) in quantitative yield.

A solution of **16** (1.60 g, 4.70 mmol) in pyridine (75 mL) containing DMAP (10 mg) was treated with additions of trityl chloride (234 mg, 0.84 mmol, 0.2 eq) every 12 hours until a final concentration of 2 eq. The mixture was stirred at room temperature for 5 days. After addition of acetic anhydride (75 mL), the mixture was stirred at room temperature overnight, poured into ice-water, and extracted with ethyl acetate. The organic layer was washed with brine and water, dried over Na_2SO_4, and concentrated. The residue was purified by flash chromatography (toluene –

ethyl acetate 9:l v/v) to afford, in order of elution: 6,6'-ditritylated sugar (903 mg, 0.84 mmol, 25%), 6'-tritylated derivative **17** (HR-MS: m/z: 896.3331 $[M+NH_4]^+$) (1.20 g, 1.37 mmol, 34%), 6-tritylated derivative (HR-MS: m/z: 901.2927 $[M+Na]^+$) (432 mg, 0.49 mmol, 12%) and peracetylated laminaribioside **15** (1.40 g, 2.06 mmol, 29%).

Acetyl *O*-(2,3,4-tri-*O*-acetyl-6-*O*-trityl-β-D-glucopyranosyl)-(1→3)-*O*-2,4,6-tri-*O*-acetyl-D-glucopyranoside **17** (α/β, 1:1): ^{1}H NMR (400MHz, $CDCl_3$) δ 7.45 – 7.18 (m, 15H, Ar), 6.26 (d, 0.5H, $J_{1,2}$ = 3.6 Hz, H-$1^{I\alpha}$), 5.66 (d, 0.5H, $J_{1,2}$ = 8.0 Hz, H-$1^{I\beta}$), 5.19 – 4.95 (m, 3H, H-3^{II}, H-4^{II}, H-2^{I}), 4.87 – 4.81 (m, 1H, H-2^{II}), 4.68 (d, 0.5H, $J_{1,2}$ = 6.4 Hz, H-1^{II}), 4.66 (d, 0.5H, $J_{1,2}$ = 6.4 Hz, H-1^{II}), 4.29 – 4.03 (m, 4H, H-3^{I}, H-6^{Ia}, H-6^{Ib}, H-4^{I}), 3.84 – 3.79 (m, 1H, H-5^{I}), 3.56 – 3.47 (m, 1H, H-5^{I}), 3.41 – 3.37 (m, 1H, H-6^{IIa}), 3.23 – 3.12 (m, 1H, H-6^{IIb}), 2.13 – 1.73 (m, 21H, CH_3).

^{13}C-NMR (400MHz, $CDCl_3$) δ 170.72 - 168.67 (CO), 143.41 (*C*Ph_3), 128.78, 127.83, 127.29 (aromatic), 100.51, 100.30 (C-1^{II}), 91.81 (C-$1^{I\beta}$), 89.37 (C-$1^{I\alpha}$), 77.53 (C-$3^{I\alpha}$), 74.79 (C-$3^{I\beta}$), 73.59, 73.26, 73.16 (C-5^{I}, C-5^{II}, C-3^{II}), 71.97, 71.66, 71.42 (C-2^{I}, C-2^{II}), 70.29, 69.12, 68.91, 67.19 (C-4^{I}, C-4^{II}), 62.49, 62.19, 61.79, 61.75 (C-6^{I}, C-6^{II}), 20-93-20.39 (*C*H_3).

Acetyl *O*-(2,3,4-tri-O-acetyl-β-D-glucopyranosyl)-(1→3)-2,4,6-tri-*O*-acetyl-D-glucopyranose (18)

Method A: A solution of **17** (0.75 g, 0.85 mmol) in 80% aq. acetic acid (70 mL) was heated at 70 ºC for 5 hours, then cooled and concentrated to dryness. TLC analysis (ethyl acetate) confirmed the reaction was complete and the presence of three new products without trityl group. The mixture was extracted with ethyl acetate, washed with saturated aq. $NaHCO_3$ and water, dried over $MgSO_4$ and concentrated.

Method B: To a solution of **17** (2.90 g, 3.40 mmol) in 60 mL of CH_2Cl_2 was added solid $FeCl_3 \cdot 6H_2O$ (1.80 g, 6.90 mmol, 2 eq). After 2 hours at RT, the reaction was complete and three detritylated products were present. After addition of water and extraction with CH_2Cl_2, the organic layer was dried over $MgSO_4$, concentrated and purified by filtration through silica using toluene 100% and later ethyl acetate 100%. 1.10 g of mixture containing **18** (HR-MS: m/z: 654.2251 $[2M+NH_4]^+$) (53% yield) was obtained.

Acetyl *O*-(2,3,4-tri-*O*-acetyl-β-D-glucopyranosyl)-(1→3)-*O*-2,4,6-tri-*O*-acetyl-D-glucopyranoside **18** (α/β, 1:1):^{1}H NMR (400MHz, $CDCl_3$) δ 6.24 (d, 0.5H, $J_{1,2}$ = 3.6 Hz, H-$1^{I\alpha}$), 5.61 (d, 0.5H, $J_{1,2}$ = 8.4 Hz, H-$1^{I\beta}$), 5.14 – 4.95 (m, 3H, H-2^{I}, H-3^{II}, H-4^{II}), 4.84 (dd, 1H, $J_{2,1}$ = 8.0 Hz, H-2^{II}), 4.61 (d, 0.5H, $J_{1,2}$ = 8.0 Hz, H-1^{II}), 4.56 (d, 0.5H, $J_{1,2}$ = 8.0 Hz, H-1^{II}), 4.26 – 4.03 (m, 4.5H, H-6^{Ia}, H-6^{Ib}, H-4^{I}, H-3^{I}, H-5^{II}), 3.93 (t, 0.5H, J = 9.6 Hz, H-3^{I}), 3.81 – 3.77 (m, 1H, H-5^{I}), 3.57 – 3.46 (m, 2H, H-6^{IIa}, H-6^{IIb}), 2.19 – 1.97 (m, 21H, CH_3).

Functionalization of C-6'. Synthesis of compounds 19i and 19ii

Several approaches were studied in order to functionalize C-6'. Compound **18** was co-evaporated with toluene and dried under vacuum at room temperature overnight prior to use in all cases.

Method A (tosylation). Synthesis of Acetyl *O*-(2,3,4-tri-*O*-acetyl-6-*O*-tosyl-β-D-glucopyranosyl)-(1→3)-2,4,6-tri-*O*-acetyl-D-glucopyranose (19i)

A solution of **18** (120 mg, 0.17 mmol) in 1.2 mL of pyridine was cooled in an ice bath. A second solution of TsCl (48 mg, 0.25 mmol, 1.3 eq) in 1.2 mL of pyridine was prepared and added dropwise to the first solution. The mixture was stirred for 30 minutes at 0 ºC and afterwards at RT. Sequential additions of TsCl (0.6 eq/addition) were added into the mixture every 12 hours at RT until reaching a total of 3.5 equivalents of TsCl in the mixture. Extractions were done with EtOAc, HCl 1N, saturated NH_4CO_3 and water and the organic phase was dried over $MgSO_4$ and dried under diminished pressure. A mixture of 51.6 mg of tosylated products containing compound **19i** was obtained**.** A small fraction was purified through preparative thin layer chromatography (EtOAc/toluene (1:1)). Compound **19i** (R_f 0.36) was the main product with a HR-MS: m/z: 808.2327 $[M+NH_4]^+$.

Acetyl *O*-(6-*O*-tosyl-2,3,4-tri-*O*-acetyl-β-D-glucopyranosyl)-(1→3)-2,3,4,6-tetra-*O*-acetyl-D-glucopyranoside **19i** (α/β, 1:1): ^{1}H NMR (400MHz, $CDCl_3$) δ 7.78 (d, 2H, J = 8 Hz, Aromatic), 7.38 (d, 2H, J = 8 Hz, Aromatic), 6.24 (d, 0.5H, $J_{1,2}$ = 4.0 Hz, H-1$^{I\alpha}$), 5.61 (d, 0.5H, J = 8.4 Hz, H-1$^{I\beta}$), 5.14 – 4.91 (m, 3H, H-2^{I}, H-3 ^{II}, H-4^{II}), 4.83 (dd, 1H, $J_{2,1}$ = 9.6 Hz, H-2^{II}), 4.65 (d, 0.5H, $J_{1,2}$ = 8.4 Hz, H-1^{II}), 4.58 (d, 0.5H, $J_{1,2}$ = 8.0 Hz, H-1^{II}), 4.26 – 4.03 (m, 5H, H-6^{Ia}, H-6^{Ib}, H-6^{IIa}, H-6^{IIb}, H-4^{I}, H-3$^{I\beta}$), 3.92 (t, 1H, $J_{3,4}$ = 9.2 Hz, H-3$^{I\alpha}$), 3.83 – 3.73 (m, 2H, H-5^{I}, H-5^{II}), 2.47 – 1.92 (m, 21H, CH_3).

Method B (bromination). Synthesis of Acetyl *O*-(2,3,4-tri-*O*-acetyl-6-bromo-6-deoxy-β-D-glucopyranosyl)-(1→3)-2,4,6-tri-*O*-acetyl-D-glucopyranose (19ii)

PPh_3 (549 mg, 2.09 mmol) was dissolved in 1.7 mL (324 mg/mL) of dry DMAc, and a second solution was prepared containing 373 mg NBS (2.09 mmol, 4 eq) in an additional 1.7 mL (220 mg/mL) of dry DMAc. The PPh_3 solution is added dropwise to another solution containing compound **18** (331 mg, 0.52 mmol) in 14 mL DMAC), followed by the dropwise addition of the NBS solution. The reaction solution is heated to 70 ºC under nitrogen. After 1 hour, the product was isolated by adding the reaction mixture slowly to 250 mL of a 50:50 (v/v) mixture of methanol and deionized water. Methanol was removed and extractions were done with EtOAc and water. The organic phase was dried with $MgSO_4$ and concentrated.

Acetyl *O*-(2,3,4-tri-*O*-acetyl-6-azido-6-deoxy-β-D-glucopyranosyl)-(1→3)-2,4,6-tri-*O*-acetyl-D-glucopyranose (20)

A solution of crude **19i** or **19ii** (51.6 mg) with sodium azide (16.3 mg, 0.24 mmol, 3 eq) in DMF (2 mL) was allowed to react at 80 ºC for 6 h. TLC analysis (toluene/ethyl acetate 1:1) showed one of the three tosylated sugars disappeared. After dilution with ethyl acetate, the mixture was washed with water, dried over $MgSO_4$ and evaporated to dryness.

A) When coming from tosylation: Purification by flash chromatography (toluene/ethyl acetate 2:1 → 1.5:1) afforded a mixture of azidated products. Compound **20** was isolated by flash chromatography obtaining 26.6 mg (0.04 mmol) in 24% yield (two step reaction yield, tosylation and azidation).

B) When coming from bromination: purification by flash chromatography (EtOAc/cyclohexane, 1.5:1) afforded compound **20.** When starting from 0.52 mmol of compound **18**, 58.4 mg (0.09 mmol) of compound 8 were obtained in 17% yield (two steps yield, bromination and azidation).

^{1}H NMR ($CDCl_3$, 400 MHz) δ 6.23 (d, 0.5H, $J_{1,2}$ = 3.7 Hz, H-$1^{I\alpha}$), 5.63 (d, 0.5H, $J_{1,2}$ = 8.3 Hz, H-$1^{I\beta}$), 5.18 – 4.83 (m, 4H, H-3^{II}, H-4^{II}, H-2^{I}, H-2^{II}), 4.73 (d, 0.5H, $J_{1,2}$ = 8.1 Hz, H-1^{II}), 4.67 (d, 0.5H, $J_{1,2}$ = 8.1 Hz, H-1^{II}), 4.26 – 3.95 (m, 4H, H-6^{Ia}, H-6^{Ib}, H-4^{I}, H-3^{I}), 3.78 – 3.64 (m, 2H, H-5^{II}, H-5^{I}), 3.45 – 3.38 (m, 1H, H-6^{IIa}), 3.26 – 3.22 (m, 1H, H-6^{IIa}), 2.19 – 1.98 (m, 21H, CH_3).

^{13}C-NMR (400MHz, $CDCl_3$) δ 170.68 - 168.76 (CO), 100.44, 100.27 (C-1^{II}), 91.68 (C-$1^{I\beta}$), 89.18 (C-$1^{I\alpha}$), 78.08 (C-$3^{I\alpha}$), 75.30 (C-$3^{I\beta}$), 73.36, 73.27 (C-5^{I}, C-5^{II}), 72.60, 71.47, 71.33, 70.07, 67.14 (C-3^{II}, C-2^{I}, C-2^{II}, C-4^{I}, C-4^{II}), 61.59 (C-6^{I}), 51.14 (C-6^{II}), 20-91-20.30 (*C*H_3).

2,3,4-tri-*O*-acetyl-6-azido-6-deoxy-β-D-glucopyranosyl-(1→3)-2,4,6-tri-*O*-acetyl-α-D-glucopyranosyl fluoride (21).

A solution of compound **20** (67 mg, 0.10 mmol) in HF-pyridine (2 mL, 7:3 v/v, 0.08 mol HF) was stirred at 0 °C for 3 hours in a plastic vial. The mixture was diluted with DCM (4 mL) and poured into an ice-cold aqueous solution of NH_3 3M (10 mL); the organic layer containing **21** was washed with saturated aqueous $NaHCO_3$ (3×) and water, dried over $MgSO_4$ and concentrated under diminished pressure. Purification by flash chromatography yielded compound **21** (MS m / z 639.2155 $[M+NH_4]^+$) (23 mg, 0.037 mmol) in 37% yield.

^{1}H NMR ($CDCl_3$, 400 MHz) δ 5.58 (dd, 1H, $J_{1,2}$ = 2.8 Hz, $J_{1,F}$ = 53.1 Hz, H-1^{I}), 5.10 – 4.78 (m, 4H, H-3^{II}, H-4^{II}, H-2^{I}, H-2^{II}), 4.67 (d, 1H, $J_{1,2}$ = 8.0 Hz, H-1^{II}), 4.18 – 4.03 (m, 4H, H-6^{Ia}, H-6^{Ib}, H-4^{I}, H-3^{I}), 3.69 – 3.58 (m, 2H, H-5^{II}, H-5^{I}), 3.34 (dd, 1H, $J_{5,6}$ = 7.4 Hz, $J_{6a,6b}$ = 13.3 Hz, H-6^{IIa}), 3.19 (dd, 1H, $J_{5,6}$ = 2.5 Hz, $J_{6a,6b}$ = 13.4 Hz, H-6^{IIb}), 2.15 – 1.91 (m, 18H, CH_3).

^{13}C-NMR (100MHz, $CDCl_3$) δ 170.78 – 169.18 (6 CO), 104.19 (d, $J_{C,F}$ = 226 Hz, C-1^{I}), 100.59 (C-1^{II}), 75.09 (C-3^{I}), 73.49, 72.85, 72.46 (d, $J_{C,F}$ = 24 Hz, C-2^{I}), 71.58, 70.44 (d, $J_{C,F}$ = 4 Hz, C-5^{I}), 69.61 (C-5^{II}, C-5^{I}, C-2^{I}, C-2^{II}, C4^{II}, C-4^{I}), 61.49 (C-6^{I}), 51.36 (C-6^{II}), 20.94 – 20.50 (6 *C*H_3).

6-Azido-6-deoxy-β-D-glucopyranosyl-(1→3)-α-D-glucopyranosyl fluoride (6N_3-Glcβ3GlcαF) (22).

Freshly prepared sodium methoxide (1M in methanol, 10 μL) was added to a stirred solution of **21** (6.3 mg, 0.010 mmol) in anhydrous methanol (252 μL), and the mixture was stirred at RT for 4 hours. The reaction mixture was neutralized with Amberlite® IR-120 (H^+) resin, filtered and lyophilized obtaining compound **22** (2.0 mg, 0.005 mmol) in 53% yield.

Laminaribiosyl fluoride donor (6N_3-Glcβ3GlcαF) (36)

Glcβ3GlcαF is prepared as previously reported[50] by treatment of peracetylated laminaribiose with hydrogen fluoride in pyridine (70%), purification of the peracetylated α-glycosyl fluoride by flash chromatography, followed by de-*O*-acetylation with sodium methoxide gives **36** in quantitative yields.

^{1}H NMR (MeOD, 400 MHz) δ 5.67 (dd, 1H, $J_{1,2}$ = 2.8 Hz, $J_{1,F}$ = 53.0 Hz, H-1^{I}), 5.18 – 5.05 (m, 2H, H-3^{II}, H-4^{II}), 4.98 – 4.88 (m, 2H, H-2^{II}, H-2^{I}), 4.66 (d, 1H, $J_{1,2}$ = 7.9 Hz, H-1^{II}), 4.37 (dd, 1H, $J_{6a,6b}$ = 4.5 Hz, $J_{6,5}$ = 12.4 Hz, H-6^{Ia}), 4.23 – 4.11 (m, 4H, H-^{4I}, H-^{6Ib}, H-5^{II}, H-6^{IIa}), 4.08 (dd, 1H, $J_{6a,6b}$ = 2.3 Hz, $J_{6,5}$ = 12.4 Hz, H-6^{IIb}), 3.71 – 3.69 (m, 1H, H-5^{I}), 2.20 – 1.99 (m, 21H, CH_3).

^{13}C-NMR (400MHz, $CDCl_3$) δ 170.44-168.85 (8C, CO), 104.99, 102.73 (C-1^{I}), 100.63 (C-1^{II}), 75.45 (C-3^{I}), 72.74 (C-3^{II}), 71.93 (d, $J_{C,F}$ = 24.5 Hz, C-2^{I}), (C-5^{II}), 71.60 (C-2^{II}), 69.92 (d, $J_{C,F}$ = 4 Hz, C-5^{I}), 67.78 (C-4^{II}), 66.59 (C-4^{I}), 61.47, 61.21 (C-6^{I}, C-6^{II}), 20.57-20.15 (8C, *C*H_3).

Synthesis of acceptors for the glycosynthase reaction *p*-nitrophenyl β-D-glucopyranoside (GlcβPNP) (31)

Triethylamine (1.79 mL, 12.81 mmol) was added to a solution of peracetylated β-D-glucopyranoside (**26**) (10.00 g, 25.62 mmol) in dry DCM under nitrogen atmosphere. $BF_3 \cdot OEt_2$ (8.04 mL, 64.05 mmol) was quickly introduced into the system and the mixture was stirred at room temperature for 96 hours. The organic phase containing the acetylated GlcβPNP (compound **30)** was washed with saturated aqueous $NaHCO_3$ and water, dried and concentrated. To a stirred solution of the reaction crude in anhydrous methanol (300 mL), freshly prepared NaOMe (1M in methanol; 6 mL) was added and the mixture was stirred for 6 hours at room temperature. Then, the mixture was neutralized with Amberlite® IR 120 resin (H^+), filtrated and evaporated to

dryness. Finally, the reaction mixture was purified by flash chromatography (Acetone-DMC 5:1) yielding GlcβPNP (**31**) (4.54 g, 15.06 mmol) in 60% yield.

^{1}H NMR (D_2O, 400 MHz) δ 8.10 (d, 2H, J_{Ar} = 9.3 Hz, arom), 7.09 (d, 2H, J_{Ar} = 9.3 Hz, *p*NP), 5.12 (d, 1H, $J_{1,2}$ = 7.7 Hz, H1), 3.82 (dd, 1H, $J_{5,6}$ = 2.2 Hz, $J_{a\,b}$ = 12.3 Hz, H-6^a), 3.63 (dd, 1H, $J_{5,6}$ = 5.7 Hz, $J_{a,b}$ = 12.3 H-6^b), 3.59 – 3.36 (m, 4H, H2, H3, H4, H5).

^{13}C NMR (D_2O, 100 MHz) δ 126.0, 116.4 (*p*NP), 99.4 (C-1), 76.2, 75.3, 72.7, 69.2 (C-2, C-3, C-4, C-5), 60.3 (C-6), 28.1 (CH_3).

p-nitrophenyl 6-azido-6-deoxy-2,3,4-tri-*O*-acetyl-β-D-glucopyranoside (6N$_3$-GlcβPNP) (35)

p-Nitrophenyl 6-azido-6-deoxy-β-D-glucopyranoside (**35**) was prepared by tosylation of the 6-OH group of **31**, acetylation with Ac_2O/py/DMAP, substitution of the tosyl group by azide, and finally de-*O*-acetylation by reaction with sodium methoxide in methanol, as follows:

4-Nitrophenyl-β-D-glucopyranoside (**31**) (2.59 g, 8.59 mmol) was dissolved in dry pyridine (26 mL) and the solution was cooled in an ice bath. A cold solution of tosyl chloride (4.91 g, 25.78 mmol) in dry pyridine (26 mL) was added and the reaction mixture was stirred for 22 hours under nitrogen atmosphere at room temperature. Acetic anhydride (52 mL) and *N*,*N*-dimethylaminopyridine (DMAP) (25 mg) were directly added to the solution. The mixture was stirred for 24 hours at room temperature. Finally, methanol (100 mL) was added to quench the reaction and, after evaporation until dryness, the product was redissolved with ethyl acetate, washed with water, the organic phase dried, and the solvent evaporated under reduced pressure to yield 9.17 g of 4-nitrophenyl 6-*O*-tosyl-2,3,4-tri-*O*-acetyl-β-D-glucopyranoside (compound **33**).

Compound **33** (9.17 g, 15.77 mmol) was dissolved in dry DMF (183 mL). Sodium azide (2.23 g, 34.37 mmol) was added and the solution stirred at 80 ºC for 14 hours. A saturated aqueous solution of sodium bicarbonate and ethyl acetate were added, and the organic phase was washed with water, dried, and the solvent evaporated. The product was purified by flash chromatography (toluene-ethyl acetate 20:1). 4-Nitrophenyl 6-azido-2,3,4-tri-*O*-acetyl-β-D-glucopyranoside (compound **34**) (1.94 g, 4.31 mmol) was obtained in 50% overall yield from **31**.

^{13}C NMR ($CDCl_3$, 100 MHz) δ 170.2, 169.6, 169.3 (CO), 126.0, 116.8 (C-Ar), 98.1 (C-1), 74.0 (C-5), 72.4, 71.0, 69.3 (C-2, C-3, C-4), 51.3 (C-6), 20.7 (CH_3).

^{1}H NMR ($CDCl_3$, 400 MHz) δ 8.23 (d, 2H, J_{Ar} = 9.1 Hz, arom), 7.10 (d, 2H, J_{Ar} = 9.1 Hz, arom), 5.33 – 5.30 (m, 2H, H2, H3), 5.24 (d, 1H, $J_{1\text{-}2}$ = 7.9 Hz, H1), 5.09 (m, 1H, H4), 3.85 (m, 1H, H5), 3.44 (dd, 1H, $J_{5,6b}$ = 7.4 Hz, $J_{6a,6b}$ = 13.4 Hz, H-6^b), 3.35 (dd, 1H, $J_{5,6a}$ = 2.7 Hz, $J_{6a,6b}$ = 13.4 H-6^a), 2.07-2.05 (m, 9H, CH_3). ESI-MS (m/z): 470.1514 $[M+NH_4]^+$

Compound **34** (200 mg, 0.44 mmol) was dissolved in methanol (7 mL) and sodium methoxide (1 mM in methanol). The mixture was stirred for 6 hours at room temperature. Then, the mixture was neutralized with Amberlite IR 120 resin (H^+), filtrated and freeze-dried. 4-Nitrophenyl 6-azido-6-deoxy-β-D-glucopyranoside (**35**) was obtained in 98% yield.

3.4.2.3.Characterization

NMR

^1H and ^{13}C NMR, COSY and HSQC spectra were recorded in a Varian Gemini 400 MHz spectrometer operated at 298 K. For ^1H NMR, chemical shifts were referenced to internal TMS (0 ppm) for solutions in $CHCl_3$ (δ_H = 7.26 ppm). For ^{13}C NMR, the central peak of the $CDCl_3$ triplet (77.16 ppm) was used as a reference. For ^{13}C NMR, the central peak of the $CDCl_3$ triplet (77.16 ppm) was used as a reference. When using MeOD as solvent, the central peak of the MeOD multiplet (49.00 ppm) was used as a reference.

HPLC-MS

Mass spectra were performed on a LC/MSD-TOF spectrometer from Agilent Technologies in positive electrospray mode.

Chromatography

Flash chromatography was performed on Merck Silica gel (40 – 63 μm) using eluents as specified. TLC was performed on Silica Gel 60 F_{254} aluminum plates with detection by development with H_2O/MeOH/H_2SO_4 (4.5/4.5/1 v/v/v) and heating at 125 ºC and/or by visualization under UV light.

3.4.2.4. Enzyme characterization

Computational docking studies

Molecular docking was performed with AUTODOCK VINA[32] Protein and ligand structures were parameterized with autodock 4.2 atom types and gasteiger charges were computed for each atom. The search space was defined as a cubic box of 33 x 34 x 22 Å centered in the active site of the enzyme. All rotable bonds of the ligand were considered free during the docking calculations, whereas the whole protein structure was kept fixed. 20 different binding modes were calculated with an exhaustiveness criterion of 8 in the VINA algorithm. The final enzyme-ligand structures were taken from the lowest energy binding modes. The final structures were analyzed with the VMD visualization program.[33]

Protein expression and purification

The glycosynthase mutant E134S was expressed and purified as described in Chapter 3 (section 3.3.5). Concentration was determined by absorbance at 280 nm using an extinction coefficient of $3.53 \cdot 10^5$ M^{-1} cm^{-1}. The protein was >95% homogeneous as judged by SDS-PAGE. It was lyophilized for storage and redissolved prior to use.

Enzyme kinetics. E134S subsite studies

All reactions were performed using 5 times higher acceptor concentration (5 mM) than donor's (1 mM) in order to avoid donor self-condensation. The control was defined by the reaction between the donor Glcβ3GlcαF and the acceptor GlcβPNP. The donor $6N_3$-Glcβ3GlcαF was combined with GlcβPNP in the study of subsite -2 while Glcβ3GlcαF and $6N_3$-GlcβPNP were used in the study of subsite +1.

After pre-incubation of the microcentrifuge tube containing the acceptor and the donor in phosphate buffer 50 mM, pH 7.0 at 35 ºC for 5 minutes, the reactions were initiated by addition of E134S mutant (1→3,1→4)-β-D-glucanase from *B. licheniformis* (0.1 μM, specific activity of 17 – 64 min^{-1} for the reference reaction Glcβ3GlcαF + GlcpNP) and kept at 35 ºC (final reaction volume of 0.3 mL). Aliquots were withdrawn in another microcentrifuge tube at regular time intervals, diluted 1:10 in formic acid 2% (v/v) to stop the enzymatic reaction and analyzed by HPLC [Agilent equipment, NovaPak® C18 (4 μm, 3.9 × 150 mm) column (Waters), flow rate 1 mL/min, 16% MeOH in water when no azide was present either in donor or acceptor, and 13% MeOH in water in the presence of azides, UV detector at 300 nm (λ)]. Initial rates were obtained from the linear progress curves of product formation (normalized area *vs* time) and expressed as v_o/[E] in inverse seconds.

3.5. REFERENCES

(1) Hein, C. D.; Liu, X.-M.; Wang, D. *Pharm. Res.* **2008**, *25*, 2216–2230.

(2) Song, Y.; Zhang, L.; Gan, W.; Zhou, J.; Zhang, L. *Colloids Surf. B. Biointerfaces* **2011**, *83*, 313–320.

(3) Takedatsu, H.; Mitsuyama, K.; Mochizuki, S.; Kobayashi, T.; Sakurai, K.; Takeda, H.; Fujiyama, Y.; Koyama, Y.; Nishihira, J.; Sata, M. *Mol. Ther.* **2012**, *20*, 1234–1241.

(4) Almant, M.; Moreau, V.; Kovensky, J.; Bouckaert, J.; Gouin, S. G. *Chem. Eur. J.* **2011**, *17*, 10029–10038.

(5) Elchinger, P.-H.; Faugeras, P.-A.; Boëns, B.; Brouillette, F.; Montplaisir, D.; Zerrouki, R.; Lucas, R. *Polymers (Basel).* **2011**, *3*, 1607–1651.

(6) Satoh, T.; Kano, H.; Nakatani, M.; Sakairi, N.; Shinkai, S.; Nagasaki, T. *Carbohydr. Res.***2006**,*341*,2406-2413.

(7) Ikeda, Y.; Adachi, Y.; Ishii, T.; Tamura, H.; Aketagawa, J.; Tanaka, S.; Ohno, N. *Biol. Pharm. Bull.* **2007**, *30*, 1384–1389.

(8) Fox, S. C.; Edgar, K. J. *Biomacromolecules* **2012**, *13*, 992–1001.

(9) Zhang, R.; Edgar, K. J. *Biomacromolecules* **2014**, *15*, 1079–1096.

(10) Faijes, M.; Imai, T.; Bulone, V.; Planas, A. *Biochem. J.* **2004**, *380*, 635–641.

(11) Clarke, A. E.; Stone, B. A. *Chemistry and Biology of (1-> 3)-B-Glucans*; La Trobe University Press: Bundoora, Australia, 1992.

(12) Hahn, M.; Olsen, O.; Politz, O.; Borriss, R.; Heinemann, U. *J. Biol. Chem.* **1995**, *270*, 3081–3088.

(13) Keitel, T.; Simontt, O.; Borrisstl, R.; Heinemann, U. *Proc. Natl. Acad. Sci. USA* **1993**, *90*, 5287–5291.

(14) Hahn, M.; Pons, J.; Planas, A.; Querol, E.; Heinemann, U. *FEBS Lett.* **1995**, *374*, 221–224.

(15) Ay, J.; Hahn, M.; Decanniere, K.; Piotukh, K.; Borriss, R.; Heinemann, U. *Proteins Struct. Funct. Genet.* **1998**, *30*, 155–167.

(16) Gaiser, O. J.; Piotukh, K.; Ponnuswamy, M. N.; Planas, A.; Borriss, R.; Heinemann, U. *J. Mol. Biol.* **2006**, *357*, 1211–1225.

(17) Piotukh, K.; Serra, V.; Borriss, R.; Planas, A. *Biochemistry* **1999**, *38*, 16092–16104.

(18) Viladot, J. L.; de Ramon, E.; Durany, O.; Planas, a. *Biochemistry* **1998**, *37*, 11332–11342.

(19) Malet, C.; Jiménez-Barbero, J.; Bernabé, M.; Brosa, C.; Planas, A. *Biochem. J.* **1993**, *296*, 753–758.

(20) Piotukh, K.; Serra, V.; Borriss, R.; Planas, A. *Biochemistry* **1999**, *38*, 16092–16104.

(21) Lohman, G. J. S.; Seeberger, P. H. *J. Org. Chem.* **2004**, *69*, 4081–4093.

(22) Kamiya, S.; Esaki, S.; Tanaka, R. *Agric. Biol. Chem.* **1985**, *49*, 55–62.

(23) Wuts, P. G. M.; Greene, T. W. *Greene's Protective Groups In Organic Synthesis*; Wiley-Interscience, Ed.; Fourth.; John Wiley & Sons: Hoboken, New Jersey, 2007.

(24) Kumar, A.; Doddi, V. R.; Vankar, Y. D. *J. Org. Chem.* **2008**, *73*, 5993–5995.

(25) Bird, P; Dolphin, D H; Withers, S. G. *Can. J. Chem.* **1990**, *68*, 1–6.

(26) Dauban, P.; Chiaroni, A.; Riche, C.; Dodd, R. H. *J. Org. Chem.* **1996**, *61*, 2488–2496.

(27) Viladot, J.-L.; Moreau, V.; Driguez, H. *J. Chem. Soc., Perkin Trans* **1997**, 2383–2387.

(28) Moreau, V.; Viladot, J.-L.; Samain, E.; Planas, A.; Driguez, H. *Bioorg. Med. Chem.* **1996**, *4*, 1849–1855.

(29) Jamois, F.; Le Goffic, F.; Yvin, J. C.; Plusquellec, D.; Ferrières, V. *Open Glycosci.* **2008**, 19–24.

(30) G Villa, T.; J Phaff, H.; Notario, V. *Carbohydr. Res.* **1979**, *74*, 369–370.

(31) Montel, E.; Hrmova, M.; Fincher, G. B.; Driguez, H. *Aust. J. Chem.* **2009**, *62*, 575–584.

(32) Wang, L. X.; Sakairi, N.; Kuzuhara, H. *Carbohydr. Res.* **1991**, *219*, 133–148.

(33) Kitaoka, M.; Matsuoka, Y.; Mori, K.; Nishimoto, M.; Hayashi, K. *Biosci. Biotechnol. Biochem.* **2012**, *76*, 343–348.

(34) Cramer, F.; Otterbach, H.; Springmann, H. *Chem. Ber.* **1959**, *92*, 384–391.

(35) Hanessian, S.; Ponpipom, M.; Lavallee, P. *Carbohydr. Res.* **1972**, *24*, 45–56.

(36) Hanessian, S.; Banoub, J. *Carbohydr. Res.* **1977**, *59*, 261–267.

(37) Jimenez Blanco, J. L.; Garcia Fernández, J. M.; Gadelle, A.; Defaye, J. *Carbohydr. Res.* **1997**, *303*, 367–372.

(38) Gouin, S. G.; Kovensky, J. *Tetrahedron Lett.* **2007**, *48*, 2875–2879.

(39) Dutton, G. G. S; Slessor, K. N. *Can. J. Chem.* **1964**, *44*, 1966.

(40) Hanessian, S.; Lavallee, P. *Carbohydr. Res.* **1973**, *28*, 303–311.

(41) Thiebault, N.; Lesur, D.; Godé, P.; Moreau, V.; Djedaïni-Pilard, F. *Carbohydr. Res.* **2008**, *343*, 2719–2728.

(42) Klemm, D.; Heinze, T.; Philipp, B.; Wagenknecht, W. *Acta Polym.* **1997**.

(43) Kern, H.; Choi, S.; Wenz, G.; Heinrich, J.; Ehrhardt, L.; Mischnick, P.; Garidel, P.; Blume, A. *Carbohydr. Res.* **2000**, *326*, 67–79.

(44) Slaghek,T.M.;Nakahara,Y.;Ogawa,T.;Kamerling, J. P.; Vliegenthart, J. F. G.*Carbohydr.Res.***1994**, *255*,61–85.

(45) Ding, X.; Wang, W.; Kong, F. *Carbohydr. Res.* **1997**, *303*, 445–448.

(46) Fink, A. L.; Hay, G. W. *Can. J. Chem.* **1969**, *47*, 845–852.

(47) Bonner, W. A. *J. Org. Chem.* **1959**, *24*, 1388–1390.

(48) Ogawa, Y.; Noda, K.; Kimura, S.; Kitaoka, M.; Wada, M. *Int. J. Biol. Macromol.* **2014**, *64*, 415–419.

(49) Fort, S.; Boyer, V.; Greffe, L.; Davies, G. J.; Moroz, O.; Christiansen, L.; Schülein, M.; Cottaz, S.; Driguez, H. *J. Am. Chem. Soc.* **2000**, *122*, 5429–5437.

(50) Malet, C.; Planas, A. *FEBS Lett.* **1998**, *440*, 208–212.

(51) Trott, O.; Olson, A. J. *J. Comput. Chem.* **2010**, *31*, 455–461.

(52) Humphrey, W.; Dalke, A.; Schulten, K. *J. Mol. Graph.* **1996**, *14*, 33–38.

APPENDIX CHAPTER 3

APPENDIX

Figure A3. 1: ^{1}H NMR of methyl 4,6-*O*-benzylidene-α-D-glucopyranoside (**2**)

Figure A3. 2: ^{1}H NMR of methyl 2-*O*-benzoyl-4,6-*O*-benzylidene-α-D-glucopyranoside (**23**)

Figure A3. 3: ^{1}H NMR of methyl 2-*O*-benzyl-4,6-*O*-benzylidene-α-D-glucopyranoside (**25**)

Figure A3. 4: ^{1}H NMR of methyl 2-*O*-allyl-4,6-*O*-benzylidene-α-D-glucopyranoside (**3**)

Figure A3. 5: ^{1}H NMR of methyl 4,6-*O*-isopropylidene-α-D-glucopyranoside

Figure A3. 6: ^{13}C NMR of a mixture of isomers benzylated at C-2 and C-3. Methyl 2-*O*-benzyl-4,6-*O*-isopropylidene-α-D-glucopyranoside (**24**) is the major product observed in the spectrum.

Figure A3. 7: ^{1}H NMR of *p*-methoxyphenyl 2-*O*-allyl-4,6-*O*-benzylidene-β-D-glucopyranoside (**29**)

Figure A3. 8: ^{1}H NMR of 2,3,4,6-tetra-*O*-acetyl-α-D-glucopyranosyl bromide (**5**)

Figure A3. 9: ^{1}H NMR (above) and ^{13}C NMR (below) of methyl *O*-(2,3,4,6-tetra-*O*-acetyl-β-D.glucopyranosyl)-(1→3)-2-*O*-allyl-4,6-*O*-benzylidene-α-D-glucopyranoside (**6**)

Figure A3. 10: HSQC (above) and NOESY (below) of methyl *O*-(2,3,4,6-tetra-*O*-acetyl-β-D.glucopyranosyl)-(1→3)-2-*O*-allyl-4,6-*O*-benzylidene-α-D-glucopyranoside (**6**)

Figure A3. 11: ^{1}H NMR (above) and ^{13}C NMR (below) of methyl *O*-(2,3,4,6-tetra-*O*-acetyl-β-D.glucopyranosyl)-(1→3)-2-*O*-allyl-4,6-di-*O*-acetyl-α-D-glucopyranoside

Figure A3. 12: HSQC of methyl *O*-(2,3,4,6-tetra-*O*-acetyl-β-D.glucopyranosyl)-(1→3)-2-*O*-allyl-4,6-di-*O*-acetyl-α-D-glucopyranoside

Figure A3. 13: ^{1}H NMR (above) and ^{13}C NMR (below) of methyl *O*-(6-azido-6-deoxy-2,3,4-tri-*O*-acetyl-β-D.glucopyranosyl)-(1→3)-2-*O*-allyl-4,6-*O*-benzylidene-α-D-glucopyranoside (**8**)

Figure A3. 14: HSQC of methyl *O*-(6-azido-6-deoxy-2,3,4-tri-*O*-acetyl-β-D.glucopyranosyl)-(1→3)-2-*O*-allyl-4,6-*O*-benzylidene-α-D-glucopyranoside (**8**)

Figure A3. 15: ^{1}H NMR (above) and ^{13}C NMR (below) of methyl *O*-(6-azido-6-deoxy-2,3,4-tri-*O*-acetyl-β-D.glucopyranosyl)-(1→3)-2-*O*-acetyl-4,6-*O*-benzylidene-α-D-glucopyranoside

Figure A3. 16: HSQC of methyl *O*-(6-azido-6-deoxy-2,3,4-tri-*O*-acetyl-β-D.glucopyranosyl)-(1→3)-2-*O*-acetyl-4,6-*O*-benzylidene-α-D-glucopyranoside

Figure A3. 17: MALDI of methyl 2-*O*-allyl-4,6-*O*-benzylidene-α-D-glucopyranoside (**3**)

Figure A3. 18: MALDI of methyl *O*-(2,3,4,6-tetra-*O*-acetyl-β-D-glucopyranosyl)-(1→3)-2-*O*-allyl-4,6-*O*-benzylidene-α-D-glucopyranoside (**6**)

Figure A3. 19: ^{1}H NMR (above) and ^{13}C NMR (below) of 2,3,4,6-tetra-*O*-acetyl-β-D-glucopyranosyl-(1→3)-1,2,4,6-tetra-*O*-acetyl-D-glucopyranose (**16**)

Figure A3. 20: HSQC of 2,3,4,6-tetra-*O*-acetyl-β-D-glucopyranosyl-(1→3)-1,2,4,6-tetra-*O*-acetyl-D-glucopyranose (**16**)

Figure A3. 21: ^{1}H NMR (above) and ^{13}C NMR (below) of the laminaribiosyl fluoride donor (Glcβ3GlcαF) (**36**)

Figure A3. 22: ^{1}H NMR (above) and ^{13}C NMR (below) of acetyl *O*-(2,3,4-tri-*O*-acetyl-6-*O*-trityl-β-D-glucopyranosyl)-(1→3)-2,4,6-tri-*O*-acetyl-D-glucopyranose (**17**)

Figure A3. 23: HSQC of laminaribiosyl fluoride donor (Glcβ3GlcαF) (**36**)

Figure A3. 24: HSQC of acetyl *O*-(2,3,4-tri-*O*-acetyl-6-*O*-trityl-β-D-glucopyranosyl)-(1→3)-2,4,6-tri-*O*-acetyl-D-glucopyranose (**17**)

Figure A3. 25: ^{1}H NMR of acetyl *O*-(2,3,4-tri-*O*-acetyl-β-D-glucopyranosyl)-(1→3)-2,4,6-tri-*O*-acetyl-D-glucopyranose **(18)**

Figure A3. 26: ^{1}H NMR of acetyl *O*-(2,3,4-tri-*O*-acetyl-6-*O*-tosyl-β-D-glucopyranosyl)-(1→3)-2,4,6-tri-*O*-acetyl-D-glucopyranose (**19i**)

Figure A3. 27: ^{1}H NMR (above) and ^{13}C NMR (below) of acetyl *O*-(2,3,4-tri-*O*-acetyl-6-azido-6-deoxy-β-D-glucopyranosyl)-(1→3)-2,4,6-tri-*O*-acetyl-D-glucopyranose (**20**)

Figure A3. 28: HSQC of acetyl *O*-(2,3,4-tri-*O*-acetyl-6-azido-6-deoxy-β-D-glucopyranosyl)-(1→3)-2,4,6-tri-*O*-acetyl-D-glucopyranose (**20**)

Figure A3. 29: ^{1}H NMR (above) and ^{13}C NMR (below) of 2,3,4-tri-*O*-acetyl-6-azido-6-deoxy-β-D-glucopyranosyl-(1→3)-2,4,6-tri-*O*-acetyl-α-D-glucopyranosyl fluoride **(21)**

Figure A3. 30: MALDI of acetyl *O*-(2,3,4-tri-*O*-acetyl-6-*O*-trityl-β-D-glucopyranosyl)-(1→3)-2,4,6-tri-*O*-acetyl-D-glucopyranose (**17**)

Figure A3. 31: MALDI of acetyl *O*-(2,3,4-tri-*O*-acetyl-β-D-glucopyranosyl)-(1→3)-2,4,6-tri-*O*-acetyl-D-glucopyranose (**18**)

Figure A3. 32: MALDI of acetyl *O*-(2,3,4-tri-*O*-acetyl-6-*O*-tosyl-β-D-glucopyranosyl)-(1→3)-2,4,6-tri-*O*-acetyl-D-glucopyranose (**19i**)

Figure A3. 33: MALDI of acetyl *O*-(2,3,4-tri-*O*-acetyl-6-azido-6-deoxy-β-D-glucopyranosyl)-(1→3)-2,4,6-tri-*O*-acetyl-D-glucopyranose (**20**)

Figure A3. 34: MALDI of 2,3,4-tri-*O*-acetyl-6-azido-6-deoxy-β-D-glucopyranosyl-(1→3)-2,4,6-tri-*O*-acetyl-α-D-glucopyranosyl fluoride (**21**)

Figure A3. 35: Degradation of curdlan. TLC (image). Each lane shows the percentage of glucose (band 1), laminaribiose Glcβ3Glc (band 2) and trisaccharides L3 (band 3) (Table left - above) present in the reaction at different times (table below).

Figure A3. 36: Tritylation study. TLC (image). Different products 6'Tr (band 1), 6Tr (band 2) and residual L (band 3) are present in the reaction when it is performed with 1.2 eq of TrCl. The image was analyzed with the program E-CAPT (table) to determine the volume of every band and the ratio between the different products.

Figure A3. 37: TLC (image). Tritylation reaction. Each lane shows the percentage of Di (band 1), 6'Tr (band 2) 6Tr (band 3) and L (band 4) (Table left - above) present when different equivalents of TrCl are used in the reaction (table below)

Figure A3. 38: Tritylation study. TLC (image). Different products Di (band 4), 6'Tr (band 6), 6Tr (band 9) and residual L (band 12) are present in the reaction when it is performed with 3.0 eq of TrCl. The image was analyzed with the program E-CAPT (table) to determine the volume of every band and the ratio between the different products.

Figure A3. 39: Tritylation study. TLC (image). Different products Di, 6'Tr, 6Tr and residual L are present in the reaction when it is performed with 4.25 eq of TrCl. The image was analyzed with the program E-CAPT (table) to determine the volume of every band and the ratio between the different products.

Table A3. 1: Translgycosylation reaction conditions (Glcβ3GlcαF + GlcβPNP). Study of subsites: control reaction

Table A3. 2: Determination of v_o (Glcβ3GlcαF + GlcβPNP). Study of subsites: control reaction

Table A3. 3: Translgycosylation reaction conditions (Glcβ3GlcαF + $6N_3$-GlcβPNP). Study of subsite +1

Table A3. 4: Determination of v_o (Glcβ3GlcαF + $6N_3$-GlcβPNP). Study of subsite +1

Table A3. 5: Translgycosylation reaction conditions (Glcβ3GlcαF + GlcβPNP). Study of subsites: control reaction

Table A3. 6: Determination of v_o (Glcβ3GlcαF + GlcβPNP). Study of subsites: control reaction

Table A3. 7: Translgycosylation reaction conditions ($6N_3$-Glcβ3GlcαF + GlcβPNP). Study of subsite –2

Table A3. 8: Determination of v_o ($6N_3$-Glcβ3GlcαF + GlcβPNP). Study of subsite –2

Table A3. 9: Degradation of curdlan. Analysis lane 1 (t = 2 hours)

Table A3. 10: Degradation of curdlan. Analysis lane 2 (t = 4 hours)

Table A3. 11: Degradation of curdlan. Analysis lane 3 (t = 6 hours)

Table A3. 12: Degradation of curdlan. Analysis lane 4 (t = 8 hours)

Table A3. 13: Degradation of curdlan. Analysis lane 5 (t = 10 hours)

Table A3. 14: Degradation of curdlan. Analysis lane 6 (t = 12 hours)

Table A3. 15: Degradation of curdlan. Analysis lane 7 (t = 14 hours)

Table A3. 16: Degradation of curdlan. Analysis lane 8 (t = 16 hours)

Table A3. 17: Degradation of curdlan. Analysis lane 9 (t = 18 hours)

Table A3. 18: Degradation of curdlan. Analysis lane 10 (t = 20 hours)

Table A3. 19: Degradation of curdlan. Ratio of the different products at different times

Table A3. 20: Tritylation study. Analysis lane 2.5 eq TrCl

Table A3. 21: Tritylation study. Analysis lane 3.5 eq TrCl

Table A3. 22: Tritylation study. Analysis lane 4.5 eq TrCl

Table A3. 23: Tritylation study. Study of maximum formation of monotritylated product *vs* equivalents of TrCl

Table A3. 24: Tritylation study. Different ratios of products are obtained when the reaction is performed with different equivalents of TrCl.

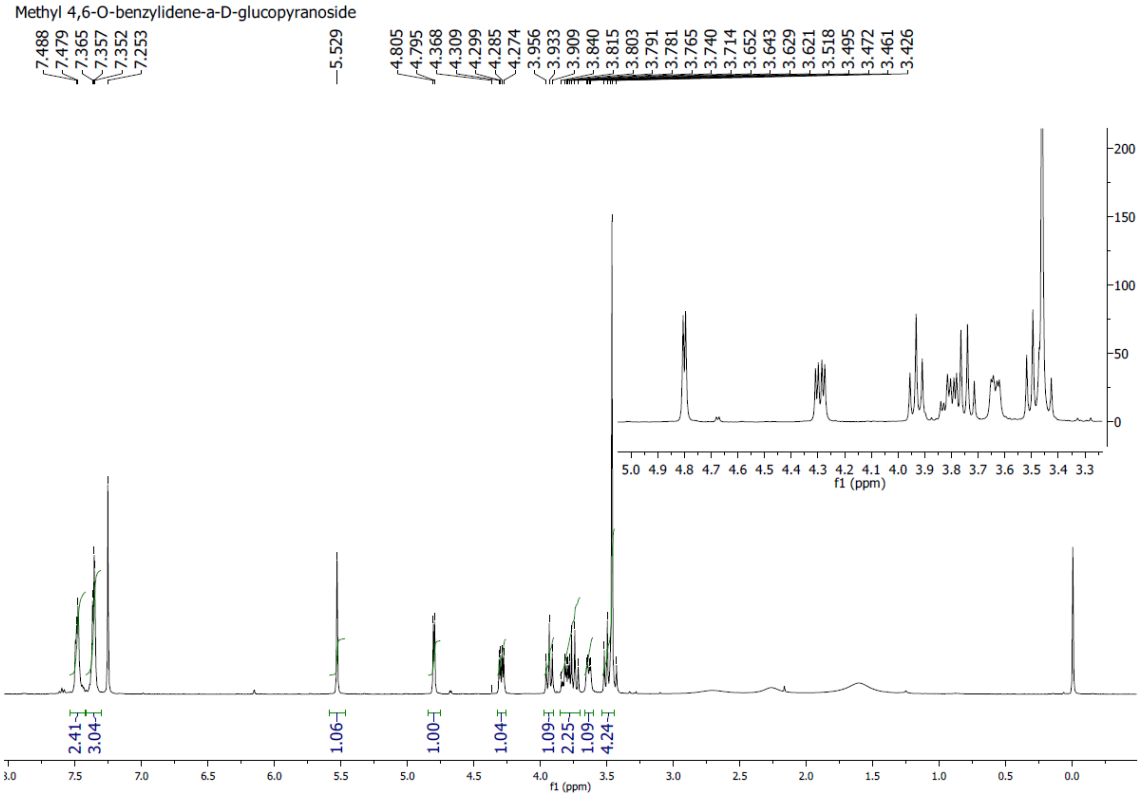

Figure A3. 1: ^{1}H NMR of methyl 4,6-*O*-benzylidene-α-D-glucopyranoside (**2**).

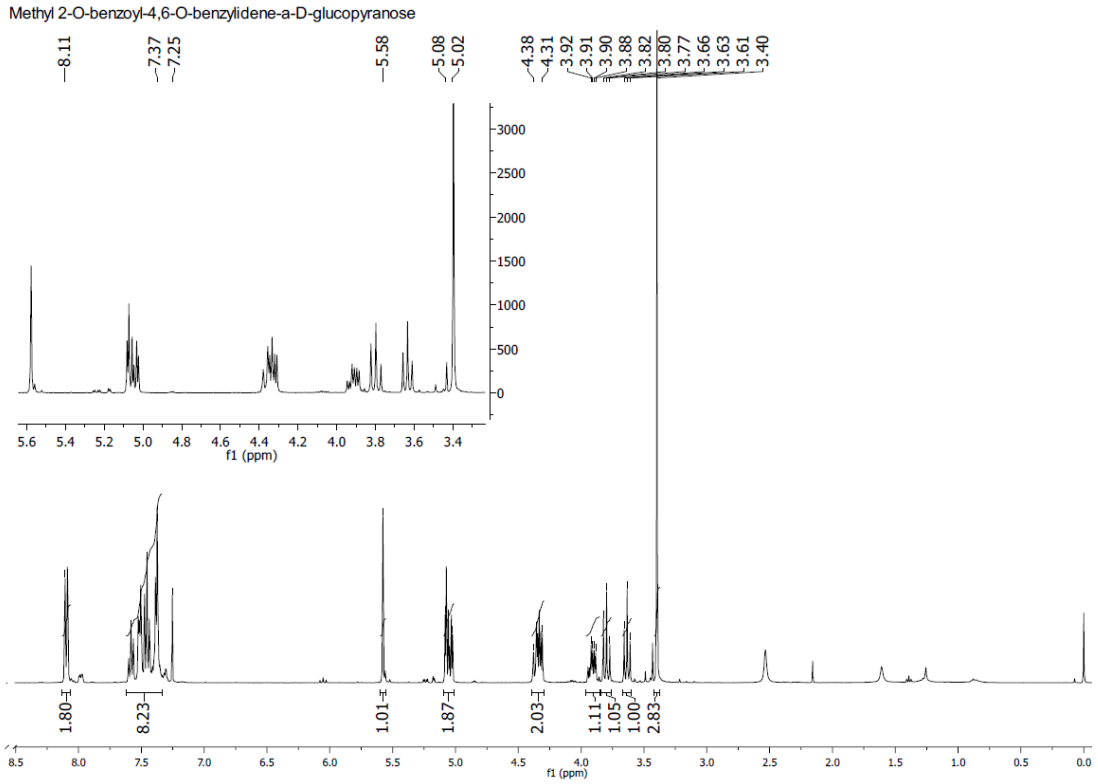

Figure A3. 2: ^{1}H NMR of methyl 2-*O*-benzoyl-4,6-*O*-benzylidene-α-D-glucopyranoside (**23**).

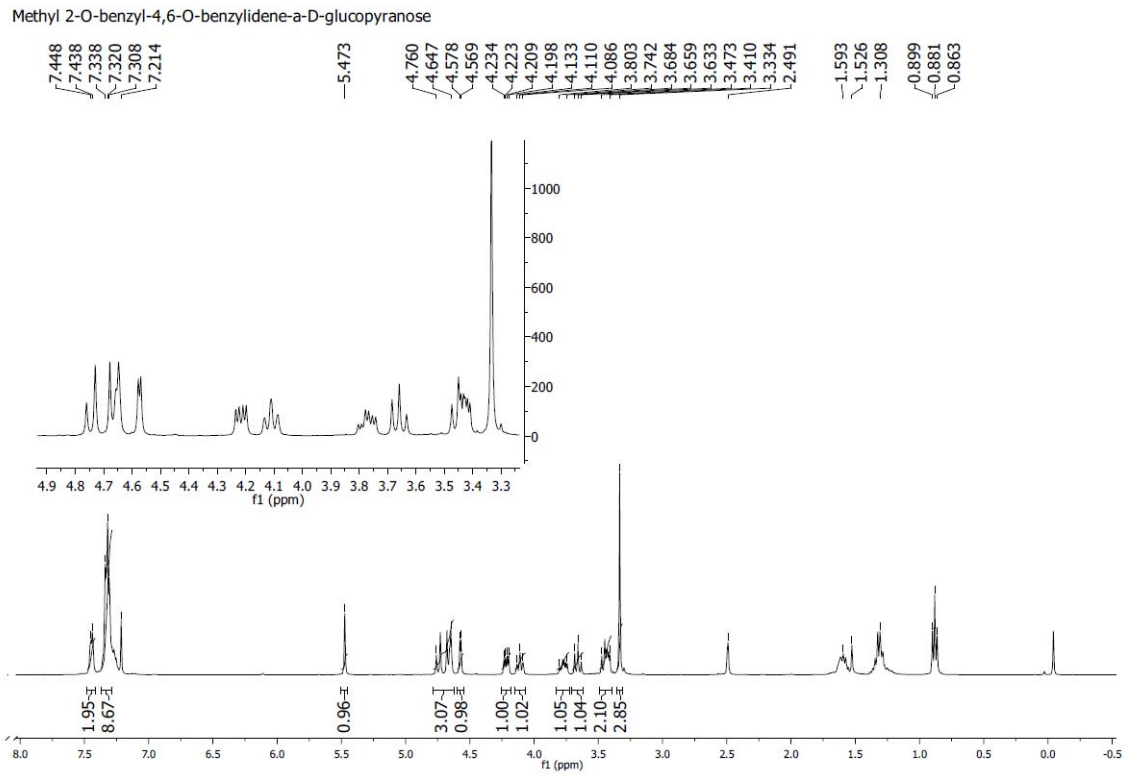

Figure A3. 3: [1]H NMR of methyl 2-*O*-benzyl-4,6-*O*-benzylidene-α-D-glucopyranoside (**25**).

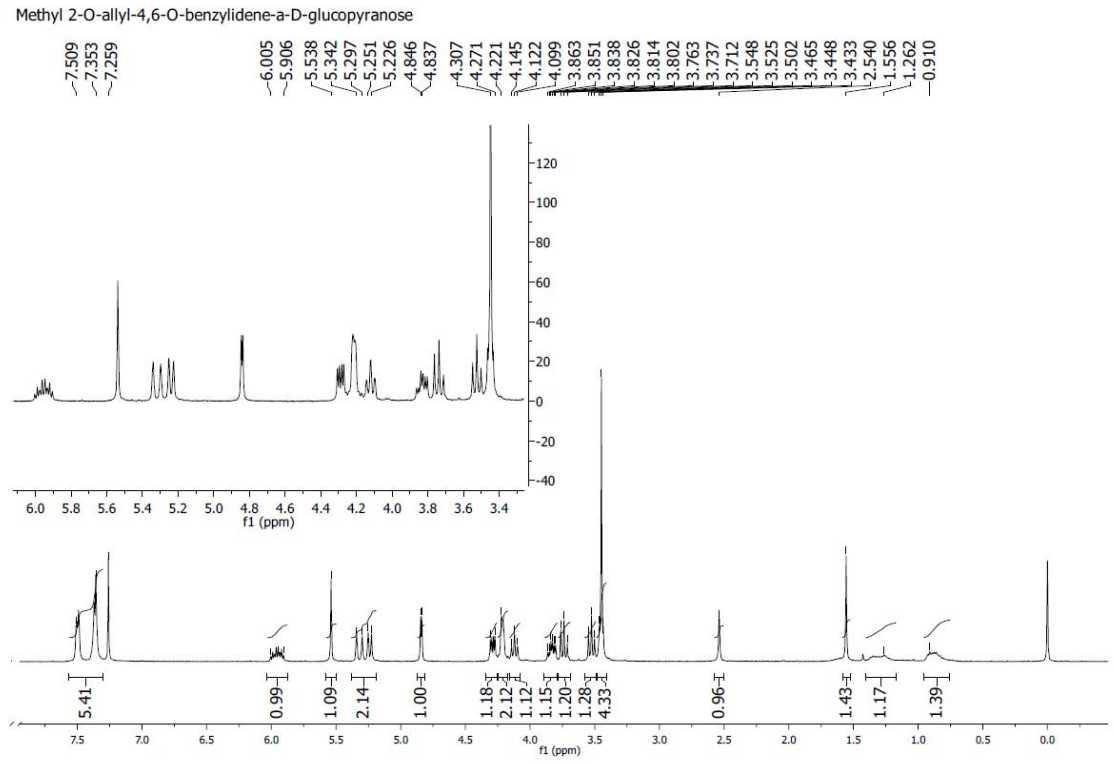

Figure A3. 4: [1]H NMR of methyl 2-*O*-allyl-4,6-*O*-benzylidene-α-D-glucopyranoside (**3**).

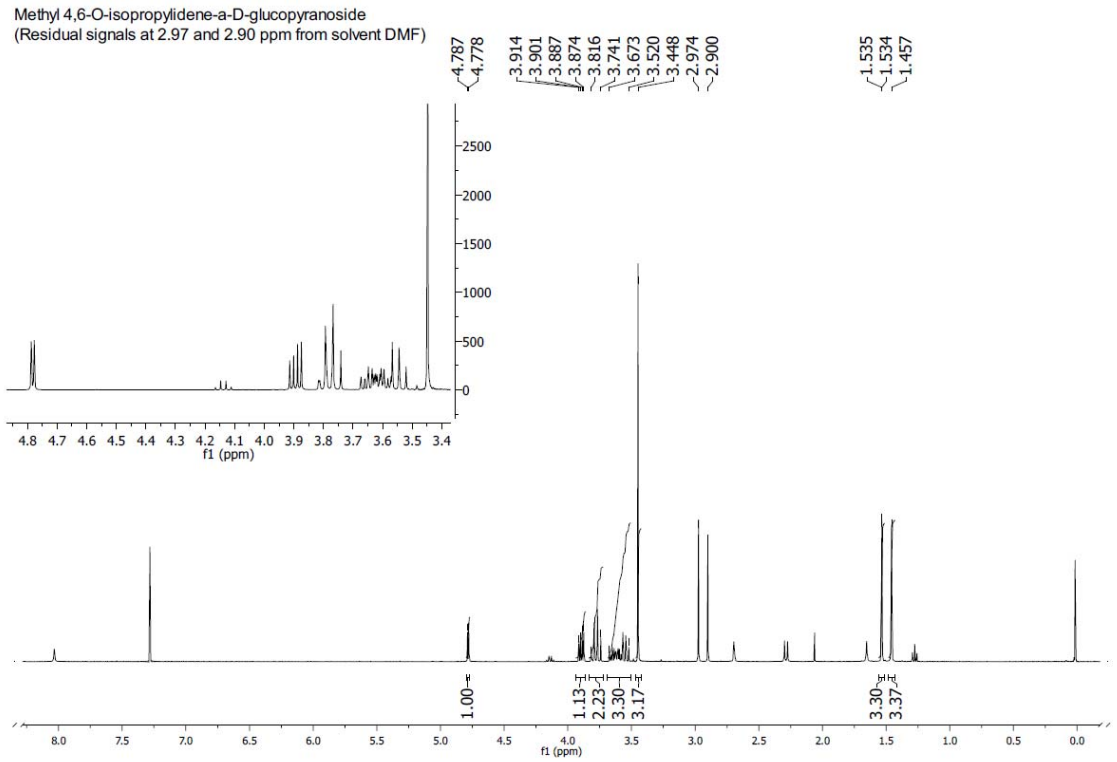

Figure A3. 5: [1]H NMR of methyl 4,6-*O*-isopropylidene-α-D-glucopyranoside.

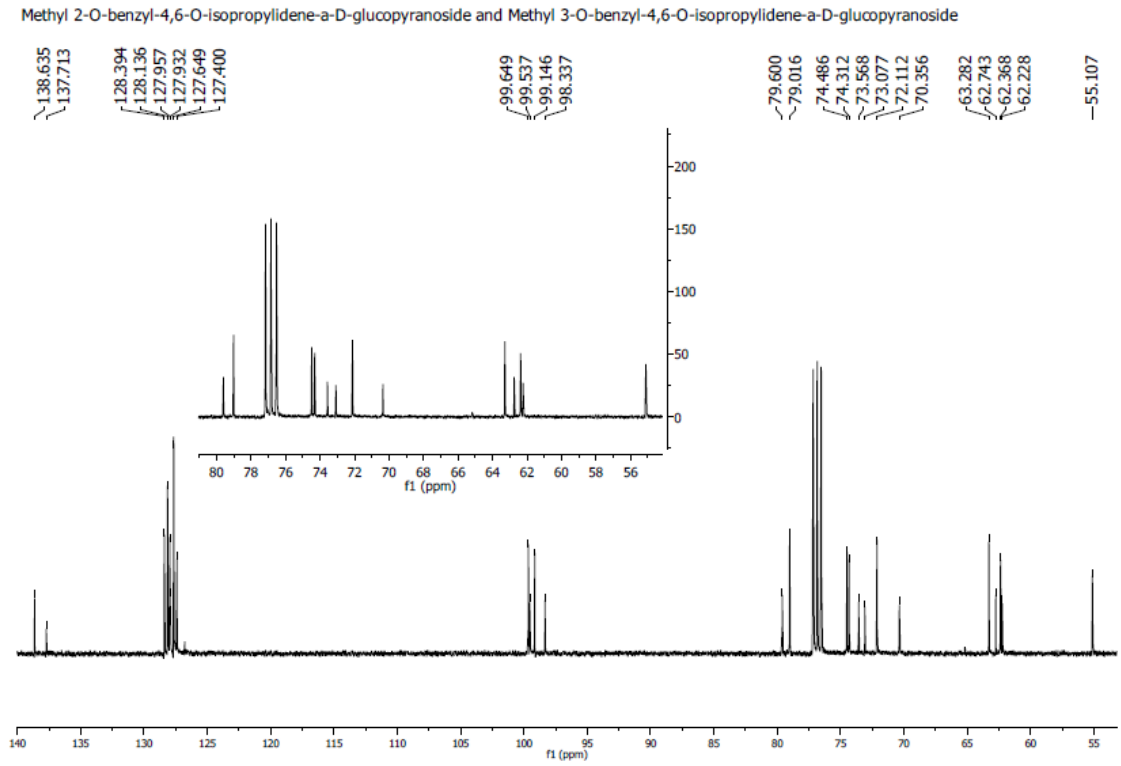

Figure A3. 6: [13]C NMR of a mixture of isomers benzylated at C-2 and C-3. Methyl 2-*O*-benzyl-4,6-*O*-isopropylidene-α-D-glucopyranoside (**24**) is the major product observed in the spectrum.

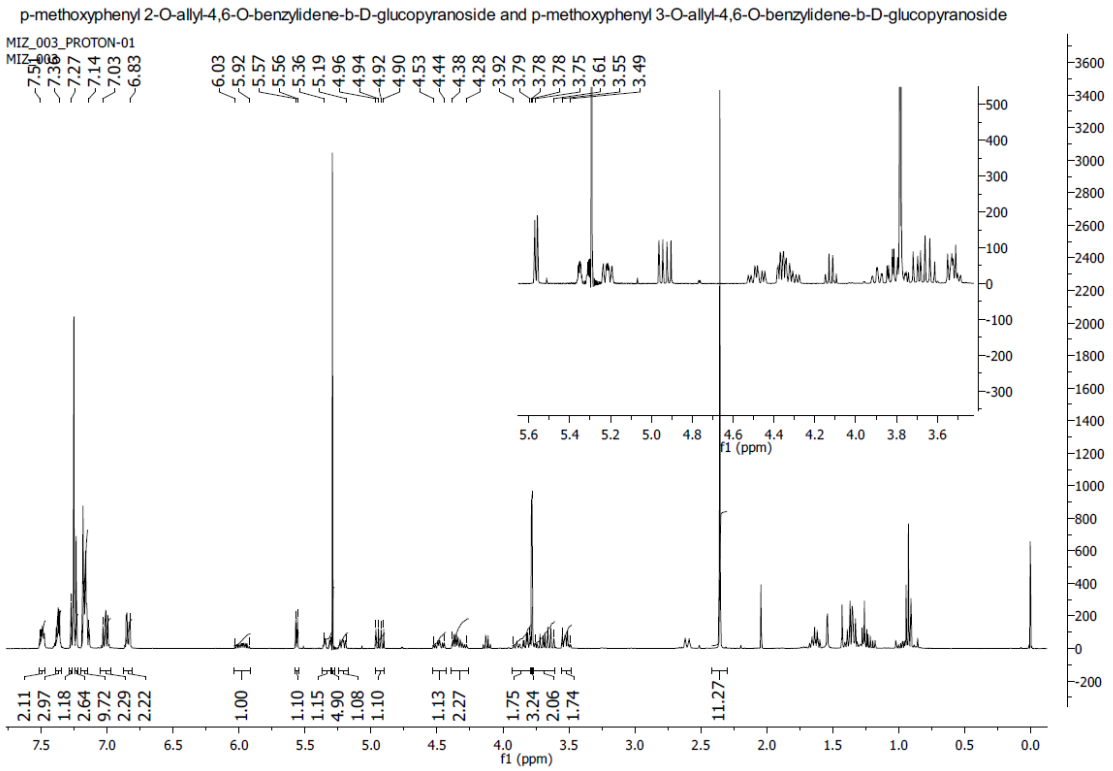

Figure A3. 7: ^{1}H NMR of *p*-methoxyphenyl 2-*O*-allyl-4,6-*O*-benzylidene-β-D-glucopyranoside (**29**).

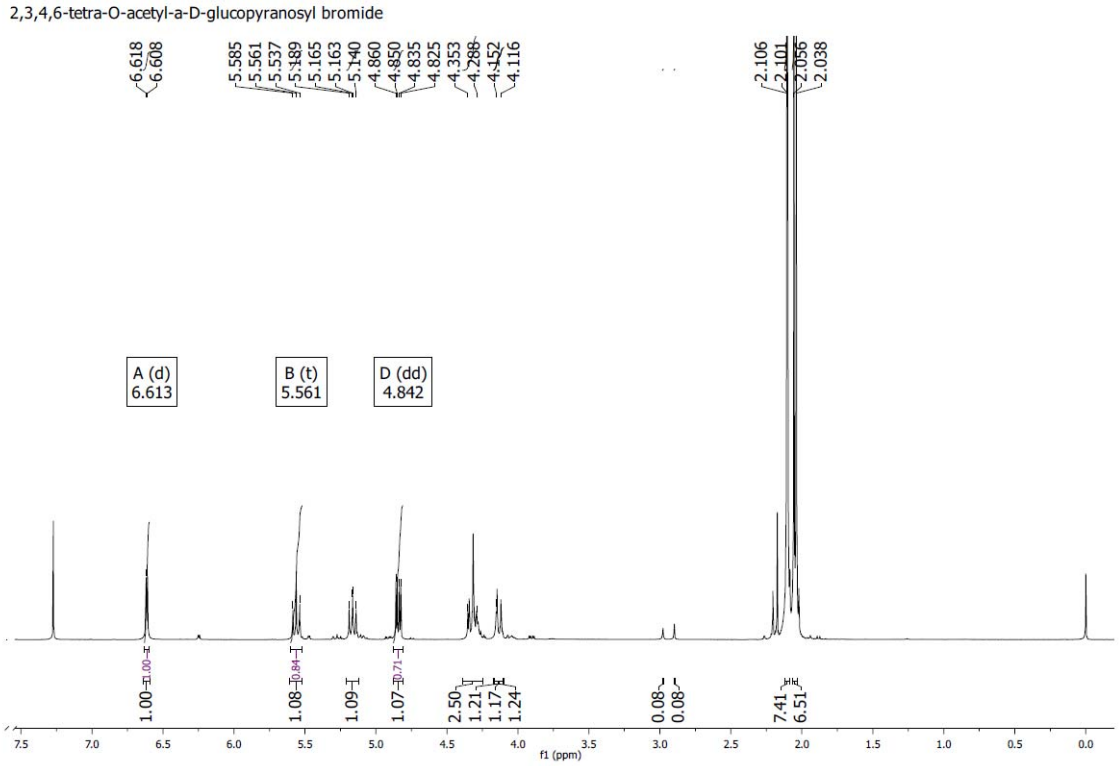

Figure A3. 8: ^{1}H NMR of 2,3,4,6-tetra-*O*-acetyl-α-D-glucopyranosyl bromide (**5**).

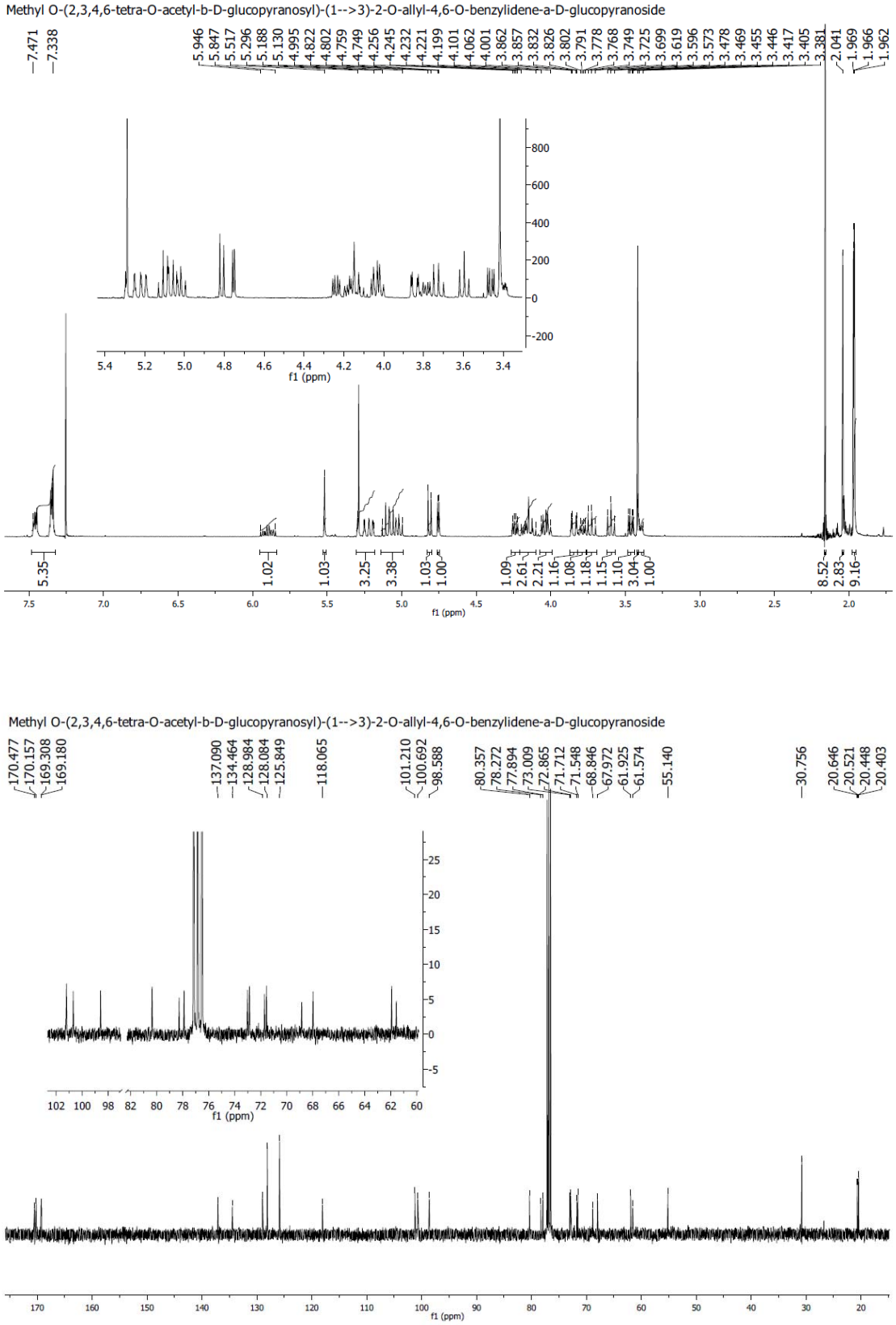

Figure A3. 9: ^{1}H NMR (above) and ^{13}C NMR (below) of methyl *O*-(2,3,4,6-tetra-*O*-acetyl-β-D.glucopyranosyl)-(1→3)-2-*O*-allyl-4,6-*O*-benzylidene-α-D-glucopyranoside (**6**).

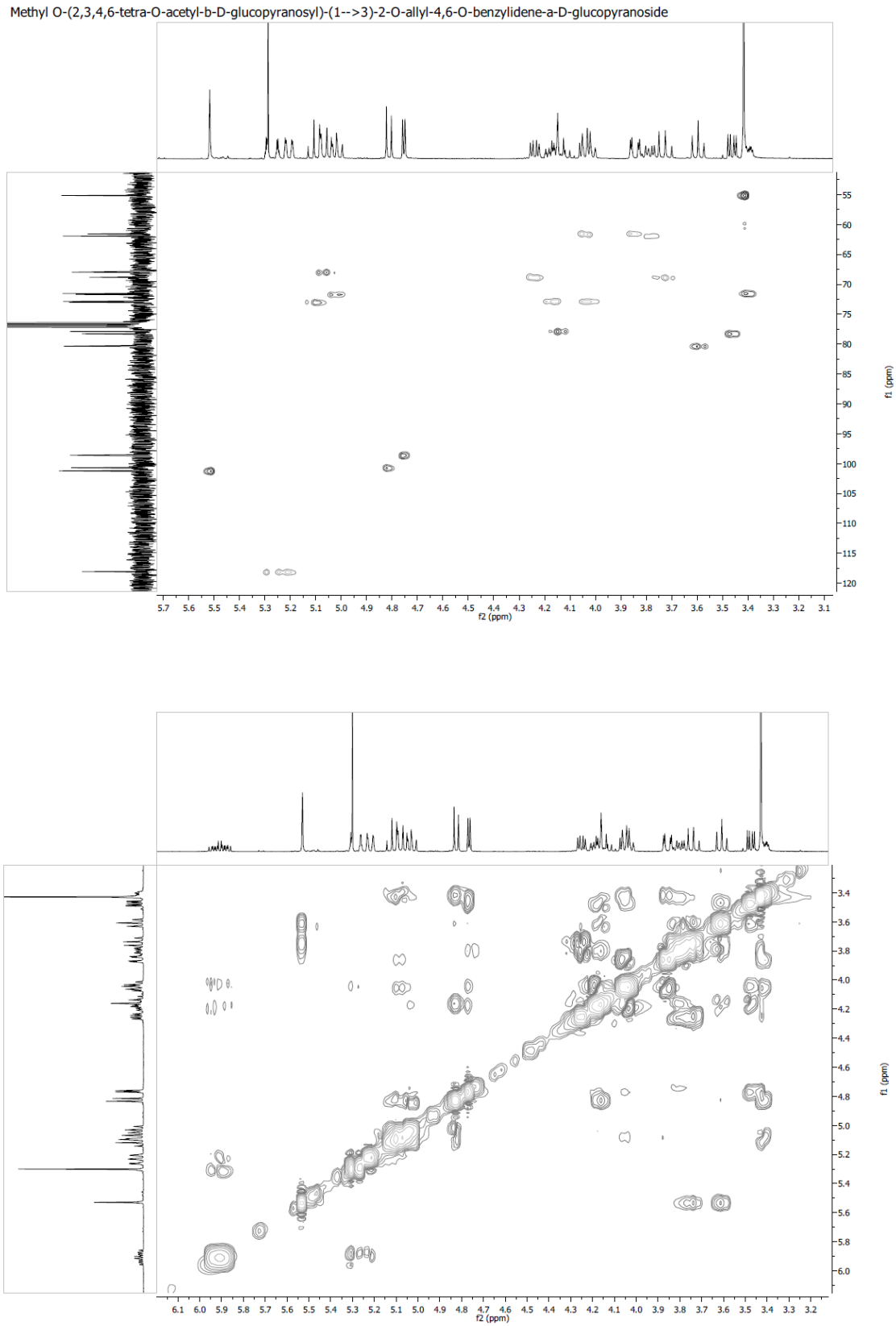

Figure A3. 10: HSQC (above) and NOESY (below) of methyl *O*-(2,3,4,6-tetra-*O*-acetyl-β-D.glucopyranosyl)-(1→3)-2-*O*-allyl-4,6-*O*-benzylidene-α-D-glucopyranoside (**6**).

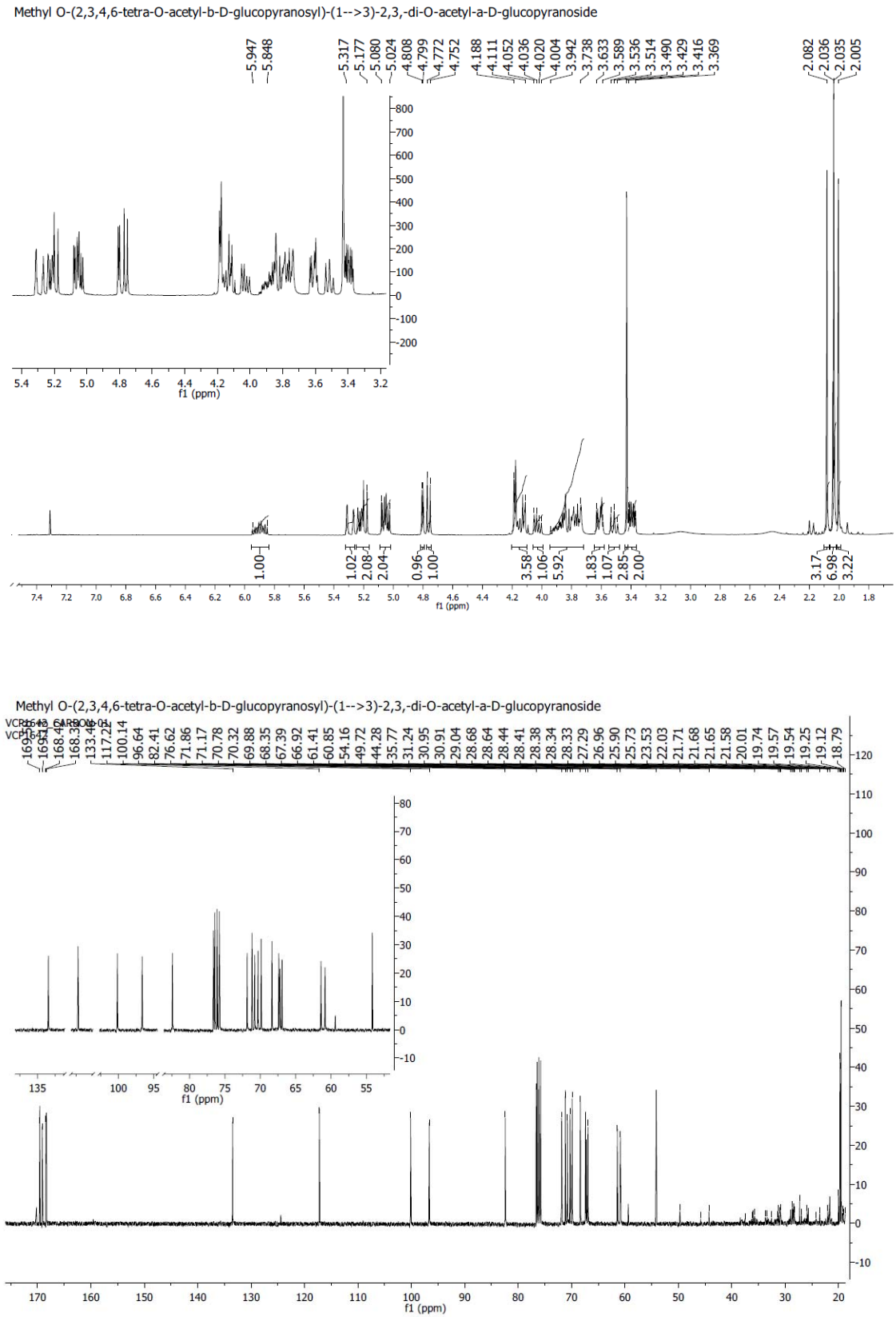

Figure A3. 11: ^{1}H NMR (above) and ^{13}C NMR (below) of methyl *O*-(2,3,4,6-tetra-*O*-acetyl-β-D-glucopyranosyl)-(1→3)-2-*O*-allyl-4,6-di-*O*-acetyl-α-D-glucopyranoside.

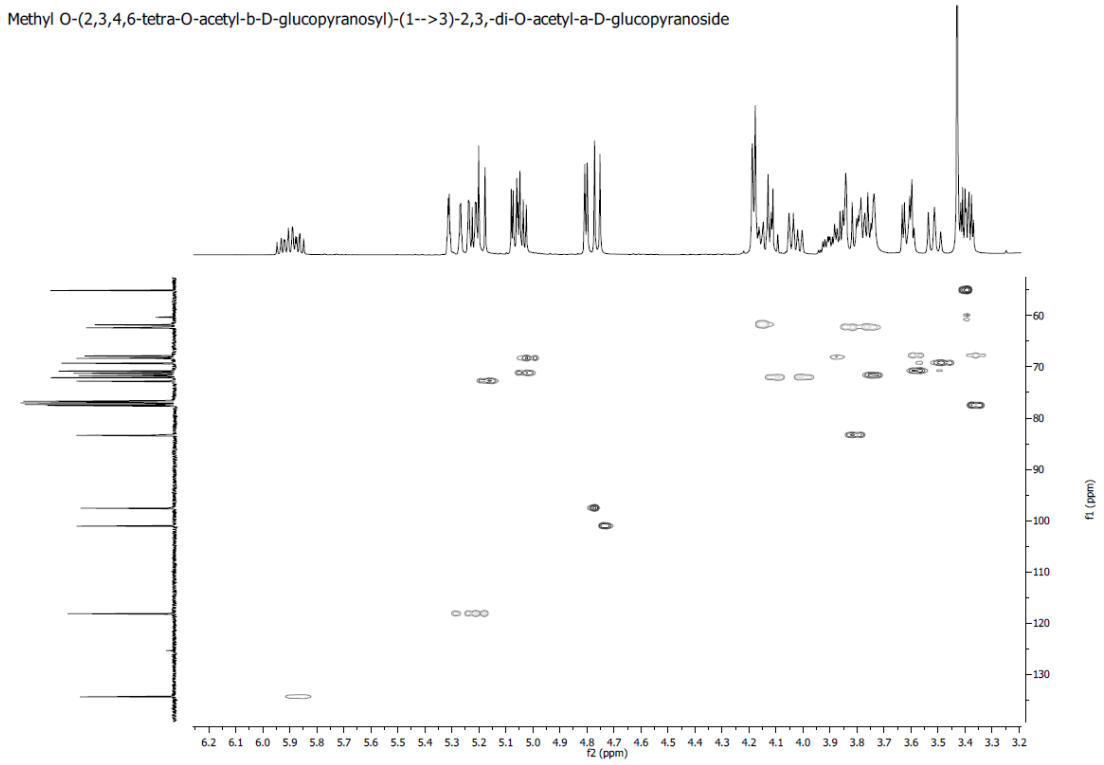

Figure A3. 12: HSQC of methyl *O*-(2,3,4,6-tetra-*O*-acetyl-β-D.glucopyranosyl)-(1→3)-2-*O*-allyl-4,6-di-*O*-acetyl-α-D-glucopyranoside.

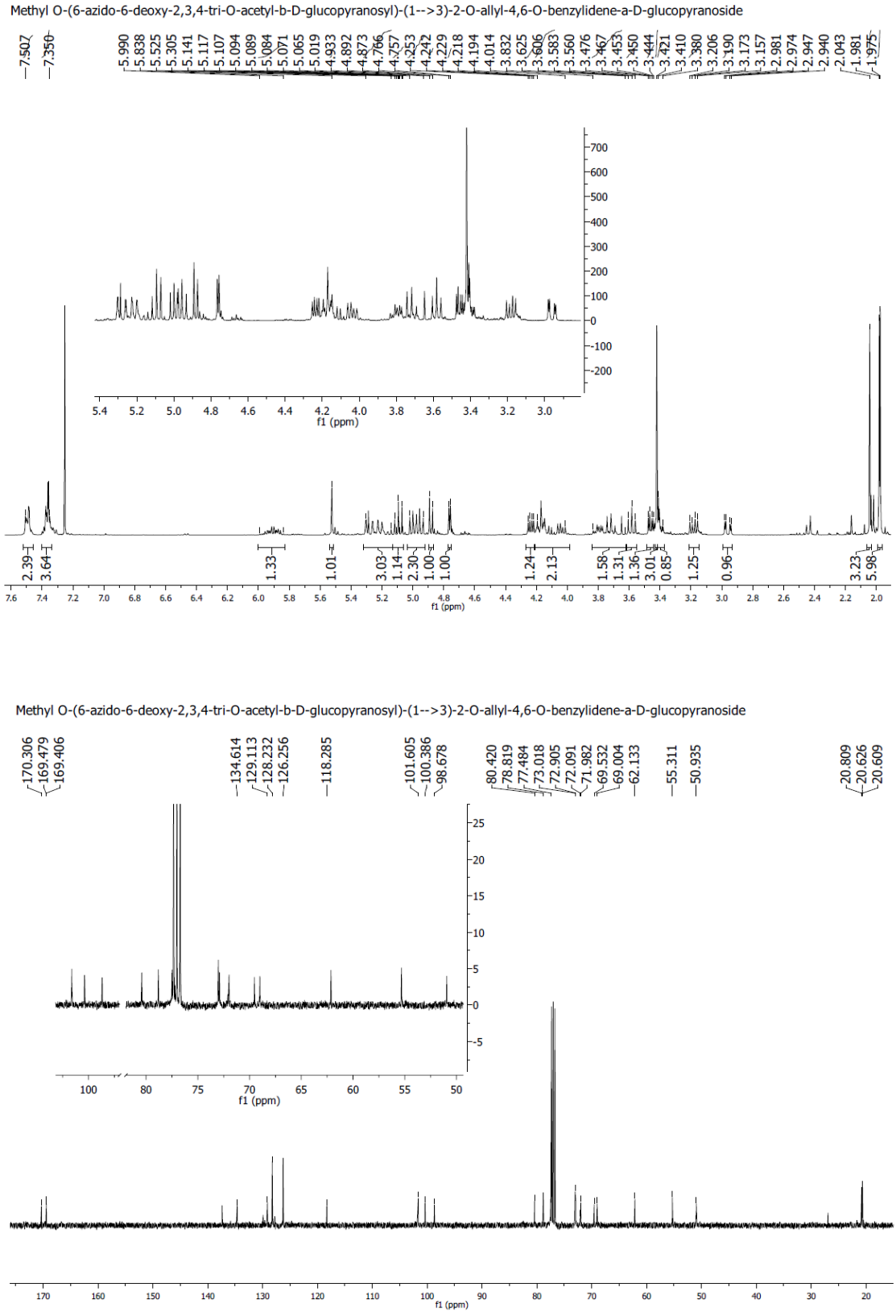

Figure A3. 13: ^{1}H NMR (above) and ^{13}C NMR (below) of methyl *O*-(6-azido-6-deoxy-2,3,4-tri-*O*-acetyl-β-D.glucopyranosyl)-(1→3)-2-*O*-allyl-4,6-*O*-benzylidene-α-D-glucopyranoside (**8**).

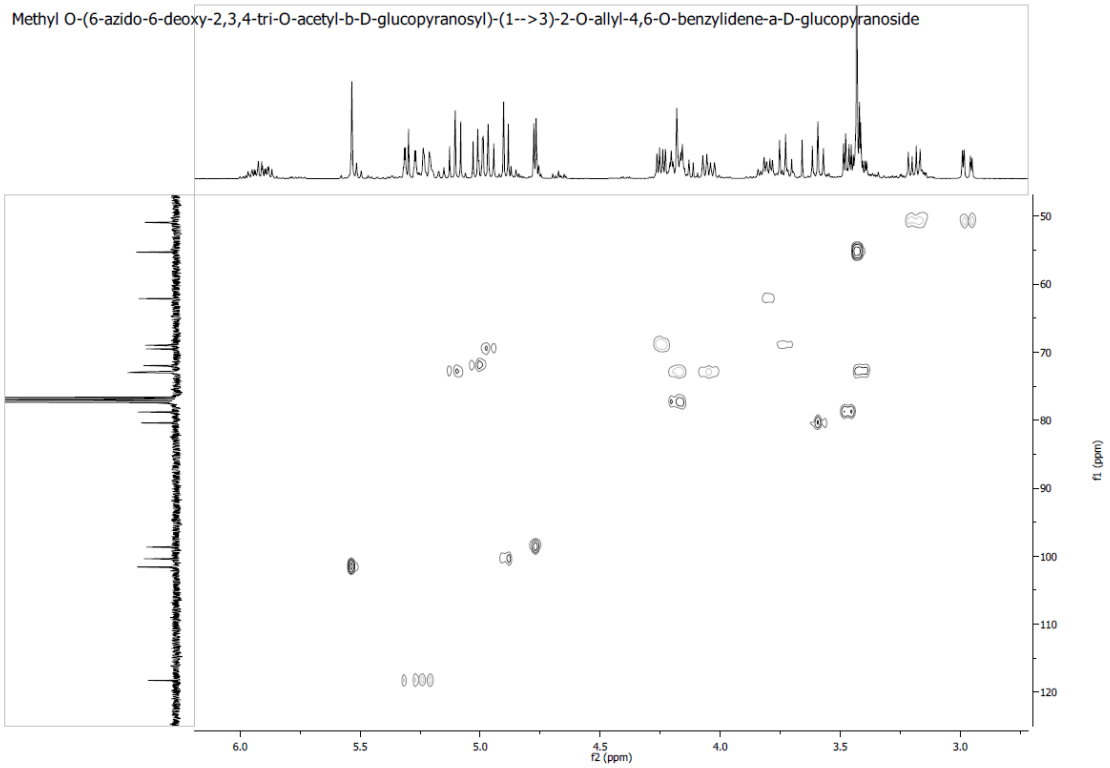

Figure A3. 14: HSQC of methyl *O*-(6-azido-6-deoxy-2,3,4-tri-*O*-acetyl-β-D.glucopyranosyl)-(1→3)-2-*O*-allyl-4,6-*O*-benzylidene-α-D-glucopyranoside (**8**).

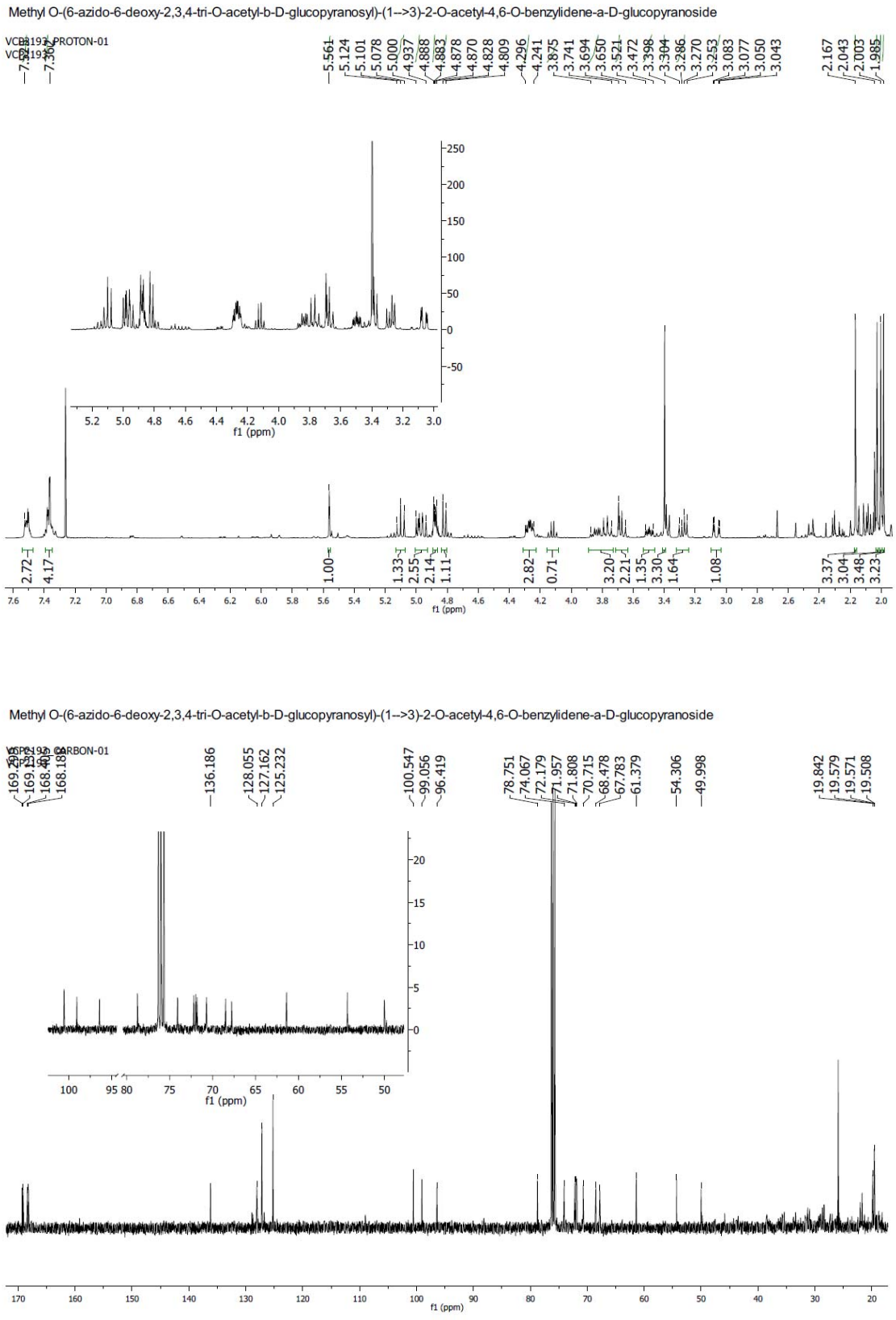

Figure A3. 15: ^{1}H NMR (above) and ^{13}C NMR (below) of methyl *O*-(6-azido-6-deoxy-2,3,4-tri-*O*-acetyl-β-D.glucopyranosyl)-(1→3)-2-*O*-acetyl-4,6-*O*-benzylidene-α-D-glucopyranoside.

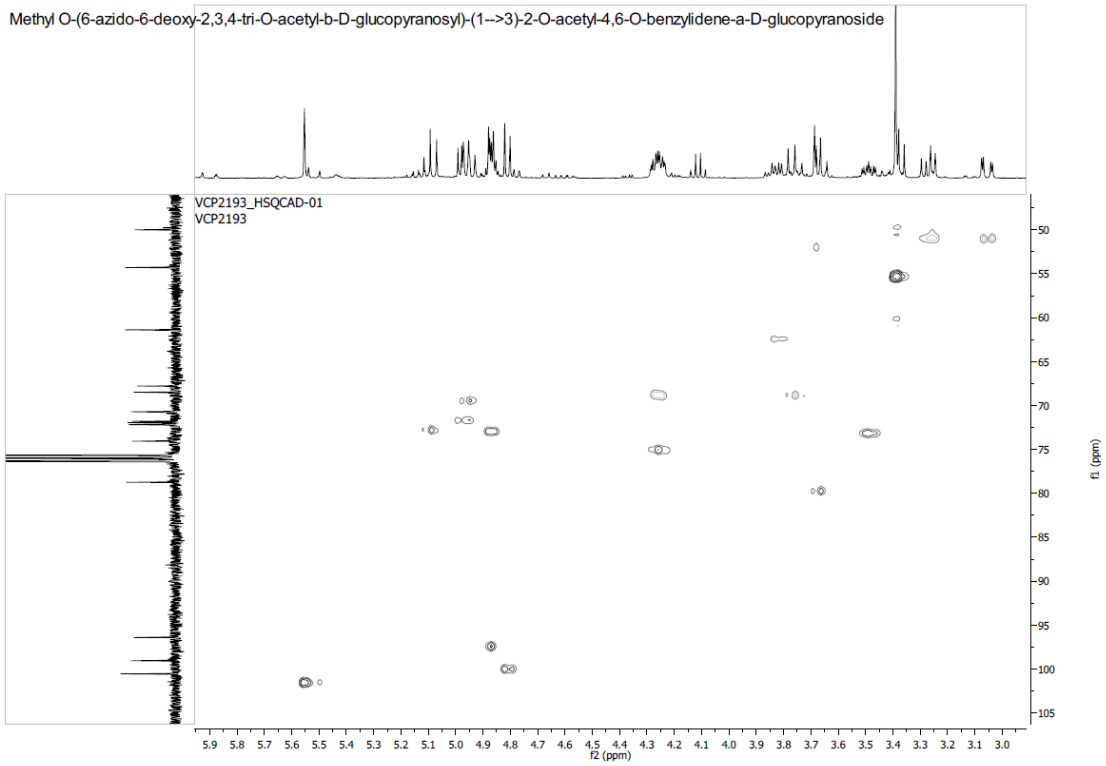

Figure A3. 16: HSQC of methyl *O*-(6-azido-6-deoxy-2,3,4-tri-*O*-acetyl-β-D.glucopyranosyl)-(1→3)-2-*O*-acetyl-4,6-*O*-benzylidene-α-D-glucopyranoside.

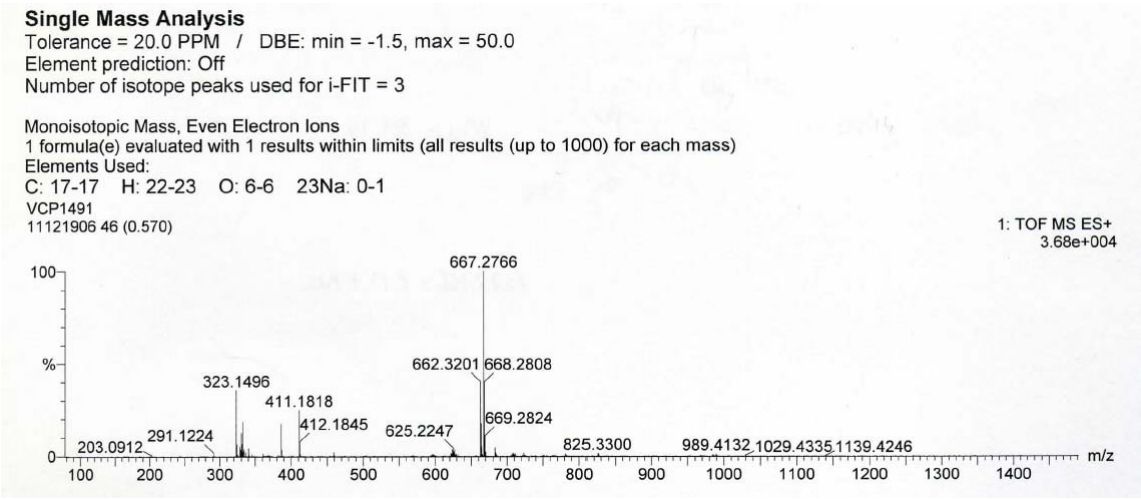

Figure A3. 17: MALDI of methyl 2-*O*-allyl-4,6-*O*-benzylidene-α-D-glucopyranoside (**3**).

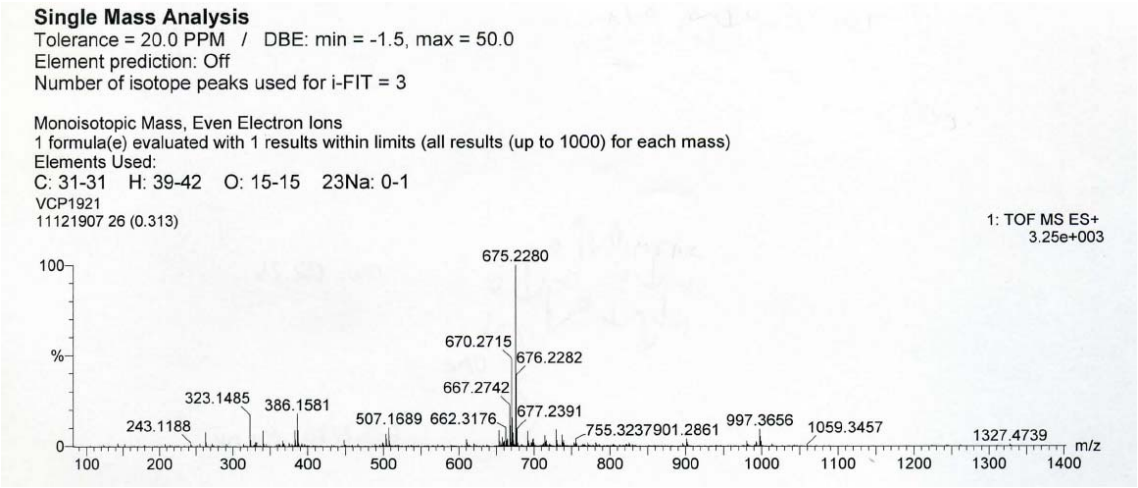

Figure A3. 18: MALDI of methyl *O*-(2,3,4,6-tetra-*O*-acetyl-β-D-glucopyranosyl)-(1→3)-2-*O*-allyl-4,6-*O*-benzylidene-α-D-glucopyranoside (**a**).

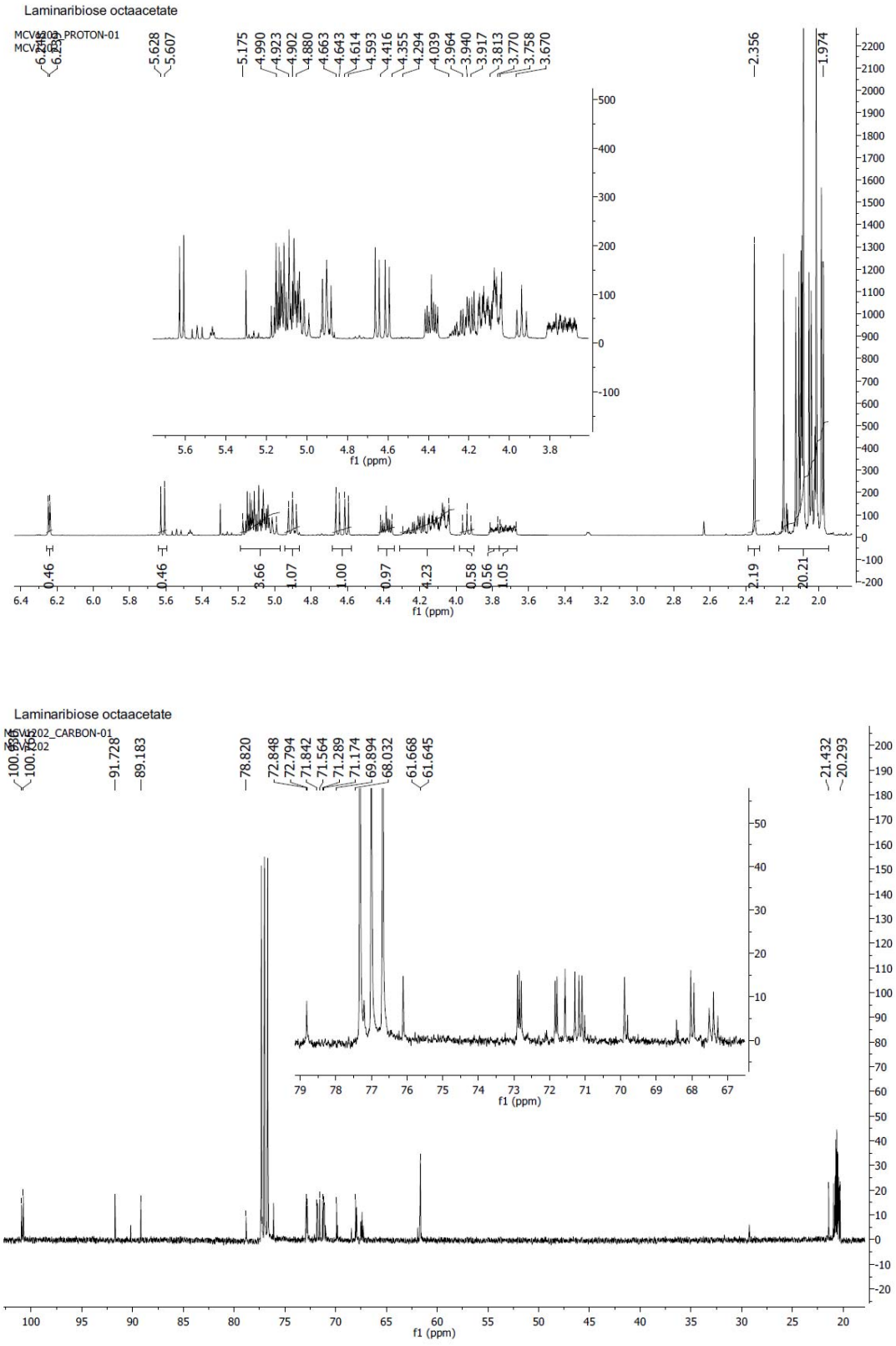

Figure A3. 19: ^{1}H NMR (above) and ^{13}C NMR (below) of 2,3,4,6-tetra-*O*-acetyl-β-D-glucopyranosyI-(1→3)-1,2,4,6-tetra-*O*-acetyl-D-glucopyranose (**16**).

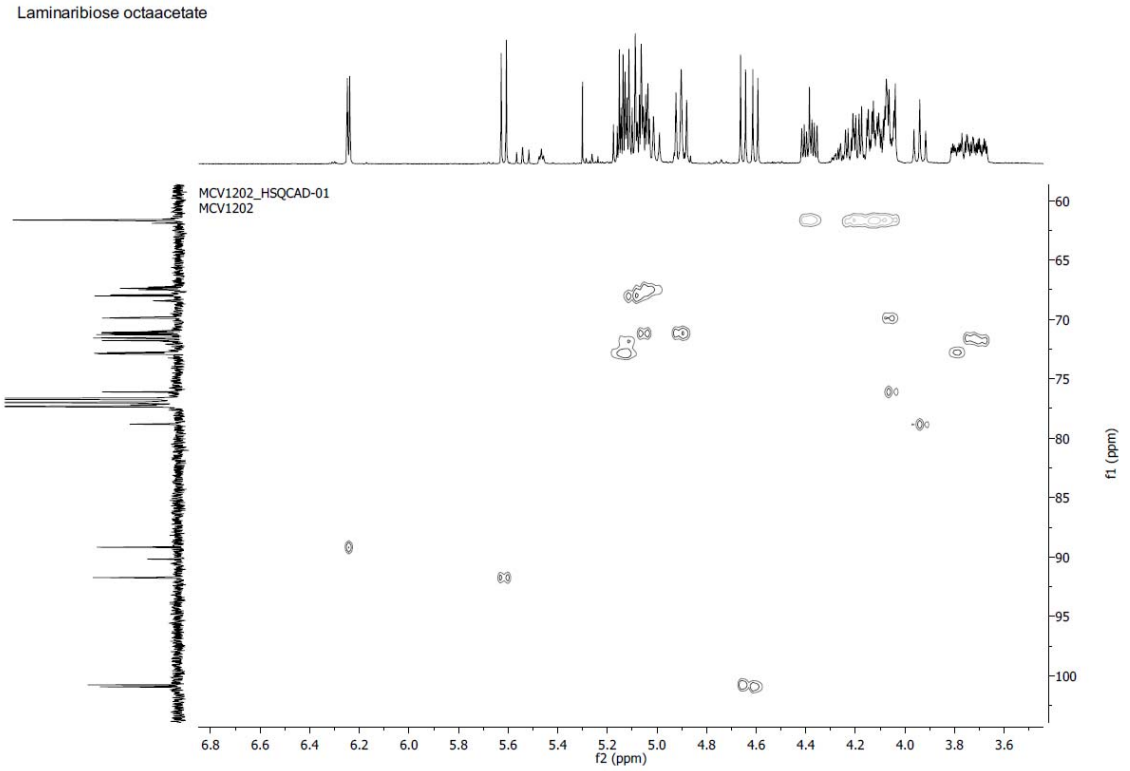

Figure A3. 20: HSQC of 2,3,4,6-tetra-*O*-acetyl-β-D-glucopyranosyI-(1→3)-1,2,4,6-tetra-*O*-acetyl-D-glucopyranose (**16**).

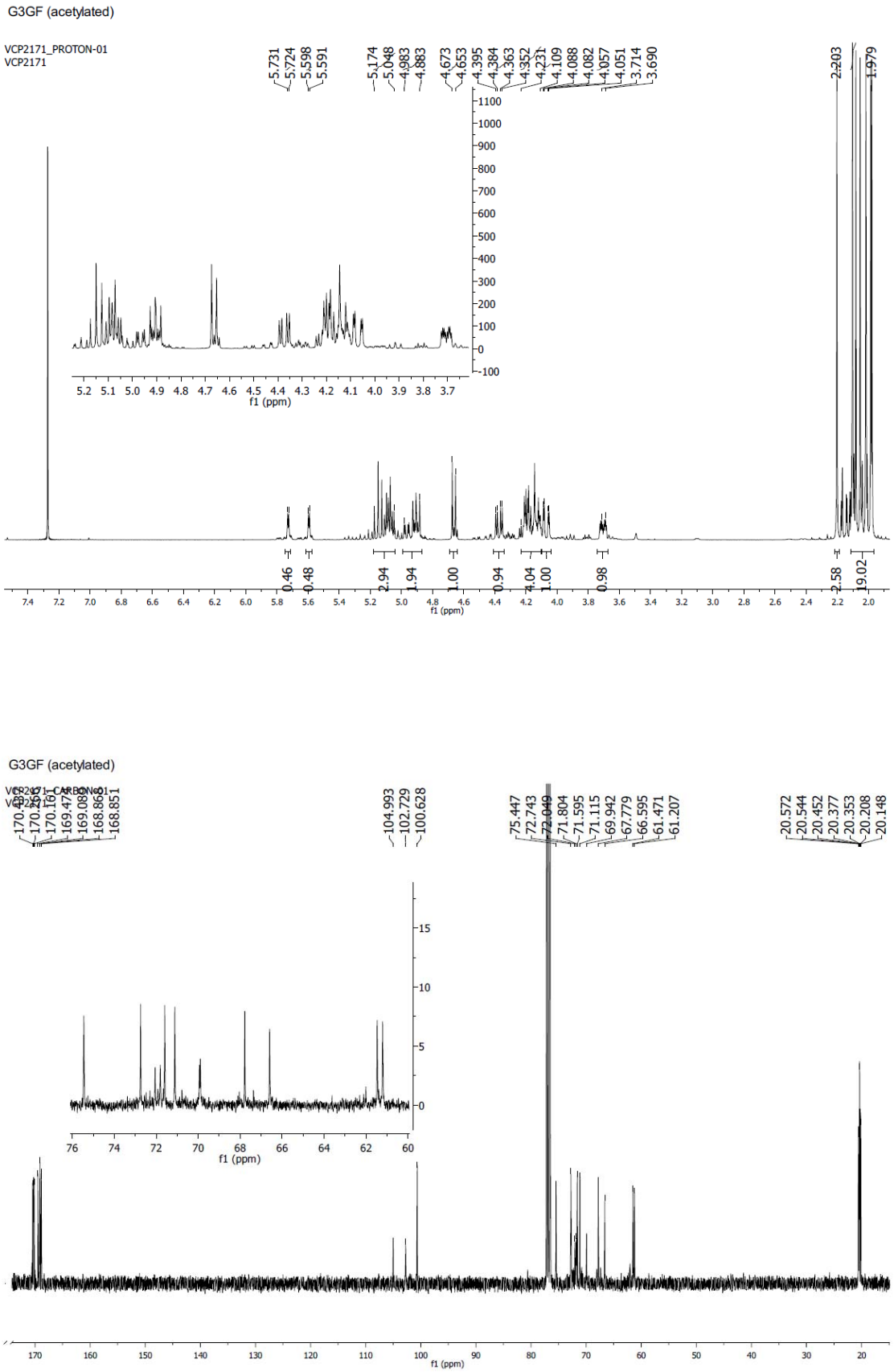

Figure A3. 21: ^{1}H NMR (above) and ^{13}C NMR (below) of the laminaribiosyl fluoride donor (Glcβ3GlcαF) (**36**).

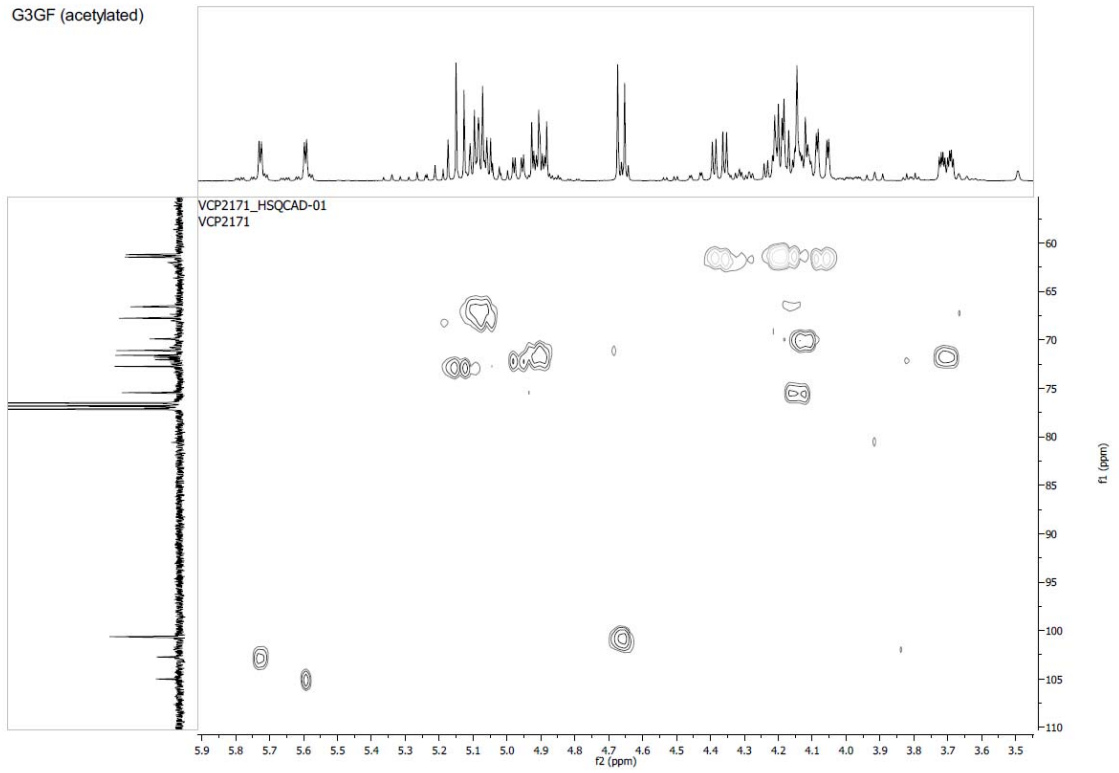

Figure A3. 22: HSQC of laminaribiosyl fluoride donor (Glcβ3GlcαF) (**36**).

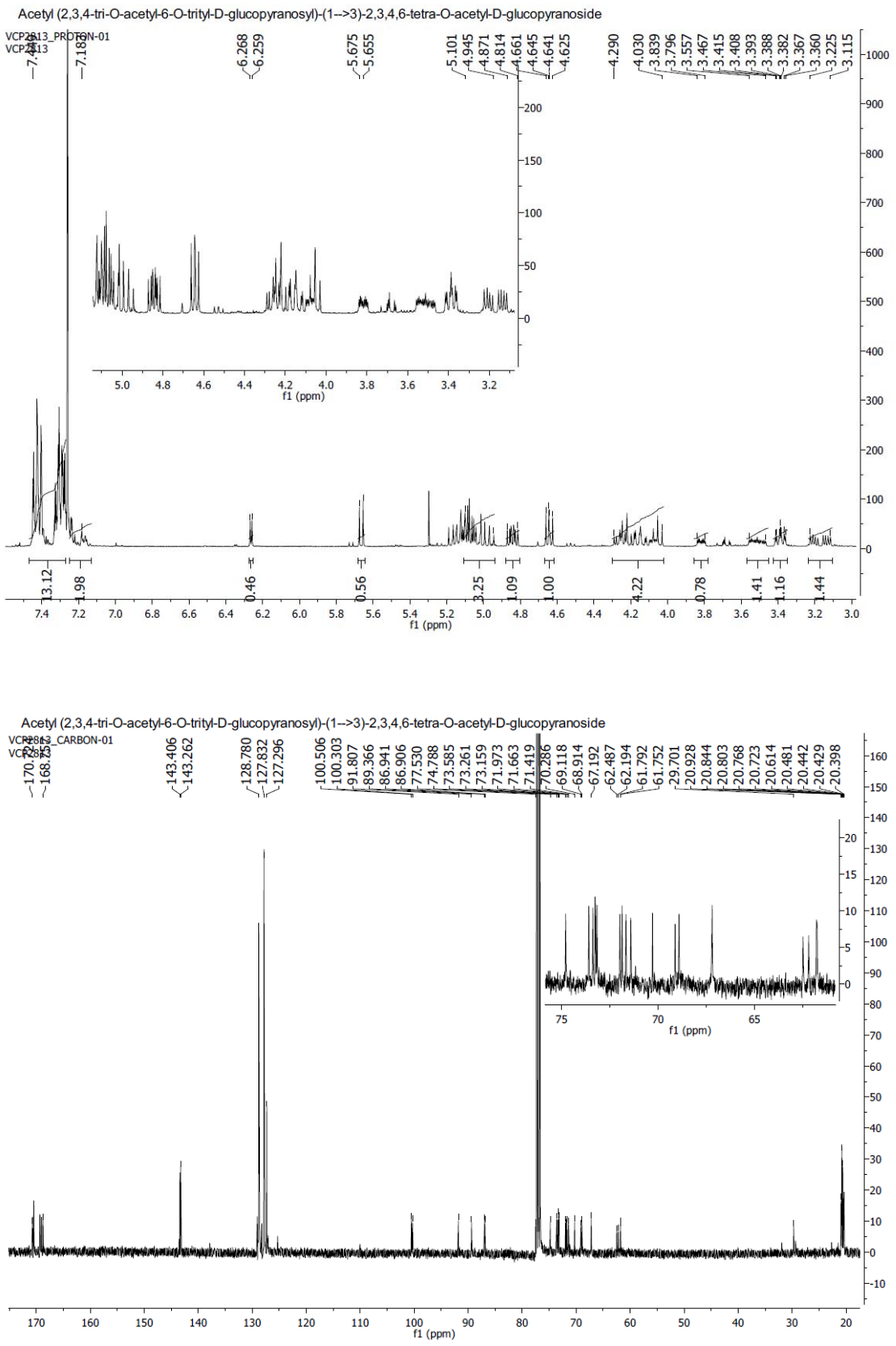

Figure A3. 23: ^{1}H NMR (above) and ^{13}C NMR (below) of acetyl *O*-(2,3,4-tri-*O*-acetyl-6-*O*-trityl-β-D-glucopyranosyl)-(1→3)-2,4,6-tri-*O*-acetyl-D-glucopyranose (**17**).

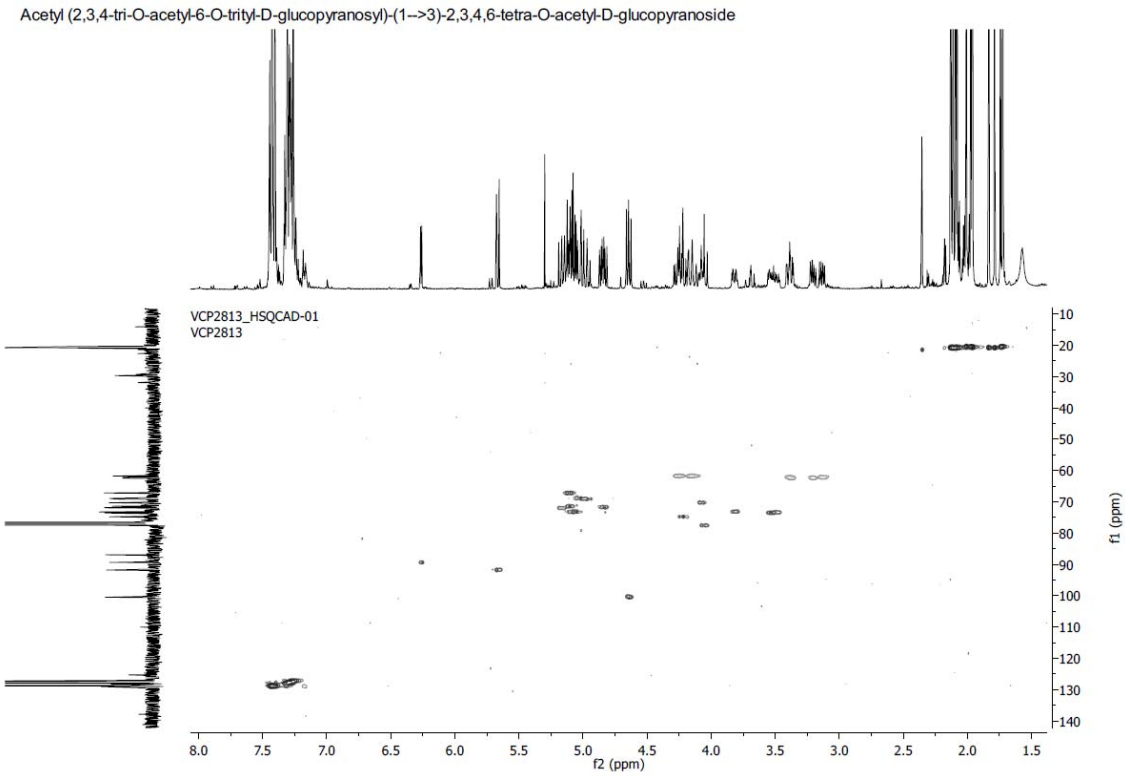

Figure A3. 24: HSQC of acetyl *O*-(2,3,4-tri-*O*-acetyl-6-*O*-trityl-β-D-glucopyranosyl)-(1→3)-2,4,6-tri-*O*-acetyl-D-glucopyranose (**17**).

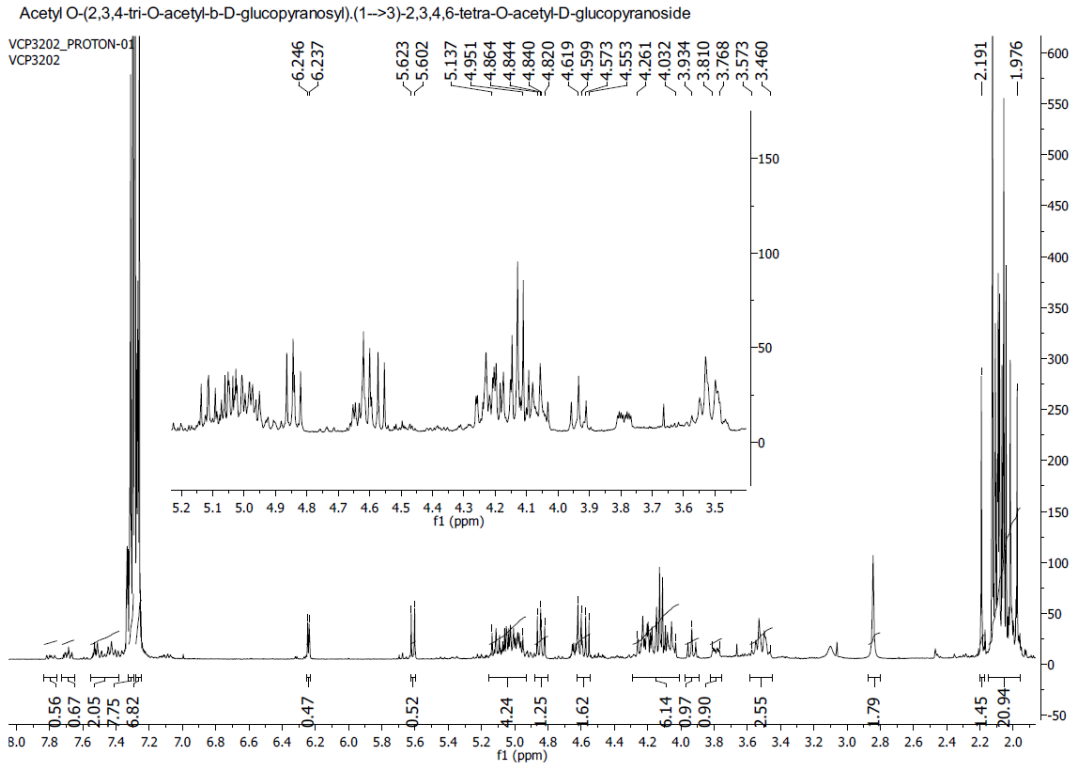

Figure A3. 25: ^{1}H NMR of acetyl *O*-(2,3,4-tri-*O*-acetyl-β-D-glucopyranosyl)-(1→3)-2,4,6-tri-*O*-acetyl-D-glucopyranose **(18).**

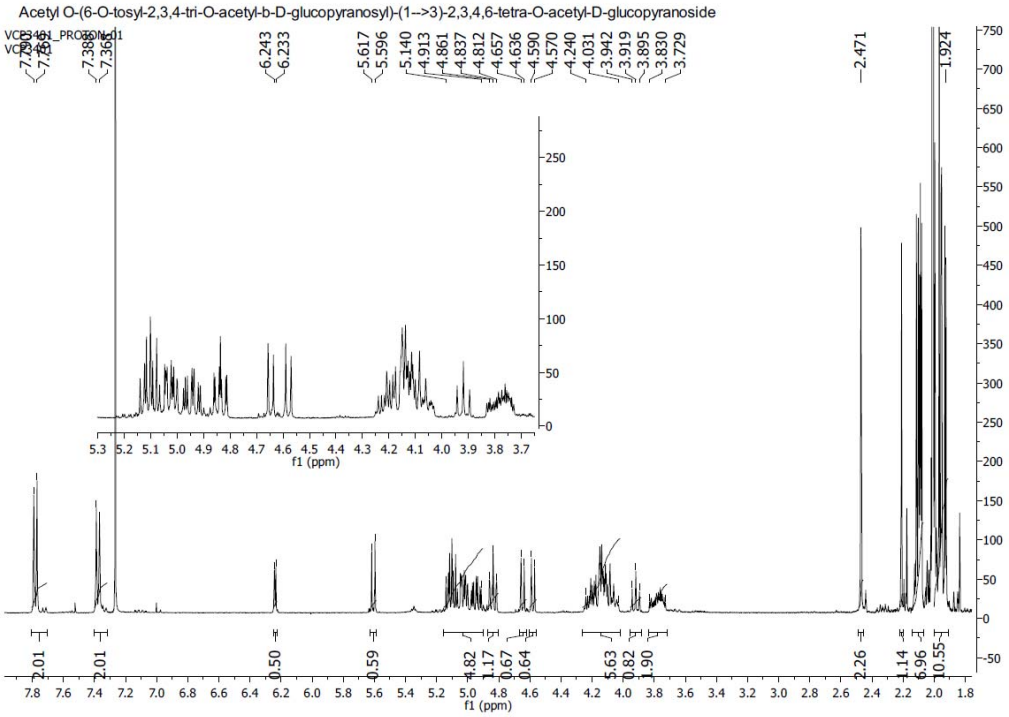

Figure A3. 26: ^{1}H NMR of acetyl *O*-(2,3,4-tri-*O*-acetyl-6-*O*-tosyl-β-D-glucopyranosyl)-(1→3)-2,4,6-tri-*O*-acetyl-D-glucopyranose (**19i**).

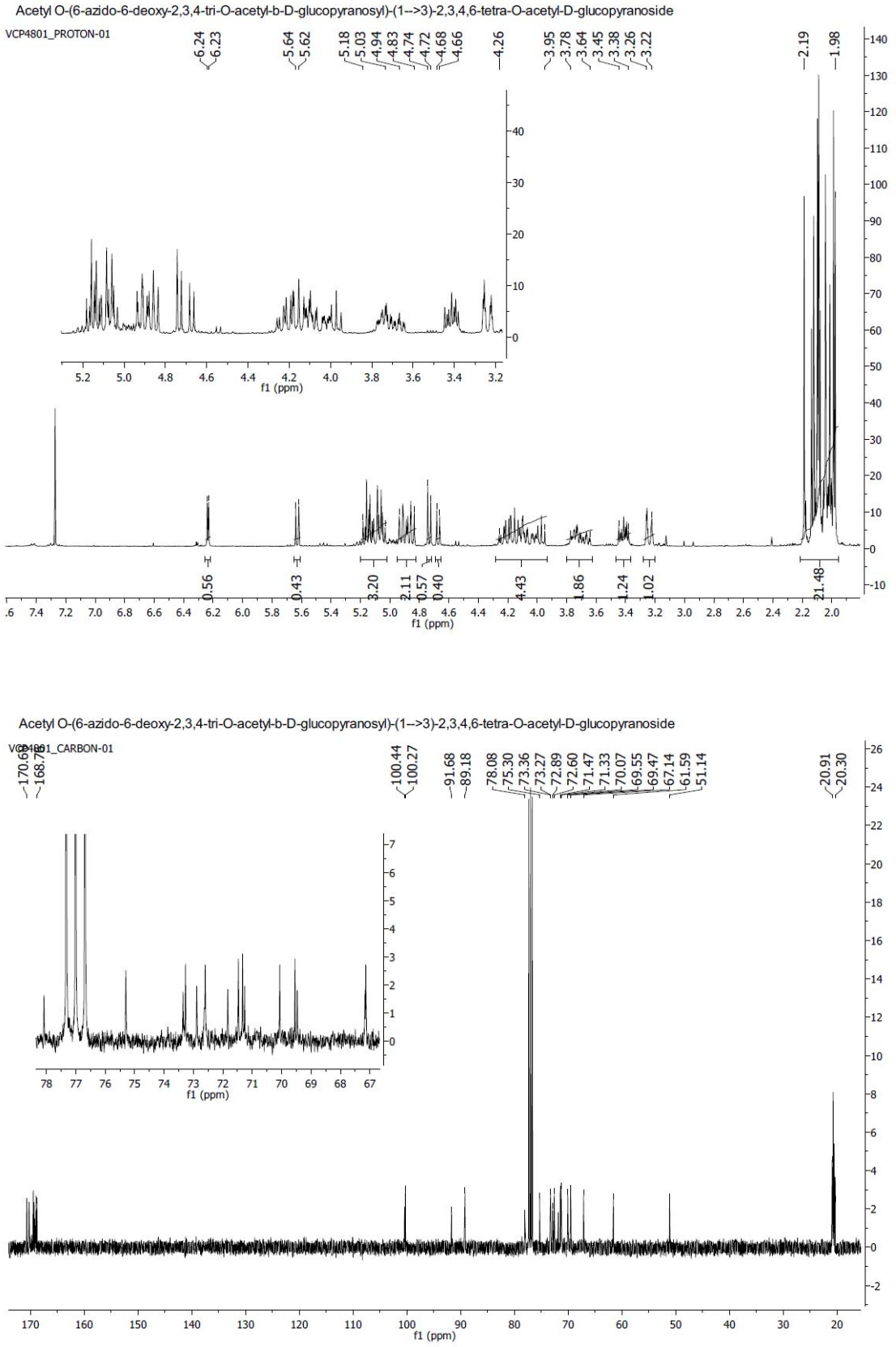

Figure A3. 27: ^{1}H NMR (above) and ^{13}C NMR (below) of acetyl *O*-(2,3,4-tri-*O*-acetyl-6-azido-6-deoxy-β-D-glucopyranosyl)-(1→3)-2,4,6-tri-*O*-acetyl-D-glucopyranose (**20**).

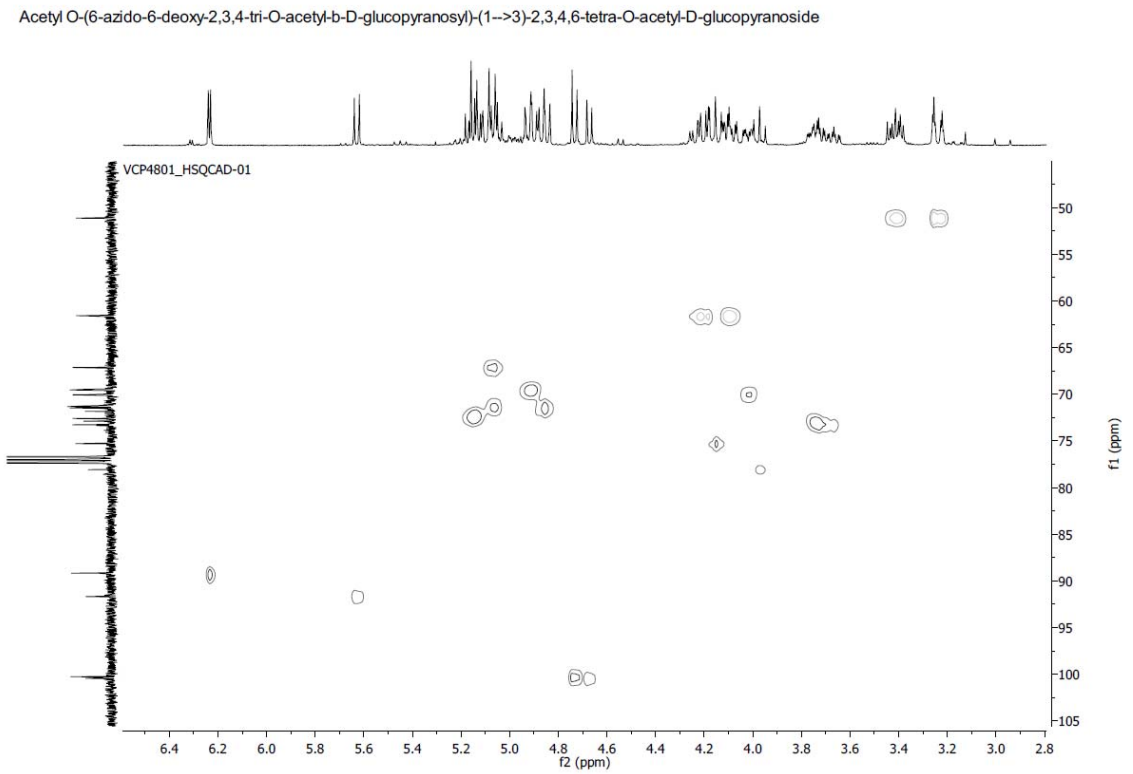

Figure A3. 28: HSQC of acetyl *O*-(2,3,4-tri-*O*-acetyl-6-azido-6-deoxy-β-D-glucopyranosyl)-(1→3)-2,4,6-tri-*O*-acetyl-D-glucopyranose (**20**).

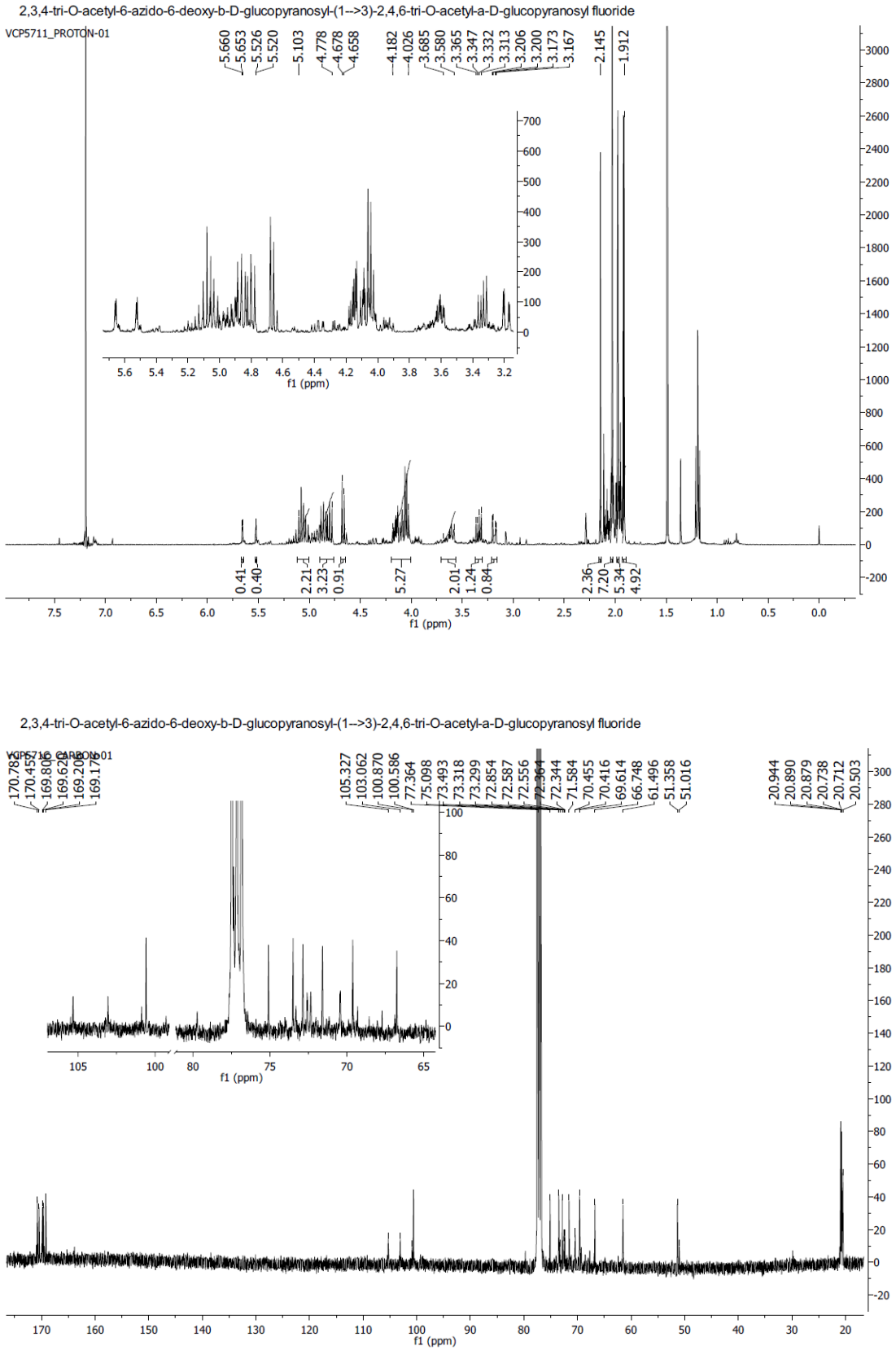

Figure A3. 29: ^{1}H NMR (above) and ^{13}C NMR (below) of 2,3,4-tri-*O*-acetyl-6-azido-6-deoxy-β-D-glucopyranosyl-(1→3)-2,4,6-tri-*O*-acetyl-α-D-glucopyranosyl fluoride **(21).**

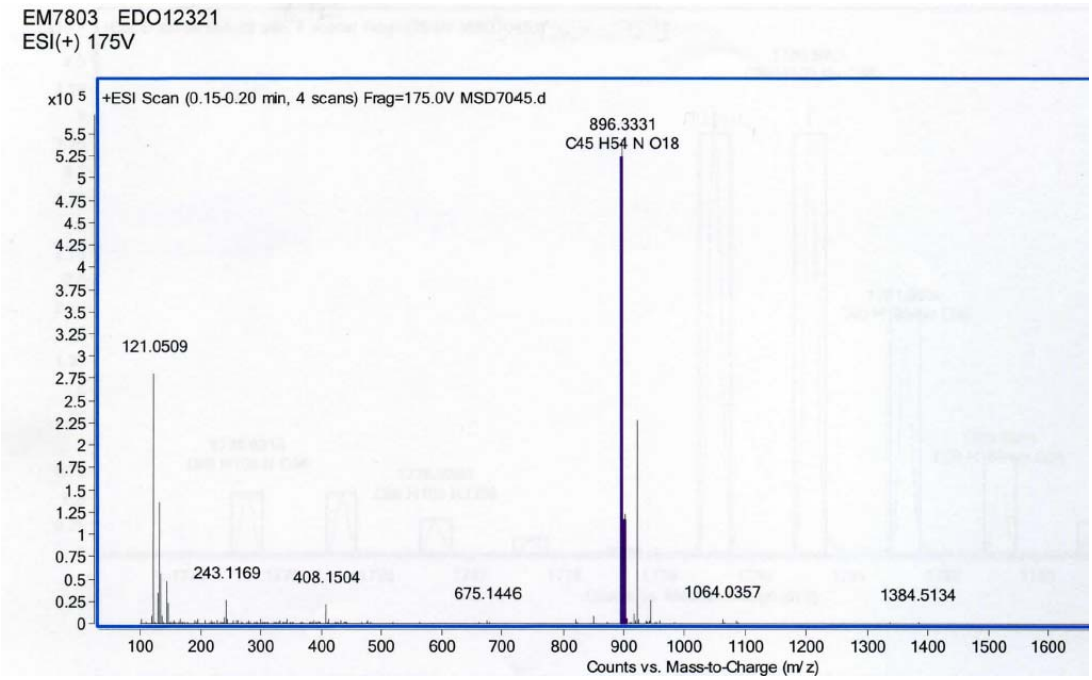

Figure A3. 30: MALDI of acetyl *O*-(2,3,4-tri-*O*-acetyl-6-*O*-trityl-β-D-glucopyranosyl)-(1→3)-2,4,6-tri-*O*-acetyl-D-glucopyranose (**17**).

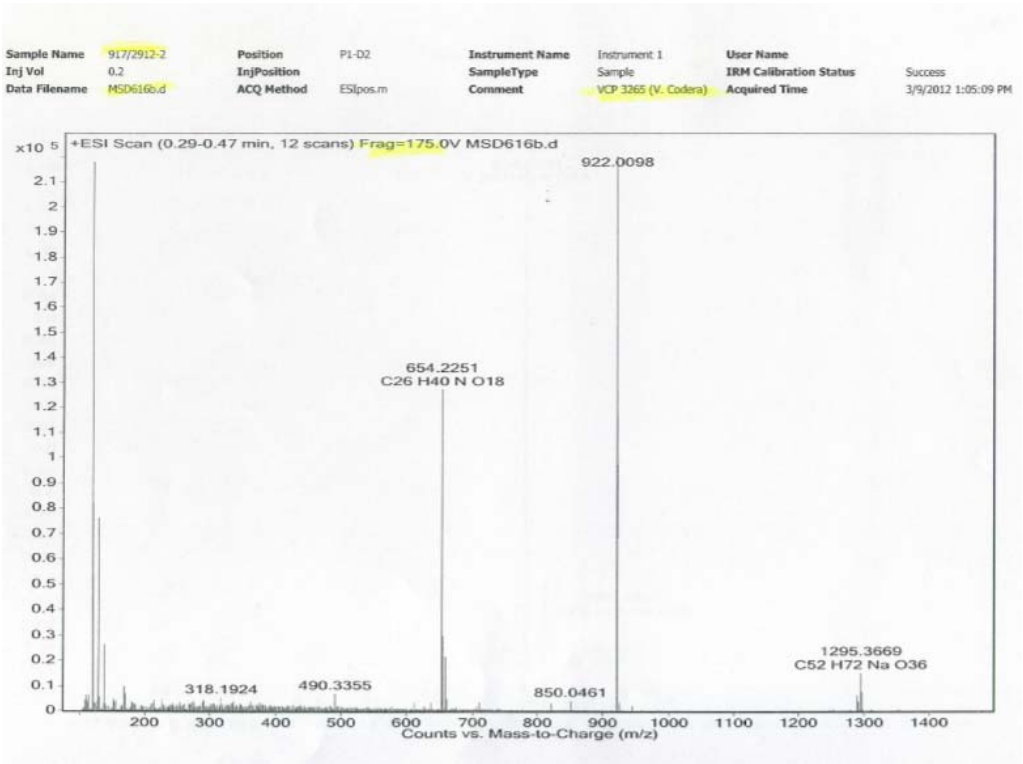

Figure A3. 31: MALDI of acetyl *O*-(2,3,4-tri-*O*-acetyl-β-D-glucopyranosyl)-(1→3)-2,4,6-tri-*O*-acetyl-D-glucopyranose (**18**).

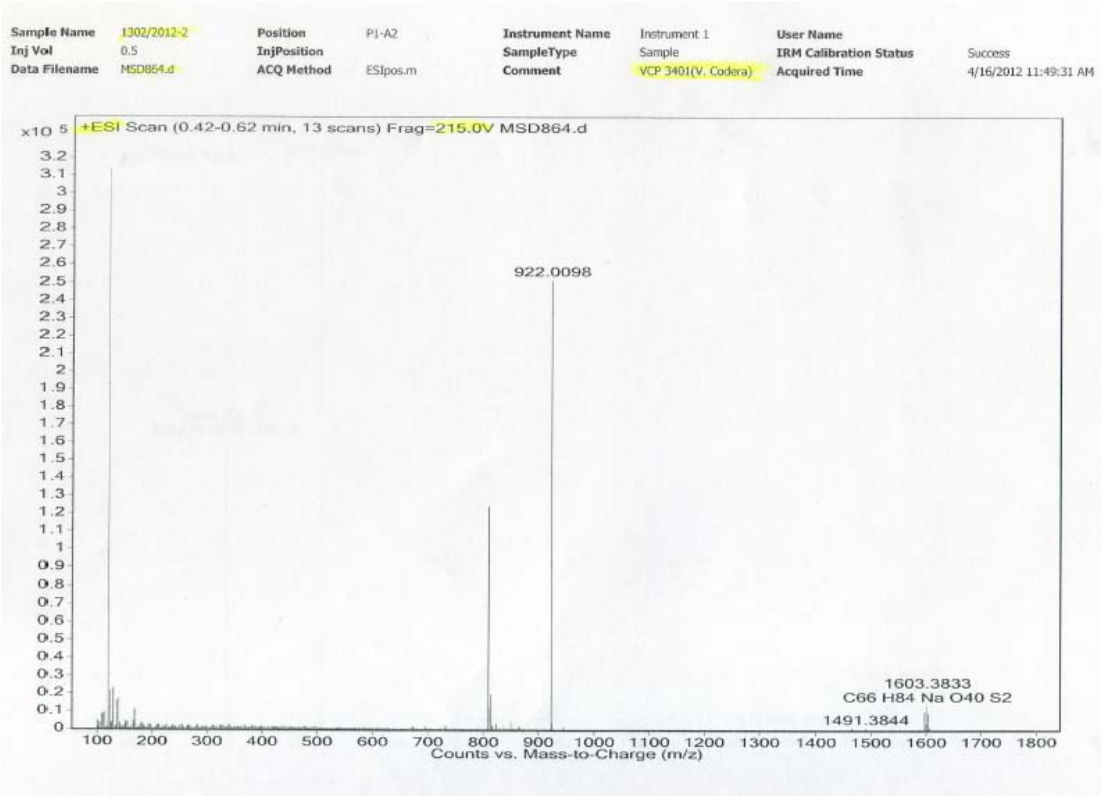

Figure A3. 32: MALDI of acetyl *O*-(2,3,4-tri-*O*-acetyl-6-*O*-tosyl-β-D-glucopyranosyl)-(1→3)-2,4,6-tri-*O*-acetyl-D-glucopyranose (**19i**).

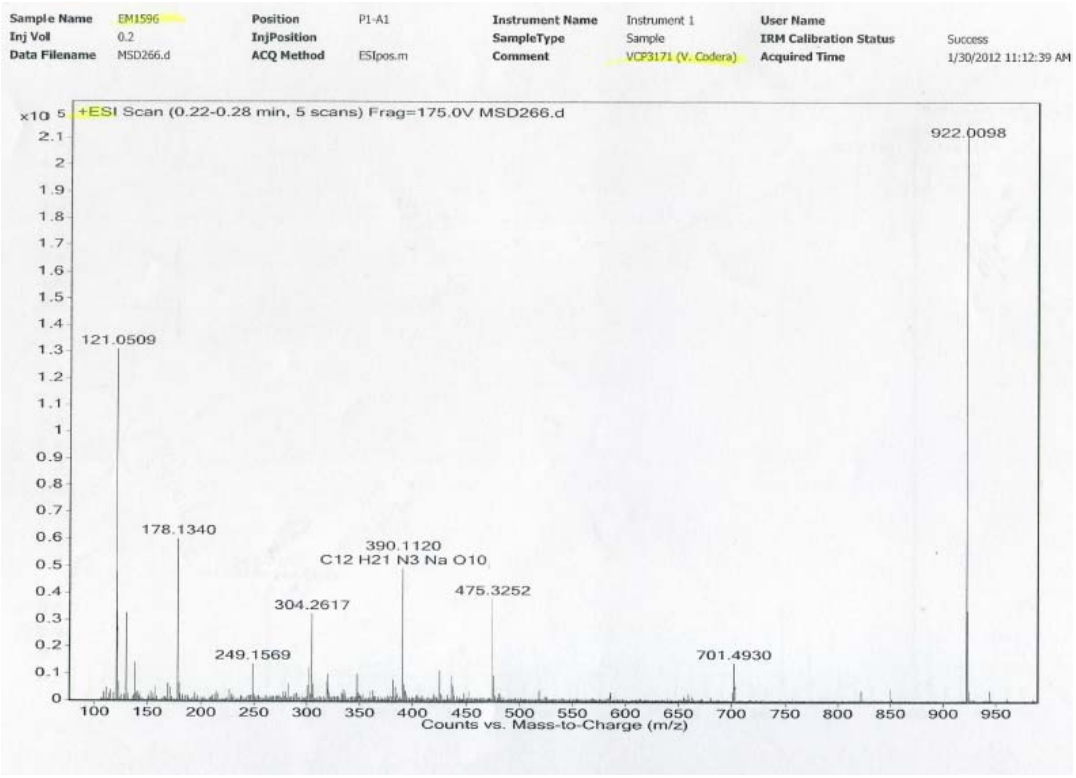

Figure A3. 33: MALDI of acetyl *O*-(2,3,4-tri-*O*-acetyl-6-azido-6-deoxy-β-D-glucopyranosyl)-(1→3)-2,4,6-tri-*O*-acetyl-D-glucopyranose (**20**).

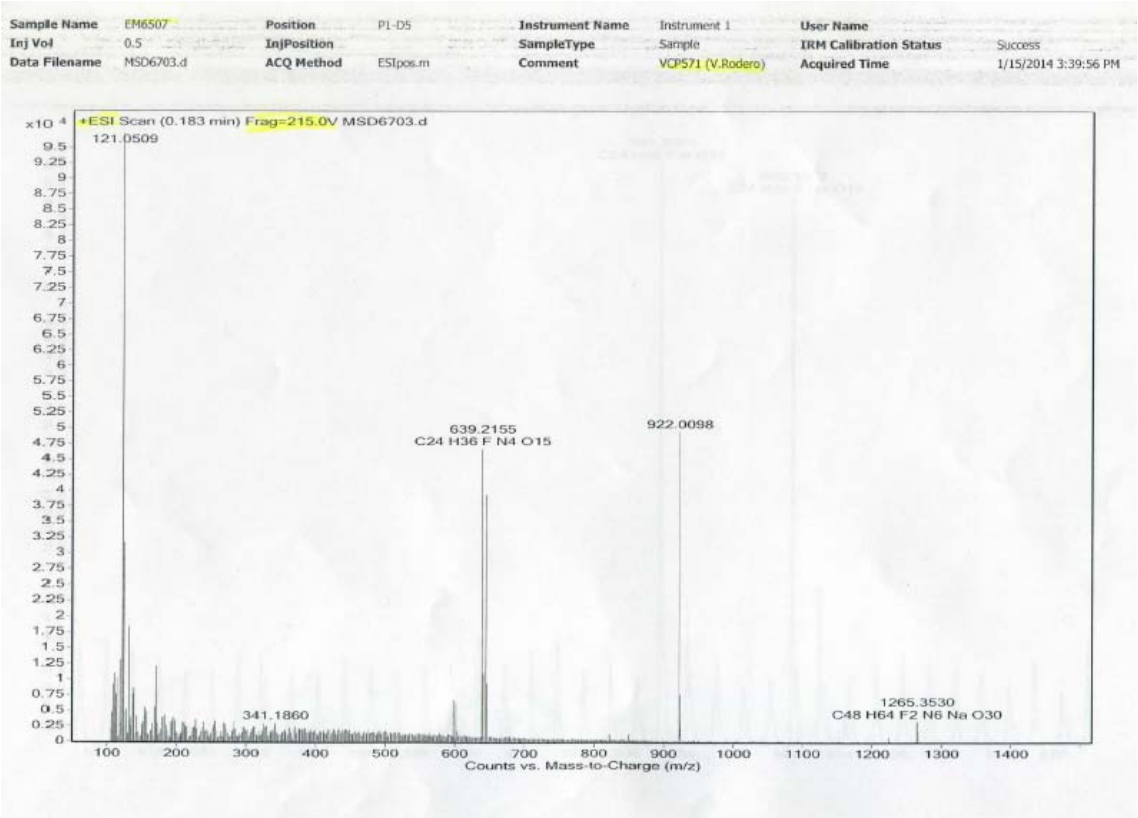

Figure A3. 34: MALDI of 2,3,4-tri-O-acetyl-6-azido-6-deoxy-β-D-glucopyranosyl-(1→3)-2,4,6-tri-O-acetyl-α-D-glucopyranosyl fluoride (**20**).

Product	Bands
Glc	Band 1
Glcβ3Glc	Band 2
L3	Band 3

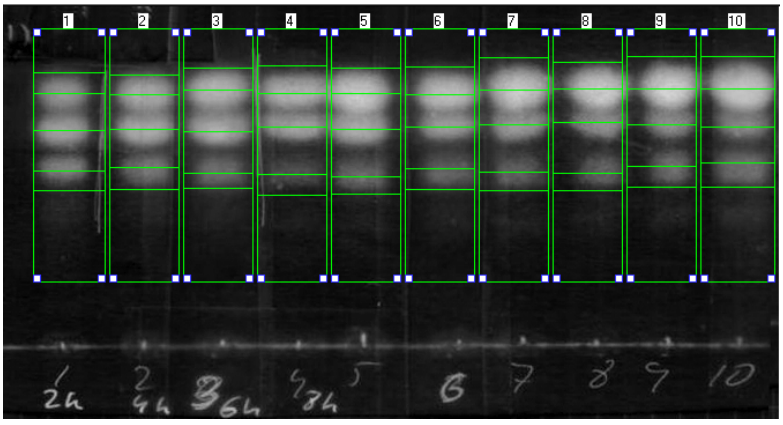

Lanes	Lane 1	Lane 2	Lane 3	Lane 4	Lane 5	Lane 6	Lane 7	Lane 8	Lane 9	Lane 10
Reaction time / h	2	4	6	8	10	12	14	16	18	20

Figure A3. 35: Degradation of curdlan. TLC (image). Each lane shows the percentage of glucose (band 1), laminaribiose Glcβ3Glc (band 2) and trisaccharides L3 (band 3) (Table left - above) present in the reaction at different times (table below).

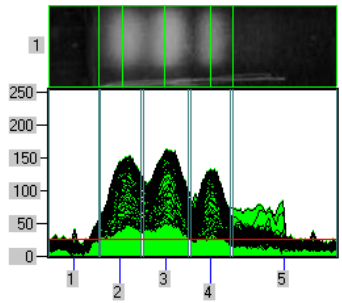

Lane 1 (2h)	Volume	Height	Area	R.F. values
Band 1 (Glc)	177414	152	2014	0.251
Band 2 (Glcβ3Glc)	220893	162	2205	0.400
Band 3 (L3)	136240	132	1868	0.563

Figure A3. 36: Degradation of curlan. Analysis of the lane (image). Every lane was analyzed with the program E-CAPT (table) to determine the volume of every band and the ratio between the different products.

Lane 1 (1.2 eq)	Volume	Height	Area	R.F. values
6'Tr	94647	120	1475	0.083
6Tr	75372	85	1722	0.473
Glcβ3Glc = L	308666	235	2664	0.834

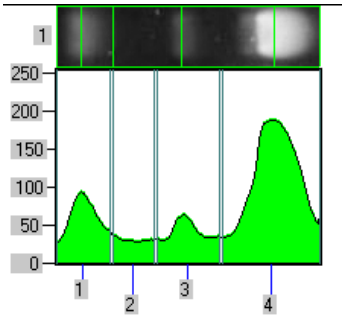

Figure A2. 37: Tritylation study. TLC (image). Different products 6'Tr (band 1), 6Tr (band 2) and residual L (band 3) are present in the reaction when it is performed with 1.2 eq of TrCl. The image was analyzed with the program E-CAPT (table) to determine the volume of every band and the ratio between the different products.

Product	Bands
6,6'-Tr = Di	Band 1
6'Tr	Band 2
6Tr	Band 3
L	Band 4

Lanes	Lane 1	Lane 2	Lane 3
TrCl eq	2.5	3.5	4.5

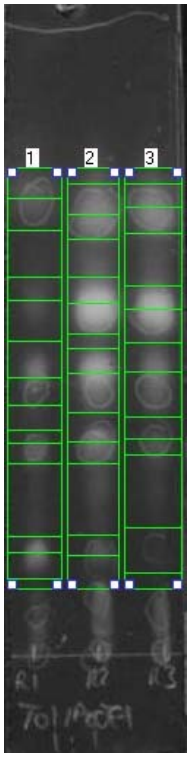

Figure A2. 38: TLC (image). Tritylation reaction. Each lane shows the percentage of Di (band 1), 6'Tr (band 2) 6Tr (band 3) and L (band 4) (Table left - above) present when different equivalents of TrCl are used in the reaction (table below).

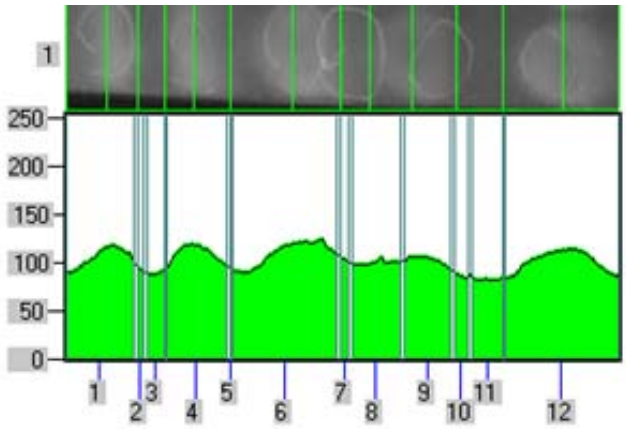

		Volume	Height	Area	R.F. values
Band 4	**Di**	208600	147	1856	0.227
Band 6	**6'Tr**	356208	168	3190	0.408
Band 9	**6Tr**	151756	141	1450	0.628
Band 12	**L**	357893	136	3479	0.904

Figure A3. 39: Tritylation study. TLC (image). Different products Di (band 4), 6'Tr (band 6), 6Tr (band 9) and residual L (band 12) are present in the reaction when it is performed with 3.0 eq of TrCl. The image was analyzed with the program E-CAPT (table) to determine the volume of every band and the ratio between the different products.

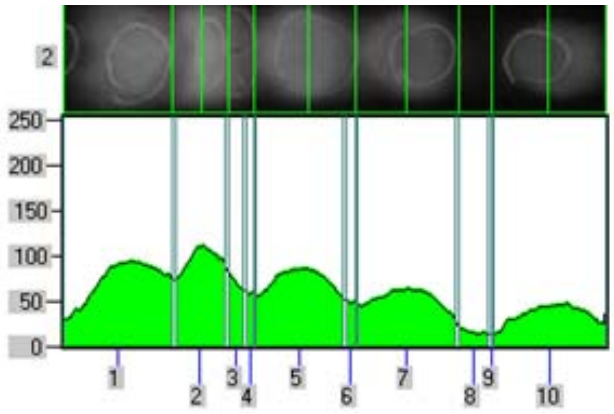

Lane 2 (4.25 eq)	Volume	Height	Area	R.F. values
Di	171693	144	1736	0.251
6'Tr	228910	121	3038	0.451
6Tr	186277	106	3410	0.634
L	143727	95	3905	0.898

Figure A3. 40: Tritylation study. TLC (image). Different products Di, 6'Tr, 6Tr and residual L are present in the reaction when it is performed with 4.25 eq of TrCl. The image was analyzed with the program E-CAPT (table) to determine the volume of every band and the ratio between the different products.

	Final concentration / mM	[Stock] / mM	Reaction volume / μL
Phosphate buffer 50 mM pH = 7.2	50	100.00	75.0
$CaCl_2$ 0.1 mM	0.1	10.00	3.0
[Glcβ3GlcαF] 1 mM	1	20.00	15.0
[GlcβPNP] 5 mM in phosphate buffer	5	10.00	150.0
E134S 0.1 μM	1.00E-04	1.26E-03	23.8
H_2O	-	-	33.2
Total volume	-		300

Table A2. 1: Translgycosylation reaction conditions (Glcβ3GlcαF + GlcβPNP). Study of subsites: control reaction.

t / min	A acceptor	Aproduct	Aa + Ap	[Product] / mM
0	5667.40	3.51	5670.91	3.10E-03
10	5550.20	89.46	5639.66	7.93E-02
21	5500.40	149.00	5649.40	1.32E-01
32	5112.60	183.10	5295.70	1.73E-01

Table A2. 2: Determination of v_o (Glcβ3GlcαF + GlcβPNP). Study of subsites: control reaction.

	Final concentration / mM	[Stock] / mM	Reaction volume / μL
Phosphate buffer 50 mM pH = 7.2	50	100.00	75.0
$CaCl_2$ 0.1 mM	0.1	10.00	3.0
[Glcβ3GlcαF] 1 mM	1	20.00	15.0
[$6N_3$-GlcβPNP] 5 mM in phosphate buffer	5	10.00	150.0
E134S 0,1 μM	1.00E-04	1.26E-03	23.8
H_2O	-	-	33.2
TOTAL	-		300

Table A2. 3: Translgycosylation reaction conditions (Glcβ3GlcαF + $6N_3$-GlcβPNP). Study of subsite +1.

t / min	Aacceptor	Aproduct	Aa + Ap	[Product] / mM
0	5449.42	4.37	5453.79	4.01E-03
22	5418.41	181.26	5599.67	1.62E-01
51	5264.02	357.39	5621.41	3.18E-01
81	5065.26	483.28	5548.54	4.35E-01

Table A2. 4: Determination of v_o (Glcβ3GlcαF + $6N_3$-GlcβPNP). Study of subsite +1.

	Final concentration / mM	[Stock] / mM	Reaction volume / μL
Phosphate buffer 50 mM pH = 7.2	50	100.00	112.5
$CaCl_2$ 0.1 mM	0.1	10.00	3.0
[Glcβ3GlcαF] 1 mM	1	20.00	15.0
[GlcβPNP] 5 mM in phosphate buffer	5	20.00	75.0
E134S 0.1 μM	2.57E-03	1.10E-02	70.1
H_2O	-	-	24.4
TOTAL	-		300

Table A2. 5: Translgycosylation reaction conditions (Glcβ3GlcαF + GlcβPNP). Study of subsites: control reaction.

t / min	Aacceptor	Aproduct	Aa + Ap	[Product] / mM
0.40	5555.10	34.80	5589.90	3.11E-02
3.45	5123.70	233.80	5357.50	2.18E-01
7.43	4900.50	368.50	5269.00	3.50E-01
12.90	4873.10	492.10	5365.20	4.59E-01
20.45	4664.50	576.40	5240.90	5.50E-01

Table A2. 6: Determination of v_o (Glcβ3GlcαF + GlcβPNP). Study of subsites: control reaction.

	Final concentration / mM	[Stock] / mM	Reaction volume / μL
Phosphate buffer 50 mM pH = 7.2	50	100.00	112.5
$CaCl_2$ 0.1 mM	0.1	10.00	3.0
[Glcβ3GlcαF] 1 mM	1	10.80	27.8
[$6N_3$-GlcβPNP] 5 mM in phosphate buffer	5	20.00	75.0
E134S 0.1 μM	2.57E-03	1.10E-02	70.1
H_2O	-		11.6
TOTAL	-		300

Table A2. 7: Translgycosylation reaction conditions ($6N_3$-Glcβ3GlcαF + GlcβPNP). Study of subsite -2

t / min	Aacceptor	Aproduct	Aa + Ap	[Product] / mM
0.42	5736.30	0.00	5736.30	0.00E+00
3.35	5653.80	1.20	5655.00	1.06E-03
7.32	5610.10	1.50	5611.60	1.34E-03
12.87	5793.50	2.10	5795.60	1.81E-03
20.20	5599.30	2.50	5601.80	2.23E-03

Table A2. 8: Determination of v_o ($6N_3$-Glcβ3GlcαF + GlcβPNP). Study of subsite -2.

Lane 1 (2h)	Volume	%
Band 1 (Glc)	177414	33%
Band 2 (Glcβ3Glc)	220893	41%
Band 3 (L3)	136240	25%
TOTAL	534547	100%

Table A2. 9: Degradation of curdlan. Analysis lane 1 (t = 2 hours).

Lane 2 (4h)	Volume	%
Band 1 (Glc)	230870	39%
Band 2 (Glcβ3Glc)	224810	38%
Band 3 (L3)	132151	22%
TOTAL	587831	100%

Table A2. 10: Degradation of curdlan. Analysis lane 2 (t = 4 hours).

Lane 3 (6h)	Volume	%
Band 1 (Glc)	267747	41%
Band 2 (Glcβ3Glc)	245493	38%
Band 3 (L3)	133304	21%
TOTAL	646544	100%

Table A2. 11: Degradation of curdlan. Analysis lane 3 (t = 6 hours).

Lane 4 (8h)	Volume	%
Band 1 (Glc)	283540	45%
Band 2 (Glcβ3Glc)	230160	36%
Band 3 (L3)	121924	19%
TOTAL	635624	100%

Table A2. 12: Degradation of curdlan. Analysis lane 4 (t = 8 hours).

Lane 5 (10h)	Volume	%
Band 1 (Glc)	315790	47%
Band 2 (Glcβ3Glc)	219899	33%
Band 3 (L3)	138734	21%
TOTAL	674423	100%

Table A2. 13: Degradation of curdlan. Analysis lane 5 (t = 10 hours).

Lane 6 (12h)	Volume	%
Band 1 (Glc)	274217	46%
Band 2 (Glcβ3Glc)	191419	32%
Band 3 (L3)	133660	22%
TOTAL	599296	100%

Table A2. 14: Degradation of curdlan. Analysis lane 6 (t = 12 hours).

Lane 7 (14h)	Volume	%
Band 1 (Glc)	347061	53%
Band 2 (Glcβ3Glc)	181032	27%
Band 3 (L3)	131298	20%
TOTAL	659391	100%

Table A2. 15: Degradation of curdlan. Analysis lane 7 (t = 14 hours).

Lane 8 (16h)	Volume	%
Band 1 (Glc)	307780	53%
Band 2 (Glcβ3Glc)	159262	28%
Band 3 (L3)	108580	19%
TOTAL	575622	100%

Table A2. 16: Degradation of curdlan. Analysis lane 8 (t = 16 hours).

Lane 9 (18h)	Volume	%
Band 1 (Glc)	336223	56%
Band 2 (Glcβ3Glc)	144223	24%
Band 3 (L3)	124556	21%
TOTAL	605002	100%

Table A2. 17: Degradation of curdlan. Analysis lane 9 (t = 18 hours).

Lane 10 (20h)	Volume	%
Band 1 (Glc)	377267	56%
Band 2 (Glcβ3Glc)	142294	21%
Band 3 (L3)	155577	23%
TOTAL	675138	100%

Table A2. 18: Degradation of curdlan. Analysis lane 10 (t = 20 hours).

Time / h	% Monosaccharide	% Disaccharide	% Trisaccharide
2	33	41	25
4	39	38	22
6	41	38	21
8	45	36	19
10	47	33	21
12	46	32	22
14	53	27	20
16	53	28	19
18	56	24	21
20	56	21	23

Table A2. 19: Degradation of curdlan. Ratio of the different products at different times.

Lane 1 (2.5 eq)	Volume	Height	Area	R.F. values
Di	86832	87	1394	0.312
6'Tr	94749	118	1341	0.498
6Tr	51633	104	792	0.656
L	62458	123	960	0.919

Table A2. 20: Tritylation study. Analysis lane 2.5 eq TrCl.

Lane 2 (3.5 eq)	Volume	Height	Area	R.F. values
Di	167661	186	1332	0.319
6'Tr	148750	166	1512	0.488
6Tr	79228	135	972	0.653
L	75380	99	1309	0.926

Table A2. 21: Tritylation study. Analysis lane 3.5 eq TrCl.

Lane 3 (4.5 eq)	Volume	Height	Area	R.F. values
Di	160388	178	1480	0.333
6'Tr	146462	126	1960	0.484
6Tr	26434	82	439	0.646
L	59281	69	1229	0.860

Table A2. 22: Tritylation study. Analysis lane 4.5 eq TrCl.

TrCl equiv.	M *vs* M+D+L	L *vs* M+D+L	D *vs* M+D+L
1.2	0.36	0.64	0.00
2.0	0.42	0.35	0.23
2.5	0.50	0.21	0.29
3.0	0.47	0.33	0.19
3.5	0.48	0.16	0.36
4.0	0.51	0.27	0.21
4.25	0.57	0.20	0.24
4.50	0.44	0.15	0.41
4.51	0.43	0.17	0.27
5.5	0.30	0.00	0.70
5.8	0.46	0.46	0.08

Table A2. 23: Tritylation study. Study of maximum formation of monotritylated product *vs* equivalents of TrCl.

TrCl (equivalents)	1.2	2.0	2.5	3.0	3.5	4.25	4.5	4.51	5.5
Glcβ3Glc	0.64	0.35	0.21	0.33	0.16	0.20	0.15	0.20	0.00
6'Tr	0.20	0.31	0.32	0.33	0.32	0.31	0.37	0.27	0.23
6Tr	0.16	0.11	0.17	0.14	0.17	0.25	0.07	0.22	0.07
Dityrityl	0.00	0.23	0.29	0.19	0.36	0.24	0.41	0.31	0.70

Table A2. 24: Tritylation study. Different ratios of products are obtained when the reaction is performed with different equivalents of TrCl.

CHAPTER 4: SYNTHESIS OF ALTERNATING 6-AZIDO-6-DEOXYCELLULOSE AND FURTHER DERIVATIZATIONS

4.1. INTRODUCTION

Synthetic aminopolysaccharide mimetics of natural chitosans have attracted recent interest in materials science to modify and improve the physicochemical and biological properties of chitosan-based biomaterials. Chitosan consists in a linear heteropolysaccharide of β-1,4-linked *N*-acetylglucosamine (GlcNAc) and glucosamine ($GlcNH_2$) units and it is obtained by chemical or enzymatic partial de-*N*-acetylation of chitin, with variable degrees of acetylation and random distribution of cationic glucosaminyl units along the polysaccharide chain.[1] The cationic nature of chitosans makes them versatile materials with a broad range of applications.[2,3,4,5,6] They are biocompatible and possess mucoadhesive**,** bacteriostatic and hemostatic properties. The positively charged chitosans are able to bind and encapsulate anionic compounds such as proteins and DNA, and interact with negatively charged compounds found in mucus and on cell surfaces, which improves the cell adhesion and proliferation properties of chitosan-based scaffolds. However, applications in drug and gene delivery systems suffer from low transfection efficiency.[7]

With the aim of mimicking and improving the biomedical properties of chitosans, different procedures to modify neutral polysaccharides have been reported.[8] Modifications of cellulose, laminarin, curdlan, and other natural polysaccharides are performed by chemical procedures, *i.e.* by functionalizing the C-6 positions with amino-substituted side chains or azido groups than can be reduced to amines or reacted by "Click" chemistry. The properties of these functionalized polysaccharides will depend on their molecular weight and degree of substitution. However, they are polydisperse with random distribution of the functional groups, requiring new methodologies to produce defined and reproducible polymeric materials.

Sequence control is one of the great remaining problems in polysaccharide synthesis. Nature creates polysaccharides often with a very high degree of control over sequence leading to highly specific biological activity, for example the active sequences of glycosaminoglycans heparin[9] and chondroitin sulfate[10] that are vital to their interactions with proteins, governing their ability to prevent thrombosis. Laborious, multi-step, low-yielding chemical syntheses have been necessary to produce even oligosaccharides of controlled sequence.[11]

Enzymatic synthesis opens up access to regular and homogeneous polysaccharides by glycosidase-catalyzed polymerization of simple glycosyl donors with regio- and stereospecificity of the newly-formed glycosidic linkages. Artificial cellulose was the first example produced by cellulase-catalyzed polymerization of β-cellobiosyl fluoride in acetonitrile/acetate buffer.[12] Few other polysaccharides such as amylose, xylan, mixed-linked β-glucans, alternating cellulose-chitin and cellulose-xylan hybrids, have been prepared by kinetically-controlled

transglycosylation using retaining glycosidases,[13,14] with moderate yields due to the intrinsic hydrolase activity of the enzymes. More recently, glycosynthases have proved their efficiency for the enzymatic synthesis of oligosaccharides, and glycoconjugates.

As it was already commented in Chapter 3 of this work, Fort *et al.*[15] explored the ability of the glycosynthase derived from the cellulase Cel7B from *Humicola insolens* (*Hi*Cel7B E197A) to accept different functionalized cellobiosyl donors. The enzyme was able to accept α-cellobiosyl fluorides that had functionalities at C-6' position such as bromine, amino and thioglucosyl groups. This particular glycosynthase offers a broad range of synthetic applications since it has also been employed for the synthesis of xyloglucan oligosaccharides.[16] We envisioned the glycosynthase technology as a potential tool for the straightforward synthesis of functionalized polysaccharides: simple glycosyl donors prepared with the specific modifications can be accepted and polymerized by the glycosynthase enzyme to produce modified polysaccharides. The glycosynthase approach could provide a new generation of polysaccharides with a functionalization pattern and polymerization degree different to those obtained by chemical modification routes.

We here address a powerful approach, whereby enzyme-catalyzed polymerization of properly modified building blocks is introduced as a simple route affording polysaccharides with controlled sequence and functionalization pattern (Figure 4. 1).

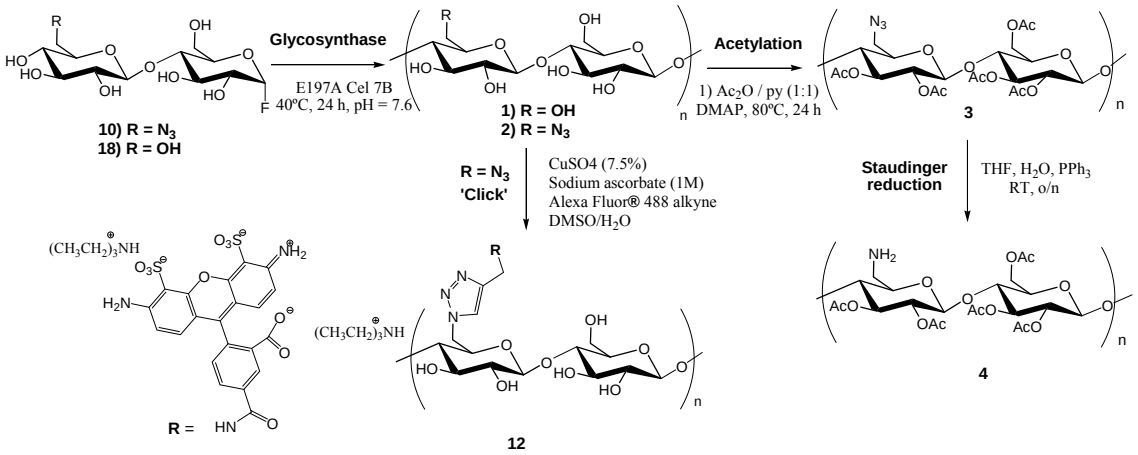

Figure 4. 1: Glycosynthase-catalyzed polymerization to produce cellulose derivatives (polymers **1 – 4**) and click chemistry with Alexa Fluor 488 alkyne (synthesis of **12**).

Targeting cellulose as a versatile scaffold for novel biomaterials, we describe the preparation of a perfectly alternating polysaccharide with repeat unit 6'-azido-6'-deoxycellobiose by a glycosynthase-catalyzed polymerization using the *H. insolens* cellulase Cel7B E197A mutant, and its further functionalization to give novel modified cellulose derivatives with a regular substitution pattern.

4.2. EXPERIMENTAL

4.2.1. Materials

1,6-anhydro-β-D-cellobiose (Carbosynth) was co-evaporated with toluene and dried under vacuum at room temperature overnight prior to use. *N*-bromosuccinimide (NBS, Sigma) was recrystallized from boiling water and dried for two days under reduced pressure over anhydrous calcium chloride. Triphenylphosphine (PPh_3, Sigma) was recrystallized from boiling ethanol and dried overnight under reduced pressure over anhydrous calcium chloride. Dimethylacetamide (DMAc, Fisher Scientific) was kept over 4 Å molecular sieves and stored under dry nitrogen after the first use.

4.2.2. Synthesis of substrates

*4.2.2.1. 2,3,4-Tri-O-acetyl-6-bromo-6-deoxy-β-D-glucopyranosyl-(1→4)-1,6-anhydro-2,3-di-O-acetyl-β-D-glucopyranose (**6**)*

1,6-anhydrous cellobiose (**5**) (2.50 g, 7.71 mmol) was dissolved in 100 mL DMAc under nitrogen. PPh_3 (7.88 g, 30.84 mmol, 4 eq) and NBS (13.80 g, 30.84 mmol, 4 eq) were dissolved each one in 25 mL of dry DMAc under nitrogen. The PPh_3 solution was added dropwise to the solution of **5**, followed by the dropwise addition of the NBS solution. The reaction solution was heated to 70ºC under nitrogen. After 1 h, 7.30 mL (7.89 g, 77.39 mmol, 10 eq) of acetic anhydride were slowly added to the reaction, and the solution was stirred overnight at 70ºC.

The product was isolated by adding the reaction mixture slowly to 400 mL of a 50:50 (v/v) mixture of methanol and deionized water. Methanol was removed and extractions were done with EtOAc and water. The organic phase was dried with $MgSO_4$ and concentrated. The product of interest **6** (890 mg, 1.49 mmol) was isolated in 20% yield through flash chromatography using a gradient of cyclohexane / EtOAc 1.5:1 (v/v) → (1 : 1) → (1 : 1.5).

^{1}H NMR ($CDCl_3$, 400 MHz) δ 5.45 (s, 1H, H-1^{I}), 5.23 (t, 1H, $J_{2,3} = J_{3,4}$ =9.4 Hz, H-3^{I}), 5.18 (m, 1H, H-3^{II}), 5.04 (m, 2H, H-2^{II}, H4^{II}), 4.94 (d, 1H, $J_{1,2}$ = 8.1 Hz, H-1^{II}), 4.61 (m, 2H, H-2^{I}, H-5^{I}), 3.97 (dd, 1H, $J_{5,6}$ = 1.1 Hz, $J_{a,b}$ = 7.7 Hz, H-6^{Ia}), 3.81 (m, 2H, H-5^{II}, H-6^{Ib}), 3.57 (s, 1H, H-4^{I}), 3.47 (dd, 1H, $J_{5,6}$ = 2.7 Hz, $J_{a\,b}$ = 11.4 Hz, H-6^{IIa}), 3.37 (dd, 1H, $J_{5,6}$ = 6.6 Hz, $J_{a,b}$ = 11.4 H-6^{IIb}), 2.17 – 1.01 (m, 15H, CH_3).

*4.2.2.2. 2,3,4-Tri-O-acetyl-6-bromo-6-deoxy-β-D-glucopyranosyl-(1→4)-1,2,3,6-tetra-O-acetyl-β-D-glucopyranose (**7**)*

A catalytic amount of triethylsilyl triflate (12 μL) was added, dropwise, to a solution of **6** (947 mg, 1.58 mmol) in acetic anhydride (12 mL) cooled at 0 ºC. The mixture was stirred at 0 ºC for 30 minutes. Then, saturated aqueous $NaHCO_3$ was added to quench the reaction and the products were extracted with DCM. The organic layers were dried, concentrated and coevaporated with toluene[1]. HBr (30% w/v in AcOH, 3.2 mL) was added to the crude anomeric mixture in DCM (6.4 mL) at 0 ºC. After stirring at 0 ºC for 30 minutes and then at room temperature for an additional hour, the reaction mixture was diluted with DCM, washed with ice-cold water and ice-cold saturated aqueous $NaHCO_3$ (3x), dried and concentrated. The resulting bromide and AgOAc (646 mg, 1.84 mmol) in a mixture of Ac_2O/AcOH (16 mL, 1:1 v/v) were stirred in the dark overnight at room temperature. The mixture was diluted with DCM and filtered through a Celite bed, and the filtrate was washed with saturated aqueous $NaHCO_3$ (3x), dried, and concentrated. Filtration through silica gel (EtOAc/petroleum ether 7:3 v/v) gives **7** (1.22 g, 1.67 mmol), 99 % three steps).

^{1}H NMR ($CDCl_3$, 400 MHz) δ 5.67 (d, 1H, $J_{1,2}$ = 8.2 Hz, H-1^{I}), 5.26 (t, 1H, $J_{1,2}$ = 9.2 Hz, H-3^{I}), 5.15 (t, 1H, $J_{2,3}$ = 9.3 Hz, H-3^{II}), 5.07 – 4.91 (m, 3H, H-2^{I}, H-2^{II}, H-4^{II}) 4.54 (d, 1H, $J_{1,2}$ = 7.8 Hz, H-1^{II}), 4.49 (dd, 1H, $J_{5,6}$ = 12.3 Hz, $J_{a,b}$ = 12.2 Hz, H-6^{Ia}), 4.14 (dd, 1H, $J_{5,6}$ = 4.7 Hz, $J_{a,b}$ = 12.2 Hz, H-6^{Ib}), 3.88 (t, 1H, $J_{2,3}$ = $J_{3,4}$ = 9 Hz, H-4^{I}), 3.79 – 3.63 (m, 2H, H-5^{I}, H-5^{II}), 3.47 (dd, 1H, $J_{5,6}$ = 2.7 Hz, $J_{a,b}$ = 11.4 Hz, H-6^{IIa}), 3.32 (dd, 1H, $J_{5,6}$ = 7 Hz, $J_{a,b}$ = 11.4 Hz, H-6^{IIb}), 2.30 – 1.98 (m, 21H, CH_3).

^{13}C NMR ($CDCl_3$, 100 MHz) δ 170.4-168.9 (CO), 100.1 (C-1^{II}), 91.8 (C-1^{I}), 75.5 (C-4^{I}), 73.8, 73.7, 72.8, 72.2, 71.8, 70.9, 70.7 (C-2^{I,II}, C-3^{I,II}, C-5^{I,II}, C-4^{II}), 61.7 (C-6^{I}), 30.4 (C-6^{II}), 21 -20.7 (CH_3).

*4.2.2.3. Acetyl 2,3,4-tri-O-acetyl-6-azido-6-deoxy-β-D-glucopyranosyl-(1→4)-2,3,6-tri-O-acetyl-D-glucopyranosyde (**8a**).*

Compound **7** (35 mg, 0.053 mmol) was dissolved in DMAc (1 mL) which contained sodium azide (15 mg, 0.230 mmol, 4.5 eq). The mixture was heated to 80 °C for 1 h and then concentrated *in vacuo*. The residue was dissolved in DCM, and the organic layer was washed with water, dried

[1] This reaction does not work in the presence of PPh_3. Compound **6** must be completely pure.

and concentrated obtaining the crude **8a**, consisting of a mixture of α/β anomers (70:30) 6'-azido-6'-deoxycellobiose determined by TLC and NMR.

*4.2.2.4. 2,3,4-Tri-O-acetyl-6-bromo-6-deoxy-β-D-glucopyranosyl-(1→4)-2,3,6-tri-O-acetyl-α-D-glucopyranosyl fluoride (**8b**).*

A solution of **7** (75 mg, 0.107 mmol) in HF-pyridine (1 mL, 7:3 v/v, 3.5 mmol HF, 326 eq HF per disaccharide) was stirred at 0 °C for 1.5 h in a plastic vial. The mixture was diluted with DCM (2 mL) and poured into ice-cold aqueous NH_3 3M (5 mL); the organic layer containing **8b** was washed with saturated aqueous $NaHCO_3$ (3×), dried and concentrated.

^{1}H NMR ($CDCl_3$, 400 MHz) δ 5.69 (dd, 1H, $J_{1,2}$ = 2.8 Hz, $J_{1,F}$ = 52.8 Hz, H-1^I), 5.47 (t, 1H, $J_{2,3}$ = $J_{3,4}$ = 9.6 Hz, H-3^I), 5.17 (t, 1H, $J_{2,3}$ = $J_{3,4}$ = 9.6 Hz, H-3^{II}), 4.99 – 4.84 (m, 3H, H-2^I, H-2^{II}, H-4^{II}), 4.59 – 4.55 (m, 2H, H-1^{II}, H-6^{Ia}), 4.19 – 4.12 (m, 2H, H-6^{Ib}, H-5^I), 3.90 (t, 1H, $J_{4,5}$ = 9.7 Hz, H-4^I), 3.69 – 3.65 (m, 1H, H-5^{II}), 3.49 – 3.46 (m, 1H, H-6^{IIa}), 3.35 – 3.29 (m, 1H, H-6^{IIb}), 2.15 – 1.99 (m, 18H, CH_3).

*4.2.2.5. 2,3,4-Tri-O-acetyl-6-azido-6-deoxy-β-D-glucopyranosyl-(1→4)-2,3,6-tri-O-acetyl-α-D-glucopyranosyl fluoride (**9**).*

Compound **8b** (524 mg, 0.813 mmol) was dissolved in DMAc (17 mL) which contained sodium azide (267 mg, 5.14 mmol, 6 eq). The mixture was heated to 80 °C for 1 h and then concentrated *in vacuo*. The residue was dissolved in DCM, and the organic layer was washed with water, dried and concentrated. Purification by flash chromatography (EtOAc – cyclohexane 1:1.5 v/v) yielded compound **9** (282 mg, 0.454 mmol) in 56%, two steps.

^{1}H NMR ($CDCl_3$, 400 MHz) δ 5.68 (dd, 1H, $J_{1,2}$ = 2.8 Hz, $J_{1,F}$ = 53.1 Hz, H-1^I), 5.47 (t, 1H, $J_{2,3}$ = $J_{3,4}$ = 9.6 Hz, H-3^I), 5.17 (t, 1H, $J_{2,3}$ = $J_{3,4}$ = 9.6 Hz, H-3^{II}), 4.98 – 4.81 (m, 3H, H-2^I, H-2^{II}, H-4^{II}), 4.60 (d, 1H, $J_{1,2}$ = 8.0 Hz, H-1^{II}), 4.59 – 4.55 (m, 1H, H-6^{Ia}), 4.15 (dd, 1H, $J_{5,6}$ = 4.1 Hz, $J_{a,b}$ = 12.2 Hz, H-6^{Ib}), 4.11 – 4.07 (m, 1H, H-5^I), 3.90 (t, 1H, J = 9.7 Hz, H-4^I), 3.66 – 3.61 (m, 1H, H-5^{II}), 3.39 – 3.36 (m, 2H, H-6^{IIa}, H-6^{IIb}), 2.15 – 1.99 (m, 18H, CH_3).

*4.2.2.6. 6-azido-6-deoxy-β-D-glucopyranosyl-(1→4)-α-D-glucopyranosyl fluoride (6'N_3-CelαF) (**10**).*

Compound **9** (329 mg, 0.529 mmol) was dissolved in 15 mL MeOH (30 mg/ mL). Then, 28 μL of 5.4 M solution of NaOMe in MeOH were added and left under stirring overnight at room temperature. The pH should be basic after the addition of NaOMe, otherwise, more salt should be added. Amberlite® IR-120 acidic resin was added to neutralize the reaction mixture. The resin

was removed by filtration, and the filtrate concentrated. Freeze-dried compound **10** (126 mg, 0.341 mmol) was obtained in 65% yield.

^{1}H NMR (MeOD, 400 MHz) δ 5.59 (dd, 1H, $J_{1,2}$ = 2.8 Hz, $J_{1,F}$ = 53.6 Hz, H-1^{I}), 4.50 (d, 1H, $J_{1,2}$ = 7.8 Hz, H-1^{II}), 3.99 – 3.50 (m, 9H, H3^{I,II}, H2^{I,II}, H4^{I,II}, H5^{I,II}, H6^{Ia}), 3.44 – 3.38 (m, 2H, H-6^{Ib}, H-6^{IIa}) , 3.29 (dd, 1H, $J_{5,6}$ = 7.9 Hz, $J_{a,b}$ = 8.9 Hz, H-6^{IIb}).

^{13}C NMR (MeOD, 100 MHz) δ 108.7 (d, $J_{C,F}$ = 224 Hz, C-1^{I}), 104.6 (C-1^{II}), 79.8, 77.6, 76.3, 74.9, 74.3, 74.3 (d, $J_{C,F}$ = 4 Hz, C-5^{I}), 73.0 (d, $J_{C,F}$ = 24 Hz, C-2^{I}), 72.7, 71.9, 61.1 (C-6^{I}), 52.7 (C-6^{II}).

*4.2.2.7. Cellobiosyl fluoride donor (CelαF) (**18**)*

CelαF is prepared as previously reported by treatment of peracetylated cellobiose with hydrogen fluoride in pyridine (70%), purification of the peracetylated α-glycosyl fluoride by flash chromatography, followed by de-*O*-acetylation with sodium methoxide gives **18** in quantitative yields[17]. The spectrum of the starting acetylated cellobiosyl fluoride presented the following signals: ^{1}H NMR (MeOD, 400 MHz) δ 5.67 (dd, 1H, $J_{1,2}$ = 2.8 Hz, $J_{1,F}$ = 53.0 Hz, H-1^{I}), 5.47 (t, 1H), 5.18 – 5.05 (m, 2H), 4.96 – 4.84 (m, 2H), 4.54 (d, 1H, $J_{1,2}$ = 7.9 Hz, H-1^{II}), 4.37 (dd, 1H, $J_{a,b}$ = 12.4, $J_{5,6}$ = 4.5 Hz, H-6^{IIb}), 4.17 – 4.04 (m, 4H), 3.83 (t, 1H), 3.71 – 3.65 (m, 1H), 2.15 – 1.99 (m, 21H, CH_3).

*4.2.2.8. Synthesis of the accpetors p-nitrophenyl β-D-glucopyranoside (GlcβpNP) (**31**) and p-nitrophenyl 6-azido-6-deoxy-2,3,4-tri-O-acetyl-β-D-glucopyranoside (6N$_3$-GlcβpNP) (**35**) for the glycosynthase reactions*

The chemical synthesis of these two compounds can be found in Chapter 3 (Experimental).

4.2.3. Enzymes

The *Humicola insolens* Cel7B E197A enzyme was kindly provided by Novozymes (Denmark). The protein was >95% homogeneous as judged by SDS-PAGE. Concentration was determined by UV spectrophotometry (ε_{280}= 6.68 x 10^{5} M^{-1}·cm^{-1}).

4.2.3.1. Kinetics of donor-acceptor condensations catalyzed by the HiCel7B E197A glycosynthase

Reactions were done in 96-well microplates. Donor and acceptor substrates in 100 mM phosphate pH 7.0 were pre-incubated at 35ºC for 5 min, then the reactions were initiated by addition of the *Hi*Cel7B E197A enzyme and kept at 35 °C (final reaction volume of 0.3 mL). Aliquots were withdrawn at regular time intervals, diluted 1:10 with formic acid 2% (v/v) to stop the enzymatic

reaction, and analyzed by HPLC (Agilent HPLC equipment, NovaPak C18 (4 µm, 3.9 × 150 mm) column (Waters), flow rate 1 mL/min, 8.5% MeOH in water when using cellobiosyl floride donor (**11**) and 12% MeOH in water for 6-azido-cellobiosyl floride donor (**10**), UV detector at 300 nm). Initial rates (v_o) were obtained from the linear progress curves of product formation (normalized area *vs* time) and expressed as v_o/[E] in inverse seconds. The initial rates of transglycosylation at different concentrations of donor were calculated from the relative areas of transglycosylation product at initial reaction times (< 10% conversion, linear progress curve). Chromatographic peaks were assigned by co-injection with independent standards.

For the determination of specific activities (data in Figure 4. 3), reactions were done at 1 mM donor (**11** or **10**), 7 mM acceptor (**31** or **35**), and 0.83 µM enzyme (specific activity of 6.2 min^{-1} for the reference reaction Glcβ4GlcαF + GlcpNP). For determination of kinetic parameters (data in Figure 4. 4), reactions were done at constant acceptor (**31**) concentration of 20 mM, varying donor (**11** or **10**) concentrations (0.025 to 2 mM), and 0.1 or 0.5 µM enzyme (specific activity of 16 min^{-1} for the reference reaction Glcβ4GlcαF + GlcpNP) for reactions with donor **11** or **10**, respectively. Kinetic parameters k_{cat}, K_M, and k_{cat}/K_M were calculated by nonlinear fitting of v_0 *vs.* donor concentration data to the Michaelis Menten model (eq. 4.1) or substrate inhibition model (eq. 4.2).

$$v_o = \frac{k_{cat}\,[E][S]}{K_M+[S]} \qquad \text{(eq. 4. 1)} \qquad v_o = \frac{k_{cat}\,[E][S]}{K_M+[S]+\frac{[S]^2}{K_I}} \qquad \text{(eq. 4. 2)}$$

Equations 4.1 and 4.2. Michaelis-Menten models.

4.2.4. Glycosynthase-catalyzed polymerizations

Reaction mixtures (0.5 mL) consisting of 30 - 50 mg donor substrate (**11** or **10**), phosphate buffer (100 mM, pH = 7.7) and *Hi*Cel7B E197A enzyme (56 µM, specific activity of 16 min^{-1} for the reference reaction Glcβ4GlcαF + GlcpNP) were incubated at 40 ºC and 250 rpm. A precipitate was formed during the reaction and no donor was observed by TLC (ACN/H_2O 8:2) after 24 hours. The precipitated product was isolated by centrifugation at 27,000 x g for 3 minutes, and the precipitate was thoroughly washed with cold water. Finally, the product was freeze-dried to yield water-insoluble polymers as white powders. Supernatants were also lyophilized to recover soluble oligomers. The products were analyzed by HPSEC to determine the polymer parameters (M_w, M_n, M_p, DP, PDI).

Synthetic cellulose (**1**).- Compound **11** (30 mg, 0.087 mmol) was dissolved in phosphate buffer (0.1 M, pH 7.0, 0.5 mL) and incubated with *Hi*Cel7B E197A enzyme (56 µM) at 40 °C. After 24

h, the isolated water-insoluble polymer was freeze-dried obtaining a white powder (29 mg, 92% yield).

Alternating 6-azido-6-deoxycellulose (**2**).- Compound **10** (30 mg, 0.081 mmol) was dissolved in phosphate buffer (0.1M, pH 7.0, 0.5 mL) and incubated with *Hi*Cel7B E197A enzyme (56 μM) at 40 °C. After 24 h the isolated water-insoluble polymer was freeze-dried obtaining a white powder (26 mg, 82% yield).

Acetylated alternating 6-azido-6-deoxycellulose (**3**).- Polymer **2** (26 mg) was mixed with pyridine (118 μL, 20 equiv), acetic anhydride (138 μL, 20 equiv) and DMAP (1 mg). The reaction solution was stirred for 24 h at 80 ºC. The product was isolated by pouring the reaction mixture in 2 mL deionized water, followed by filtration. The precipitate was dried overnight in a vacuum oven at 50 °C. DS = 2.1 determined by ^{1}H NMR spectroscopy. FTIR: 3439 cm^{-1} (OH), 2109 cm^{-1} (N_3), 1757 cm^{-1} (C=O).

4.2.5. Functionalization of polysaccharides 2 and 3

Conjugated alternating 6-azido-6-deoxycellulose with Alexa Fluor® 488 alkyne (**12**).- A solution of Alexa Fluor® 488 alkyne (Life Technologies) (2.0 mg, 2.56 μmol) in water (1 mL) and freshly prepared solution of sodium L-ascorbate (1M, 20 mL, Sigma-Aldrich) were added to a solution of polymer **2** (1.0 mg, 2.6 μmol/anhydrous cellobiose Unit) in DMSO (1mL). Then, 7.5% aqueous cupric sulfate (24 μL, 7.21 μmol) was added to the reaction mixture, which was stirred overnight at 24ºC. The unreacted Alexa Fluor reagent was removed by dialysis (Pur-A-Lyzer^{TM} Mega 1000 Dialysis Kit, Sigma-Aldrich) against water. The functionalized polymer **12** (1.0 mg, 1.07 μmol) was obtained after lyophilization in 41 % yield.

Acetylated alternating 6-aminocellulose (**4**).- Polymer **3** (20 mg) was dissolved in 2 mL of THF, followed by the dropwise addition of 13 μL of deionized water. Then, Ph_3P (2 eq. per acetylated glucosyl unit) was added, and the solution allowed to react at room temperature for 12h in a sealed flask. The solution was transferred to a 3500 MWCO dialysis tubing that was placed in a beaker containing 600 mL ethanol. As the dialysis proceeded, a precipitate was slowly formed. After one day of dialysis, the contents inside the tubing were removed, and the precipitate was isolated by filtration. The precipitate (polymer **4**) was dried in a vacuum oven at 50 °C.

FTIR: 3431 cm^{-1} (OH, NH_2), 1763 cm^{-1} (C=O).

4.2.6. Structural characterization of the polysaccharides

FTIR.- A Thermo Electron Nicolet 8700 FTIR was used to perform infrared spectroscopy analyses of the samples as pressed KBr pellets. All samples were dried in a vacuum oven prior to analysis to avoid moisture. *In situ* FTIR spectra were obtained using a Mettler Toledo ReactIR 45M with a SiComp fiber optic ATR probe.

NMR.- ^{1}H and ^{13}C NMR, COSY and HSQC spectra were recorded on a Varian Gemini 400 MHz spectrometer operated at 298 K. For ^{1}H NMR, the TMS peak (0 ppm) was used as reference. When using MeOD as solvent, the central peak of the MeOD multiplet (3.31 ppm) was used as a reference. For ^{13}C NMR, the central peak of the $CDCl_3$ triplet (77.16 ppm) was used as a reference. When using MeOD as solvent, the central peak of the MeOD multiplet (49.00 ppm) was used as a reference[18].

Synthetic cellulose and functionalized cellulose ^{13}C NMR spectra were obtained on Varian INOVA and Varian UNITY 400 MHz spectrometers with a minimum of 5,000 scans in $CDCl_3$. Chemical shifts are reported relative to the solvent peaks.

Mass spectrometry.- MALDI-TOF spectra were obtained in a Bruker Daltonics spectrometer with 2,5-dihydroxybenzoic acid as matrix. Reflectron, positive ion mode, 19 kV acceleration voltage, and 20 kV reflector voltage were used.

Size exclusion chromatography.- HPSEC analyses to determine molecular mass profiles were performed on an Agilent 1100 HPLC system equipped with a refractive index detector using a PSS Gram column (8.0 x 300 mm, 100Å, 10 um) and a PSS Gram pre-column (9.0 x 50 mm, 100 Å, 10 um) thermostated at 50ºC, and DMSO with lithium bromide (5 g/L) as eluent at a flow rate of 0.5 mL/min. The calibration curve was obtained with dextrans as standards (American Polymer Standards Corporation DXT1 – DXT55 kDa). Freeze dried polymers and standards were dissolved in DMSO and filtered. From the chromatograms, M_p (molecular mass of the peak maximum), M_w (weight average molecular mass), M_n (number average molecular mass), DP (degree of polymerization), and PDI (polydispersity index) were calculated.[19]

Scanning electron microscopy.- For SEM experiments, the dried product was fixed on a graphite tape, coated with gold/palladium by ion-sputtering, and observed at an accelerating voltage of 10 kV and working distance of 16 mm using a JEOL JSM-5310 microscope.

Fluorescence microscopy.- Polysaccharide **12** was observed with a Stereoscopic microscope Nikon Eclipse TE 2000-U using a Piston GFP filter, excitation 450-490 nm, emission: 500-530 nm, and images were acquired with a cooled CCD camera.

4.3. RESULTS AND DISCUSSION

A substrate that acts both as a good donor and acceptor can efficiently self-condense in a glycosynthase polymerization reaction. Structural and kinetic studies of different endo-glycosidases on their disaccharide substrates revealed that the introduction of a functionalization at C-6 with an azido group could compromise the enzyme-substrate binding.[20,21,22] By contrast, at position C-6' interactions seem less restrictive. Therefore, we tentatively proposed that 6'N_3-CelαF could be accepted as donor as well as acceptor by the E197A glycosynthase mutant.

4.3.1. Synthesis of azido substrates

To explore the possibility of using HiCel7B E197A for the glycosynthase-catalyzed polymerization reaction of 6'N_3-CelαF, we tested the enzyme on different azido substrates and evaluated its effect on donor and acceptor subsites.

The synthesis of 6'-azido-6'-deoxy-cellobiosyl fluoride (6'N_3-CelαF) was prepared essentially as reported in Fort *et al*.[15] exploring some additional modifications (Figure 4. 2). Starting from 1,6-anhydro-β-D-cellobiose (**5**), selective bromination was performed at position C-6' with *N*-bromosuccinimide and triphenylphosphine in dimethylacetamide for 1 hour at 80 ºC. Addition of acetic anhydride was added to protect the free hydroxyls of the disaccharide and isolate the brominated product (**6**). Acetolysis of the 1,6-anhydro ring was developed as in Fort *et al.* with hydrobromic acid in acetic acid and further acetylation with silver acetate yielding the β-anomer in quantitative yields (**7**). The first strategy for the synthesis of the desired donor 6'N_3-CelαF consisted on treatment with sodium azide in DMF, acetylation followed by fluorination, but a mixture of 6'-azido-6-'deoxy-D-cellobiose anomers (α/β 70:30) (**8a**) were obtained which decreased fluorination yields. Therefore, the beta anomer was first fluorinated (**8b**) and then azidated (**9**) as in Fort's work. Finally, deacetylation with sodium methoxide in MeOH afforded the new glycosynthase donor 6'N_3-CelαF (**10**) (see characterization of the products in the Experimental section).

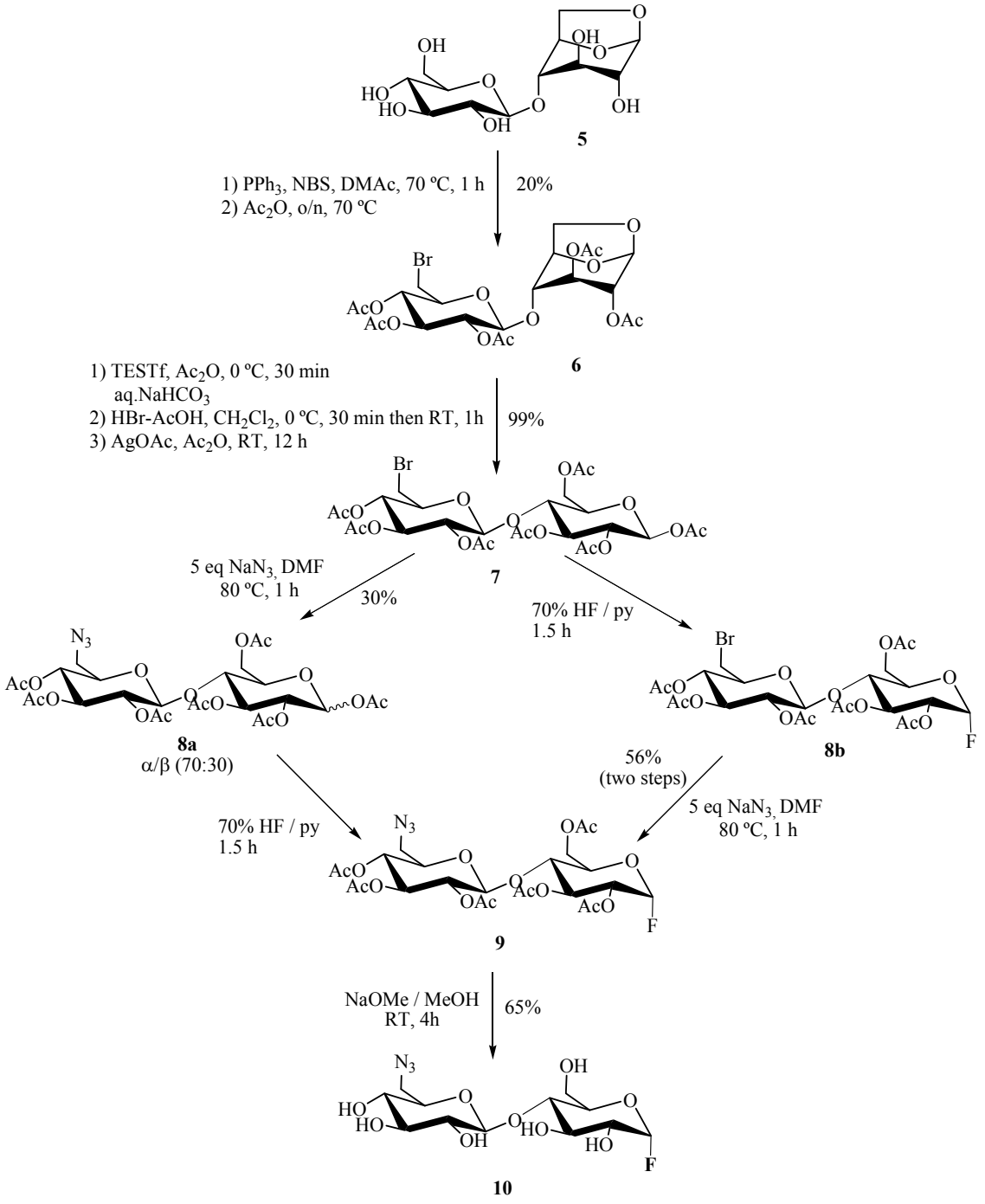

Figure 4. 2: Synthesis of the cellobiosyl fluoride donor 6'N_3-CelαF (**10**).

Acceptors *p*-nitrophenyl 6-azido-6-deoxy-β-D-glucoside (6N_3-GlcβpNP, **35**) was obtained after regiospecific tosylation of *p*-nitrophenyl β-D-glucoside (GlcβpNP, **31**) and further substitution by sodium azide with an overall yield of 50% as decribed in Chapter 3 (Figure 3. 26).

4.3.2. Kinetic characterization of HiCel7B E197A glycosynthase for azido substrates

To evaluate the ability of the *Hi*Cel7B E197A glycosynthase to accept azido-substituted substrates, different donor-acceptor pairs were kinetically analyzed (Figure 4. 3). With CelαF (**11**) as donor substrate, specific activities with acceptors GlcβpNP (**31**) and 6N_3-GlcβpNP (**35**) are essentially the same, indicating that the azido group can be accommodated in subsite +1 of the enzyme's binding cleft. With 6'N_3-CelαF (**10**) donor and 6N_3-GlcβpNP (**35**) acceptor substrates, activity is just 2-fold lower than the reference **11**+**31** reaction, concluding that subsite -2 also tolerates an azido substitution.

11 R_1 = OH
10 R_1 = N_3

31 R_2 = OH
35 R_2= N_3

Reaction	R_1	R_2	s.a. (%)[1]
11 + 31	OH	OH	100
11 + 35	OH	N_3	102
10 + 31	N_3	OH	48

Figure 4. 3: Donor-acceptor condensations catalyzed by the *Hi*Cel7B E197A glycosynthase. [1)] Specific activities (s.a.) at 1 mM donor (**11** or **10**), 7 mM acceptor (**31** or **35**), 0.83 µM enzyme in 100 mM phosphate buffer pH 7.0, 35ºC.

Kinetics with different donor concentrations at saturating GlcβpNP acceptor (**31**) concentration are plotted in Figure 4. 4. CelαF (**11**) follows saturation kinetics with k_{cat} of 17 min^{-1}, whereas 6'N_3-CelαF (**10**) has the same k_{cat} (16.4 min^{-1}) but shows substrate inhibition at high donor concentration. Therefore, subsites -2 and +1 accept the 6-azido substitution, a requirement to evaluate donor self-condensation to yield alternating 6-azido polymers.

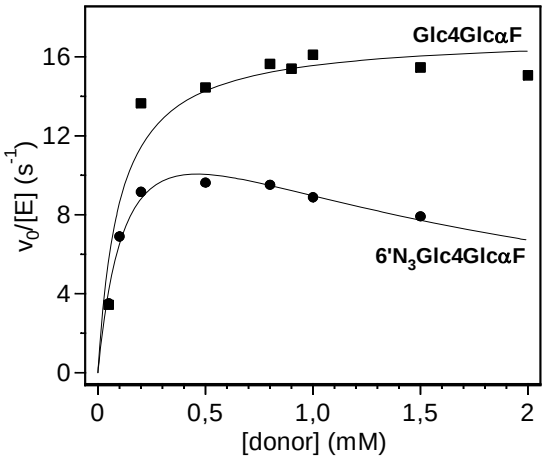

Donor	k_{cat} (min^{-1})	K_M (mM)	K_I (mM)	k_{cat}/K_M ($mM^{-1}min^{-1}$)
18	17.1 ± 0.9	0.10 ± 0.03	--	173
10	16.4 ± 2.4	0.15 ± 0.04	1.5 ± 0.5	113

Figure 4. 4: Kinetics of *Hi*Cel7B E197A glycosynthase for donors Glcβ4GlcαF (**11**, ■) and 6'-N_3Glcβ4GlcαF (**10**, ●) at saturating (20 mM) GlcβpNP (**31**) acceptor in 100 mM phosphate buffer pH 7.0, 35 ºC.

4.3.3. Glycosynthase-catalyzed polymerization

Glycosynthase-catalyzed polymerizations were performed at high donor concentration, pH 7.8 and 40 ºC (Figure 4. 1, Table 4. 1). Polymeric products precipitated as a white powder after 24 h reactions. TLC analysis showed that the polymerizations proceeded quantitatively and neither fluoride donors nor their hydrolysis products were detected. The water-insoluble polymers were isolated in good yields (>90%) after centrifugation, washes with water, and lyophilization, and they were structurally characterized.

Analysis of the degree of polymerization and molecular mass distribution of the insoluble polysaccharides by HPSEC showed that cellulose (**1**) (entry 1, Table 4. 1) presents a monomodal profile with a M_W value of 4.3 kDa which corresponds to $(4Glc\beta4Glc\beta)_n$, n=13, and the alternating 6-azido-6-deoxycellulose (**2**) (entry 2) has a M_W value of 5.8 kDa ($(4[6'N_3\text{-}Glc]\beta4Glc\beta)_n$, n=17) (Figure 4. 5). Same results were obtained after acetylation of the 6-azido polysaccharide with Ac_2O and pyridine (entry 3, polymer **3**).

Entry	[donor] (mM)	[enz] (μM)	yield (%)	M_w (kDa)	n (DP)[d]	M_n (kDa)	PDI	M_p[e] (kDa)
CelαF								
1	174	56	92	4.3	13 (26)	2.9	1.5	3.7
6'N_3-CelαF								
2	162	56	75 - 90	5.8	17 (34)	4.9	1.2	4.7
3[a]	162	56	88[b]	9[c]	16 (32)	7	1.2	8

Table 4. 1: Polysaccharide parameters obtained after HPSEC. [a]Glycosynthase-catalyzed reaction followed by further acetylation. [b]average yield (4 reactions). [c]acetylated M_w. [d]n, number of condensations. (DP), number of glucosyl units for the weight average molecular mass polysaccharide (M_w). [e]M_p, molecular mass of the maximum peak in HPSEC chromatograms. Two values correspond to bimodal profiles.

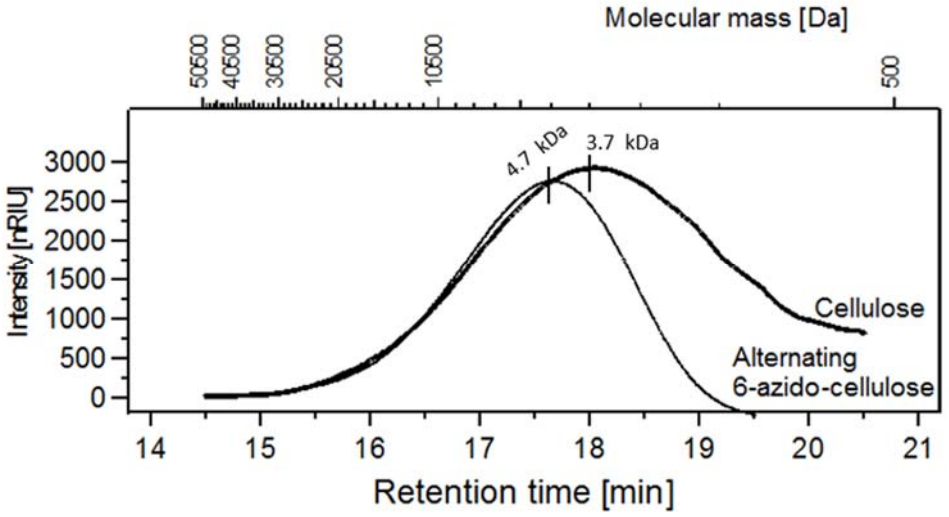

Figure 4. 5. HPSEC chromatograms of polymers **1** (cellulose) and **2** (alternating 6-azido-6-deoxycellulose) obtained under different conditions, where labels correspond to entries in Table 4. 1. M_p values (maximum of the peaks) are indicated in kDa.

MALDI-TOF MS shows a series of peaks up to 5.5 kDa corresponding to the low molecular mass oligomers, peaks separated by Δm/z of 324 and 349 for polymer **1** and **2**, respectively, which correspond to the theoretical mass of the repeating (Glcβ4Glc) unit for polymer **1** and the (6'N_3-Glcβ4Glc) unit for polymer **2,** and Δm/z of 560 for the acetylated polymer **3** (Figure 4. 6).

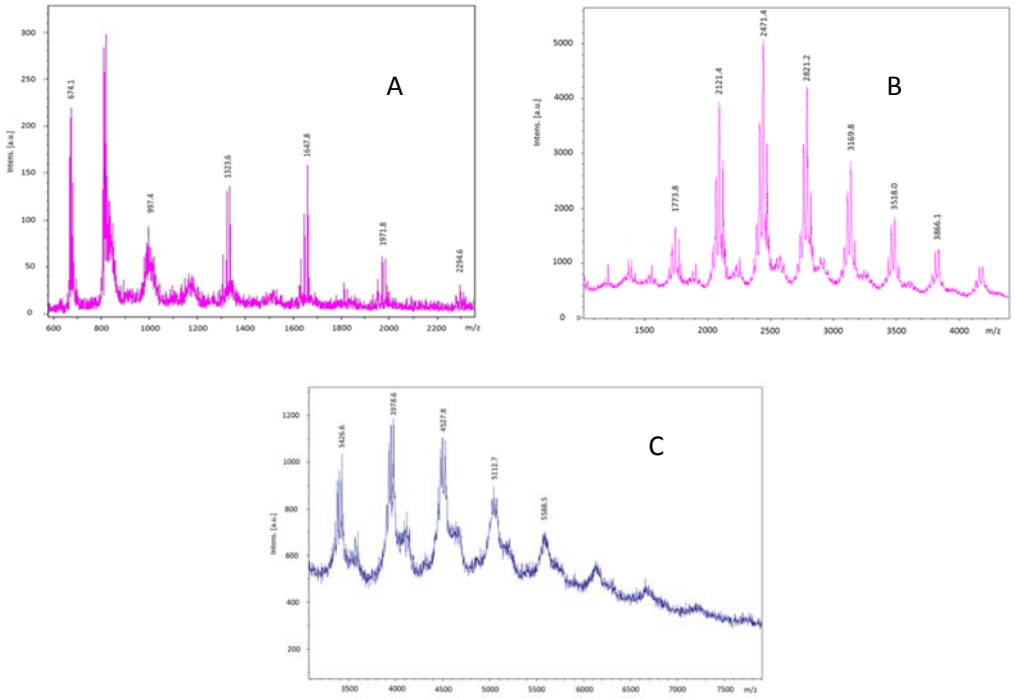

Figure 4. 6. MALDI-TOF spectra of A) synthetic cellulose (**1**), B) 6-azido 6-deoxycellulose (**2**), C) acetylated 6-azido 6-deoxycellulose (**3**).

Analysis of the acetylated polymer **3** by ^{1}H NMR presented a degree of acetylation (DA) of 2.1 (maximum theoretical DA = 2.5) (Figure 4. 7). ^{13}C NMR (Figure 4. 8A) showed the formation of the new β-1,4 glycosidic linkage (δ_H 76 ppm) and disappearance of the signal at δ_H 69 ppm assignable to the unsubstituted C-4 of the nonreducing end of the cellobiosyl donor. The signal at δ_C 62 ppm corresponds to the acetylated C-6 positions while the signal at δ_C 51 ppm was assigned to the azidated C-6' positions consistent with the presence of azido groups every two glucosyl units.

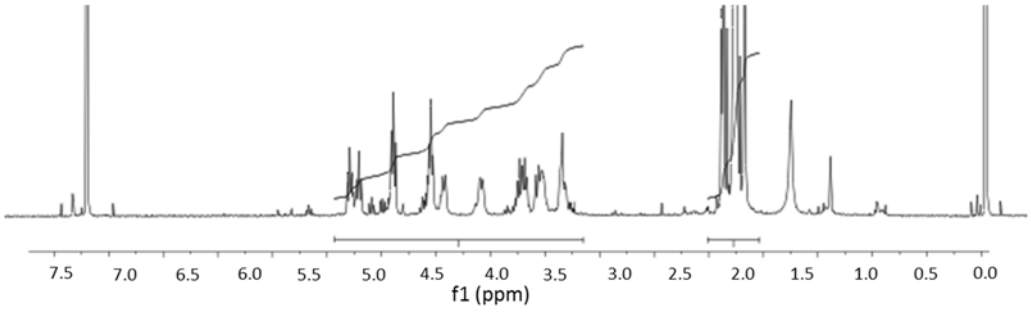

Figure 4. 7: ^{1}H NMR spectrum of alternating acetylated 6-azido 6-deoxycellulose (**3**).

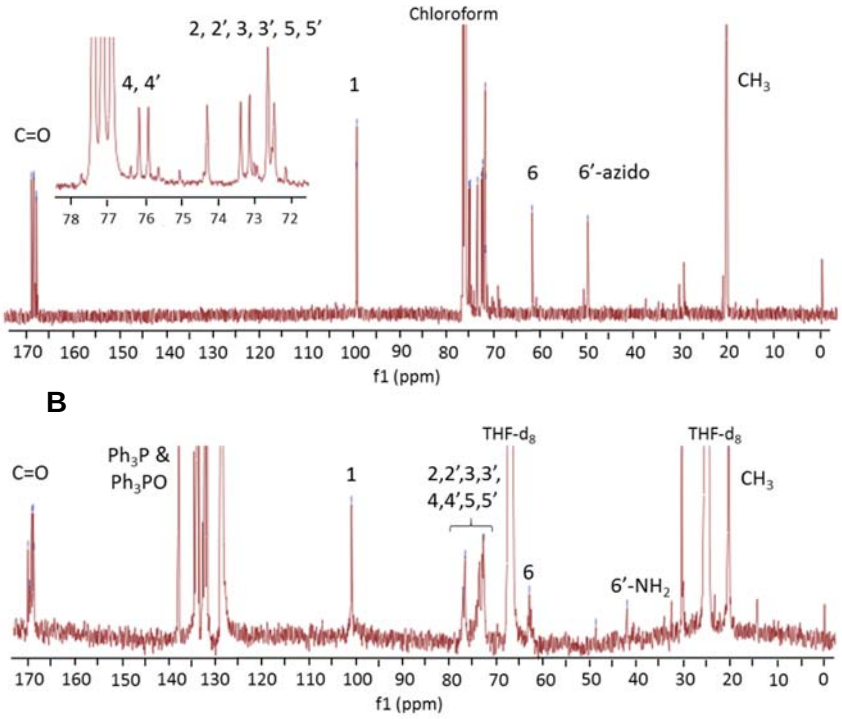

Figure 4. 8: ^{13}C NMR spectra of (A) acetylated alternating 6-azido-6-deoxycellulose (**3**), and (B) acetylated alternating 6-amino-6-deoxycellulose (**4**).

The FTIR spectrum of the alternating 6-azido-cellulose (**2**) (Figure 4. 9A) shown an intense stretching band of the azido group at 2110 cm^{-1}, and the absorption band of the sugar OH groups at 3480 cm^{-1}, whereas the acetylated polymer **3** (Figure 4. 9B) retains the azide band at 2110 cm^{-1}, a new band at 1750 cm^{-1} for the C=O of the acetyl groups, but still contains a small absorption band at 3480 cm^{-1} due to free hydroxyl groups resulting from the incomplete acetylation reaction.

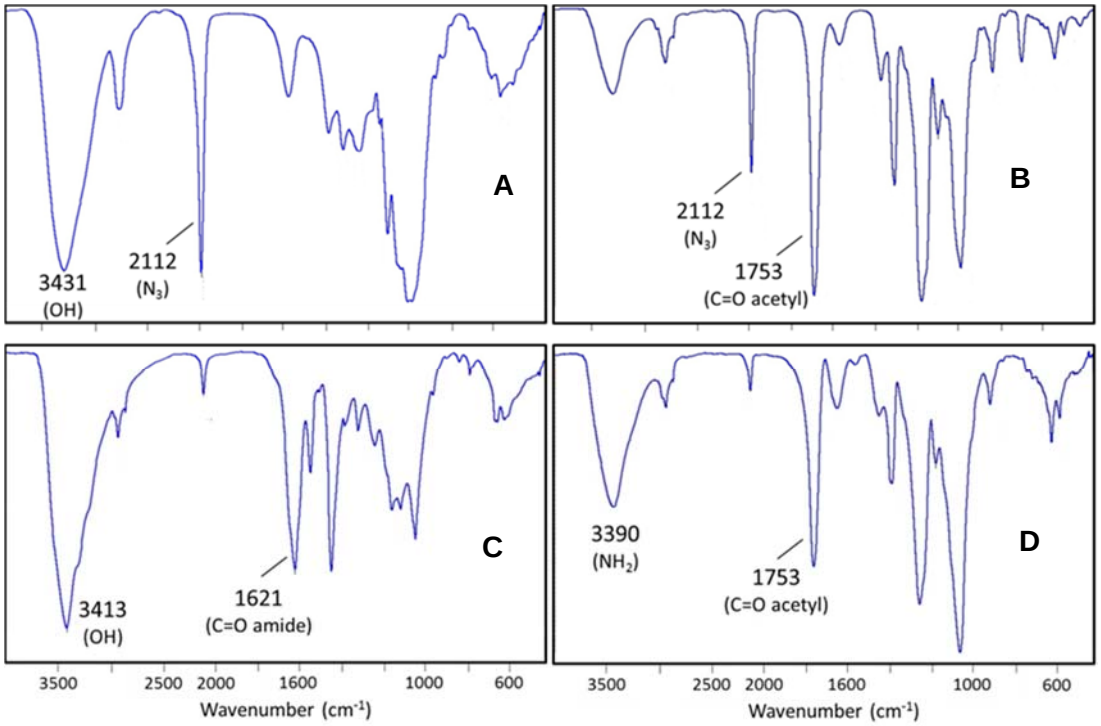

Figure 4. 9: FTIR spectra of alternating 6-azido 6-deoxycellulose and their derivatives. A) 6-azido 6-deoxycellulose (**2**). B) acetylated 6-azido 6-deoxycellulose (**3**). C) conjugated 6-azido 6-deoxycellulose with Alexa Fluor (**12**). D) acetylated 6-amino 6-deoxycellulose (**4**).

Polysaccharide morphologies were analyzed by SEM revealing that the 6-azido-cellulose (**2**) formed porous spherulites like the non-modified cellulose (**1**), although they seem to be larger, with 5-7 µm versus 2-4 µm average diameter, respectively (Figure 4. 10). These artificial polysaccharides notably differ from natural cellulose such as MCC (microcrystalline cellulose), whose particles of 10-50 µm are composed of aggregate bundles of multi-sized cellulose microfibrils.[23] The spherulite morphology with variable porosity seems to be common for artificial polysaccharides produced by *in vitro* enzymatic syntheses, as previously seen in the first artificial cellulose obtained by transglycosylation with *T.viridiae* cellulase[24] or alternating β-1,3/1,4 glucan obtained by a glycosynthase-catalyzed polymerization.[25,26]

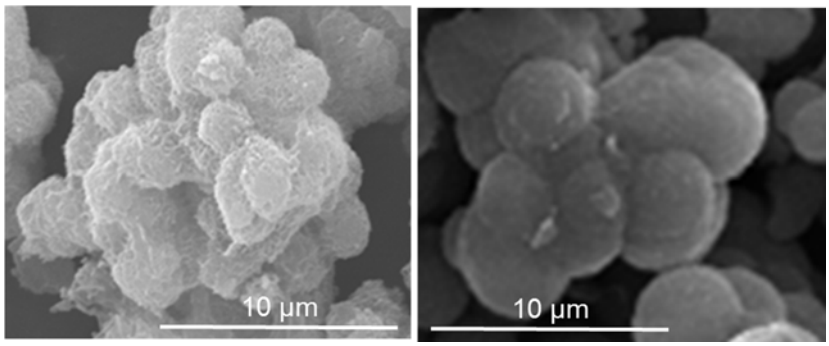

Figure 4. 10: SEM of the polysaccharides **4** (left) and **5** (right).

4.3.4. Functionalization of polysaccharides 2 and 3

The azido cellulose **2** and the acetylated derivative **3** are reactive intermediates for further modifications (Figure 4. 1). The accessibility and reactivity of the 6-azido groups was first tested by "click" chemistry (Figure 4. 11).[27]

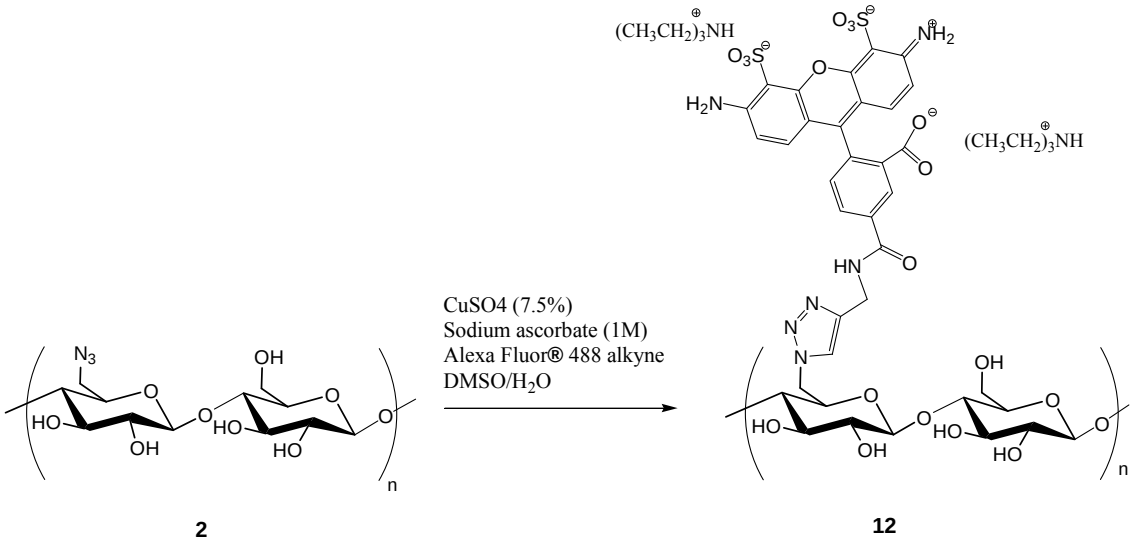

Figure 4. 11: Derivatization of 6-azido-6-deoxycellulose with the fluorescent Alexa Fluor dye.

The alternating 6-azido-6-deoxycellulose (**2**) was subjected to a copper-catalyzed azide/alkyne cycloaddition (Huisgen reaction)[28] with the alkyne-functionalized Alexa Fluor dye. After isolation of the water soluble product (**12**) by dialysis and lyophilization, FTIR spectroscopy (Figure 4. 9C) showed the appearance of a new absorption band at 1621 cm^{-1} corresponding to the carbonyl group of the Alexa Fluor amide function, and the disappearance of the stretching band of the azido groups at 2110 cm^{-1}, although some residual band was apparent due to incomplete reaction. The dye-labeled polymer **12** was observed as a green fluorescent solid by fluorescence microscopy (Figure 4. 12).

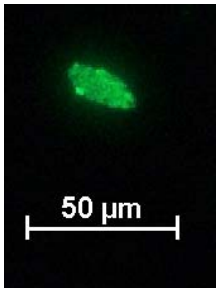

Figure 4. 12: Fluorescent-labelled 6-azido 6-deoxycellulose with Alexa Fluor® 488 (**19**) observed by fluorescence microscopy.

Next, reduction of the azido groups to amines was studied. Staudinger reduction has been recently applied to acylated 6-azido-6-deoxycelluloses with DS (azido) of 0.9-0.95 to selectively reduce the azido groups to amines in the presence of easily reducible ester groups (Figure 4. 13).[30]

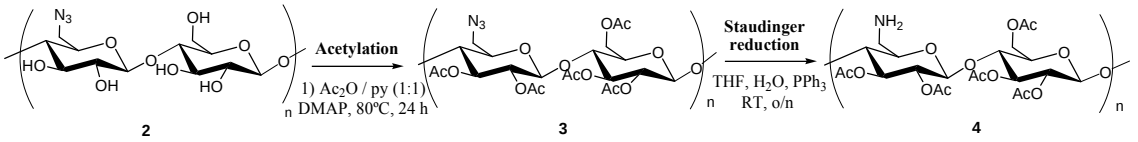

Figure 4. 13: Acetylation of 6-azido-6-deoxycellulose and further reduction of the azide.

The same protocol was here applied to reduce the acetylated alternating 6-azido polymer **3** with the aim of obtaining a novel 6-amino-6-deoxy cellulose derivative with a regular pattern of one amino group every two glucosyl units in the polysaccharide chain. The reaction was performed by reacting the acetylated polymer **3** dissolved in THF with Ph_3P to form a phosphazide which evolves to an iminophosphorane. It is then hydrolyzed by water to produce the polymer **4** and triphenylphosphine oxide. Unfortunately, this new polysaccharide has poor solubility in water and common organic solvents, alike the reported acylated 6-aminocelluloses obtained from MCC.[30] Due to the solubility issues, the reaction was performed in deuterated THF and the ^{13}C NMR spectrum of the crude reaction mixture was directly recorded (Figure 4. 8B). The spectrum showed the formation of the amine (δ_C 43 ppm assigned to C-6'-NH_2) and some residual azide (signal at δ_C 51 ppm for C-6-N_3). FTIR analysis confirms the presence of the free amine (broad N−H stretching band at 3390 cm^{-1} and the N−H bend at 1570 cm^{-1}) but shows a residual signal of the azide at 2110 cm^{-1}, while the carbonyl signal of the acetyl groups remains at 1755 cm^{-1} (Figure 4. 9D).

Substituted celluloses at C-6 have been achieved by chemical modification of MCC, where bromination of cellulose is completely selective at C-6,[29] but further SN_2 displacement of the bromide is limited due to the poor solubility of the 6-bromo-6-deoxycellulose. Edgar and coworkers[30] showed that esterification of brominated cellulose broadens the applications for

further modifications. In this way, 6-azido-6-deoxy-2,3-di-*O*-acyl cellulose was obtained from MCC resulting in a polysaccharide of DP 50 and DS (azide) of 0.92.[31] The enzymatic protocol here reported provides access to novel structures, where azide substitutions are regularly distributed at C-6 every two glucosyl units on a cellulose chain with free hydroxyl groups, with DP of about 40 and DS (azide) of 0.5. By extension, the same strategy with homologous azido-cellooligosaccharide donors (*i.e.* 6''-azidocellotriosyl and 6'''-cellotetraosyl fluoride donors) will afford other regularly functionalized celluloses with different substitution patterns.

4.4. CONCLUSIONS

As opposed to chemically modified celluloses where the substitution pattern is intrinsically random, the glycosynthase-catalyzed polymerization of properly modified glycosyl donors gives access to novel functionalized celluloses with defined and regular substitution patterns.

The glycosynthase *Hi*Cel7B E197A has been explored to act on azido functionalized substrates. Kinetic studies demonstrated that *Hi*Cel7B E197 accommodates the azido substitution of 6'N_3-CelαF in subsite –2 and 6N_3-GlcβpNP in subsite +1 reacting with similar catalytic efficiency than the corresponding non-functionalized substrates. We have shown that a 6'-azido-cellobiosyl donor is readily polymerized to give alternating 6-azido-6-deoxycellulose with a regular pattern of one azido group every two glucosyl units, which can be further reacted to install different functional groups or substituents.

The alternating 6-azido-6-deoxycellulose was acetylated improving its solubility in organic solvents and the azides were reduced to amines through the Staudinger reaction obtaining the alternating 6-amino-6-deoxycellulose. Furthermore, the reactivity of the azido groups was also demonstrated by performing the copper-catalyzed azide/alkyne cycloaddition between the alternating 6-azido-6-deoxycellulose and a fluorescence probe (Alexa Fluor® 488 alkyne). The resulting fluorescent product was soluble in water and had the same Ex/Em than the attached fluorescent probe. In the future, the attachment of bioactive molecules might be attempted on the alternating 6-azido-6-deoxycellulose for further biomaterial studies.

The glycosynthase strategy can be extended to other functionalized donors, *i.e.* tri- or tetrasaccharide donors, to afford other regularly functionalized glycopolymers with different substitution patterns. Likewise, other functional groups may be introduced in the glycosyl donor (*i.e.* –COOH, -$CONH_2$, -SH) provided that the donor is accepted as a substrate by the glycosynthase, which otherwise can be engineered for the desired specificity by protein engineering and directed evolution approaches. This strategy opens the access to novel polysaccharide structures with promising applications.

4.5. REFERENCES

(1) Varki A., Cummings R.D., Esko J.D., Freeze, H.H., Stanley, P., Bertozzi, C.R., Hart, G.W., Etzler, M. E. *Essentials of Glycobiology*; Second.; Cold Spring Harbor Press: Cold Spring Harbor (NY), 2009.

(2) Dash, M.; Chiellini, F.; Ottenbrite, R. M.; Chiellini, E. *Prog. Polym. Sci.* **2011**, *36*, 981–1014.

(3) Kumar, M. N. V. R.; Muzzarelli, R. a a; Muzzarelli, C.; Sashiwa, H.; Domb, a J. *Chem. Rev.* **2004**, *104*, 6017–6084.

(4) Patel, M. P.; Patel, R. R.; Patel, J. K. *J Pharm Pharm. Sci* **2010**, *13*, 536–557.

(5) Duceppe, N.; Tabrizian, M. *Expert. Opin. Drug Deliv.* **2010**, *7*, 1191–1207.

(6) Shukla, S. K.; Mishra, A. K.; Arotiba, O. a; Mamba, B. B. *Int. J. Biol. Macromol.* **2013**, *59*, 46–58.

(7) Jayakumar, R.; Chennazhi, K. P.; Muzzarelli, R. a. a.; Tamura, H.; Nair, S. V.; Selvamurugan, N. *Carbohydr. Polym.* **2010**, *79*, 1–8.

(8) Cumpstey, I. *ISRN Org. Chem.* **2013**, *2013*, 1–27.

(9) Desai, U. R.; Petitou, M.; Bjo, I.; Olson, S. T. *J. Biol. Chem.* **1998**, *273*, 7478–7487.

(10) Gama, C. I.; Tully, S. E.; Sotogaku, N.; Clark, P. M.; Rawat, M.; Vaidehi, N.; Goddard, W. a; Nishi, A.; Hsieh-Wilson, L. C. *Nat. Chem. Biol.* **2006**, *2*, 467–473.

(11) Rawat, M.; Gama, C. I.; Matson, J. B.; Hsieh-wilson, L. C. *J. Am. Chem. Soc.* **2008**, *130*, 2959–2961.

(12) Kobayashi, S.; Kashiwa, K.; Kawasaki, T.; Shoda, S. *J. Am. Chem. Soc.* **1991**, *113*, 3079–3084.

(13) Faijes, M.; Planas, A. *Carbohydr. Res.* **2007**, *342*, 1581–1594.

(14) Kadokawa, J.; Kobayashi, S. *Curr. Opin. Chem. Biol.* **2010**, *14*, 145–153.

(15) Fort, S.; Boyer, V.; Greffe, L.; Davies, G. J.; Moroz, O.; Christiansen, L.; Schülein, M.; Cottaz, S.; Driguez, H. *J. Am. Chem. Soc.* **2000**, *122*, 5429–5437.

(16) Gullfot, F.; Ibatullin, F. M.; Sundqvist, G.; Davies, G. J.; Brumer, H. *Biomacromolecules* **2009**, *10*, 1782–1788.

(17) Malet, C.; Planas, A. *FEBS Lett.* **1998**, *440*, 208–212.

(18) Gottlieb, H. E.; Kotlyar, V.; Nudelman, A. *J. Org. Chem.* **1997**, *62*, 7512–7515.

(19) Carraher, C. E. J. *Seymour/Carraher's Polymer Chemistry*; 2007.

(20) Gaiser, O. J.; Piotukh, K.; Ponnuswamy, M. N.; Planas, A.; Borriss, R.; Heinemann, U. *J. Mol. Biol.* **2006**, *357*, 1211–1225.

(21) Piotukh, K.; Serra, V.; Borriss, R.; Planas, A. *Biochemistry* **1999**, *38*, 16092–16104.

(22) Malet, C.; Viladot, J. L.; Ochoa, A.; Gállego, B.; Brosa, C.; Planas, A. *Carbohydr. Res.* **1995**, *274*, 285–301.

(23) Moon, R. J.; Martini, A.; Nairn, J.; Simonsen, J.; Youngblood, J. *Chem. Soc. Rev.* **2011**, *40*, 3941–3994.

(24) Kobayashi, S.; Hobson, L. J.; Sakamoto, J.; Kimura, S.; Sugiyama, J.; Imai, T.; Itoh, T. *Biomacromolecules* **2000**, *1*, 168–173.

(25) Faijes, M.; Imai, T.; Bulone, V.; Planas, A. *Biochem. J.* **2004**, *380*, 635–641.

(26) Pérez, X.; Faijes, M.; Planas, A. *Biomacromolecules* **2011**, *12*, 494–501.

(27) Liebert, T.; Hänsch, C.; Heinze, T. *Macromol. Rapid Commun.* **2006**, *27*, 208–213.

(28) Meldal, M.; Tornøe, C. W. *Chem. Rev.* **2008**, *108*, 2952–3015.

(29) Furuhata, K.; Koganei, K.; Chang, H.; Aoki, N. *Carbohydr. Res.* **1992**, *230*, 165–177.

(30) Fox, S. C.; Edgar, K. J. *Cellulose* **2011**, *18*, 1305–1314.

(31) Fox, S. C.; Edgar, K. J. *Biomacromolecules* **2012**, *13*, 992–1001.

APPENDIX CHAPTER 4

APPENDIX

Figure A4. 1: ^{1}H NMR (above) and HSQC (below) of 2,3,4-tri-*O*-acetyl-6-bromo-6-deoxy-β-D-glucopyranosyl-(1→4)-1,6-anhydro-2,3-di-*O*-acetyl-β-D-glucopyranose (**6**)

Figure A4. 2: ^{1}H NMR (above) and ^{13}C NMR (below) of 2,3,4-tri-*O*-acetyl-6-bromo-6-deoxy-β-D-glucopyranosyl-(1→4)-1,2,3,6-tetra-*O*-acetyl-β-D-glucopyranose (**7**)

Figure A4. 3: HSQC of 2,3,4-tri-*O*-acetyl-6-bromo-6-deoxy-β-D-glucopyranosyl-(1→4)-1,2,3,6-tetra-*O*-acetyl-β-D-glucopyranose (**7**)

Figure A4. 4: ^{1}H NMR of 2,3,4-tri-*O*-acetyl-6-bromo-6-deoxy-β-D-glucopyranosyl-(1→4)-2,3,6-tri-*O*-acetyl-α-D-glucopyranosyl fluoride (**8b**)

Figure A4. 5: ^{1}H NMR 2,3,4-tri-*O*-acetyl-6-azido-6-deoxy-β-D-glucopyranosyl-(1→4)-2,3,6-tri-*O*-acetyl-α-D-glucopyranosyl fluoride (**9**)

Figure A4. 6: ^{1}H NMR (above) and ^{13}C NMR (below) of 6-azido-6-deoxy-β-D-glucopyranosyl-(1→4)-α-D-glucopyranosyl fluoride (6'N_3-CelαF) (**10**)

Figure A4. 7: ^{1}H NMR (above) and ^{13}C NMR (below) of acetylated alternating 6-azido-6-deoxycellulose (**3**) ($CDCl_3$)

Figure A4. 8: ^{13}C NMR of acetylated alternating 6-azido-6-deoxycellulose (**3**) (THF)

Figure A4. 9: ^{13}C NMR of acetylated alternating 6-amino-6-deoxycellulose (**4**) ($CDCl_3$)

Figure A4. 10: ^{1}H NMR (above) and ^{13}C NMR (below) of *p*-nitrophenyl β-D-glucopyranoside (GlcβpNP) (**31**)

Figure A4. 11: HSQC of *p*-nitrophenyl β-D-glucopyranoside (GlcβpNP) (**31**)

Figure A4. 12: ^{1}H NMR (above) and ^{13}C NMR (below) of *p*-nitrophenyl 6-azido-6-deoxy-2,3,4-tri-*O*-acetyl-β-D-glucopyranoside (6N_3-GlcβpNP) (**34**)

Figure A4. 13: HSQC of *p*-nitrophenyl 6-azido-6-deoxy-2,3,4-tri-*O*-acetyl-β-D-glucopyranoside (6N_3-GlcβpNP) (**34**)

Figure A4. 14: MALDI spectrum of *p*-nitrophenyl 6-azido-6-deoxy-β-D-glucopyranoside (6N_3-GlcβpNP) (**35**)

Table A4. 13: Determination of v_o (CelαF + $6N_3$-GlcβpNP). Study of subsite +1

Table A4. 14: Translgycosylation reaction conditions ($6'N_3$-CelαF + GlcβpNP). Study of subsite -2

Table A4. 15: Determination of v_o ($6'N_3$-CelαF + GlcβpNP). Study of subsite -2

Table A4. 16: Summary of results (Michaelis-Menten reaction and subsite studies) when [Donor] = 1 mM

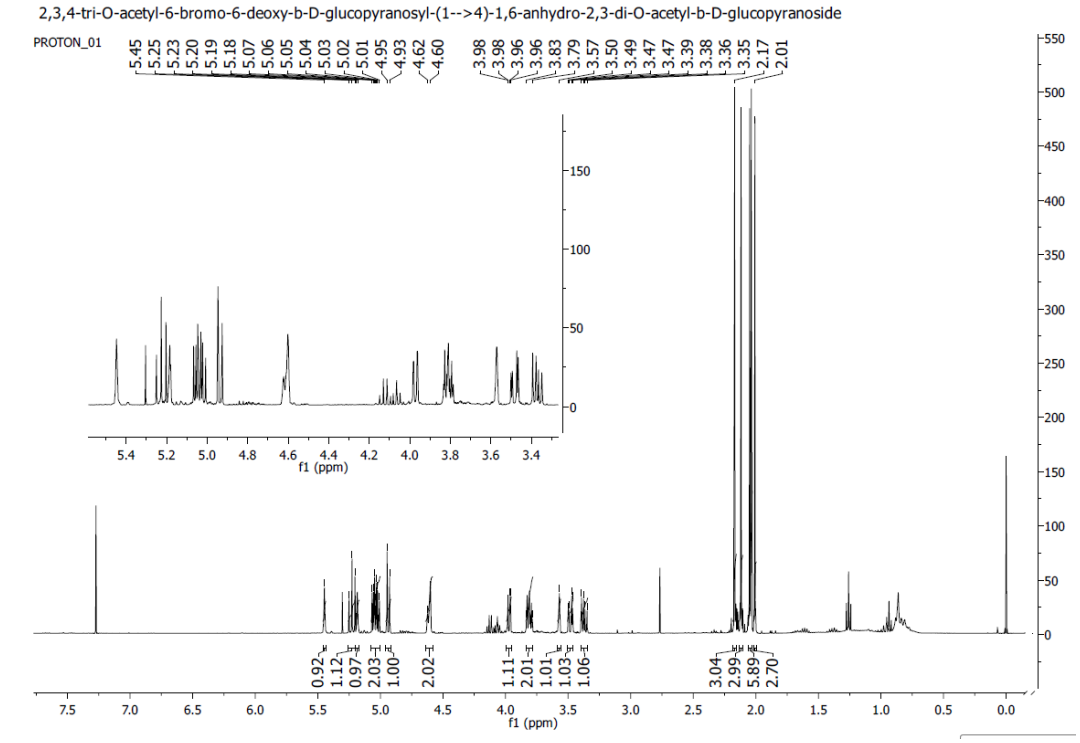

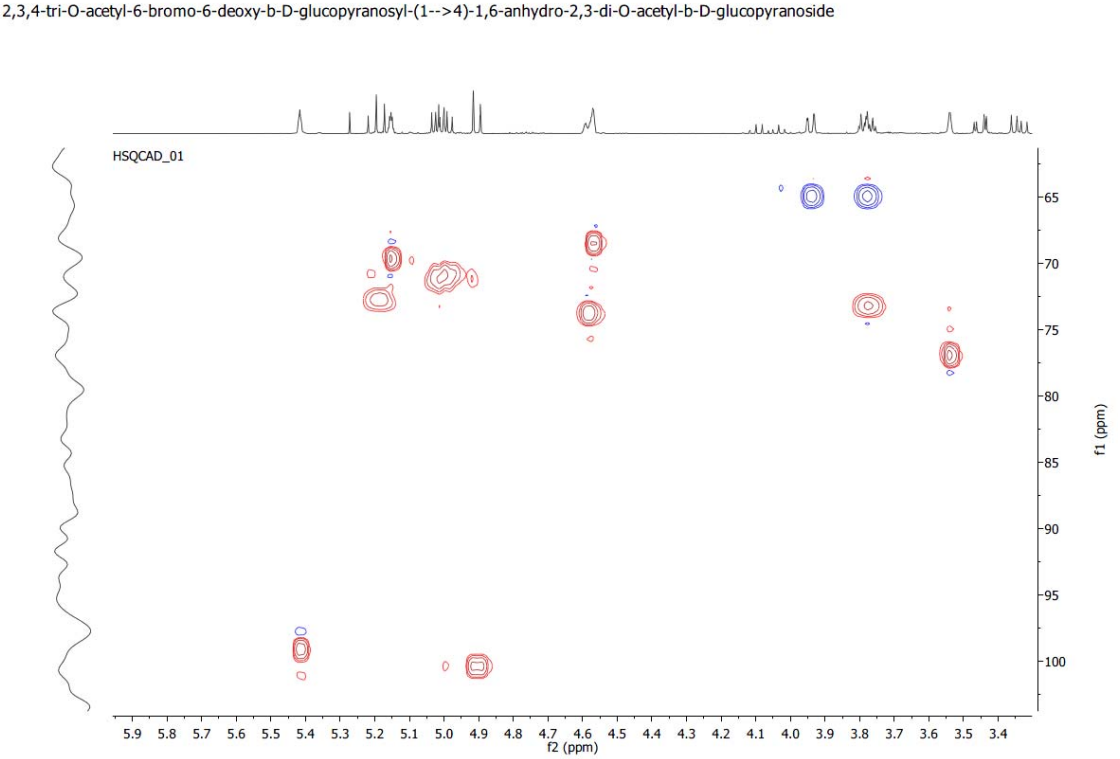

Figure A4. 1: [1]H NMR (above) and HSQC (below) of 2,3,4-tri-*O*-acetyl-6-bromo-6-deoxy-β-D-glucopyranosyl-(1→4)-1,6-anhydro-2,3-di-*O*-acetyl-β-D-glucopyranose **(6).**

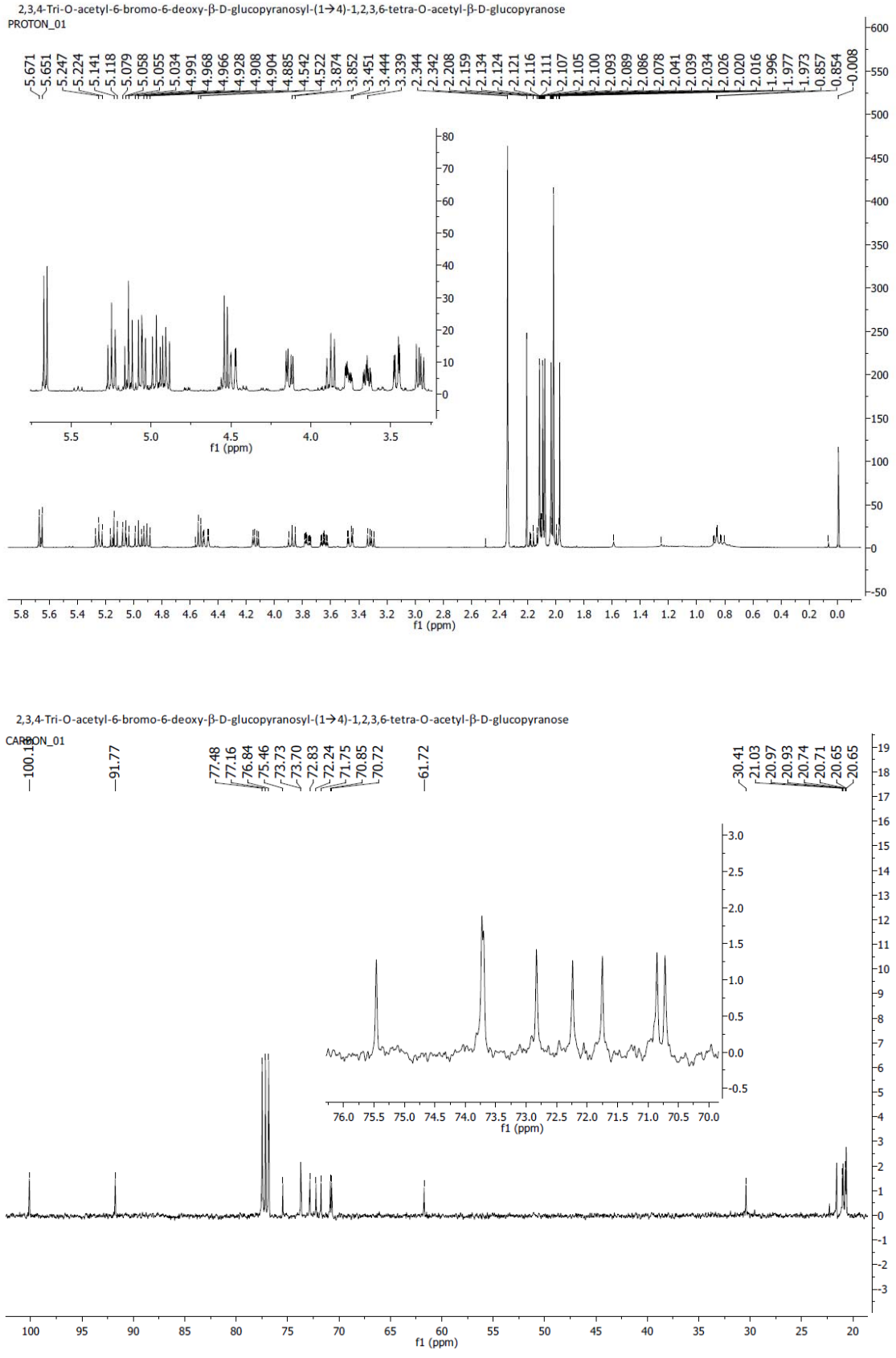

Figure A4. 2: ^{1}H NMR (above) and ^{13}C NMR (below) of 2,3,4-tri-*O*-acetyl-6-bromo-6-deoxy-β-D-glucopyranosyl-(1→4)-1,2,3,6-tetra-*O*-acetyl-β-D-glucopyranose **(7).**

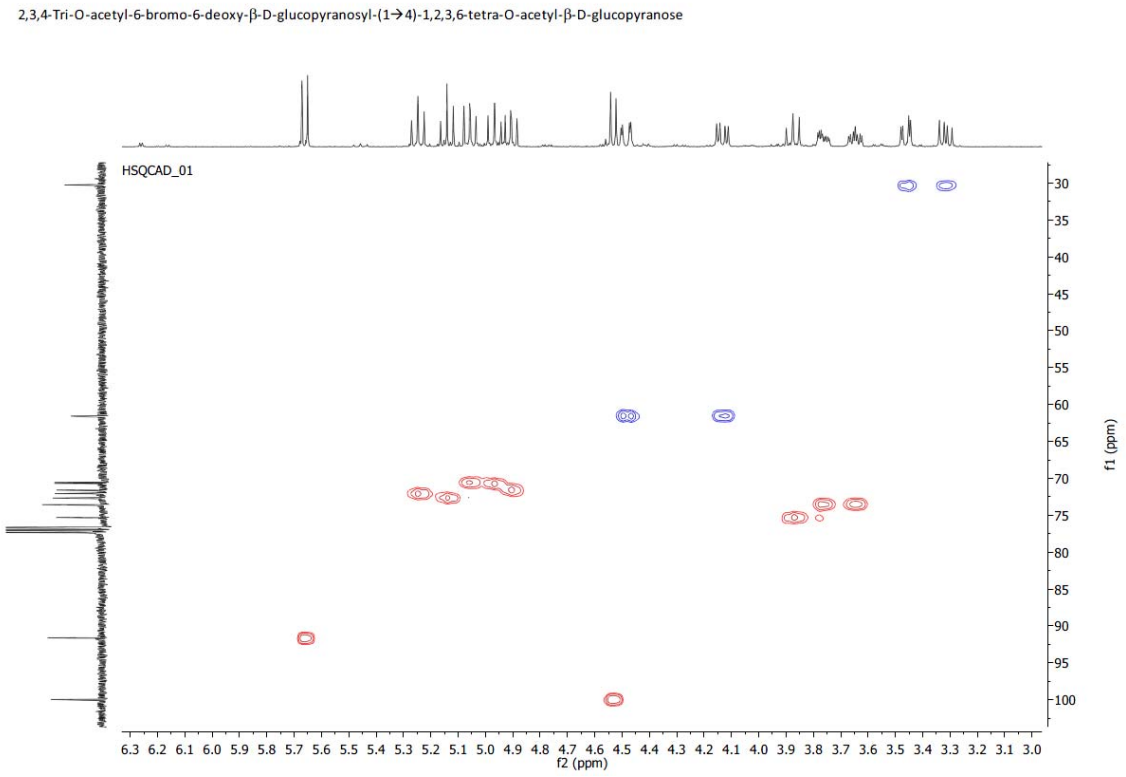

Figure A4. 3: HSQC of 2,3,4-tri-*O*-acetyl-6-bromo-6-deoxy-β-D-glucopyranosyl-(1→4)-1,2,3,6-tetra-*O*-acetyl-β-D-glucopyranose **(7).**

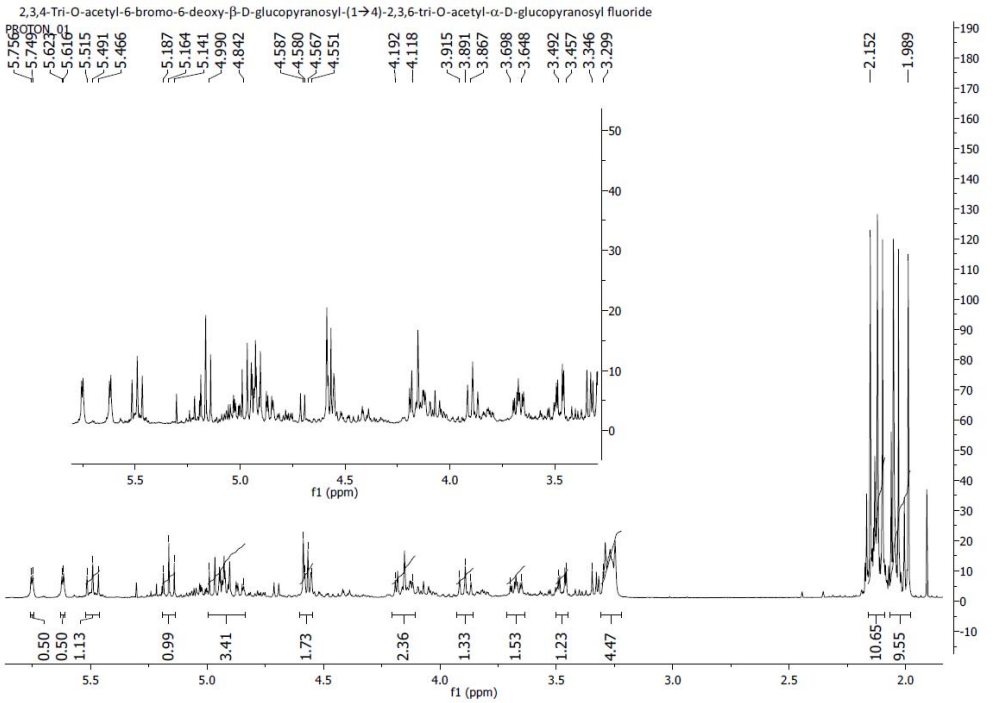

Figure A4. 4: ^{1}H NMR of 2,3,4-tri-*O*-acetyl-6-bromo-6-deoxy-β-D-glucopyranosyl-(1→4)-2,3,6-tri-*O*-acetyl-α-D-glucopyranosyl fluoride (**8b**).

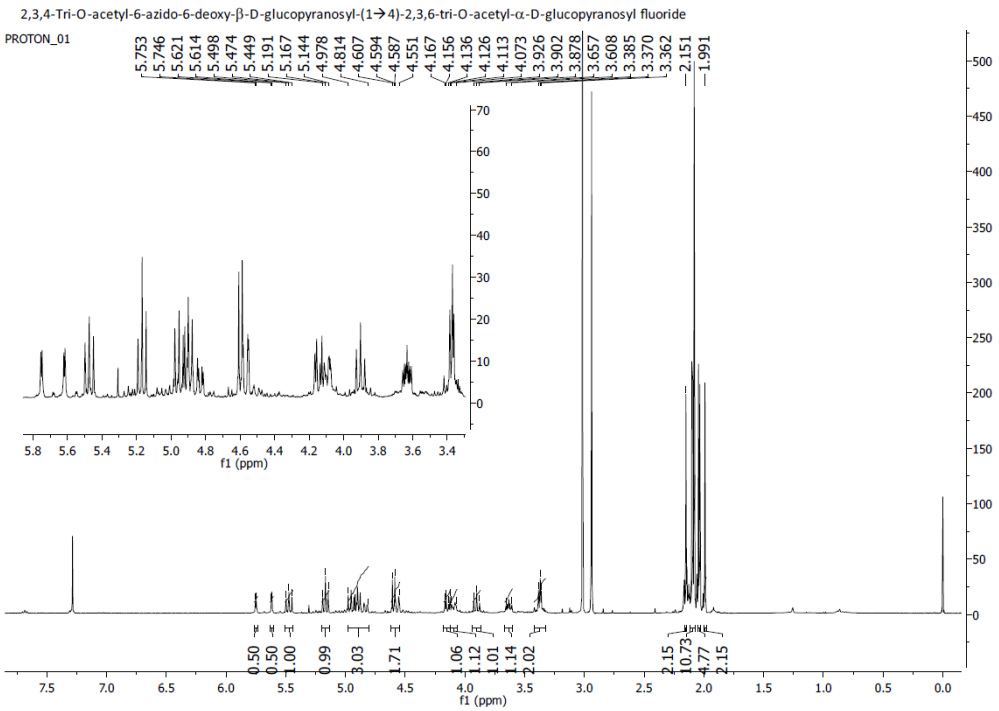

Figure A4. 5: ^{1}H NMR 2,3,4-tri-*O*-acetyl-6-azido-6-deoxy-β-D-glucopyranosyl-(1→4)-2,3,6-tri-*O*-acetyl-α-D-glucopyranosyl fluoride (**9**).

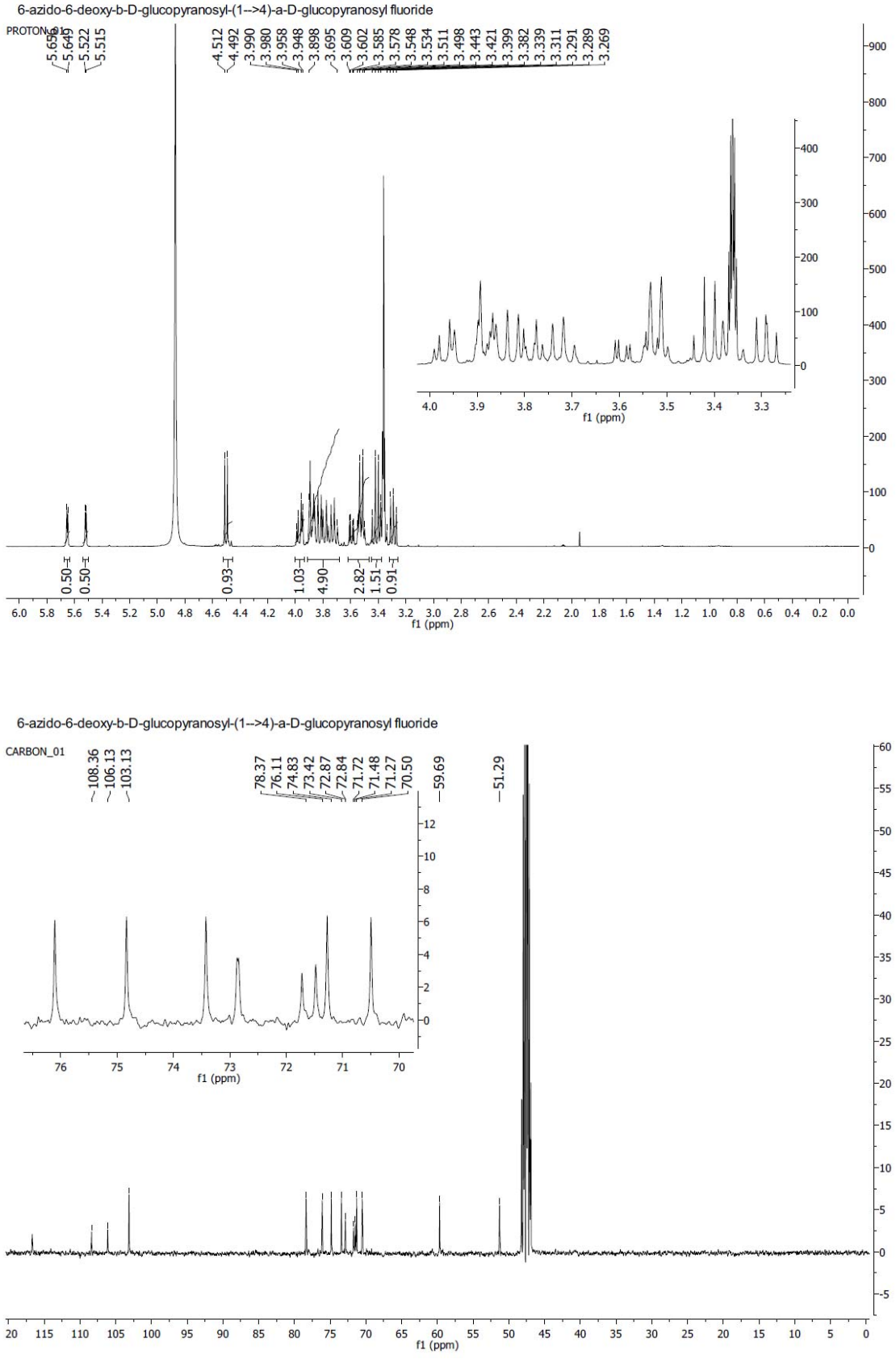

Figure A4. 6: ^{1}H NMR (above) and ^{13}C NMR (below) of 6-azido-6-deoxy-β-D-glucopyranosyl-(1→4)-α-D-glucopyranosyl fluoride (6'N_3-CelαF) (**10**).

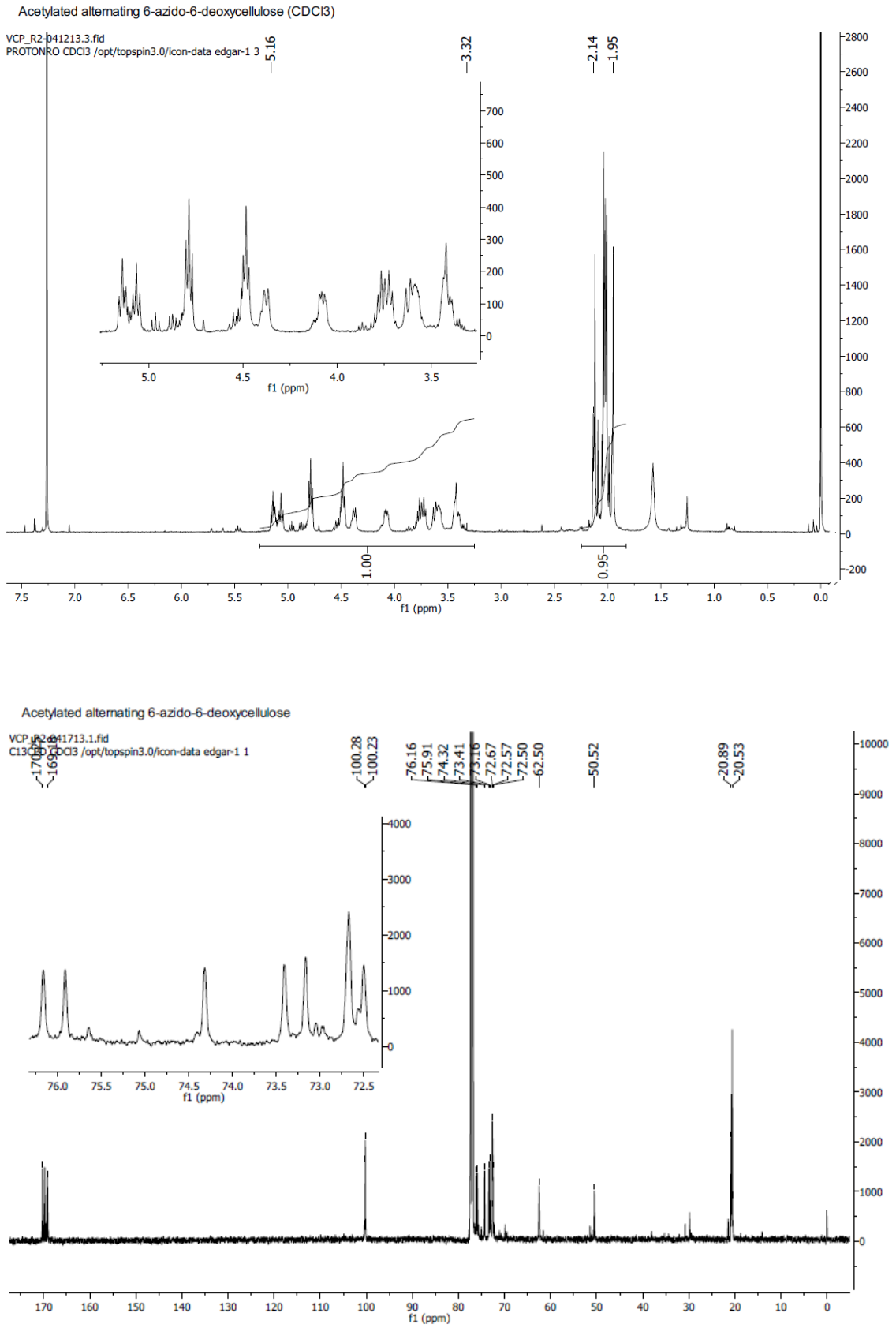

Figure A4. 7: ^{1}H NMR (above) and ^{13}C NMR (below) of acetylated alternating 6-azido-6-deoxycellulose (**3**) ($CDCl_3$).

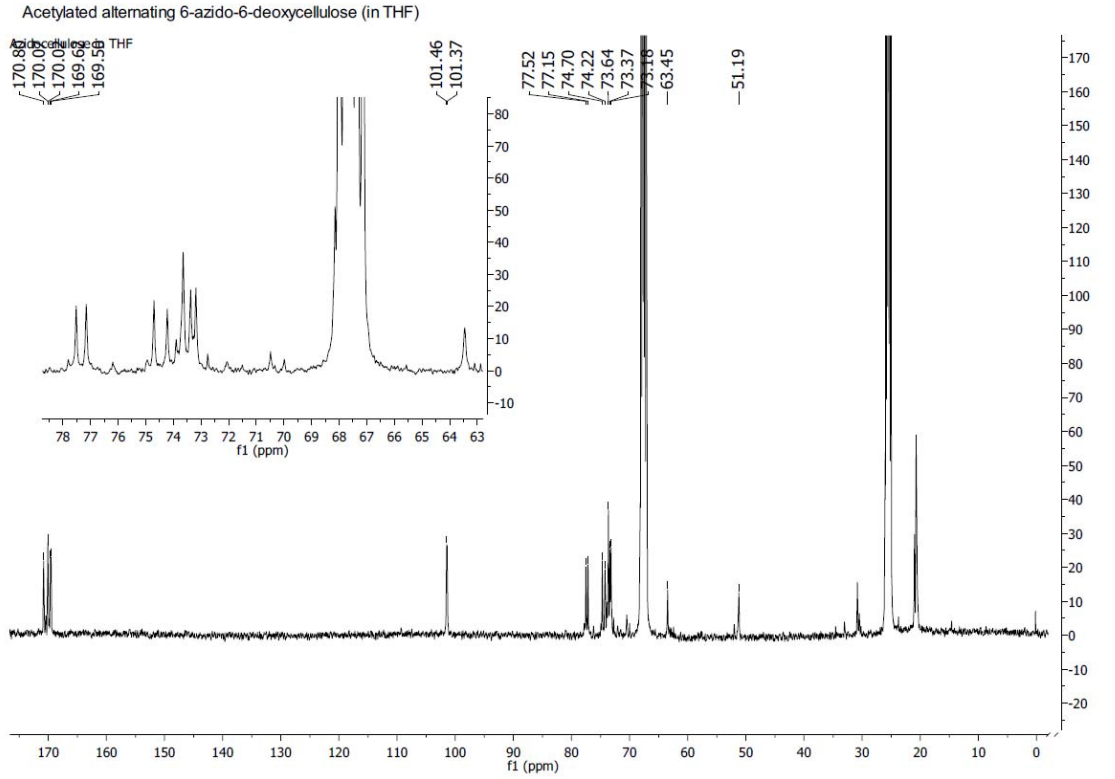

Figure A4. 8: ^{13}C NMR of acetylated alternating 6-azido-6-deoxycellulose (**3**) (THF).

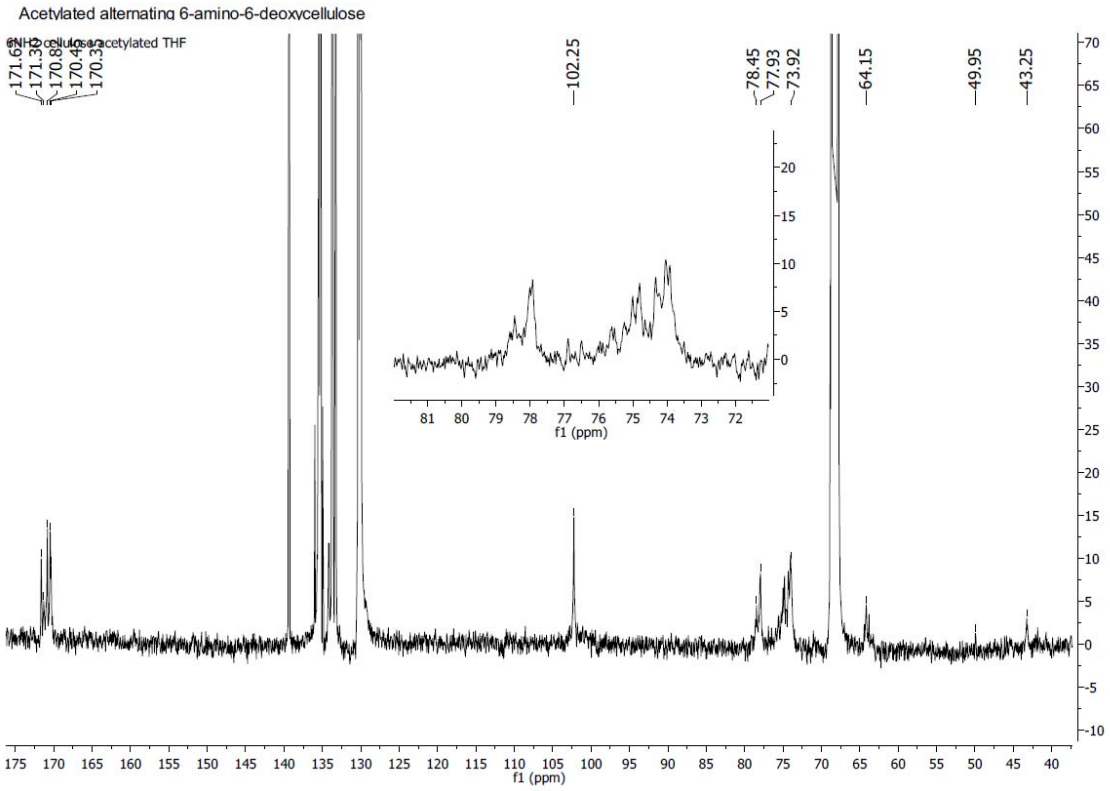

Figure A4. 9: ^{13}C NMR of acetylated alternating 6-amino-6-deoxycellulose (**4**) ($CDCl_3$).

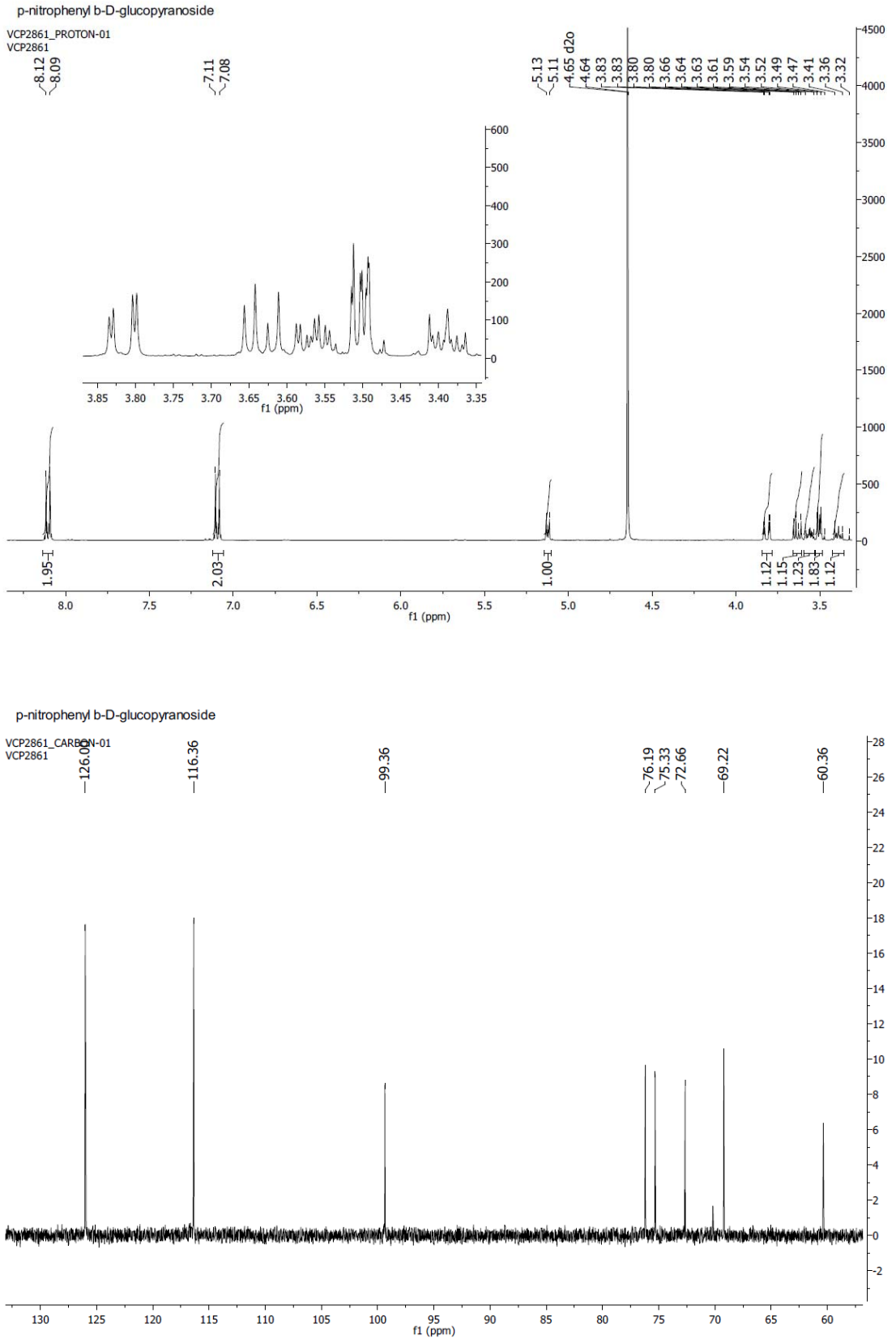

Figure A4. 10: ^{1}H NMR (above) and ^{13}C NMR (below) of *p*-nitrophenyl β-D-glucopyranoside (GlcβpNP) (**31**).

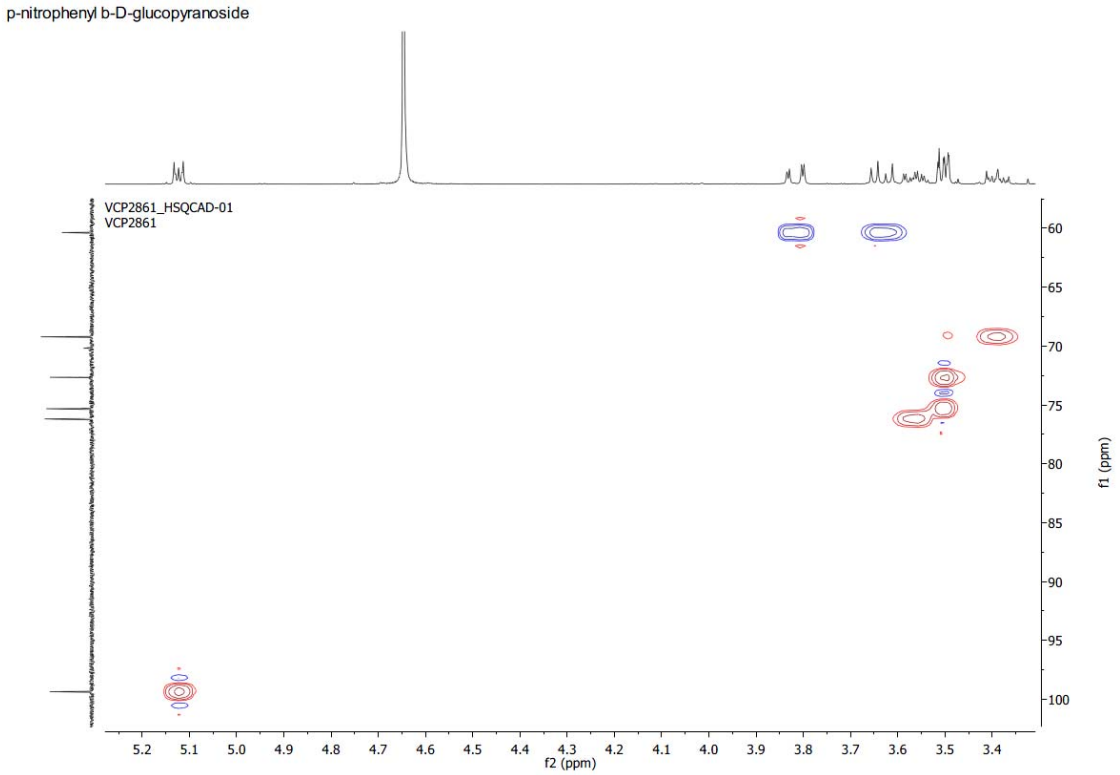

Figure A4. 11: HSQC of *p*-nitrophenyl β-D-glucopyranoside (GlcβpNP) (**31**).

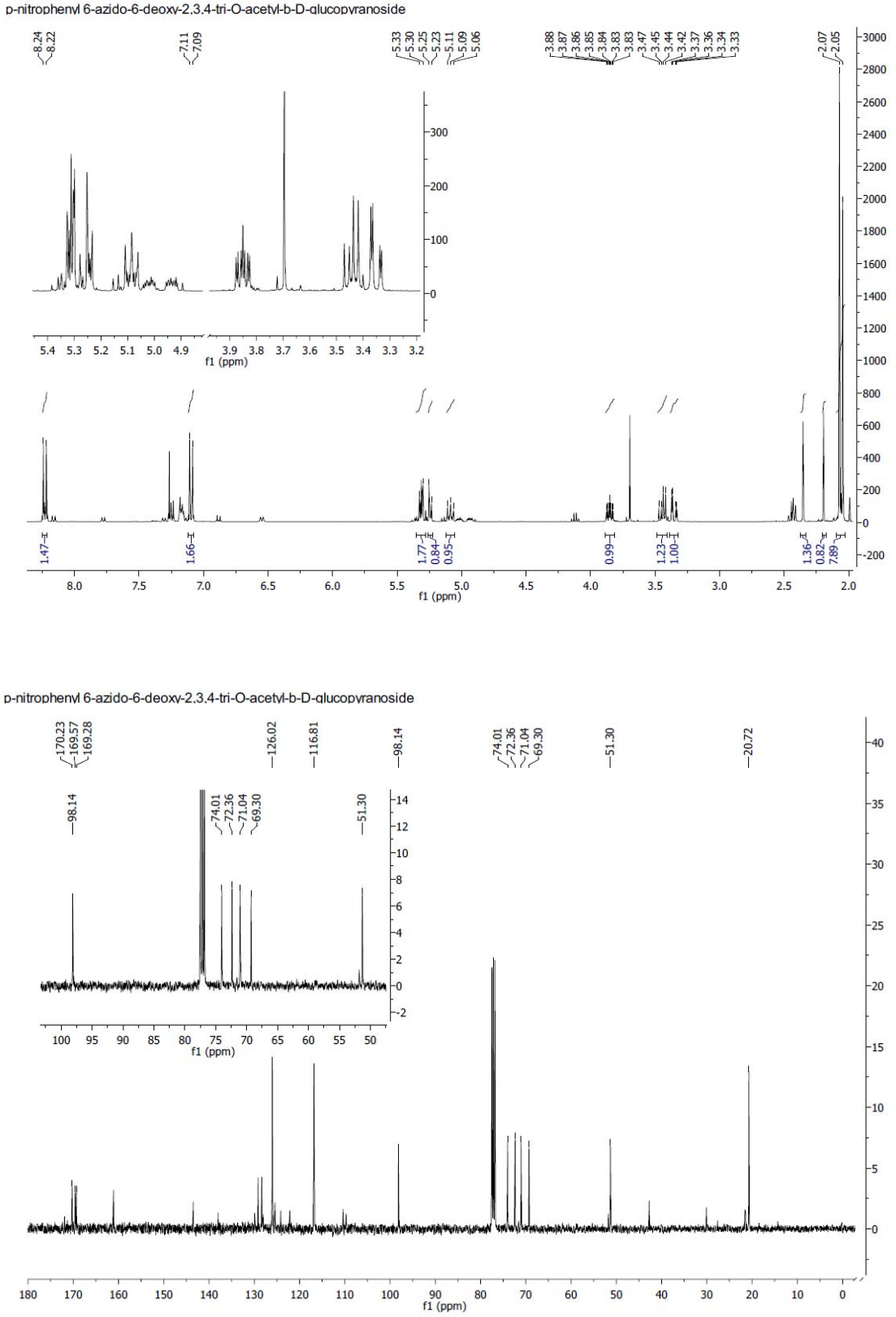

Figure A4. 12: ^{1}H NMR (above) and ^{13}C NMR (below) of *p*-nitrophenyl 6-azido-6-deoxy-2,3,4-tri-*O*-acetyl-β-D-glucopyranoside ($6N_3$-GlcβpNP) (**34**).

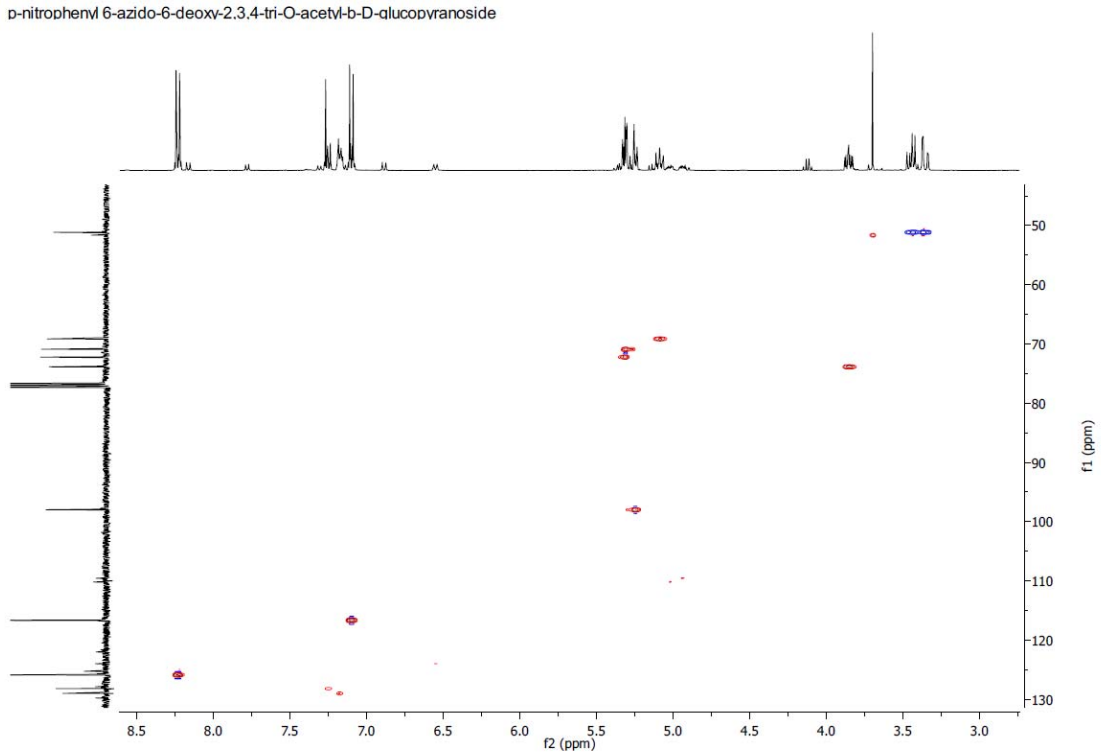

Figure A4. 13: HSQC of *p*-nitrophenyl 6-azido-6-deoxy-2,3,4-tri-*O*-acetyl-β-D-glucopyranoside ($6N_3$-GlcβpNP) (**34**).

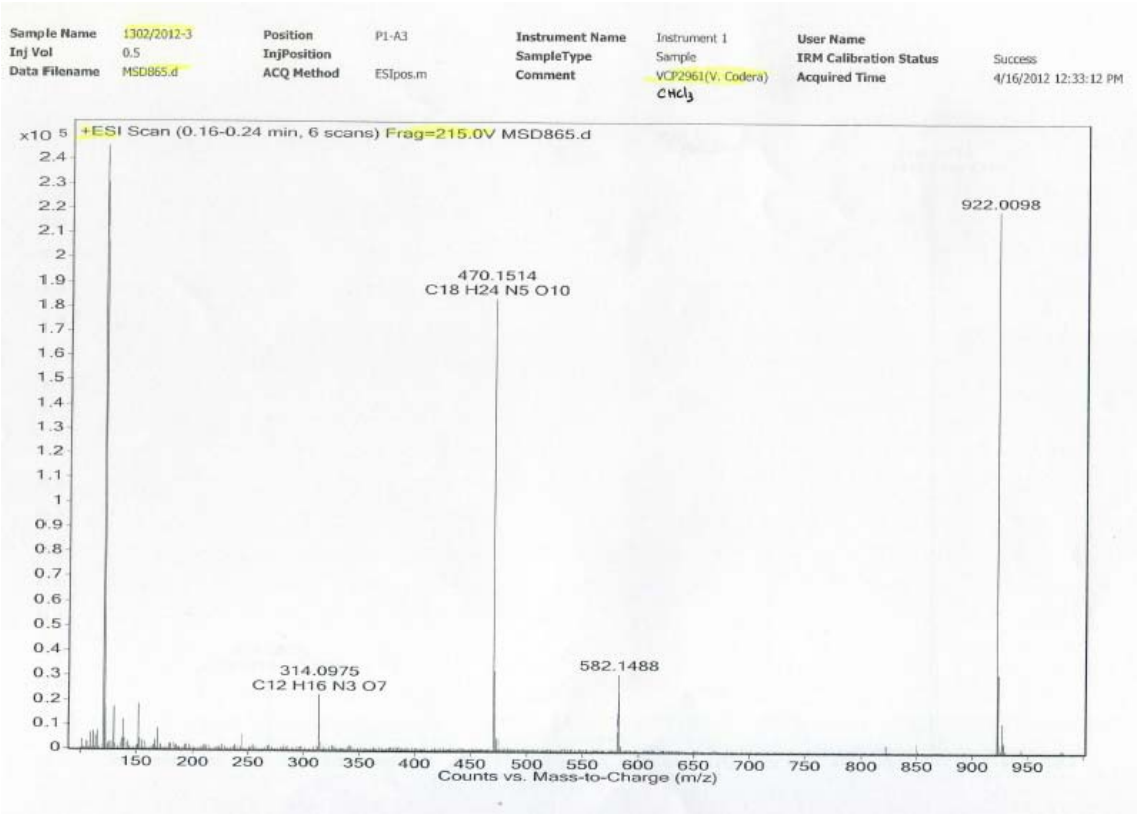

Figure A4. 14: MALDI spectrum of *p*-nitrophenyl 6-azido-6-deoxy-β-D-glucopyranoside ($6N_3$-GlcβpNP) (**35**).

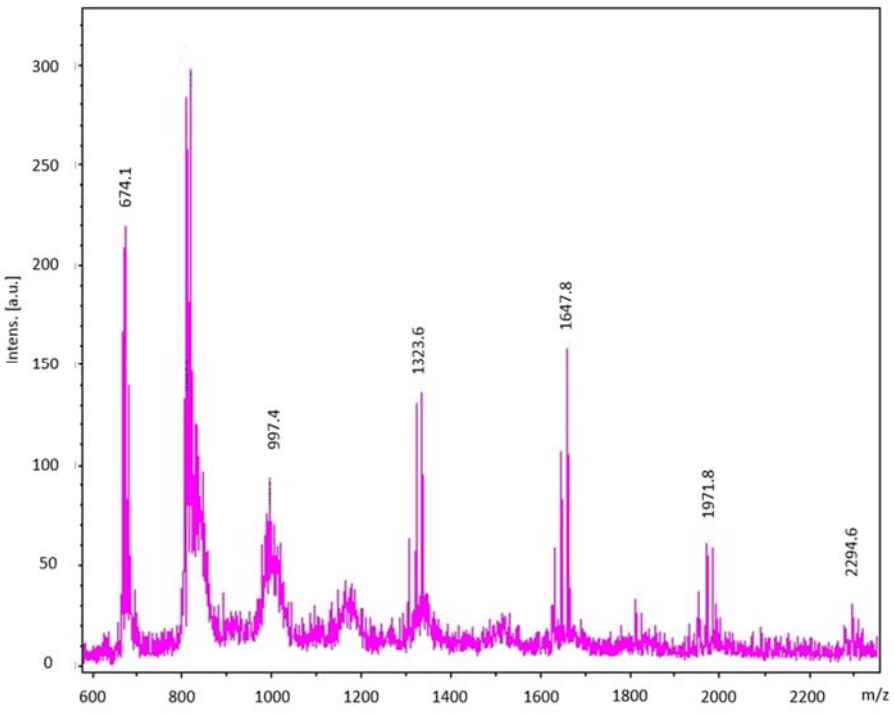

Figure A4. 15: MALDI-TOF spectrum of cellulose (**1**).

Δ mass	m/z experimental	# Glu	[M-OH+Na]$^{1+}$	Error % 1Na	[M-2OH+2Na]$^{2+}$	Error % 2 Na	[M-2OH+H+K]$^{2+}$	Error % H+K
	674.11	4	674.2	-0.02	680.2	-0.90	674.3	-0.03
323.24	997.35	6	999.3	-0.20	1005.3	-0.79	999.4	-0.21
326.28	1323.63	8	1324.4	-0.06	1330.4	-0.51	1324.6	-0.07
324.15	1647.78	10	1649.5	-0.11	1655.5	-0.47	1649.7	-0.11
324.02	1971.8	12	1974.7	-0.14	1980.6	-0.45	1974.8	-0.15
322.84	2294.64	13	2299.8	-0.22	2305.8	-0.48	2299.9	-0.23
Average 324.11			Error	-0.13		-0.60		-0.13

Table A4. 1: Assignment of main peaks in representative MALDI-TOF spectrum of cellulose (**1**).

Δ mass	m/z experimental	# Glu	[M-OH+Na]1+	Error % 1Na	[M-OH+H+K]2+	Error % H+K
	1773.8	10	1774.6	-0.04	1774.7	-0.05
347.5	2121.4	12	2124.7	-0.16	2124.8	-0.16
350.1	2471.4	14	2474.8	-0.14	2475.0	-0.14
349.7	2821.2	16	2825.0	-0.13	2825.1	-0.14
348.7	3169.8	18	3175.1	-0.17	3175.2	-0.17
348.2	3518.0	20	3525.2	-0.20	3525.3	-0.21
348.1	3866.1	22	3875.3	-0.24	3875.4	-0.24
348.7			Mean error:	-0.15		-0.16

Table A4. 2: Assignment of main peaks in representative MALDI-TOF spectrum of alternating 6-azido-6-deoxycellulose (**2**).

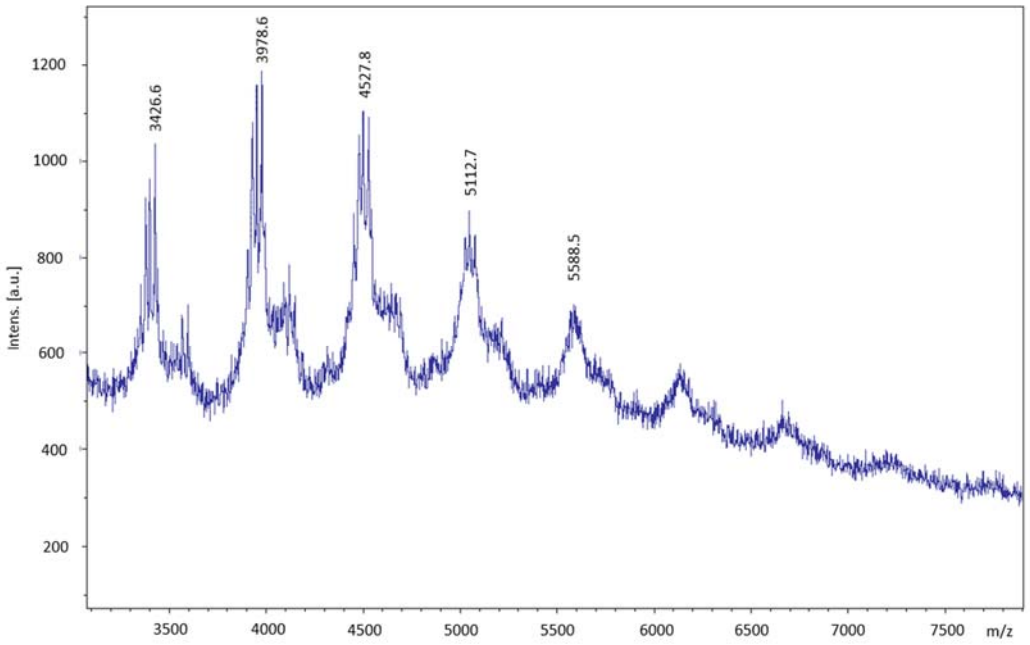

Figure A4. 16: MALDI-TOF spectrum of acetylated alternating 6-azido-6-deoxycellulose (**3**).

Δ mass	m/z experimental	# Glu	$[M\text{-}OH+Na]^{1+}$	Error % 1Na	$[M\text{-}OH+H+K]^{2+}$	Error % H+K
	3426.6	12	3427.0	-0.01	3429.2	-0.08
551.8	3978.4	23	3987.2	-0.22	3989.3	-0.27
549.4	4527.8	26	4547.4	-0.43	4549.5	-0.48
584.9	5112.7	29	5107.5	0.10	5109.7	0.06
Average 562.0			Error	-0.14		-0.19

Table A4. 3: Assignment of main peaks in representative MALDI-TOF spectrum of acetylated alternating 6-azido-6-deoxycellulose (**3**).

	Calculated mass	Δ mass
1) Cellulose	324.11	324.11
2) $6N_3$-cellulose	350.12	348.70
3) Acetylated $6N_3$cellulose	560.17	562.00

Table A4. 4: Summary. MW repeating units determined by MALDI-TOF.

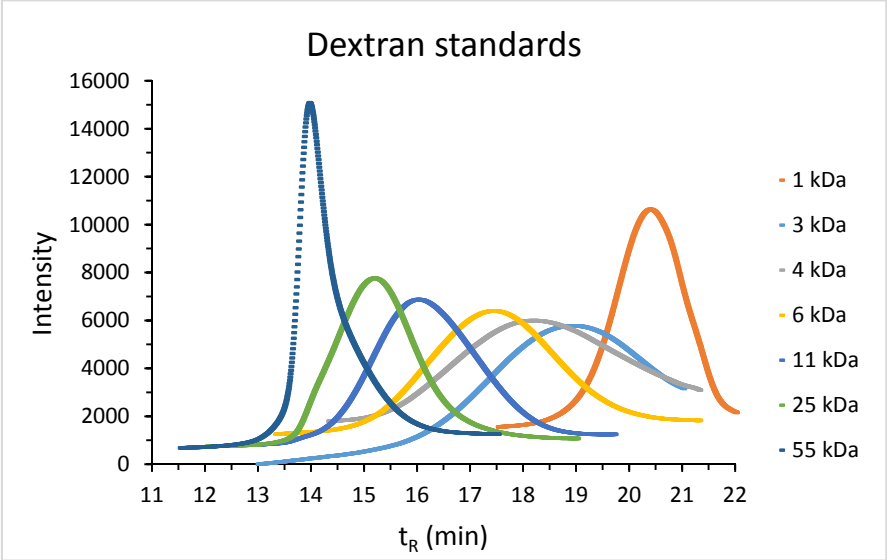

Figure A4. 17: HPSEC dextran standards.

M_p Standard	log M_p	t_r (min)
1000	3.0000	20.3688
2800	3.4472	18.9072
3400	3.5315	18.1692
4440	3.6474	17.4204
9900	3.9956	15.9948
20500	4.3118	15.1632
50200	4.7007	13.9392

Table A4. 5: Determination of the retention time (t_r) of dextran standards.

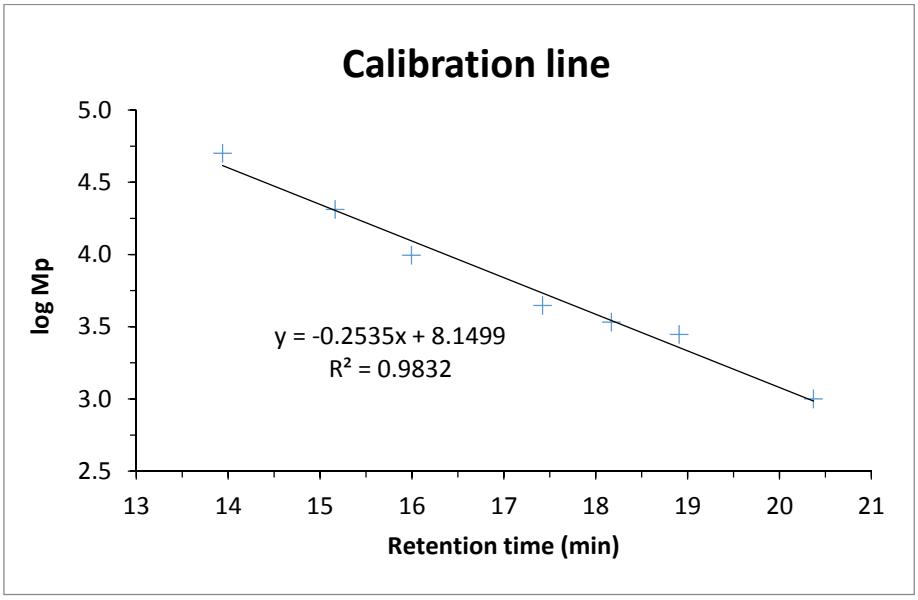

Figure A4. 18: HPSEC. Standards calibration line.

	Donor								
	2 mM	1.5 mM	1 mM	0.9 mM	0.8 mM	0.7 mM	0.5 mM	0.2 mM	0.05 mM
t / min	[Product] / μM								
0.33	0.00	0.00	0.00	0.00	0.00	0.00	0.00	0.00	0.00
1.80	0.00	0.00	0.00	0.00	0.00	0.00	0.00	0.00	0.00
3.87	2.99	2.99	2.50	2.58	2.34	0.00	0.00	0.00	0.00
7.90	7.34	7.10	7.34	5.65	6.54	4.60	5.25	0.00	0.00
16.30	24.54	22.76	22.36	21.15	20.34	15.17	15.66	6.54	0.00
30.05	45.68	44.87	43.99	41.89	43.34	46.09	38.26	25.34	8.31
42.98	59.81	62.15	65.70	62.55	63.20	68.28	55.61	47.30	14.69

Table A4. 6: Determination of v_o (CelαF + GlcβpNP).

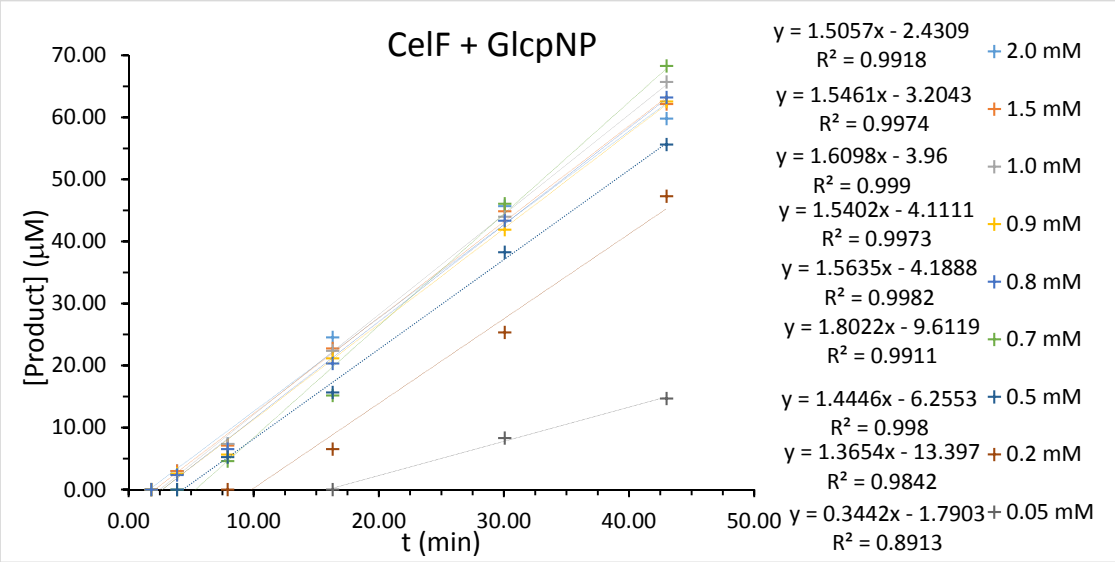

Figure A4. 19: Determination of v_o (CelαF + GlcβpNP). Reaction kinetics of Cel7B Glycosynthase. 4-nitrophenyl β-D-glucopyranoside acceptor (20 mM). Reactions performed at pH 7.0 and 35 °C.

[CelαF] / mM	v_o/[E] (min^{-1})
0.05	3.44
0.2	13.65
0.5	14.45
0.8	15.64
0.9	15.40
1.0	16.10
1.5	15.46
2.0	15.06

Table A4. 7: Michaelis-Menten data (CelαF + GlcβpNP).

	[6'N_3-CelαF] donor								
	2 mM	1.5 mM	1mM	0.8 mM	0.5 mM	0.3 mM	0.2 mM	0.1 mM	0.05 mM
t / min	[Product] / µM								
0.30	1.03	0.00	0.00	0.00	0.00	0.00	0.00	0.00	0.00
1.92	5.32	5.79	0.00	0.00	0.00	0.00	0.00	0.00	0.00
3.92	11.43	13.89	15.40	17.06	15.16	15.16	16.51	14.92	11.90
8.27	30.40	32.06	33.49	36.75	35.63	34.84	34.60	30.87	23.33
14.83	64.92	61.67	62.46	71.35	63.89	64.60	66.27	52.70	31.59
29.92	119.60	116.11	130.56	140.40	140.32	127.62	103.49	71.35	35.08
44.93	149.60	151.11	166.83	175.56	166.90	139.52	114.21	73.33	34.84

Table A4. 8: Determination of v_o (6'N_3-CelαF + GlcβpNP).

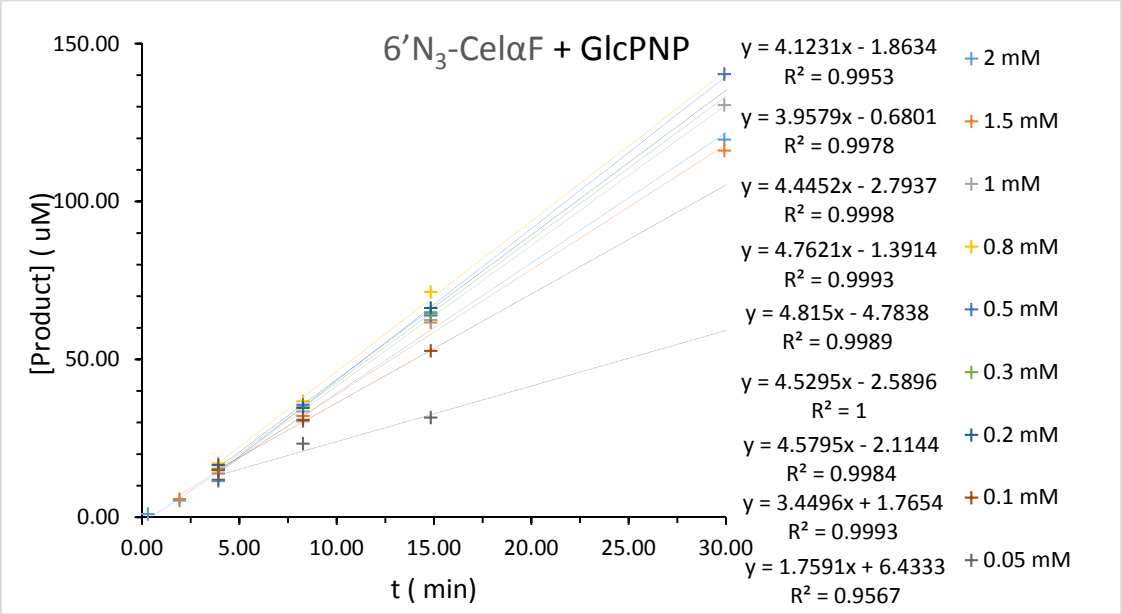

Figure A4. 20: Determination of v_o (6'N_3-CelαF + GlcβpNP). Reaction kinetics of Cel7B Glycosynthase. 4-nitrophenyl β-D-glucopyranoside acceptor (20 mM). Reactions performed at pH 7.0 and 35 °C.

[CelαF] / mM	v_o/[E] (min^{-1})
0.05	3.52
0.1	6.90
0.2	9.16
0.5	9.63
0.8	9.52
1.0	8.89
1.5	7.92

Table A4. 9: Michaelis-Menten data (6'N_3-CelαF + GlcβpNP).

	Desired final concentration / mM	Stock / mM	Reaction volume / mL
Phosphate buffer pH =7	100	200	98
[CelαF] in H_2O	1	30.8	10
[GlcβpNP] in phosphate buffer 100 mM	7	20	105
Cel7B in H_2O	8.30E-04	7.00E-03	35
H_2O	-	-	52
TOTAL	-		300

Table A4. 10: Translgycosylation reaction conditions (CelαF + GlcβpNP). Study of subsites: control reaction.

t / min	Aacceptor	Aproduct	Aa + Ap	[Product] / μM
0.08	7907.40	3.60	7911.00	3.21
6.10	7867.90	36.50	7904.40	32.57
10.00	7518.30	63.50	7581.80	56.67
15.33	7564.20	90.20	7654.40	80.49
25.32	7513.50	130.10	7643.60	116.10
40.65	7457.80	168.50	7626.30	150.37

Table A4. 11: Determination of v_o (CelαF + GlcβpNP). Study of subsites: control reaction.

	Final concentration / mM	[Stock] / mM	Reaction volume / mL
Phosphate buffer pH =7	100	200	45
[CelαF] in H_2O	1	30.8	10
[6N_3-GlcβpNP] in phosphate buffer 100 mM	7	10	210
Cel7B in H_2O	8.30E-04	7.00E-03	35
H_2O	**-**	-	0
TOTAL	**-**		300

Table A4. 12: Translgycosylation reaction conditions (CelαF + 6N_3-GlcβpNP). Study of subsite +1.

t / min	Aacceptor	Aproduct	Aa + Ap	[Product] / μM
0.08	8215.40	2.60	8218.00	2.05
5.00	8367.70	34.20	8401.90	26.97
9.00	8489.00	63.90	8552.90	50.39
14.00	8351.60	94.60	8446.20	74.61
24.20	8183.50	153.00	8336.50	120.66
39.62	7993.50	212.50	8206.00	167.59

Table A4. 13: Determination of v_o (CelαF + 6N_3-GlcβpNP). Study of subsite +1.

	Final concentration / mM	[Stock] / mM	Reaction volume / mL
Phosphate buffer pH =7	100	200	98
[6'N_3-CelαF] in H_2O	1	10	30
[GlcβpNP] in phosphate buffer 100 mM	7	20	105
Cel7B in H_2O	8.30E-04	7.00E-03	35
H_2O	-	-	32
TOTAL	-		300

Table A4. 14: Translgycosylation reaction conditions (6'N_3-CelαF + GlcβpNP). Study of subsite -2.

t / min	Aacep	Aproduct 1	Aa + Ap	[Product] / μM
1.98	8817.30	13.60	8830.90	11.07
6.27	9068.60	26.70	9095.30	21.74
8.08	9043.10	32.00	9075.10	26.05
10.23	9034.30	38.30	9072.60	31.18

Table A4. 15: Determination of v_o (6'N_3-CelαF + GlcpNP). Study of subsite -2.

	Michaelis- Menten (July 2013)		Subsite studies (November 2013)		
	CelαF + GlcβpNP	6'N_3-CelαF + GlcβpNP	Control (CelαF + GlcβpNP)	Subsite -2 (6'N_3-CelαF + GlcβpNP)	Subsite +1 (CelαF + N_3GlcβpNP)
Donor (mM)	1	1	1	1	1
Acceptor (mM)	20	20	7	7	7
[Enzyme] (uM)	0.1	0.5	0.83	0.83	0.83
v_o (μM/min)	1.61	4.45	5.14	2.46	5.26
v_o/E (min^{-1})	16.10	8.89	6.19	2.97	6.34

Table A4. 16: Summary of results (Michaelis-Menten reaction and subsite studies) when [Donor] = 1 mM.

CONCLUSIONS

CONCLUSIONS

1. The effect of the CBM11 was explored on glycosynthase-catalyzed polymerizations to generate mixed-linked 1,3-1,4-β-glucans with regular sequences. The observed effect is dependent on the rate of polysaccharide formation. At high polymerization rates, polymer yields are higher than 80% and CBM11, either as a discrete protein or appended to E134S (fusion protein), has no effect on the DP. In contrast, when the rate of polymerization is low and polymer yields are below 80%, the CBM11 facilitates the polymerization resulting in 25% increase in DP.
2. In the case of the alternating polysaccharide $(4Glc\beta3Glc\beta)_n$, the presence of the CBM disrupts the crystallinity of the insoluble polymer yielding amorphous precipitates instead of the characteristic spherulite morphology.
3. The production of laminaribiose from the degradation of curdlan with the kitilase from *Rhizoctonia solani* was optimized obtaining a mixture of 45% glucose, 46% laminaribiose and 9% trisaccharide.
4. Selective tritylation was performed on laminaribiose to obtain the 6'-tritylated compound. A preferential reactivity for 6'-tritylation compared to 6-tritylation was always observed in ratios 2 – 2.5 to 1. The ratio of trityl chloride – disaccharide was crucial for the complete protection of the C-6 and C-6' primary positions.
5. Acyl migrations were observed after detritylation with aqueous acetic acid. The addition of NaI avoid acyl migrations but the reaction was incomplete and not reproducible. The use of $FeCl_3 \cdot 6H_2O$ was finally chosen for the deprotection of the trityl group despite it did not avoid further acyl migrations.
6. Condensation reactions between different laminaribiosyl fluoride donors (Glcβ3GlcαF and $6N_3$-Glcβ3GlcαF) and different *p*-nitrophenyl glucoside acceptors (GlcβPNP and $6N_3$-GlcβPNP) by the E134S glycosynthase mutant concluded that the N_3 functional group can be accommodated at both donor and acceptor subsites. However, the specific activity with the $6N_3$-Glcβ3GlcαF donor was 0.15% compared to the unsubstituted donor. Donor polymerization was not studied in this work because of this low activity. Further directed evolution approaches will be required to improve the specific activity.
7. The ability of the *Hi*Cel7B E197A glycosynthase to accept azido-substituted substrates was evaluated demonstrating that it can accommodate a functionalized azido substrate in both donor and acceptor subsites, with preference for subsite +1 than subsite -2.
8. Glycosynthase-catalyzed polymerizations of 6'N3-CelαF as substrates yielded water-insoluble alternating 6-azido-6-deoxycellulose that precipitated as porous spherulites.

9. The alternating 6-azido-6-deoxycellulose consisted of a regular pattern of one azido group every two glucosyl units, which were further reacted to install different functional groups or substituents. In the future, the strategy opens the access to novel polysaccharide structures with promising applications. It can be extended to other functionalized donors to afford other regularly functionalized glycopolymers with different substitution patterns. Furthermore, other functional groups may be introduced in the glycosyl donor provided that the donor is accepted as a substrate by the glycosynthase, which otherwise can be engineered for the desired specificity by protein engineering and directed evolution approaches.